ISSN 2408-2384 (ONLINE)

Environment and Natural Resources Journal

Volume 23 Number 5 September - October 2025

The endangered green peafowl (*Pavo muticus*). The species distribution modeling reveals how climate change and habitat factors threaten the green peafowl's remaining strongholds in Thailand.

Source: Prommakul K, Noowong J, Charaspet K, Kaewdee B, Siripattaranukul K, Duengkae P, Simchareon S, Sukmasuang R. Predicting habitat suitability for the endangered green peafowl (*Pavo muticus* L., 1766) in Thailand's Western Stronghold under future climate scenarios. Page 469-482

Scopus Clarivate Analytics EBSCO HOST DOAJ ASEAN CITATION INDEX TCI Thai-Journal Citation Index Centre

Environment and Natural Resources Journal (EnNRJ)
Volume 23, Number 5, September - October 2025 ISSN: 2408-2384 (Online)

FOCUS AND SCOPE

Environment and Natural Resources Journal (EnNRJ) is a peer-reviewed journal which provides a platform for exchanging and distributing knowledge and cutting-edge research in environmental science and natural resource management to academicians, scientists, and researchers.

The scope of the journal covers the integration of multidisciplinary sciences for prevention, control, treatment, environmental clean-up, and restoration. The study of existing or emerging problems related to the environment and natural resources in Southeast Asia and the development of innovative knowledge and/or creative recommendations for mitigation measures and sustainable development are emphasized. The subject areas are diverse, but specific topics of interest include:

- Biodiversity
- Climate change
- Detection and monitoring of pollutants and their sources (e.g., agriculture, industry, mining, urban activities, accidents)
- Disaster (e.g., forest fires, flooding, earthquakes, tsunamis or tidal waves)
- Ecological/Environmental modelling
- Emerging contaminants/hazardous wastes investigations and remediation
- Environmental dynamics (e.g., coastal erosion, rising sea levels)
- Environmental assessment tools, policy, and management [e.g., GIS, remote sensing, and Environmental Management Systems (EMS)]
- Pollution control and innovative solutions for pollution reduction
- Remediation technology in contaminated environments
- Transboundary pollution
- Waste and wastewater treatments and disposal technology

Schedule
Environment and Natural Resources Journal (EnNRJ) is published 6 issues per year in January-February, March-April, May-June, July-August, September-October, and November-December.

Publication Fees
An article publication fee in the Environment and Natural Resources Journal is set at a rate of 250 USD per article, payable after the final acceptance of the manuscript.

Ethics in publishing
EnNRJ follows closely a set of guidelines and recommendations published by Committee on Publication Ethics (COPE).

Environment and Natural Resources Journal (EnNRJ)
Volume 23, Number 5, September - October 2025 ISSN: 2408-2384 (Online)

EXECUTIVE CONSULTANT TO EDITOR

Professor Dr. Benjaphorn Prapagdee
(Mahidol University, Thailand)
Associate Professor Dr. Kitikorn Charmondusit
(Mahidol University, Thailand)

EDITOR

Associate Professor Dr. Noppol Arunrat
(Mahidol University, Thailand)

ASSOCIATE EDITOR

Assistant Professor Dr. Piangjai Peerakiatkhajohn
(Mahidol University, Thailand)
Dr. Jakkapon Phanthuwongpakdee
(Mahidol University, Thailand)

EDITORIAL BOARD

Professor Dr. Aysegul Pala
(Dokuz Eylul University, Türkiye)
Professor Dr. Hermann Knoflacher
(Vienna University of Technology, Austria)
Professor Dr. Hideki Nakayama
(Nagasaki University, Japan)
Professor Dr. Jung-Ho Yun
(Kyung Hee University, South Korea)
Professor Dr. Sompon Wanwimolruk
(Mahidol University, Thailand)
Professor Dr. Uwe Strotmann
(University of Applied Sciences, Germany)
Associate Professor Dr. Chuleemas Boonthai IWAI
(Khon Kaen University, Thailand)
Associate Professor Dr. Devi N. Choesin
(School of Life Sciences and Technology, Indonesia)
Associate Professor Dr. Pasicha Chaikaew
(Chulalongkorn University, Thailand)
Associate Professor Dr. Pirom Noisumdaeng
(Thammasat University, Thailand)
Associate Professor Dr. Pongchai Dumrongrojwatthana
(Chulalongkorn University, Thailand)
Associate Professor Dr. Sate Sampattagul
(Chiang Mai University, Thailand)

Associate Professor Dr. Schradh Saenton
(Chiang Mai University, Thailand)
Associate Professor Dr. Takehiko Kenzaka
(Setsunan University, Japan)
Associate Professor Dr. Vimoltip Singtuen
(Khon Kaen University, Thailand)
Associate Professor Dr. Xu Tian
(Shanghai Jiao Tong University, China)
Assistant Professor Dr. Anish Ghimire
(Asian Institute of Technology, Thailand)
Assistant Professor Dr. Said Munir
(University of Leeds, United Kingdom)
Assistant Professor Dr. Toru Hamamoto
(Tohoku University, Japan)
Dr. Davide Poggio (Research Associate)
(University of Sheffield, United Kingdom)
Dr. Ho Ngo Anh Dao
(Ton Duc Thang University, Viet Nam)
Dr. Miaoqiang Lyu
(The University of Queensland, Australia
Dr. Mohamed F. Yassin
(Kuwait Institute for Scientific Research, Kuwait)

ASSISTANT TO EDITOR

Assistant Professor Dr. Thunyapat Sattraburut
Dr. Praewa Wongburi
Dr. Tatiya Siripongpreda
Dr. Shreema Rana
Mr. William Thorn

JOURNAL MANAGER

Isaree Apinya

JOURNAL EDITORIAL OFFICER

Nattakarn Ratchakun
Parynya Chowwiwattanaporn

Editorial Office Address
Research and Academic Service, Research Management Unit,
Faculty of Environment and Resource Studies, Mahidol University
999, Phutthamonthon Sai 4 Road, Salaya, Phutthamonthon, Nakhon Pathom, Thailand, 73170
Phone +662 441 5000 ext. 2108
Website: https://ph02.tci-thaijo.org/index.php/ennrj/index
E-mail: ennrjournal@gmail.com

Environment and Natural Resources Journal (EnNRJ)
Volume 23, Number 5, September - October 2025 ISSN: 2408-2384 (Online)

CONTENT

Environment and Natural Resources Journal

Volume 23
Issue 5
2025

Heavy Metal Contamination in Taft River Sediments Affected by Bagacay Mine Post-Operation in Hinabangan, Samar, Philippines

Jessie Sabijon[1*], Venecio Ultra Jr[2], Marcos Bollido[3], Eduardo Espejon Jr[1], and Zaldee Niño Tan[1]

[1]Department of Agriculture and Related Programs, Northwest Samar State University, San Jorge Campus, Philippines
[2]Department of Sustainable Natural Resources, School of Earth Sciences and Engineering, Botswana International University of Science and Technology, Palapye, Botswana
[3]College of Agriculture, Forestry and Environmental Sciences, Western Philippines University, Philippines

ARTICLE INFO

Received: 29 Jan 2025
Received in revised: 2 May 2025
Accepted: 6 May 2025
Published online: 23 Jul 2025
DOI: 10.32526/ennrj/23/20250026

Keywords:
Heavy metals/ Sediments/ Taft River Basin/ Bagacay Mines

*** Corresponding author:**
E-mail:
jessie.sabijon@nwssu.edu.ph

ABSTRACT

The purpose of this study was to assess the level of heavy metal contamination in the sediments of the Taft River Basin in Taft Eastern Samar, Philippines. The concentrations and levels of heavy metal contamination in sediments were assessed using the Pollution Load index (PLi), the Contamination Factor (Cfi), and the Geoaccumulation Index (Igeo). Our findings revealed moderate to high levels of potentially toxic elements (PTEs) such as Ti, Cr, Mn, Ni, Cu, Zn, As, Mo, Cd, and Pb. The CF and Igeo values indicated significant pollution, with Igeo values ranging from class 2 to class 6. The CFi indicated moderate to high contamination in river bank sediments following the order of Pb>As>Zn>Mo>Mn>Cu>Ni>Cr>Ti>Cd, and Pb>Cu>Zn>As>Mn>Cr>Ni>Mo>Ti>Cd in river bottom sediments. The PLi values exceeded the critical threshold of 1, confirming severe contamination, especially in the upper reaches of the river near the Bagacay mining site. The contamination showed a consistent presence of heavy metals, with Pb, As, Zn, and Mo being dominant in river bank sediments, and Cu, Pb, Zn, and As in river bottom sediments. Downstream attenuation of PTE levels was observed and is attributed to dilution and sedimentation processes. Overall, the study confirmed the contamination of these heavy metals in the sediments and underscored the need for rehabilitating the Bagacay mine to prevent the buildup of these contaminated sediments in the basin. It is recommended to expand monitoring to include groundwater and biotic components to better assess long-term ecological risks. Regular sediment quality assessments, and multi-stakeholder watershed management are essential for the sustainable health of the Taft River and its surrounding communities.

1. INTRODUCTION

Concerns over the effects of mining on the aquatic ecosystem are growing (Gabrielyan et al., 2018). Aquatic ecosystems like rivers are considered sinks of contaminants because they are open systems and are therefore more vulnerable to contamination. The accumulation of contaminants in rivers impacted by mining activities is a prevalent issue in many developing countries (Islam et al., 2014). In the Philippines, inactive and abandoned mines expose and disturb heavy metal-laden soils and sediments, posing significant environmental and health risks (Samaniego et al., 2024).

A notable example is the Bagacay Mines in Samar, which was abandoned after years of operation, leaving behind massive amounts of mining waste containing extremely high concentrations of heavy metals. These pollutants have significantly affected the quality of the Taft River Basin, which receives drainage from the mining site. The conditions of the Taft River before the mining operation supported a relatively intact aquatic environment. However, post-

Citation: Sabijon J, Jr VU, Bollido M, Jr EE, Tan ZN. Heavy metal contamination in Taft River sediments affected by Bagacay Mine post-operation in Hinabangan, Samar, Philippines. Environ. Nat. Resour. J. 2025;23(5):390-408. (https://doi.org/10.32526/ennrj/23/20250026)

mining activities, especially the unrehabilitated waste piles, have contributed to the degradation of the river ecosystem. The riverbed sediments of the primary tributaries stretching from the Bagacay mine site to the Taft River have exhibited levels of heavy metal contamination exceeding critical limits, such as those set by the U.S. Environmental Protection Agency (EPA) and the Canadian Environmental Quality Guidelines (CEQG) for heavy metals in sediments. These excessive levels include arsenic (9.79 mg/kg), lead (50 mg/kg), and cadmium (1.0 mg/kg) (Dayang, 2017).

Heavy metal contamination of sediments has aroused significant concern due to the toxicity, persistence, and bioaccumulation of these pollutants (Yang et al., 2012), as well as the potential risks they pose to human health and aquatic organisms (da Silva et al., 2017). Despite this, most river monitoring practices focus on water quality alone, often overlooking the role of sediments, which continuously interact with the river system (Duncan et al., 2018). In fact, most heavy metals entering the aquatic environment become incorporated into the sediments through flocculation and precipitation (Zhou et al., 2023). Under certain conditions, these heavy metals can also be released from the sediment and reintroduced into the water column, making sediments both sinks and potential secondary sources of contamination.

The presence of toxic heavy metals in sediments threatens the health and balance of the aquatic ecosystem. They can accumulate in microorganisms, aquatic animals, and plants, potentially entering the food chain and posing a serious threat to human health (Feng et al., 2024; Kang et al., 2020). For instance, crustaceans such as mud crabs and shrimp found in the Taft River have shown elevated levels of heavy metals (Cabahug et al., 2023), highlighting the river's contamination from mining pollutants. These organisms, which occupy the lower trophic levels, absorb heavy metals from polluted water and sediments, posing a serious risk to local biodiversity and potentially affecting human populations who rely on them for food. Furthermore, heavy metal-laden sediments may be transported by runoff and precipitation, causing erosion of riverbanks and deposition of pollutants into nearby coastal areas. These sediments act as long-term storage for heavy metals and may affect marine ecosystems and public health (Sabijon et al., 2024). Once bound to sediments, heavy metals become persistent and are considered among the most hazardous pollutants in aquatic environments. Contamination of Cu, Hg, Cd, Fe, and Zn in the sediments of Ambon Bay, located in Maluku Province, Indonesia, was reported by Manullang et al. (2017). Similarly, surface sediments of the Mangonbangon River in Tacloban City have shown the presence of Fe>Mn>Zn>Cu>Cr>Ni>Co (Decena et al., 2018). Belyaeva (2012) likewise reported high concentrations of heavy metals and trace elements such as As, Cu, Mo, Sb, Co, Ni, and Zn in the surface waters and sediments of the Voghji River Basin in Ararat Plain region of Armenia.

Since heavy metal concentrations in sediments are typically much higher than those in surface water, it is critical to evaluate sediment quality as a reliable indicator of pollution (Wang et al., 2014). Unlike water, metal concentrations in sediments remain relatively stable over time (Tupan et al., 2014). However, despite the known environmental risks posed by the Bagacay Mines, limited information is available on the contamination of sediments in the Taft River Basin. Therefore, this study was conducted to assess the extent of heavy metal contamination in the sediments of the Taft River Basin, particularly as affected by post-operational discharges and waste from the Bagacay Mines.

2. METHODOLOGY

2.1 Study area

The study was done in the Taft River Basin, located between 11°54′N latitude and 125°25′E longitude. The region where the site is located experiences a humid tropical monsoon climate (Cayanan et al., 2018) with annual rainfall ranging from 2,500 mm in Northwest Leyte to over 3,000 mm in Borongan, Eastern Samar, and an average temperature of approximately 28°C. The study area is specifically located in the Taft River in Hinabangan, Samar, Philippines, a region with a documented history of mining and agricultural activities. A significant contributor to environmental degradation in the area was inefficient waste management and the unprogrammed abandonment of Bagacay Mine, which was operational from the mid-20th century until its closure in 1996. The mine was primarily engaged in the extraction of nickel and copper, and its operations led to substantial discharge of mine tailings and heavy metal contaminants into nearby rivers, including the Taft River (MGB, 2005; Dayang, 2017). These contaminants, such as nickel, copper, zinc, and

arsenic, remain in the soil and aquatic systems due to their persistent and mobile nature.

The geology of the Bagacay area is predominantly composed of Miocene to Pliocene volcanic and volcaniclastic rocks, including andesitic to basaltic flows, pyroclastics, and tuffaceous sediments, which are part of the Bagacay Formation (MGB, 2005). The area hosts polymetallic sulfide mineralization, consisting mainly of copper, lead, zinc, gold, and silver, associated with hydrothermal alteration zones such as silicification and argillic alteration. Mineralization occurs along vein and fracture systems, indicating that the deposit is structurally controlled, and suggests characteristics of a volcanogenic massive sulfide (VMS) or epithermal-type deposit. The mining activities in the area have exposed mineralized zones and left behind tailings rich in heavy metals, contributing to long-term environmental impacts (MGB, 2005).

A preliminary survey of the Taft River floodplain was conducted to identify representative sampling sites and document ecological conditions. Field observations revealed signs of environmental degradation, including discolored water, sediment plumes, and riverbed alteration, suggesting continued pollution. Soil samples collected across the floodplain showed elevated heavy metal concentration (Sabijon et al., 2024).

The soils in the area which area classified as Eutrudepts derived from limestone (calcite-rich) parent material, have undergone extensive degradation due to decades of cultivation, flooding, and erosion (Asio et al., 2006). Today, agricultural use is limited, and vegetation consists mainly of grasses, shrubs, and isolated crops. In addition to mining, periodic flooding and soil erosion have contributed to the downstream transport and deposition of contaminated sediments, compounding the environmental risks and underscoring the need for ongoing monitoring and rehabilitation efforts.

2.2 Sediment sample collection and analysis

Figure 1 and Table 1 show the selected sample collection points in different barangays along the Taft River in Eastern Samar. The barangays are a rural village in Eastern Samar and the smallest administrative unit in the Philippines, functions similarly to a village or neighborhood in other countries. Sediment samples were collected during the rainy season (27 October to 03 November 2020) to capture the potential peak influx of heavy metals associated with surface runoff from the Bagacay Mining site. Rainfall events significantly enhance the mobilization and transport of heavy metals from exposed soils, mine tailings, and disturbed catchments into the Taft river system. Sampling during this period provides a more accurate representation of heavy metal input into sediments. The air-dried sediment samples were pulverized using a wooden mallet to prevent contamination from metallic tools, which can introduce trace metals and affect the accuracy of heavy metal analysis (US EPA, 1996). The pulverized samples were then passed through a 2 mm mesh sieve to remove coarse debris and to isolate the fine fraction, which is more representative of heavy metal accumulation due to its higher surface area and binding capacity (US EPA, 1996). Prepared samples were subjected to laboratory analyses to evaluate their heavy metal concentrations. The analysis for heavy metal concentrations was conducted following the same procedure (Figure 2) of Ultra (2020) and Sabijon et al. (2024) at the Soil Sciensce Laboratory of the Department of Sustainable Natural Resources, School of Earth Sciences and Engineering, Botswana International University of Science and Technology, Palapye, Botswana.

Table 1. Coordinates and relative proximity of the sampling sites from the Bagacay Mines

Sampling Sites	Latitude	Longitude	Distance from Bagacay Mines (km)
San Rafael	11.80861111	125.2952778	5.332
Binaloan	11.85194444	125.3247222	13.172
Malinao	11.873824	125.347566	17.482
San Pablo	11.88027778	125.36	20.112
Mabuhay	11.89777778	125.3688889	22.637
Gayam	11.88531	125.39912	26.629
Pob.6	11.90916667	125.4152778	32.049
Pob. 1	11.90138889	125.4216667	33.131
Polangi	11.88777778	125.4219444	34.917

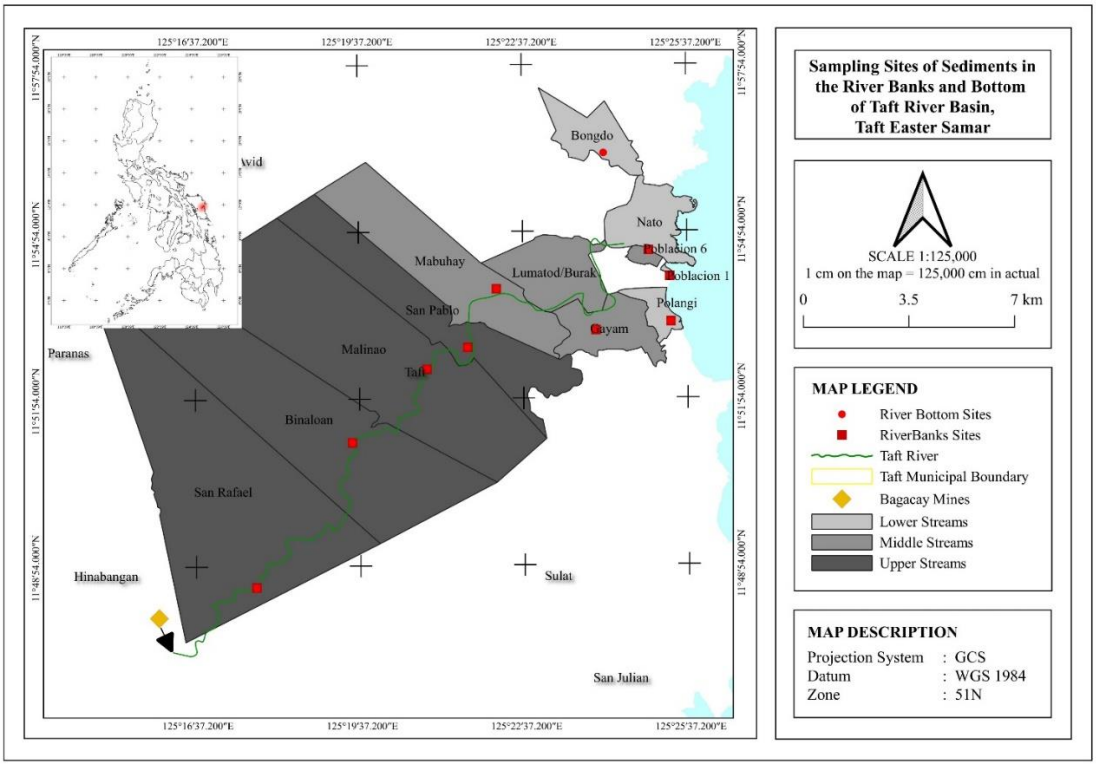

Figure 1. Map showing the sampling sites of sediments in Taft River Basin

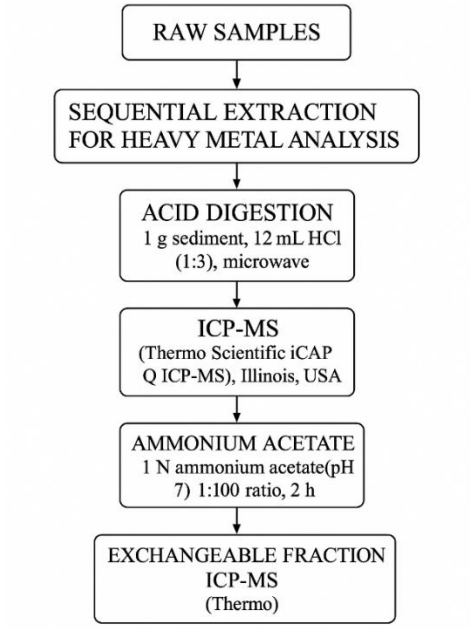

Figure 2. Flow chart of the procedural analyses for heavy metals

2.3 Sediment contamination indices

2.3.1 Geoaccumulation index

The geoaccumulation index was used to determine the degree of contamination in a sample (Müller, 1979) whuch was estimated using the formula:

$$\text{Igeo} = \log_2\left(\frac{\text{Cn}}{1.5\text{Bn}}\right) \quad (1)$$

Where; Cn is the metal (n) concentration measured in the study area's sediments, Bn is the background value of the corresponding metal (n), and factor 1.5 is the background matrix correction for lithogenic effects (Salomons and Forstner, 1984).

2.3.2. Contamination factor

The contamination factor (CFi), a single metric, is regarded as a simple and useful instrument for monitoring heavy metal contamination (Shen et al., 2019). CFi is calculated using this equation:

$$\text{CFi} = \frac{\text{Ci}}{\text{Bi}} \quad (2)$$

Where; Ci and Bi are the measured concentration and background value of metal i, respectively. CFi is an indicator of heavy metal contamination in sediments. The background concentrations of heavy metals (in mg/kg) were determined from non-contaminated samples collected within the same area. The values were as follows: Ti (3697), Cr (43.2), Mn (242), Ni (38), Cu (15), Zn (55.6), As (8.7), Mo (3.4), Cd (6.6), and Pb (5.5).

2.3.3 Pollution load index (PLi)

Tomlinson et al. (1980) employed the PLi to determine the site's total amount of heavy metals. The PLi value for a site in the sediments was computed using the following formula:

$$PLi = (CF1 \times CF2 \times CF3 \times \ldots x\ CFn)1/N \quad (3)$$

Where; CFi is the ratio of the observed concentration (Ci) to the number of heavy metals. PLi>1 indicates contaminated, while PLi<1 indicates unpolluted. A PLI level value of 0 denotes excellence, a PLI value of 1 reflects baseline pollution levels, and a PLI value of =>1 indicates progressive degradation of sediment quality.

The Kriging interpolation method was applied in the study using QGIS to create the Pollution Load Index (PLI) map of heavy metals in river sediments, owing to its ability to model spatial autocorrelation and deliver statistically reliable predictions. Kriging is preferred over simpler methods like IDW because it not only interpolates values but also quantifies uncertainty, making it well-suited for environmental assessments. Its effectiveness in mapping heavy metal contamination in soils and sediments has been widely supported in the literature (Zhang et al., 2011; Eze et al., 2018).

3. RESULTS

3.1 Total concentrations of heavy metals in river sediments

In Figures 3(a-j) and 4(a-j), the Ti concentrations in most of the collected river sediments were higher than the permissible concentration (WHO, 1982). The concentration ranged from 2,869-6,012 mg/kg in the river bank sediments and 2,914-6,224 mg/kg in the river bottom sediments. The highest concentration in river bank sediments was observed in Barangay ("Brgy") Poblacion 6 (lower stream), and in Brgy. Malinao (upper stream) for bottom sediments.

According to Kabata-Pendias and Pendias (2001), the overall concentrations of Cr in sediments were higher than the critical threshold of 75-100 mg/kg, except for the river bank sediments of Brgy. Polangi (lower stream) and river bottom sediments of Brgy. Binaloan (upper stream). Cr concentrations in most river bank sediments and river bottom sediments ranged from 112.24-624.20 mg/kg and 140-1,768 mg/kg, respectively. These values are 1.4-17.7 times and 1.1-6.2 times higher than the critical limit. The highest Cr concentration in river bank sediments was found in Brgy. Burak, and in Brgy. Bungdo (both middle stream) for river bottom sediments.

Also, Mn concentrations of river sediments in all sites were found to be lower compared to the critical level of 600 mg/kg (Vodyanitskii, 2016), except for Brgy. San Pablo (upper stream) which recorded 720 mg/kg. Generally, all river sediments were found to have have safe concentrations of Mn.

Additionally, the total Ni concentration in the river bank sediments of Barangays San Rafael, Binaloan (upper stream), Gayam (middle stream), Poblacion 6, Poblacion 1, and Polangi (lower stream) exceeded the 100 mg/kg threshold level (Kabata-Pendias and Pendias, 2001). The river bank sediments around Brgy. Polangi recorded the highest concentration, which was 98 times greater than the threshold amount (98,194 mg/kg). For bottom sediments, only samples from Brgys. Malinao (upper stream), Gayam and Bungdo (middle stream), and Polangi (lower stream) had Ni concentrations above the critical level. The highest Ni concentration was observed in Brgy. Bungdo (middle stream) at 435 mg/kg, which is four times higher than the critical limit. Relatively higher total Cu concentrations above the critical level of 60-125 mg/kg were observed in most of the river bank sediments, except for samples from Brgy. Poblacion 1 and Brgy. Polangi (lower stream), and in all bottom sediments except for Brgy. Bungdo (middle stream). River bank and bottom sediment Cu concentrations ranged from 144-1,244 mg/kg and 144-3,116 mg/kg, respectively.

The highest concentration in river bank sediments was recorded in Brgy. San Rafael (upper stream) at 1,244 mg/kg, which is ten times higher than the highest critical threshold. In bottom sediments, the highest Cu concentration was detected in samples from Brgy. San Pablo (upper stream) at 3,116 mg/kg. A higher concentration trend of Cu was observed in samples from the upper stream, likely due to proximity to a mining site.

The majority of the river bank and bottom sediments contained high quantities of Zn. Zn concentrations were above the minimum critical value of 70 mg/kg (Kabata-Pendias and Pendias, 2001), ranging from 196-2,276 mg/kg in river bank sediments and 167-5,064 mg/kg in river bottom sediments. Brgy. Poblacion 6 (lower stream) had the greatest Zn concentrations in both river bank (2,276 mg/kg) and river bottom sediments (5,064 mg/kg), which are 33 and 72 times higher than the minimum critical level,

respectively. The same trend was observed for arsenic (As), which was higher in all river sediments. Values for both river bank and bottom sediments were above the critical level of 1-40 mg/kg (ATSDR, 2007), ranging from 123-6,252 mg/kg. The highest As concentrations were found in both river bank and bottom sediments of Brgy. Poblacion 6 (lower stream).

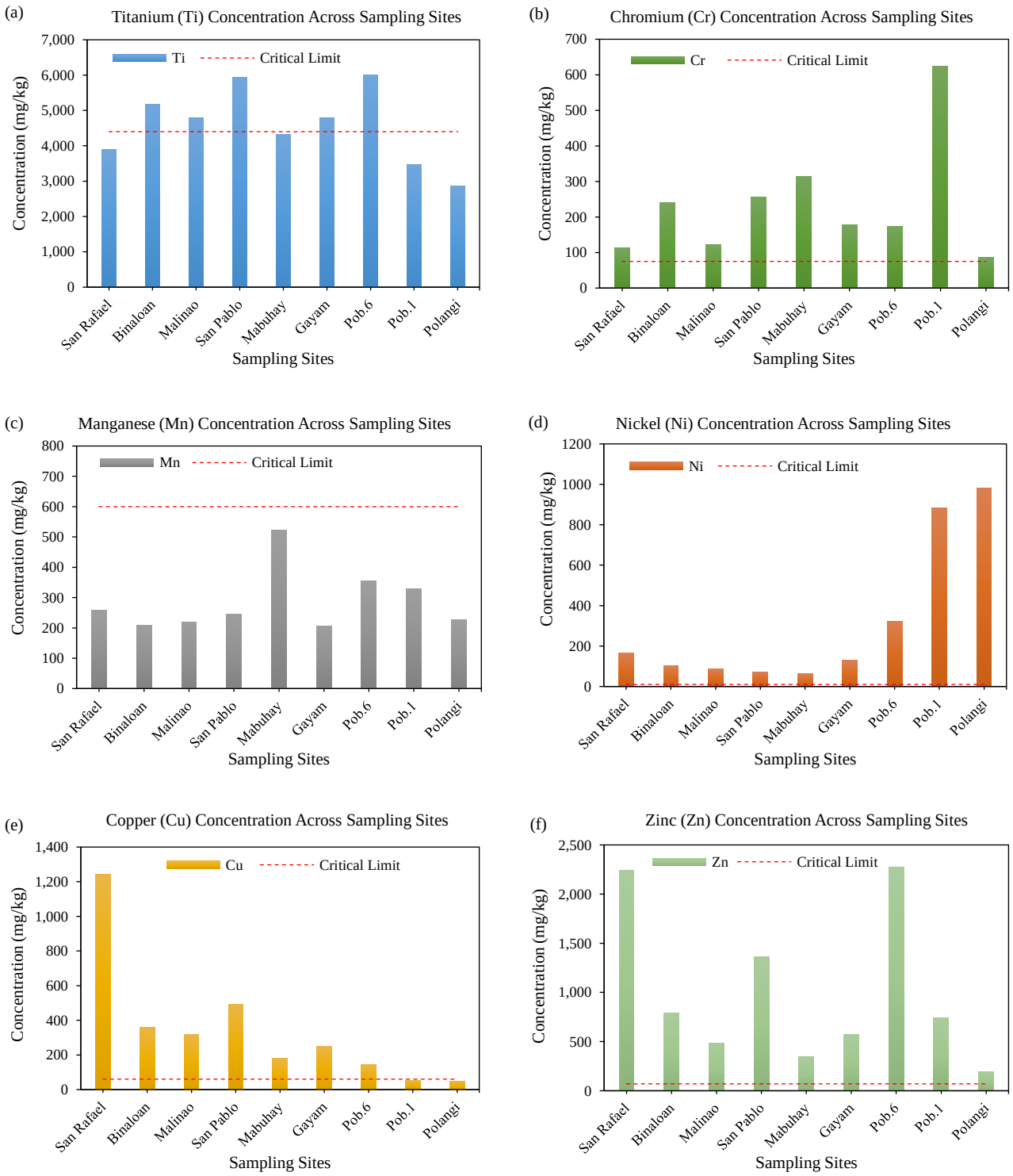

Figure 3. Total concentrations of (a) Ti, (b) Cr, (c) Mn, (d) Ni, (e) Cu, (f) Zn, (g) As, (h) Mo, (i) Cd, (j) Pb, in river bank sediments

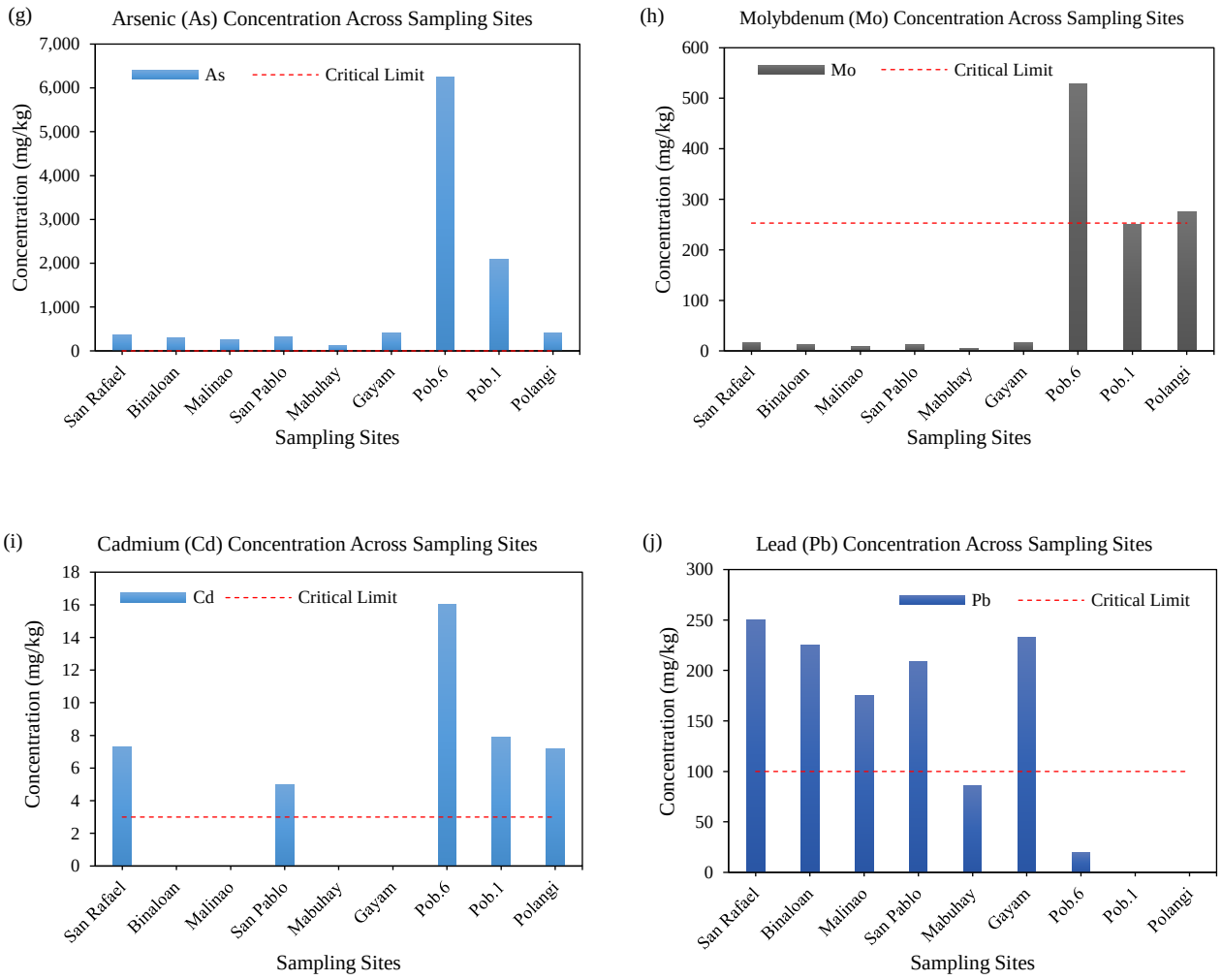

Figure 3. Total concentrations of (a) Ti, (b) Cr, (c) Mn, (d) Ni, (e) Cu, (f) Zn, (g) As, (h) Mo, (i) Cd, (j) Pb, in river bank sediments (cont.)

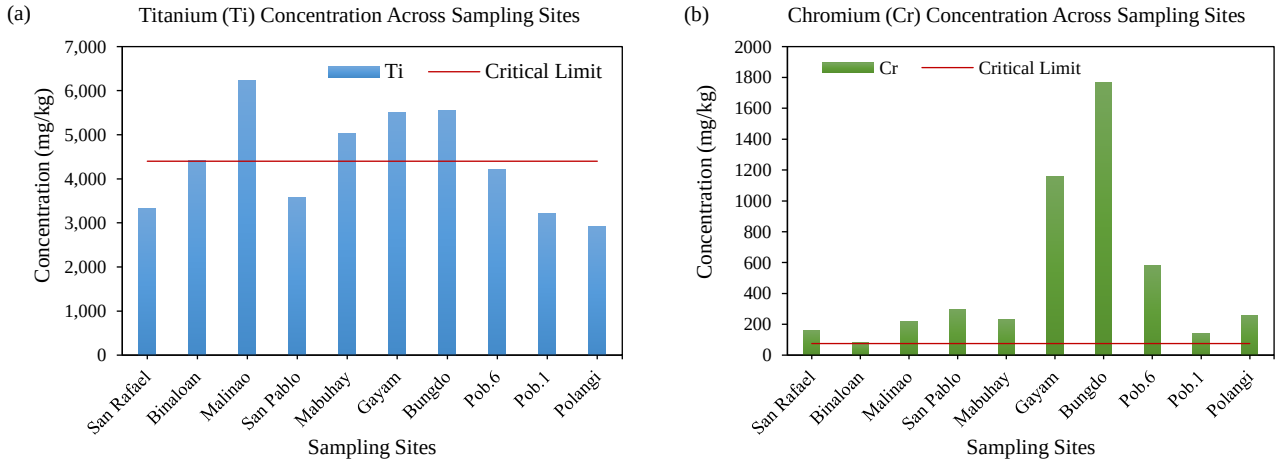

Figure 4. Total concentrations of (a) Ti, (b) Cr, (c) Mn, (d) Ni, (e) Cu, (f) Zn, (g) As, (h) Mo, (i) Cd, (j) Pb, in river bottom sediments

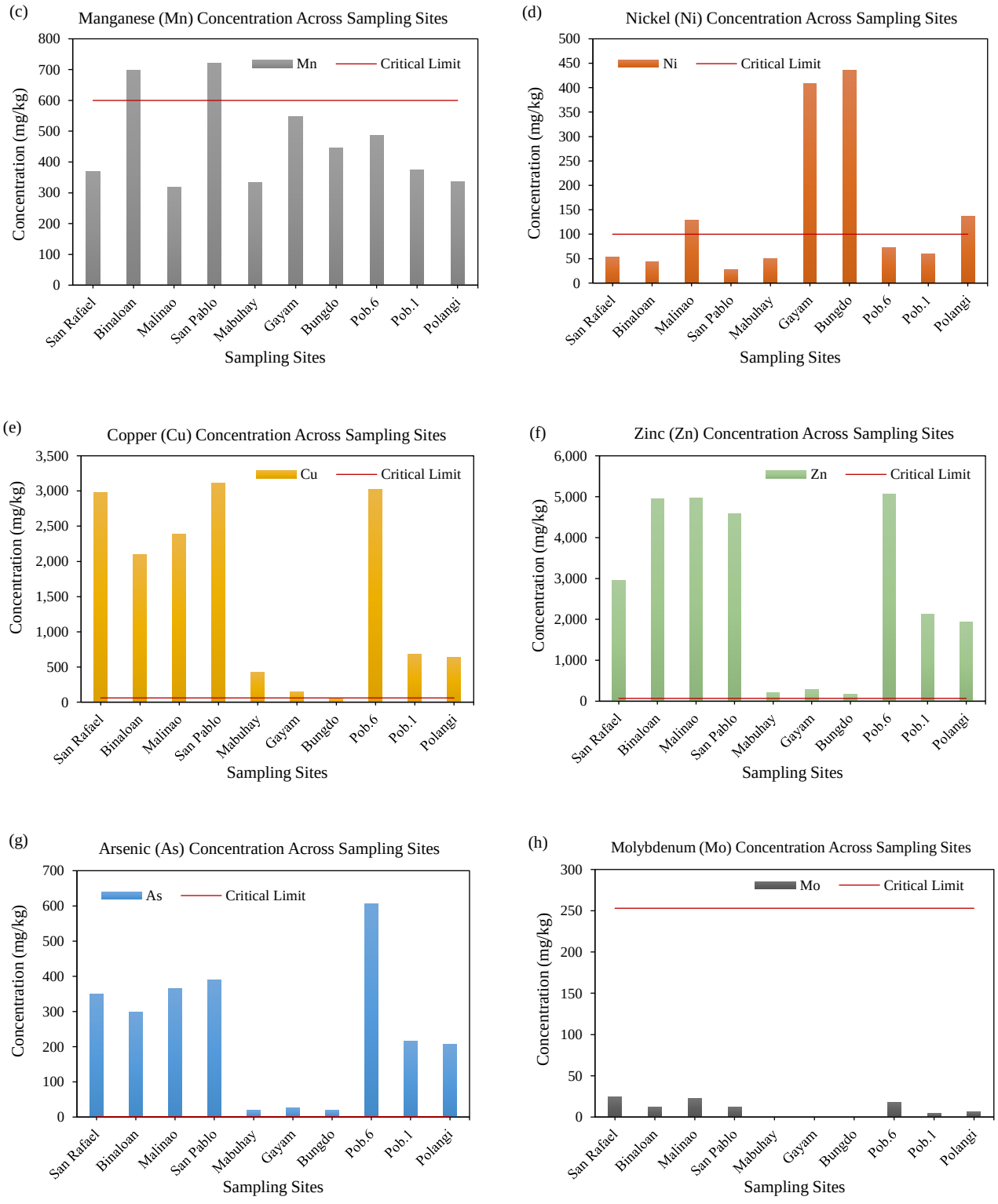

Figure 4. Total concentrations of (a) Ti, (b) Cr, (c) Mn, (d) Ni, (e) Cu, (f) Zn, (g) As, (h) Mo, (i) Cd, (j) Pb, in river bottom sediments (cont.)

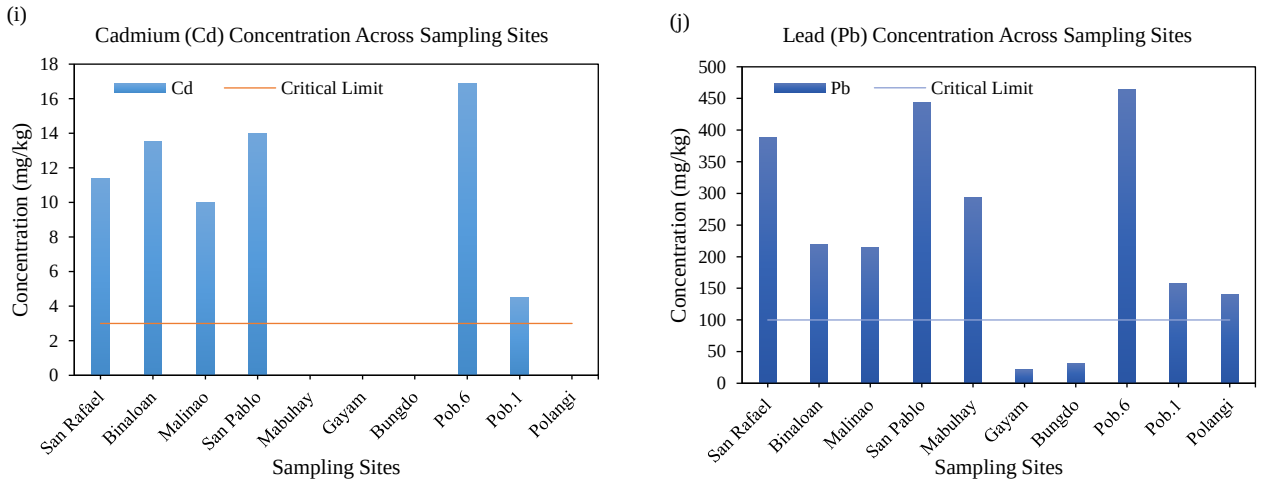

Figure 4. Total concentrations of (a) Ti, (b) Cr, (c) Mn, (d) Ni, (e) Cu, (f) Zn, (g) As, (h) Mo, (i) Cd, (j) Pb, in river bottom sediments (cont.)

In the case of molybdenum (Mo), concentrations in river sediments were below the critical level of 253 mg/kg. Similarly, most samples had Cd concentrations below the critical limit of 3-8 mg/kg. Only river bank sediment samples from Brgy. San Rafael, Brgy. San Pablo (upper stream), Brgy. Poblacion 6, Brgy. Poblacion 1, and Brgy. Polangi (lower stream) were within or above the critical level, especially in the middle stream. The highest Cd concentration (16 mg/kg) was found in samples from Brgy. Poblacion 6 (lower stream).

River bottom sediment samples from Brgy. San Rafael, Binaloan, Malinao, San Pablo (upper stream), and Poblacion 6, Poblacion 1 (lower stream) also showed Cd concentrations above the critical level. All other samples from different barangays, particularly in the middle stream, had Cd concentrations below the critical level. Furthermore, total Pb concentrations in river bank and bottom sediments were higher than the critical level of 100-400 mg/kg. Pb concentrations were highest in the river bank sediments of Brgy. San Rafael (upper stream) at 250 mg/kg, and in the bottom sediments of Brgy. Poblacion 6 (lower stream) at 464.00 mg/kg.

3.2 Contamination and pollution of sediments

The results indicated that the total heavy metal concentrations in riverbank sediments followed a decreasing order of Ti > Ni > Zn > As > Cu > Cr > Mn > Mo > Cd > Pb, while in river bottom sediments, the distribution followed Ti > Zn > Cu > Cr > Mn > Ni > As > Pb > Mo > Cd. The critical and permissible levels used as comparison thresholds for each metal were based on values reported in relevant scientific literature. “Critical levels” refer to the concentrations above which adverse environmental or biological effects may occur (Kabata-Pendias and Pendias, 2001; ATSDR, 2007), while “permissible limits” are typically regulatory standards such as those from WHO (1982).

In Figures 5(a-j) to 6(a-j), the majority of the quantifiable heavy metals corresponded to Class 2 to 6 based on the geo-accumulation index (Igeo) proposed by Müller (1979), indicating that most of the river sediments in the Taft River Basin were moderately to extremely polluted. In riverbank sediments, all sites were classified as very highly contaminated (Igeo>5, Class 6) with titanium (Ti), nickel (Ni), zinc (Zn), arsenic (As), copper (Cu), chromium (Cr), and manganese (Mn). Molybdenum (Mo) contamination ranged from moderately to very highly contaminated (Igeo 2->5, Class 2-6), while cadmium (Cd) ranged from uncontaminated to highly contaminated (Igeo 0-5, Class 1-5). Lead (Pb) contamination was absent (Igeo=0, Class 0) in Brgy. Binaloan and Brgy. Malinao (both Upper Stream), and Brgy. Mabuhay and Brgy. Gayam (Middle Stream), but all other barangays, particularly those in the Lower Stream areas such as Brgy. Poblacion 6 and Brgy. Polangi, showed moderate to high Pb contamination.

In the river bottom sediments, all sites were classified as very highly contaminated (Igeo>5, Class 6) with Ti, Zn, Cu, Cr, Mn, Ni, and As. No Pb, Mo, or Cd contamination (Igeo=0, Class 0) was observed in Brgy. Mabuhay, Brgy. Gayam, and Brgy. Bungdo (Middle Stream). Additionally, no Mo contamination was recorded in Brgy. Poblacion 1 (Lower Stream), and no Cd contamination was found in both Brgy.

Poblacion 1 and Brgy. Polangi (Lower Stream). In contrast, all other bottom sediment samples showed moderate to high contamination levels (Igeo 2-4, Class 2-4) for Pb, Mo, and Cd.

When grouped according to stream location, the Lower Stream barangays (Brgy. Poblacion 6, Brgy. Poblacion 1, and Brgy. Polangi) were observed to be the most highly contaminated, showing extreme Igeo values especially for Zn, Cu, Pb, and As. The Middle Stream barangays (Brgy. Mabuhay, Brgy. Gayam, Brgy. Bungdo, and Brgy. Burak) exhibited moderate contamination, with minimal Pb, Mo, and Cd contamination in some areas.

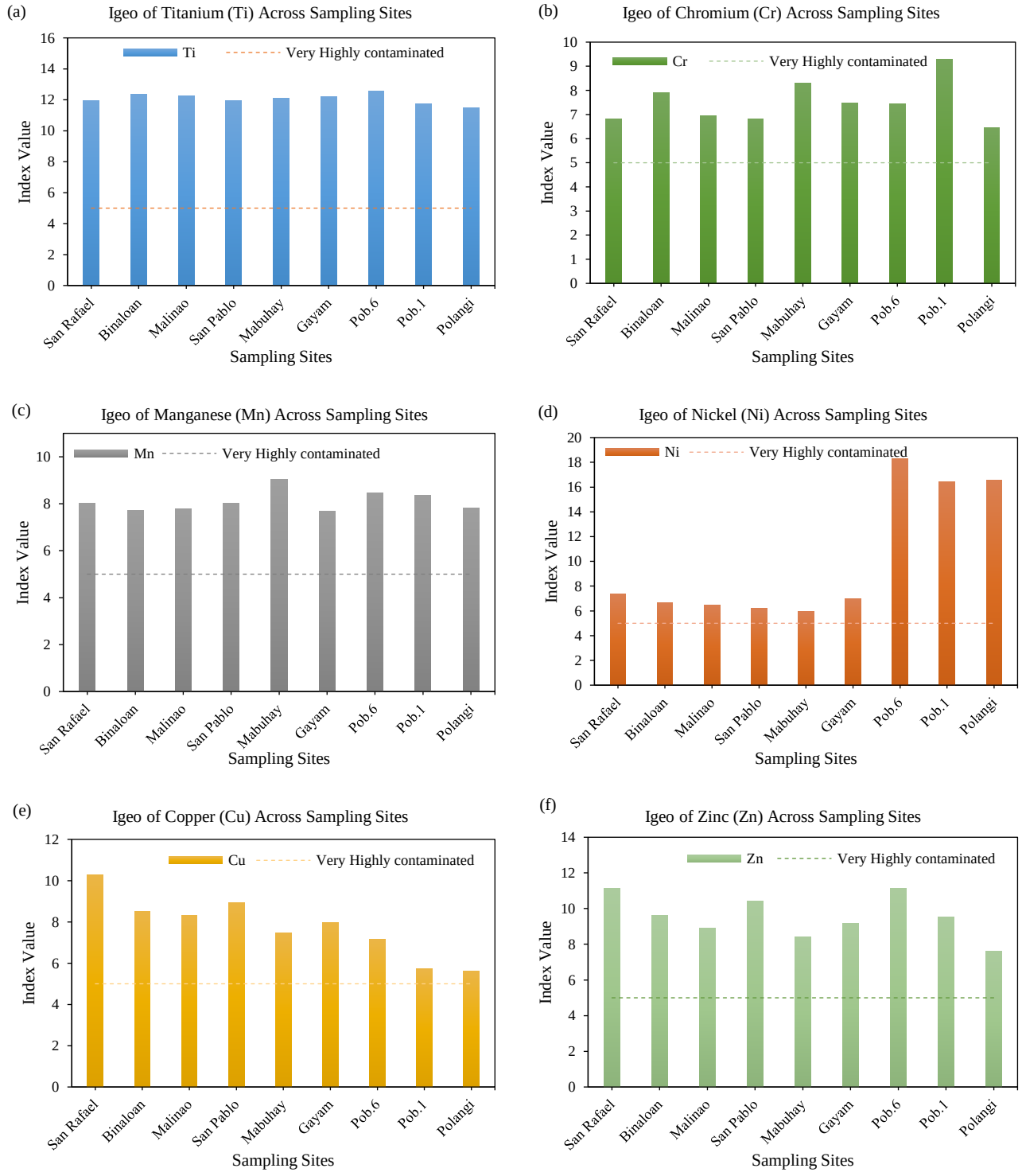

Figure 5. Geo-accumulation of (a) Ti, (b) Cr, (c) Mn, (d) Ni, (e) Cu, (f) Zn, (g) As, (h) Mo, (i) Cd, (j) Pb, in river bank sediments

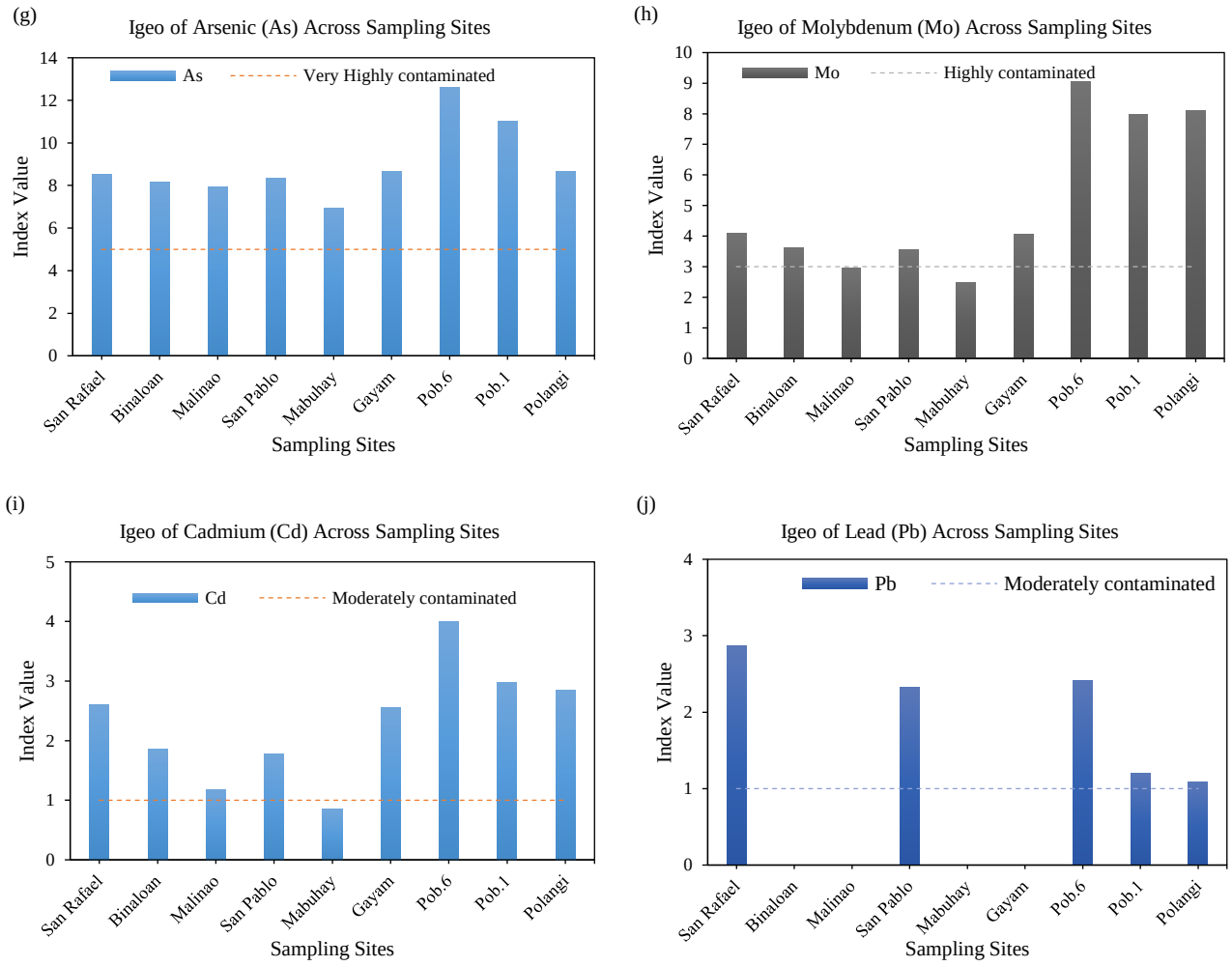

Figure 5. Geo-accumulation of (a) Ti, (b) Cr, (c) Mn, (d) Ni, (e) Cu, (f) Zn, (g) As, (h) Mo, (i) Cd, (j) Pb, in river bank sediments (cont.)

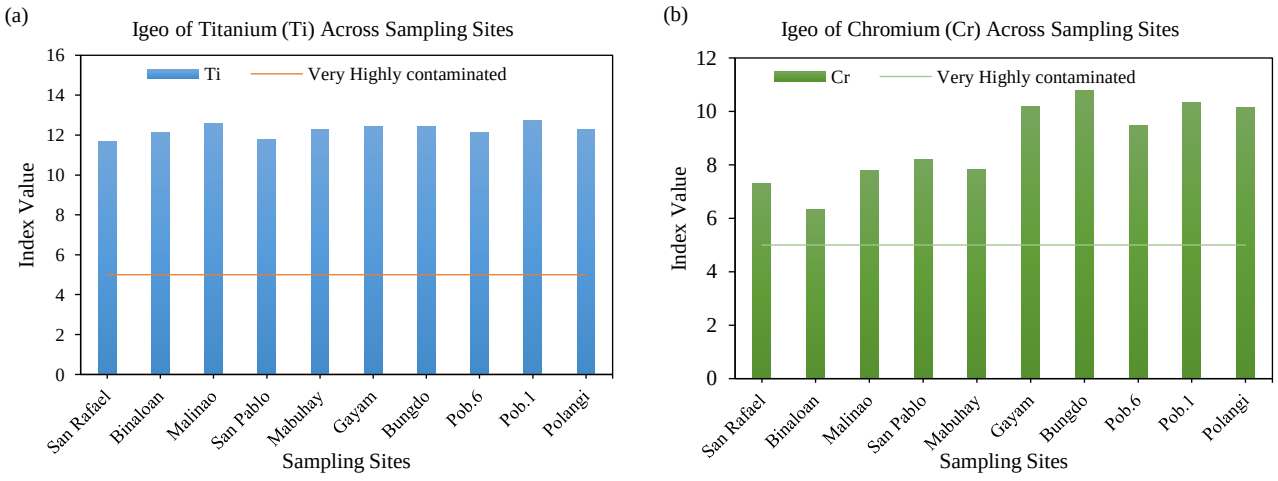

Figure 6. Geo-accumulation of (a) Ti, (b) Cr, (c) Mn, (d) Ni, (e) Cu, (f) Zn, (g) As, (h) Mo, (i) Cd, (j) Pb, in river bottom sediments

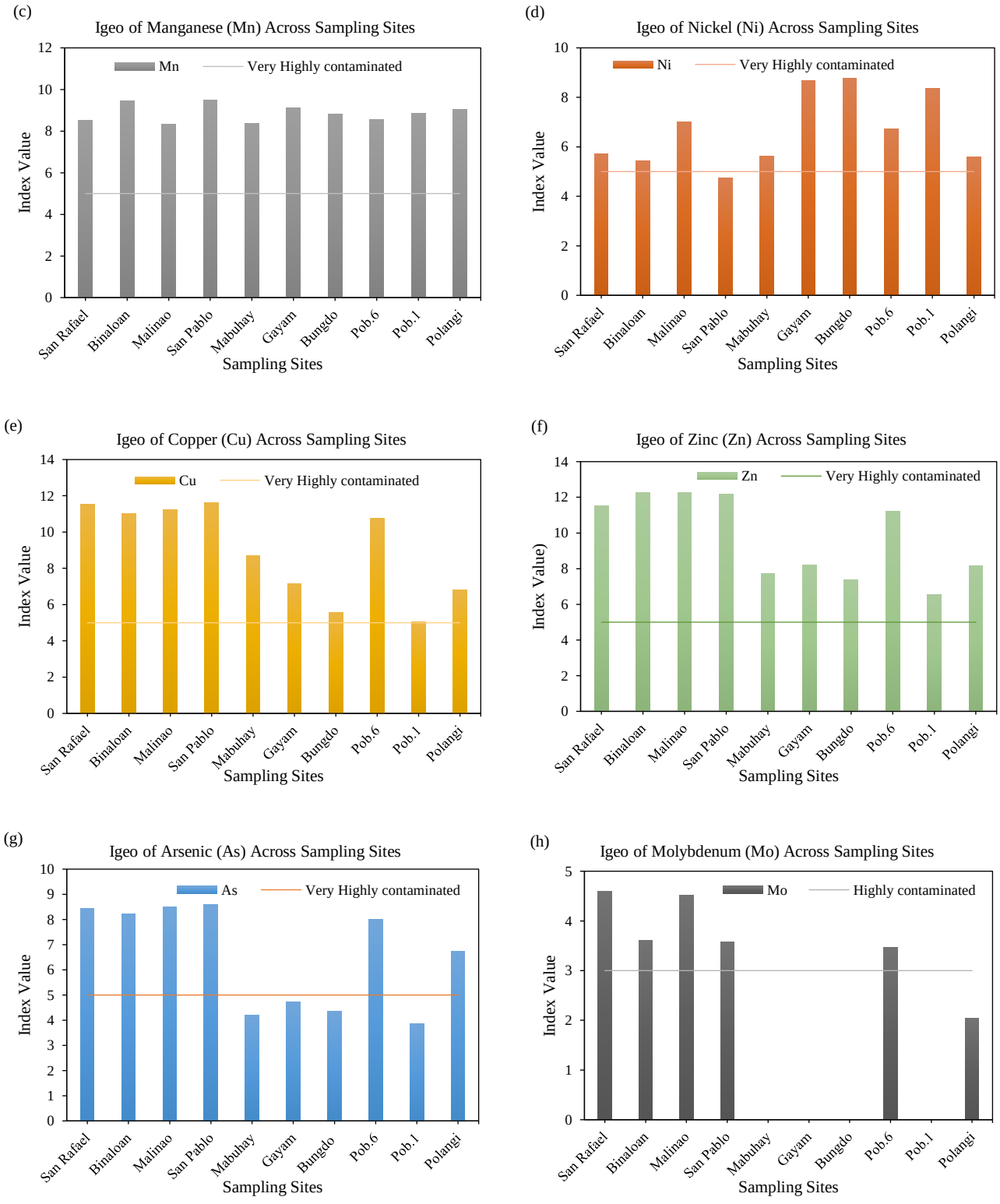

Figure 6. Geo-accumulation of (a) Ti, (b) Cr, (c) Mn, (d) Ni, (e) Cu, (f) Zn, (g) As, (h) Mo, (i) Cd, (j) Pb, in river bottom sediments (cont.)

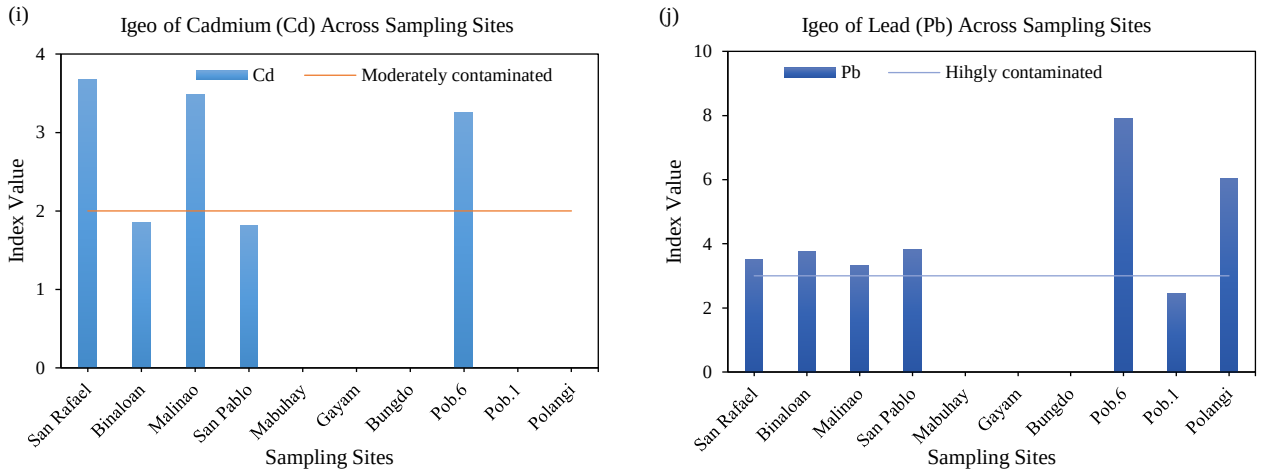

Figure 6. Geo-accumulation of (a) Ti, (b) Cr, (c) Mn, (d) Ni, (e) Cu, (f) Zn, (g) As, (h) Mo, (i) Cd, (j) Pb, in river bottom sediments (cont.)

The Pollution Load Index (PLI), used to assess the degree of heavy metal contamination in sediments, varied across all the riverbank and river bottom sediments studied in the Taft River Basin (Figures 7(a) and 7(b); Figures 8(a) and 8(b)). According to standard classification, PLI values below 1 (PLI<1) indicate no pollution; values between 1-1.5 suggest high contamination with potential for rehabilitation and safe reuse; and values greater than 1.5 (PLI>1.5) indicate that the sediment is unsuitable for crop production due to heavy contamination. In this study, all sediment samples recorded PLI values greater than 1, with riverbank sediments ranging from 1.43 to 1.65, and river bottom sediments from 1.50 to 1.71. These values reflect a general trend of gradual degradation of sediment quality and confirm that the Taft River Basin is heavily contaminated with heavy metals.

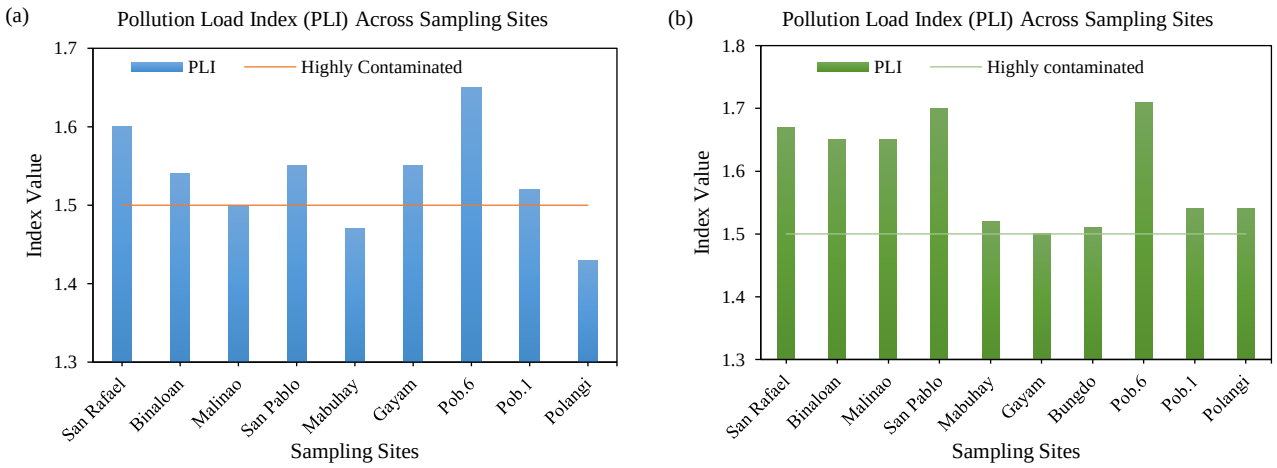

Figure 7. Contamination and Pollution of heavy metals in river bank sediments (a) and river bottom sediments (b)

4. DISCUSSION

4.1 Heavy metal concentrations in river sediments

Heavy metals are present in the sediments of river systems due to their capacity to act as carriers, sources, and sinks of pollutants (Zhu et al., 2018). Because river sediments serve as effective environmental indicators for monitoring pollution levels in aquatic ecosystems (Sun et al., 2018), this study assessed the concentrations of Ti, Cr, Cu, Zn, Mn, Ni, As, Mo, Cd, and Pb in the Taft River Basin, particularly in areas influenced by the post-operational impacts of the Bagacay mining site. The results showed that most heavy metal concentrations in both riverbank and river bottom sediments exceeded their respective critical or permissible limits, with the exception of Mn, Mo, and Cd (Figures 3 and 4). These concentrations were found to vary across different locations, reflecting the evident spatial distribution of heavy metals at the surface of the sediments.

(a)

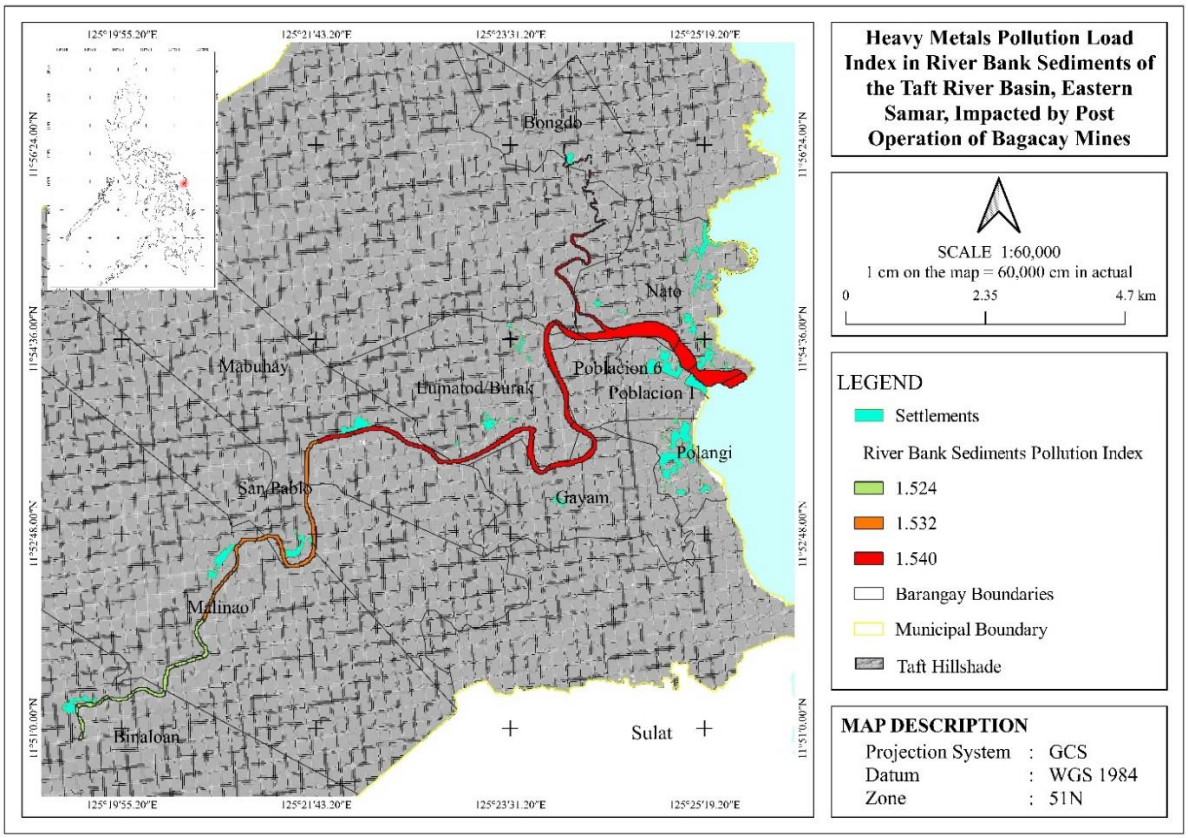

(b)

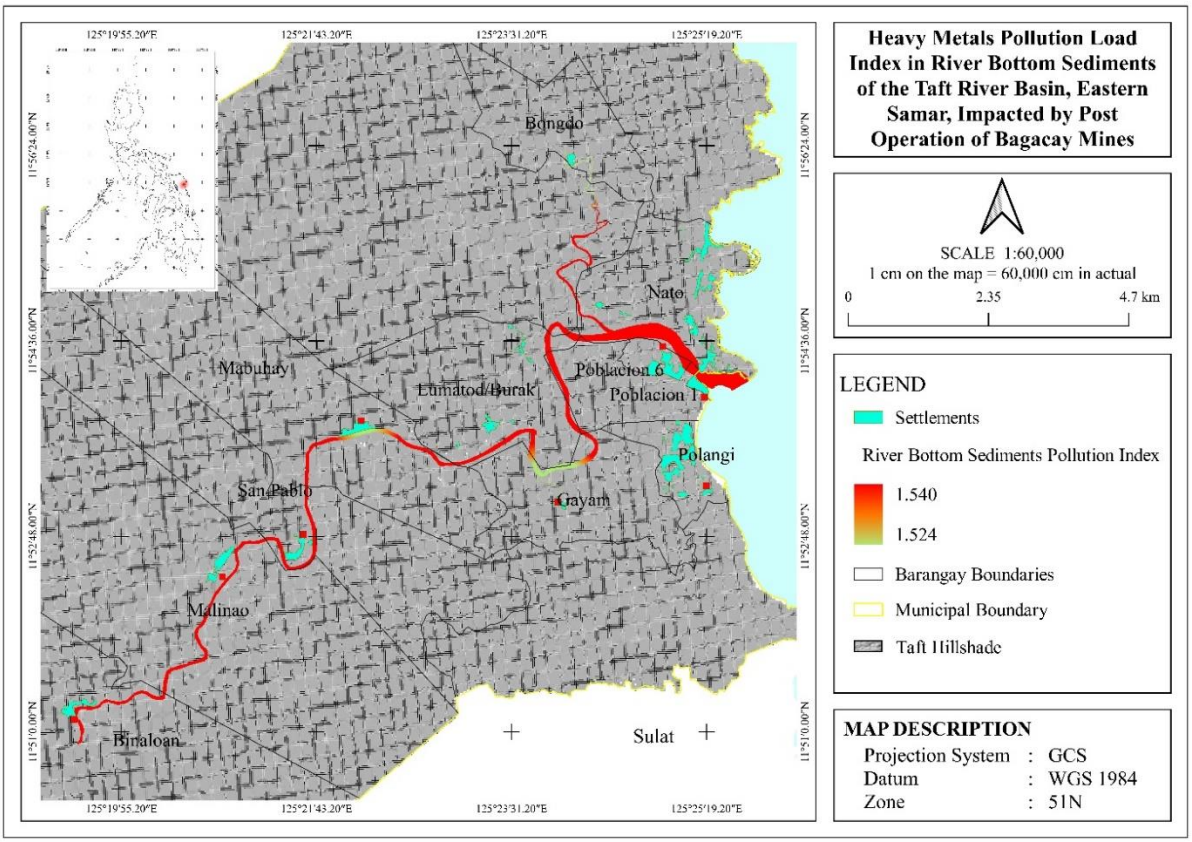

Figure 8. Pollution index map of river bank (a) and bottom sediments (b)

The varying concentrations of heavy metals in sediments are likely influenced by several dynamic processes within the river system. This is consistent with the findings of Weber and Opp (2020), who highlighted that the distribution of heavy metals in rivers and floodplains is affected by numerous environmental and anthropogenic factors. One of these processes is flooding, which contributes significantly to the transfer and redistribution of waste materials from upper to lower stream sections, thereby increasing the concentration of contaminants downstream (Sabijon et al., 2024). In this study, elevated levels of Ti, Cr, Cu, Zn, Ni, As, and Pb were observed across all sampled sediments within the Taft River Basin.

Supporting these observations, Dayang (2017) also reported excessive levels of heavy metal contamination including As, Cu, Pb, Hg, Zn, and Fe in both water and sediment samples from the Bagacay mine downstream to the Taft River. Similarly, Sabijon et al. (2024) documented that heavy metal concentrations in the surface soils of the Taft River floodplain followed a decreasing trend of Ti > Cr > Mn > Zn > Cu > Ni > As > Pb > Mo > Cd, which further confirms the sediment data presented in this study. Other regional and international studies provide similar evidence: Manullang et al. (2017) identified Fe, Cu, Zn, Pb, Cd, and Hg contamination in the surface sediments of Ambon Bay; Decena et al. (2018) observed Fe, Mn, Zn, Cu, Cr, and Ni in the Mangonbangon River; and Gabrielyan et al. (2018) reported high concentrations of As, Cu, Mo, Sb, Co, Ni, and Zn in the Voghji River Basin. Likewise, the Fenhe River sediments have shown variable heavy metal concentrations, including cadmium (0.040-0.296 mg/kg), lead (20.30-39.60 mg/kg), chromium (50.00-177.70 mg/kg), nickel (20.70-49.60 mg/kg), mercury (0.053-0.101 mg/kg), arsenic (5.76-10.10 mg/kg), copper (16.90-56.80 mg/kg), and zinc (72.30-233.60 mg/kg), further substantiating the widespread occurrence and environmental relevance of heavy metal pollution in riverine sediments (Chen et al., 2020).

4.2 Contamination and pollution of heavy metals in river sediments

The contamination of river sediments by heavy metals has garnered increasing attention in the context of water quality and ecological research (Edokpayi et al., 2022). In this study, moderate to high contamination of Ti, Cr, Mn, Ni, Cu, Zn, As, Mo, Cd, and Pb in the sediments of the Taft River basin was observed (Salomons and Forstner, 1984). These levels significantly exceeded the critical limits for heavy metals (Figures 3 and 4) across all sampling sites. River bank sediments exhibited high contamination levels for Pb, As, Zn, Mo, Mn, and Cu, while moderate contamination was found for Ni, Cr, Ti, and Cd (Figures 5-8). In river bottom sediments, the contamination followed a similar trend, with high contamination of Cu, Pb, Zn, As, Mn, Cr, and Ni, while Mo, Ti, and Cd showed moderate contamination (Figures 5-8). The contamination sequence for river bank and bottom sediments was as follows: Pb > As > Zn > Mo > Mn > Cu > Ni > Cr > Ti > Cd, and Cu > Pb > Zn > As > Mn > Cr > Ni > Mo > Ti > Cd, respectively.

The calculated pollution load index (PLI) values (Figures 7(a) and 7(b); Figures 8(a) and 8(b)) suggested a progressive deterioration of river sediments, with PLI>1 indicating moderate to severe contamination (Shen et al., 2019). These results confirmed that all the sediments in the riverbanks and bottoms of the Taft River Basin are polluted with heavy metals. Notably, higher pollution levels were observed in the upper (1.55, 1.67) and lower (1.53, 1.60) stream sites, with the highest pollution observed in the river bottom sediments at Poblacion 6 (lower stream), reaching a PLI of 1.71. The highest pollution values were predominantly observed in the upper stream, which is geographically closer to the Bagacay mining site, corroborating findings by Sabijon et al. (2024). The greater contamination observed in the upper stream may be attributed to the proximity of the Bagacay Mines, with contaminants being carried downstream by hydrological processes. The observed reduction in heavy metal levels downstream could be explained by the dilution effect of unpolluted water inflow as contaminants spread over greater distances (Luo et al., 2020).

Heavy metals are known to be poorly soluble in water (Zahra et al., 2014), with a significant portion being adsorbed onto particulates that eventually accumulate as bottom sediments (Zheng et al., 2008). This explains why heavy metal contamination is especially evident in the bottom sediments, as these sediments have a remarkable ability to accumulate low levels of contaminants over time (Islam et al., 2018). Additionally, disturbed sediments are more likely to be transported along hydrological gradients, spreading contamination to a wider area (Zhang et al., 2019).

Another important consideration for the potential influence to the increase in heavy metal contamination is the study areas natural geology. The

Taft River Basin is known to have certain mineral-rich geological formations, such as titanium-bearing rocks, which could naturally result in higher concentrations of elements like Ti, even without anthropogenic contamination. Heavy metals such as Ti, a common component of rocks and sediments, are naturally occurring and may not necessarily indicate pollution (Zhu et al., 2018).

Beyond the Bagacay Mines, potential sources of contamination could include agricultural runoff, industrial discharges, or other local anthropogenic activities in the region. Such sources may have contributed to the elevated levels of heavy metals in the river sediments, particularly in areas where industrial and agricultural practices are prevalent. Several other studies have also highlighted the contamination of sediments in river systems, confirming similar findings. For example, Sabijon et al. (2024) observed moderate to high contamination in Cu, Cr, Pb, As, Zn, Ni, Ti, Mo, and Cd in the sediments of the Taft River Basin. Similarly, Basir et al. (2022) reported heavy metal contamination (Hg < Zn < Pb < As) in the Mahakam river sediments of Indonesia, and Arifin et al. (2015) found that artisanal and small-scale gold mining (ASGM) activities in Indonesia's Bone River and Wubudu River contaminated these rivers with mercury, arsenic, and lead. Furthermore, research from China's Daniangkou Reservoir indicated high ecological risks due to surface sediment contamination with Cd and Cr (Lei et al., 2013). Other studies from large Chinese reservoirs, such as the Three Gorges Reservoir and the Liujiaxia and Xiaolangdi Reservoirs on the Yellow River, have reported heavy metal buildup and contamination in sediment profiles, including metals like Pb, Cd, Zn, and Cr (Zhao et al., 2015).

The evidence from this study revealed that the Taft River Basin is affected by heavy metal contamination, though a more comprehensive understanding of natural geological conditions and additional local pollution sources is necessary for a thorough assessment of the river's overall ecological health.

The comparative analysis in Table 2 underscores the global prevalence of heavy metal contamination in riverine sediments, positioning the Taft River within a broader environmental context of pollution linked to anthropogenic activities. Notably, the Taft River's contamination profile marked by the presence of ten potentially toxic elements (PTEs) reflects a complex and multifaceted pollution scenario. This mirrors patterns observed in similarly impacted rivers such as the Voghji River in Armenia and the Fenhe River in China, where intensive mining and industrial operations have been identified as primary contributors to elevated heavy metal concentrations.

Table 2. Comparison of potentially toxic elements in sediments from Taft River and other rivers

River/Location	Country	PTEs detected	Contamination level	Source/Notes
Taft River (Present Study)	Philippines	Ti, Cr, Mn, Ni, Cu, Zn, As, Mo, Cd, Pb	Moderate to High (PLI > 1)	Highest in upper and lower stream; linked to Bagacay Mines
Taft River (Sabijon et al., 2024)	Philippines	Cu, Cr, Pb, As, Zn, Ni, Ti, Mo, Cd	Moderate to High	Confirms multi-metal contamination in the same basin
Mangonbangon River (Decena et al., 2018)	Philippines	Pb, Cd, Cr, Zn	Moderate to High	Possible sources include domestic and urban runoff
Bone and Wubudu Rivers (Arifin et al., 2015)	Indonesia	Hg, As, Pb	High	Contamination from ASGM activities
Mahakam River (Basir et al., 2022)	Indonesia	Hg, Zn, Pb, As	Moderate to High	Prioritization sequence: Hg < Zn < Pb < As
Daniangkou Reservoir (Lei et al., 2013)	China	Cd, Cr	High	High ecological risk due to sediment contamination
Three Gorges Reservoir (Zhao et al., 2015)	China	Pb, Cd, Zn, Cr	Moderate to High	Heavy metal buildup observed in sediment profiles
Liujiaxia and Xiaolangdi Reservoirs (Zhao et al., 2015)	China	Pb, Cd, Zn, Cr	Moderate to High	Found along Yellow River; evidence of sediment pollution
Fenhe River (Chen et al., 2020)	China	Cu, Pb, Zn, Cd, Cr	High	Related to industrial wastewater and coal mining
Voghji River Basin (Gabrielyan et al., 2018)	Armenia	As, Cd, Cr, Cu, Ni, Pb, Zn	High	Contamination linked to mining in the Zangezur Copper Mine

Among Philippine rivers, the Taft River demonstrates broader contamination than the Mangonbangon River, which shows fewer PTEs but still registers high levels of Pb, Cd, Cr, and Zn. This could be attributed to the stronger industrial influence and proximity to the Bagacay mining site in the Taft River area. On the other hand, urban runoff appears to be the primary contamination source in the Mangonbangon River, indicative of different anthropogenic pressures.

Compared to international sites, the Taft River's PLI (Figures 7(a) to 8(b)) values suggest similar or slightly lower contamination severity than those of the Bone and Wubudu Rivers in Indonesia and the Voghji River in Armenia. These rivers are heavily affected by mining operations (ASGM and large-scale copper mining, respectively), which are known for introducing persistent and toxic metals into aquatic ecosystems.

Chinese rivers and reservoirs, such as the Three Gorges, Daniangkou, and Fenhe Rivers, also exhibit similar heavy metal profiles, although the Fenhe River shows extreme contamination due to both industrial effluents and coal mining. These comparisons underscore the critical role that mining and industrial activities play in shaping sediment contamination profiles and offer insight into how Philippine rivers like the Taft could follow similar contamination trajectories without appropriate environmental controls.

Overall, this comparison underscores the urgent need for national strategies in river monitoring, mining waste management, and pollution remediation. The Taft River's contamination profile, while alarming, is not unique but rather it is part of a global trend that demands integrated and science-based responses.

5. CONCLUSION

This study reveals that sediments in the Taft River Basin are moderately to highly contaminate with potentially toxic elements (PTEs), including Ti, Cr, Mn, Ni, Cu, Zn, As, Mo, Cd, and Pb. The contamination factors (CF) and geo-accumulation index (Igeo) values indicate significant pollution, with Igeo values ranging from class 2 to class 6. The contamination order: Pb>As>Zn>Mo>Mn>Cu>Ni> Cr>Ti>Cd in riverbank sediments and Cu>Pb>Zn>As >Mn>Cr>Ni>Mo>Ti>Cd in bottom sediments highlights a consistent presence of heavy metal inputs.

Pollution Load Index (PLI) values across all sites exceeded the critical threshold (PLI>1), confirming a deteriorated sediment quality. The highest contamination levels were found near the upper reaches of the river, particularly at sites closest to the Bagacay mining area, underscoring mining as a primary contributor. Downstream attenuation of PTE concentrations appears influenced by dilution and sedimentation dynamics.

Recommendations include the urgent need to rehabilitate the Bagacay mine site through acid mine drainage treatment, waste containment, and reforestation. Broader monitoring should also be implemented, encompassing groundwater and biotic components, to evaluate long-term ecological risks. Regular sediment quality assessments and the application of mining best practices must be institutionalized to mitigate further pollution. Finally, multi-stakeholder watershed management is critical to ensure the sustainable health of the Taft River and its surrounding communities.

ACKNOWLEDGEMENTS

This work is funded by Grant in Aid from Department of Science and Technology - Philippine Council for Agriculture, Aquatic and Natural Resources Research and Development (PCAARRD) and Northwest Samar State University.

AUTHOR CONTRIBUTIONS

Conceptualization, Sabijon, Jessie. and Ultra, Venecio.; Methodology, Sabijon, Jessie, Espejon, Eduardo and Bollido, Marcos.; Software, Tan, Zaldee Nino.; Writing-Original Draft Preparation, Sabijon, Jessie.; Writing-Review and Editing, Ultra, Venecio.

DECLARATION OF CONFLICT OF INTEREST

The authors have no competing interests to declare that are relevant to the content of this article.

REFERENCES

Agency for Toxic Substances and Disease Registry (ATSDR). Toxicological Profile for Arsenic. Atlanta, GA: US Department of Health and Human Services, Public Health Service; 2007.

Arifin YI, Sakakibara M, Sera K. Impacts of artisanal and small-scale gold mining (ASGM) on environment and human health of Gorontalo Utara Regency, Gorontalo Province, Indonesia. Geosciences 2015;5(2):160-76.

Asio VB, Cabunos Jr CC, Chen ZS. Morphology, physiochemical characteristics, and fertility of soils from quaternary limestone in Leyte, Philippines. Soil Science 2006;171(8):648-61.

Belyaeva OA. Impact of mining enterprises of the city of Kapan on adjacent agroecosystems. Natural Science 2012; 2(19):26-30.

Basir, Kimijima S, Sakakibara M, Pateda SM, Sera K. Contamination level in geo-accumulation index of river

sediments at artisanal and small-scale gold mining area in Gorontalo Province, Indonesia. International Journal of Environmental Research and Public Health 2022; 19(10):Article No. 6094.

Cabahug M, Ultra V, Morallos S, Lanuza N, Espejon E, Tan ZN, et al. Heavy metal concentrations in Mollusks and Crustaceans harvested from Eastern Samar's Taft River in the Philippine and the health risks posed to consumers. Philippine Journal of Science 2023;152(4):1349-62.

Cayanan EA, Estudillo CE. Characterization of the Climate of the Philippines based on the Latest 30-Year Normal (1981-2010) Data. Philippine Atmospheric, Geophysical, and Astronomical Services Administration (PAGASA); 2018.

Chen J, Lu J, Zhang Z, Zhao R. Assessment of heavy metal pollution and human health risk in urban river sediments: A case study of Fenhe River, China. Environmental Science and Pollution Research International 2020;27(26):26949-63.

da Silva Y, Cantalice J, do Nascimento C, Singh V, da Silva Y, Silva C, et al. Bedload as an indicator of heavy metal contamination in a Brazilian anthropized watershed. Catena 2017;153:106-13.

Dayang JR. Revegetating Bagacay Mining Site: A review of potential tropical species for phytoremediation of non-essential heavy metals. Journal of Degraded and Mining Lands Management 2017;4(3):807-14.

Decena C, Sanita M, Liporada R. Assessing heavy metal contamination in surface sediments in an urban river in the Philippines. Polish Journal of Environmental Studies 2018;27(5):1983-95.

Duncan AE, de Vries N, Nyarko KB. Assessment of heavy metal pollution in the sediments of the River Pra and its tributaries. Water, Air, and Soil Pollution 2018;229(1):Article No. 272.

Edokpayi J, Nkhumeleni M, Enitan-Folami A, Olaniyi F. Water quality assessment and potential ecological risk of trace metals in sediments of some selected rivers in Vhembe District, South Africa. Physics and Chemistry of the Earth, Parts A/B/C 2022;126:Article No. 103111.

United States Environmental Protection Agency (US EPA). Method 3050B: Acid Digestion of Sediments, Sludges, and Soils. Report No:SW-846. Washington (DC): US EPA; 1996.

Eze PN, Zhang Y, Wang L. Using geostatistics and GIS techniques to assess heavy metal contamination in soils around a coal mine area in South Africa. Environmental Earth Science 2018;77(6):Article No. 230.

World Health Organization (WHO). Environmental Health Criteria 24-Titanium. International Programme on Chemical Safety; 1982.

Feng W, Tao Y, Liu M, Deng Y, Yang F, Liao H, et al. Distribution and risk assessment of nutrients and heavy metals from sediments in the world-class water transfer projects. Environmental Sciences Europe 2024;36(1):Article No. 140.

Gabrielyan A, Shahnazaryan G, Minasyan S. Distribution and identification of sources of heavy metals in the Voghji River basin impacted by mining activities (Armenia). Journal of Chemistry 2018;1:Article No. 7172426.

Islam MS, Ahmed MK, Habibullah-Al-Mamun M, Islam KN, Ibrahim M, Masunaga S. Arsenic and lead in foods: A potential threat to human health in Bangladesh. Food Additives and Contaminants: Part A 2014;31(12):1982-92.

Kabata-Pendias A. Trace Elements in Soils and Plants. 2nd ed. CRC Press; 2001.

Kang M, Tian Y, Zhang H, Lan Q. Distribution, ecological risk assessment, and source identification of heavy metals in river sediments from Hai River and its tributaries, Tianjin, China. Water, Air, and Soil Pollution 2020;231:Arcticle No. 38.

Lei P, Zhang H, Shan BQ. Analysis of heavy metals pollution and ecological risk assessment in the sediments from the representative river mouths and tributaries of the Danjiangkou Reservoir. Resources and Environment in the Yangtze Basin 2013;22(1):110-7.

Luo C, Routh J, Dario M, Sarkar S, Wei L, Luo D, et al. Distribution and mobilization of heavy metals at an acid mine drainage affected region in South China, a post-remediation study. Science of the Total Environment 2020;724: Article No. 138122.

Manullang CY, Lestari TY, Arifin Z. Assessment of Fe, Cu, Zn, Pb, Cd, and Hg in Ambon Bay surface sediments. Marine Research in Indonesia 2017;42(2):77-86.

Mineral Resources and Geosciences Bureau (MGB). Environmental Impact Assessment of Mining Operations in the Philippines. Manila: Department of Environment and Natural Resources; 2005.

Müller G. Heavy metals in the sediments of the Rhine - changes since 1979. Review in Science and Technology 1981; 81(24):778-83.

Sabijon J, Ultra Jr V, Bollido M, Openiano M, Poliquit D, Aquino R, et al. Nutrients and heavy metal contents on surface of agricultural soils in the flood-plains of Taft River Basin impacted by Bagacay Mines, Philippines. Philippine Journal of Science 2024;153(1):375-90.

Salomons W, Forstner U. Metals in the Hydrocycle. Berlin, Heidelberg, New York: Springer-Verlag; 1984. p. 349.

Samaniego JO, Gibaga CR, Tanciongco AM, Quierrez RN. Abandoned and inactive mines in the Philippines: Current environmental conditions, ongoing rehabilitation efforts and future opportunities. In: Derelict Mines. CRC Press; 2024. p. 189-207.

Shen F, Mao L, Sun R, Du J, Tan Z, Ding M. Contamination evaluation and source identification of heavy metals in the sediments from the Lishui River Watershed, Southern China. International Journal of Environmental Research and Public Health 2019;16(3):Article No. 336.

Sun Z, Xie X, Wang P, Hu Y, Cheng H. Heavy metal pollution caused by small-scale metal ore mining activities: A case study from a polymetallic mine in South China. Science of the Total Environment 2018;639:217-27.

Tomlinson D, Wilson J, Harris C, Jeffrey D. Problems in the assessment of heavy-metal levels in estuaries and the formation of a pollution index. Helgoländer Meeresuntersuchungen 1980;33:566-75.

Tupan C, Herawati EY, Arfiati D. Detection of phytochelatin and glutathione in seagrass *Thalassia hemprichii* as a detoxification mechanism due to lead heavy metal exposure. Aquatic Science and Technology 2014;2(1):67-78.

Ultra Jr VU. Fly ash and compost amendments and Mycorrhizal inoculation enhanced the survival and growth of *Delonix regia* in Cu-Ni mine tailings. Philippine Journal of Science 2020;149(3):479-89.

Vodyanitskii YN. Standards for the contents of heavy metals in soils of some states. Annals of Agrarian Science 2016; 14(3):257-63.

Wang J, Liu R, Zhang P, Yu W, Shen Z, Feng C. Spatial variation, environmental assessment and source identification of heavy metals in sediments of the Yangtze River Estuary. Marine Pollution Bulletin 2014;87(1-2):364-73.

Weber CJ, Opp C. Spatial patterns of mesoplastics and coarse microplastics in floodplain soils as resulting from land use and fluvial processes. Environmental Pollution 2020;267:Article No. 115390.

Yang Y, Chen F, Zhang L, Liu J, Wu S, Kang M. Comprehensive assessment of heavy metal contamination in sediment of the Pearl River Estuary and adjacent shelf. Marine Pollution Bulletin 2012;64(9):1947-55.

Zahra A, Hashmi MZ, Malik RN, Ahmed Z. Enrichment and geo-accumulation of heavy metals and risk assessment of sediments of the Kurang Nallah-feeding tributary of the Rawal Lake Reservoir, Pakistan. Science of the Total Environment 2014;470:925-33.

Zhang M, He P, Qiao G, Huang J, Yuan X, Li Q. Heavy metal contamination assessment of surface sediments of the Subei Shoal, China: Spatial distribution, source apportionment and ecological risk. Chemosphere 2019;223:211-22.

Zhang C, Selinus O, Sjövall K. Geostatistical interpolation of heavy metals in soils using the OK and IDW methods in a coal mining area. Environmental Monitoring Assessment 2011;176(1-4):361-77.

Zhao D, Wan S, Yu Z, Huang J. Distribution, enrichment and sources of heavy metals in surface sediments of Hainan Island rivers, China. Environmental Earth Sciences 2015;74: 5097-110.

Zheng NA, Wang Q, Liang Z, Zheng D. Characterization of heavy metal concentrations in the sediments of three freshwater rivers in Huludao City, Northeast China. Environmental Pollution 2008;154(1):135-42.

Zhou F, Li P, Xing XL, Weng MZ, Liu L, Zhang Y, et al. Distribution characteristics and ecological risk assessment of heavy metals in sediments of Longyang Lake and Moshui Lake in Wuhan. China Environmental Science 2023;43: 5433-43.

Zhu D, Wu S, Han J, Wang L, Qi M. Evaluation of nutrients and heavy metals in the sediments of the Heer River, Shenzhen, China. Environmental Monitoring and Assessment 2018;190(7):Article No. 380.

Environment and Natural Resources Journal

Volume 23
Issue 5
2025

Strategy of Implementing Incinerator for Port Solid Waste Management: Case Study of Tanjung Luar Fishing Port, Indonesia

Mustaruddin[1*], Iin Solihin[1], Gondo Puspito[1], Syifa Nurul Aini[2], Eko Sri Wiyono[1], and Fis Purwangka[1]

[1]Department of Fishery Resources Utilization, Faculty of Fisheries and Marine Sciences, IPB University, Bogor, Indonesia
[2]Department of Resource and Environmental Economics, Faculty of Economics and Management, IPB University, Bogor, Indonesia

ARTICLE INFO

Received: 15 Jan 2025
Received in revised: 20 May 2025
Accepted: 26 May 2025
Published online: 16 Jul 2025
DOI: 10.32526/ennrj/23/20250020

Keywords:
Environment/ Fishing/ Fishing boat/ Fishing port/ Port industry/ Solid waste

*** Corresponding author:**
E-mail:
mustaruddin@apps.ipb.ac.id;
mus_m03@yahoo.com

ABSTRACT

The study aimed to (a) analyze fisheries' activities and the suitability of incinerators for port solid waste management, (b) formulate priority strategies for implementing incinerator technology in Tanjung Luar Fishing Port. The methods used were descriptive analysis, score methods, and Analytic Hierarchy Process (AHP) methods. The developing fishery activities analyzed in Tanjung Luar were fishing boat activities, fish marketing, port industries and fish processing, sea supply kiosk, provision of sea fuels, provision of ice for fish, food stalls, and other fishery services. The suitability of incinerators for port solid waste management was relatively high, which was indicated by the fulfillment of 'good compliance' criteria (3.20 on a scale of 1-4) and 'very good beyond compliance' criteria (3.52 on a scale of 1-4). Developing an environmental control system in incinerator operations (CONT) was priority strategy I of implementing incineration into solid waste management in fishing ports (IR=0.245, inconsistency 0.05). The supporting strategy was the recruitment of skilled incinerator managers from the community (MANG) (IR=0.232, inconsistency 0.05). The implementation of incinerators is believed to be able to save the management cost of port solid waste reaching 26,584.62 USD per year, prevent waste hazards to fish caught, fisheries actors, visitors, and the community around the port (9,768 people), and improve the performance of fishery activities in the port (8 activities). In the future, it is hoped that research will be conducted on the development of energy sources for fishing ports that utilize combustion heat in incinerators.

HIGHLIGHTS

This study highlights fishery activities in a fishing port and the potential for solid waste produced. Furthermore, it analyses the suitability of incinerators if applied to manage the port's solid waste. Finally, it formulates a priority strategy for implementing incinerator technology after it is declared suitable for the Fishing Port.

1. INTRODUCTION

Fishing ports are the centre of fisheries activities in many regions in Indonesia. This is because fishing ports are a place for unloading fish caught by fishing boats, a place where fish processing industries obtain raw fish, a place where fish marketing activities are carried out, and a place where supporting fisheries businesses develop. One of the fishing ports that plays this role is the Tanjung Luar Fishing Port (FP), East Lombok Regency. According to the Department of Marine Affairs and Fisheries (DMAF) of East Lombok Regency (2024), the Tanjung Luar FP was the main centre of fisheries activities in West Nusa Tenggara (WNT) Province, where fish production reached 4,382 tons/year or 58.66% of the total marine fish production in 2023 in East Lombok Regency. Meanwhile, East Lombok Regency mainly contributed to WNT's fisheries and marine products (Mustaruddin et al., 2022a; Firdaus et al., 2020).

However, these fishery activities also had a negative impact on the environment of the fishing port, namely producing various solid, liquid and gas waste. Solid waste was the type of waste that most

Citation: Mustaruddin, Solihin I, Puspito G, Aini SN, Wiyono ES, Purwangka F. Strategy of implementing incinerator for port solid waste management: Case study of Tanjung Luar Fishing Port, Indonesia. Environ. Nat. Resour. J. 2025;23(5):409-419. (https://doi.org/10.32526/ennrj/23/20250020)

produced by fishery activities at Tanjung Luar FP. According to the Department of Environment and Sanitation (DES) of East Lombok Regency (2024), almost all fishery activities at the Tanjung Luar FP produced solid waste. The activities of fishing vessels, fish marketing, and sea supply kiosks were the main contributors of solid waste, especially from net scraps, used containers and plastics, leftover supplies, fallen fish, and fish pieces (Shofa and Hadi, 2017; Subhan, 2018; Liu et al., 2022). Solid waste at the Tanjung Luar FP also comes from community activities around the port. Meanwhile, liquid and gas waste generally come from fisheries processing and transportation activities, but the amount is not as much as solid waste. The volume of daily solid waste at the Tanjung Luar FP tends to increase, and its condition is concerning because it has spread to the port ponds. In 2022, a cleaning activity for the port and coastal area involved fisheries stakeholders, village trustee army, and the community. In 2023, DES of East Lombok Regency carried out a marathon garbage sweeping activity in the coastal and port areas (DMAF of East Lombok Regency, 2024). However, these activities were limited to collecting and sorting waste, but no waste processing system in place. As a result, the solid waste/garbage that had been collected spread again and polluted the fishing port area.

One effort that can be made in aim to solve the solid waste problem is to apply incinerator technology. An incinerator is a solid waste processing technology that is operated at high temperatures. This temperature is produced by developing a closed combustion technique, where heat is optimised for burning and nothing is released into the environment (Ji et al., 2022; Yang et al., 2019). This incineration technique is considered suitable for solid waste from fishing ports, which are usually wet, contain lots of used sacks, pieces of containers, fish scraps/pieces, net scraps, fibres, and plastic packaging (Liu et al., 2022; Hendrawan, 2022). The organic and inorganic components in the waste are mixed, wet, with various sizes that are difficult to separate. This will complicate the application of other technologies, such as composting and bio-digesters. These two technologies only process organic waste from fish scraps and food waste, while used sacks, net scraps, fibre and plastic packaging cannot be processed (Subhan, 2018; Ozkaynak and Icemer, 2024; Vaio et al., 2019). Incinerator technology can process all types of solid waste. However, in order to be widely operated, waste processing technology must meet the proper criteria stated in Ministry of Environment and Forestry (MEF) of Indonesia (2021) and be well received by local fisheries stakeholders (McClanahan et al., 2024; Caramuta et al., 2021).

The study helps to ensure this, thus facilitating the implementation of incinerator technology in the Tanjung Luar FP area. The study aimed to (a) analyse fishery activities and the suitability of incinerators for solid waste management at the fishing port, and (b) formulate priority strategies of implementing incinerator technology for solid waste management in fishing ports.

2. METHODOLOGY

2.1 Study location

The location of the study was the Tanjung Luar FP Area, East Lombok Regency, WNT Province, Indonesia (Figure 1). The study was conducted in June-August 2024.

2.2 Data collection

The data collected consisted of fisheries activity data, dominant fish landed data, solid waste data, incinerator suitability data for solid waste management, and views regarding the application of incinerators for port solid waste management. Statistics collection methods included field exploration, questionnaire distribution, training, and focus group discussions (FGD). Field exploration was intended to collect information on fisheries activities and dominant fish landed at the Tanjung Luar FP. The distribution of questionnaires was designed to collect information on solid waste and the suitability of incinerators for their management. Training and FGD were intended to raise awareness of waste management while obtaining information/views regarding the application of incinerator technology for port solid waste management. Training and FGD were carried out by combining the concepts of the classroom and field method. This combination of methods was used to optimise the impact of awareness and the depth of information obtained from FGD participants.

Questionnaire respondents and FGD participants were selected purposively from fisheries stakeholders who are active in the Tanjung Luar FP Area. The selection criteria were active fisheries actors who have been active in the Tanjung Luar FP Area for at least two years. Specifically for questionnaire respondents, added with minimum education criteria of junior high school graduates (Ozkaynak and Icemer, 2024; Kamargo et al.,

2018). The questionnaire respondents amounted to 15 people consisting of 4 fishermen, 3 fish industry/ processors, 3 fish traders, 3 supporting service actors, and 2 port managers.

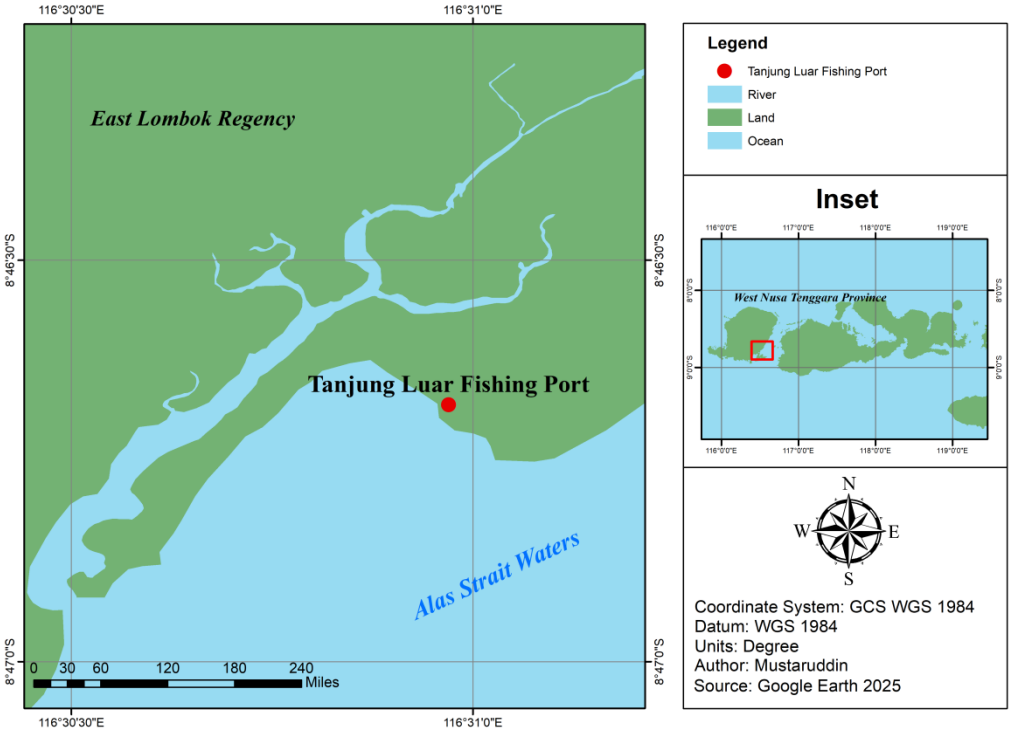

Figure 1. Map of the study area

2.3 Data analysis

Data analysis used descriptive analysis, score methods, and analytical hierarchy process (AHP) methods. Descriptive analysis was used to describe fisheries activities in the Tanjung Luar FP Area and the potential solid waste they generate. Score methods were used to evaluate the suitability of incinerators with proper criteria for port solid waste management. According to MEF of Indonesia (2021), there were two proper criteria, namely compliance criteria and beyond compliance criteria. Aspects assessed in the compliance criteria include water pollution control, air pollution control, toxic and hazardous waste management, and control of potential land damage. Beyond compliance criteria include energy efficiency efforts, implementation of reduce, reuse and recycle (R3), protection of biodiversity, and community development programs.

The AHP method was used to formulate priority strategies for the application of incinerator technology in the management of fishery port solid waste. According to Mustaruddin et al. (2011) and Caramuta et al. (2021), the AHP method is divided into four analysis hierarchies, namely goals, criteria, sub-criteria (optional), and alternative strategies. In this study, the goal was the strategy of implementing incinerator technology for solid waste management in fishing ports. The criteria used were compliance criteria and beyond compliance criteria. Sub-criteria were not developed because the substance of both criteria was complete and accommodated applicable regulations (MEF of Indonesia, 2021). Alternative strategies were further determined from the results of FGD and questionnaire distribution. Analysis of each hierarchy used a paired comparison test (Saaty, 1993). Furthermore, the results of the AHP analysis were tested for inconsistency and sensitivity. The results of the AHP analysis could be trusted if they have an inconsistency <0.1 and are not too sensitive (Mustaruddin et al., 2011).

3. RESULTS AND DISCUSSION

3.1 Fishery activities and solid waste potential at the Tanjung Luar Fishing Port

Fishery activities at the Tanjung Luar FP generally supported the production of fish docking at the port. These activities consisted of fishing boat activities, fish marketing, port industry and fish processing, provision of supplies for going to sea at supply kiosks, provision of fuel for going to sea,

provision of ice for fish, food stalls, and other fishery services. The dominant fish landed were squid, yellowtail, sardinella, pinkear emperor, selar, cob, mackerel tuna, and bullet tuna (Table 1). This fishing was generally carried out by small fishermen who operate outboard motorboats (DMAF of East Lombok Regency 2024). This type of boat is widely chosen because of more flexible in its operation. Larger boats are rare and are used for fishing in more distant waters, such as the waters of Sumbawa Island and the waters of East Nusa Tenggara.

Table 1. The dominant fish landed at Tanjung Luar Fishing Port

No	Fish species	Semester 1 in 2023 (kg)	Semester 2 in 2023 (kg)	Total (kg)	Potential waste of fishing
1	Squid (*Loligo chinensis*)	24,742	357,966	382,708	squid pieces (tentacles), fishing line pieces
2	Yellowtail (*Paracaesio kusakarii*)	164,943	5,230	170,173	bait scraps, fishing line pieces
3	Sardinella (*Sardinella albella*)	14,616	219,675	234,291	fallen fish, net scraps
4	Pinkear emperor (*Lethrinus amboinensis*)	312,809	39,646	352,455	fallen fish, net scraps, fishing line pieces
5	Selar (*Selar crumenophthalmus*)	5,315	161,865	167,180	fish pieces, net scraps
6	Cob (*Auxis thazard*)	14,074	164,994	179,068	fish pieces, scales and guts, net scraps, fishing line pieces
7	Mackerel tuna (*Euthynnus affinis*)	36,508	200,810	237,318	fish pieces, scales and guts, net scraps
8	Bullet tuna (*Auxis rochei*)	68,777	374,802	443,579	fish pieces, scales and guts, net scraps

Source: data processed from DMAF of East Lombok Regency (2024)

In semester 1 (January-June), the fish that were caught the most were yellowtail (*Paracaesio kusakarii*) and pinkear emperor (*Lethrinus amboinensis*). This is thought to be because in semester 1, the frequency of rain is higher (rainy season), so that the salinity of sea water is lower and many nutrient components from land enter the waters. Yellowtail and pinkear emperor are types of reef fish that like low salinity and inhabit sandy areas with lots of coral (Kamargo et al., 2018; Wahyudin et al., 2019). Nutrients carried by floods from land will settle at the bottom of the waters and accelerate the increase in the population of both types of fish. In semester 2 (July-December), squid production increased drastically, allegedly due to longer sunlight (dry season) in those months. Mustaruddin et al. (2022a) and Rosalina et al. (2011) argued that squid prefer shallow waters with dim lighting. In these conditions, squid will grow large and reproduce rapidly. This encourages increased fish production and increased fishing activities in the Tajung Luar FP, while increasing the amount of waste produced.

The solid waste generated by fishing activities was very diverse, including net scraps, fallen fish, used cardboard, used plastic, fish container waste, used sacks, used styrofoam, pieces of rope, and food waste (Table 2). The diversity of the waste was influenced by the scope of the business and the type of demand received by fishery business actors/stakeholders in the Tanjung Luar FP area. The results of distributing questionnaires and FGDs stated that the potential for solid waste tends to increase from year to year due to the increase in fish landing services and variations in needs in fishing, fish processing, and fish marketing. The waste was generally wet because it came from handling fresh fish, cooling fish, providing ice, and handling processed fish, especially salted fish. Fresh fish and salted fish are the main products produced in the Tanjung Luar FP area (Mustaruddin et al., 2022a; Firdaus et al., 2020).

Currently, solid waste at Tanjung Luar FP (Table 2) has not been handled optimally. The local authorities only handled around 37% of the waste, by taking it to the waste disposal site. The rest was just piled up, then scattered again until it enters the port pool. This continued to happen until it became news in many mass media (Subhan, 2018; DES of East Lombok Regency, 2024). Cleaning efforts were carried out, for example through cleaning activities for the port and coastal areas in 2022, and marathon sweeping of coastal and port waste in 2024 (DMAF of East Lombok Regency, 2024). However, these activities were not carried out routinely, so that solid waste to the port continued to spread and pollute the environment.

Table 2. Fishery activities and solid waste potential at Tanjung Luar Fishing Port

No	Fishery activities	Products/services	Potential solid waste
1	Fishing boat	fish caught	net scraps, fishing line pieces, used cardboard supplies, used plastic, fallen fish, pieces of fish, fish guts
2	Fish marketing	fish caught	fish tank waste, fallen fish, fish guts, pieces of rope
3	Port industry and fish processing	loading and unloading fish, processed fish	waste from fish landing, fish handling, fish containers, spice containers, fish pieces, fish scales and guts, leftover burning wood
4	Sea supply kiosk	fishing supplies	used cardboard, wooden crates, used sacks, leftover packages
5	Provision of fuel	fishing fuel	used jerry cans, pipe pieces and used hoses
6	Provision of ice for fish	Ice for fishing	leftover ice containers, used styrofoams
7	Food stalls	ready to eat food	used cardboard, used plastic, leaves, leftover food, leftover packages
8	Fishery services	fish handling and transportation	used cardboard, used spare parts, pieces of rigging

3.2 Suitability of incinerators for port solid waste management

An incinerator is a waste processing technology developed to overcome the problem of solid waste in the field, especially if the waste is wet and has various sources. The incinerator proposed in this study is a closed combustion type whose combustion heat can be increased to 800-1,200ºC. The incinerator components were initiated to be installed vertically. The goal is that it can be operated in fishing ports with narrow land and can be moved. The vertical installation is intended so that the incinerator does not take up much space for fisheries activities in the port. This is because the activity zone is already full at Tanjung Luar FP. The incinerator that was initiated has a capacity of 15-20 tons/day. This capacity is more than enough to handle solid waste from the fishing port and its surroundings which reaches 12-15 tons/day. However, the development of incinerators in fishing ports must meet the proper criteria required in MEF of Indonesia (2021). It is important so that the incinerator can be operated properly on site, its utilization level is optimal, and it is safe for the environment (Cheng et al., 2020; Thanassekos and Scheld, 2020; Hendrawan, 2022).

Figure 2 presents the distribution of incinerator suitability values for solid waste management in the Tanjung Luar FP area, and Figure 3 presents the level of fulfillment of the required compliance criteria and beyond compliance criteria. The values is scaled from 1 to 4, where values 1, 2, 3, and 4 mean bad, moderate, good, and very good respectively.

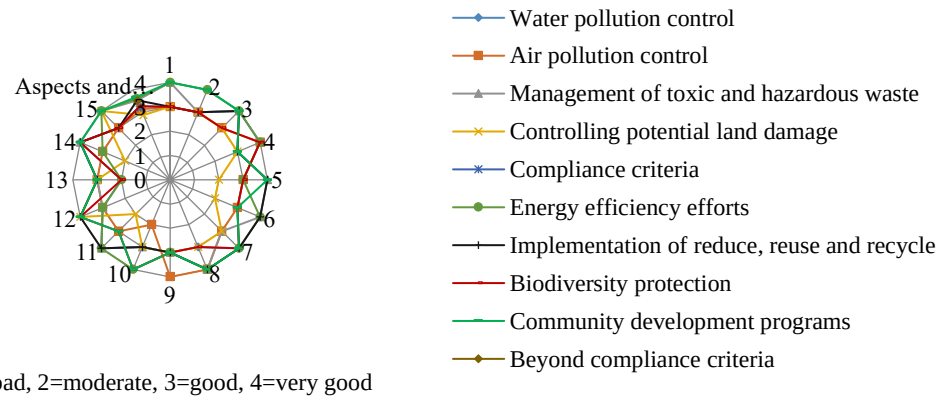

Figure 2. Distribution of incinerator suitability values for solid waste management in the Tanjung Luar Fishing Port Area.

Based on Figure 2, solid waste management with incinerators had received quite diverse responses from fisheries stakeholders, but no one gave a bad score. This shows that there was no social rejection of incinerators (Ji et al., 2022; Osmundsen, 2023). The incinerator technology also met the compliance criteria good (3.20 on a scale of 1-4) and the beyond compliance criteria very good (3.52 on a scale of 1-4) for application in fishing ports (Figure 3). This shows that incinerators could be widely applied for solid

waste management in the Tanjung Luar FP area. In the compliance criteria, the aspect that was met very good was water pollution control (3.53 on a scale of 1-4). In the beyond compliance criteria, the aspects that were met very good were energy efficiency efforts, implementation of reduce, reuse, and recycle (R3), and community development programs with values of 3.60; 3.53; and 3.67 on a scale of 1-4, respectively. The only aspect with a relatively low value was controlling potential land damage (2.87 on a scale of 1-4). In the implementation of R3, the reduction aspect could be optimised because the incinerator could reduce the volume of solid waste by up to 70% (Ji et al., 2022; Hendrawan, 2022). Ash from the burning of used cardboard, fallen fish, leftover food, used wooden crates, and fish pieces can be used as fertiliser (recycle) in greening at Tanjung Luar FP and its surroundings.

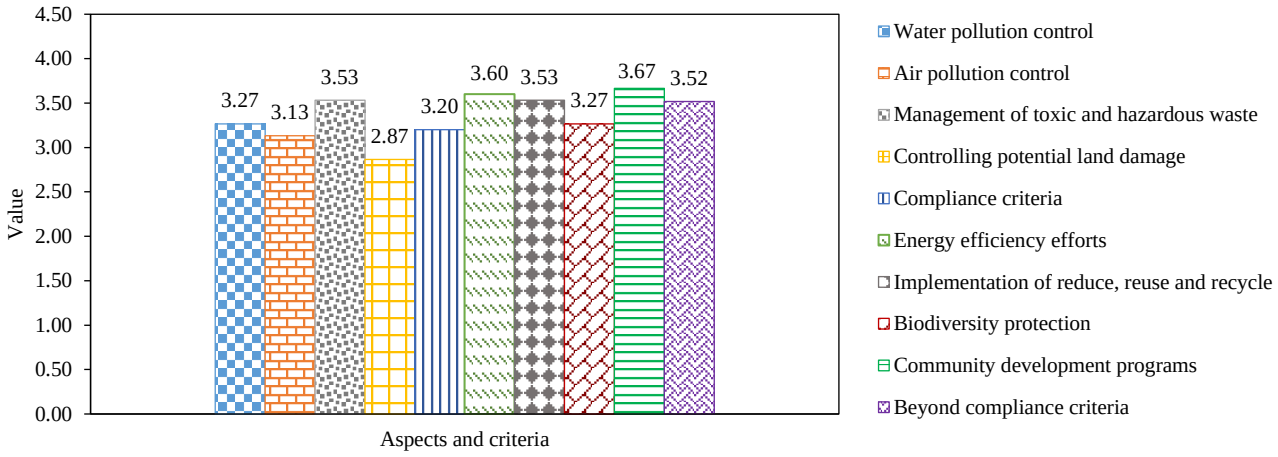

Figure 3. Compliance of incinerator technology with respect to compliance and beyond compliance criteria for application in fishing ports.

The highest value in the community development aspect was thought to be because the incinerator opens great opportunities for the involvement of fishermen, port industry and fish processing players, fish traders, and supporting service actors at the port, especially in sorting solid waste and operating the incinerator. Fisheries stakeholders can bring their waste/garbage, although not too dry, because the incinerator is designed to operate with high combustion heat (Yang et al., 2019; Ji et al., 2022). The operation of the incinerator is also relatively easy and is closed combustion, so the risk of accidents can be minimised (Shofa and Hadi, 2017; Cheng et al., 2020). The value in the aspect of controlling potential land damage (Figure 3) was not high but was quite good. This was because the application of the incinerator was only focused on the port area (not on a large area). However, fishery activities at the Tanjung Luar FP were very complex (Table 2) and occur every day (DMAF of East Lombok Regency, 2024), so the volume of waste remained high. Fishery activities at the Tanjung Luar FP were always busy because it was the main destination for fish landings from boats operating in the Alas Strait waters and many other waters in WPPRI-573 (Firdaus et al., 2020; Mustaruddin et al., 2022a).

3.3 Strategy of implementing incinerator technology for port solid waste management

The success of implementing incinerator technology in the Tanjung Luar FP Area was greatly influenced by the strategy chosen. Therefore, the alternative strategies offered in the study come from the aspirations and interests of fisheries stakeholders in the location. These alternative strategies were: (a) Recruitment of skilled incinerator managers from the community (MANG), (b) Development of appropriate incinerators collectively (COLL), (c) Cooperation in incinerator development with private companies (COOP), (d) Development of environmental control systems in incinerator operations (CONT), and (e) Development of tariff systems in incinerator operations (TARF). In addition, the continuity of the strategy application also depended on the level of fulfilment of the strategy against applicable standards/criteria that underlie its positive assessment (Caramuta et al., 2021; Mustaruddin et al., 2022a). In this study, the criteria referred to the applicable regulations on proper (MEF of Indonesia, 2021). The

hierarchical tree for determining priority strategies is presented in Figure 4. Furthermore, the results of the analysis related to the urgency of the criteria and the achievements of each alternative strategy in meeting these criteria are presented in Table 3.

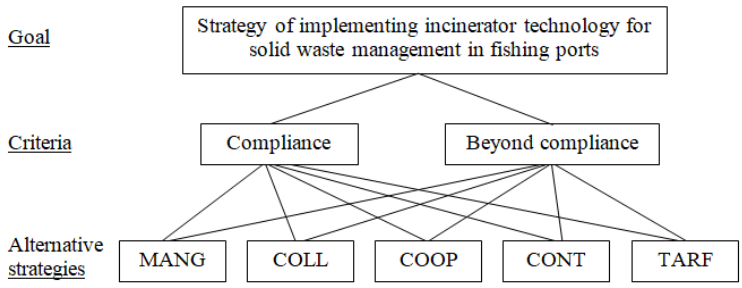

Figure 4. Hierarchy tree for determining the priority of strategy of implementing incinerator technology for solid waste management in fishing ports

Table 3. Results of the analysis of the urgency of proper criteria and the achievement of each alternative strategy in meeting these criteria

Proper criteria	Alternative strategy	IR	Achievements	Inconsistency
Compliance (IR: 0.333)	MANG	0.249	0.098	
Compliance (IR: 0.333)	COLL	0.181	0.071	
Compliance (IR: 0.333)	COOP	0.197	0.078	0.06
Compliance (IR: 0.333)	CONT	0.124	0.049	
Compliance (IR: 0.333)	TARF	0.249	0.098	
Beyond compliance (IR: 0.667)	MANG	0.222	0.134	
Beyond compliance (IR: 0.667)	COLL	0.143	0.087	
Beyond compliance (IR: 0.667)	COOP	0.191	0.116	0.04
Beyond compliance (IR: 0.667)	CONT	0.323	0.196	
Beyond compliance (IR: 0.667)	TARF	0.122	0.074	

Based on Table 3, the beyond compliance criteria were the most urgent proper criteria (IR=0.667) to be fulfilled in the implementation of incinerator technology in the Tanjung Luar FP Area. It was thought to be because the beyond compliance criteria were more accommodating to the dynamics and needs of the field, for example, related to energy efficiency and the existence of community development programs. According to Ewell et al. (2020) and Ross et al. (2024), the beyond compliance criteria pay attention to the best environmental management practices in the community and the dynamics of global environmental issues. The results of the analysis were also in line with the level of fulfilment of the incinerator in Figure 3, which prioritised the beyond compliance criteria. However, both proper criteria must still be fulfilled to support the legality and continuity of the implementation of incinerators for port solid waste management. The compliance criteria provide a portion of 33.3% (IR=0.333) for the legality of the application.

The strategy of recruiting skilled incinerator managers from the community (MANG) and the strategy of developing a tariff system in incinerator operations (TARF) met the compliance criteria good, namely with each achievement of 0.98 at a trusted inconsistency of 0.06. It is quite reasonable because skilled managers are believed to have a better understanding of applicable waste management regulations, while the tariff system is a manifestation of compliance with these regulations (Ewell et al., 2020; McClanahan et al., 2022). For the beyond compliance criteria, it was very good met by the strategy of developing an environmental control system in incinerator operations (CONT), namely with an achievement of 0.196 at a trusted inconsistency of 0.04. According to McClanahan et al. (2022), Azeez et al. (2022), and Subhan (2018), the development of an environmental control system has a major impact on protecting fish quality, public health, and the comfort of activities in the port area. The strategy of recruiting skilled incinerator managers from the

community (MANG) and the strategy of cooperation in incinerator development with private companies (COOP) also met the criteria good, with achievements of 0.134 and 0.116, respectively (inconsistency 0.04). Both strategies expanded community involvement through recruitment and cooperation programs.

By considering the urgency of each criterion and the achievement of each alternative strategy, the strategy of implementing incinerator technology for solid waste management in fishing ports could be formulated with a priority order, as presented in Figure 5.

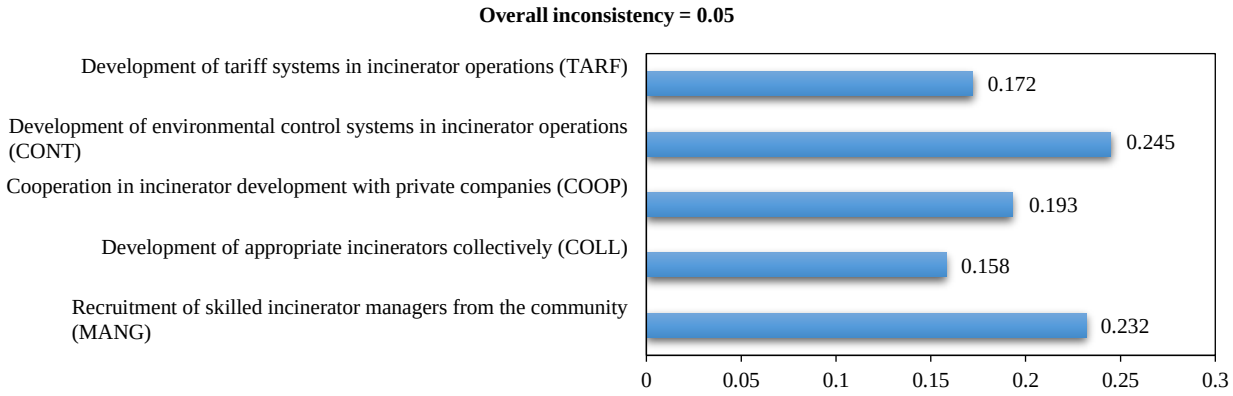

Figure 5. Analysis results of strategic priorities of implementing incinerator technology for port solid waste management

Based on Figure 5, the strategy for developing an environmental control system in incinerator operations (CONT) is a priority I (IR=0.245, inconsistency 0.05) if incinerator technology was applied in the Tanjung Luar FP area. According to Ji et al. (2022) and Liu et al. (2022), an environmental control system is very much needed in waste management because it directly controls the operations and outputs it produces. The environmental control system protects fishermen and the community from the impacts of neglected fisheries and port activities (Mustaruddin et al., 2022b; Cheng et al., 2020; Shofa and Hadi, 2017). The CONT strategy was also not too sensitive because it only changed when there was a decrease in the program's orientation towards the community (IR beyond compliance criteria <0.632), while the decrease/unclear regulations were relatively stable (Figure 6). According to Caramuta et al. (2021) and Firdaus et al. (2020), a strategy that was oriented towards community welfare needs to be prioritised because in addition to its high acceptance, it was also effective in its implementation in fishing ports.

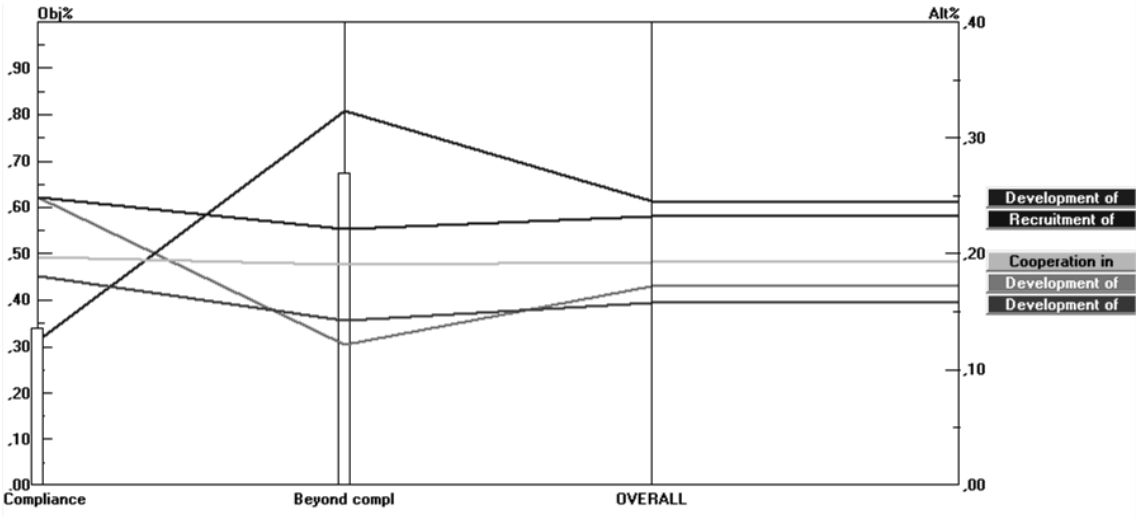

Figure 6. Results of the sensitivity analysis of the strategy for developing an environmental control system in incinerator operations (CONT) in fishing ports

The environmental control system developed in the CONT strategy can include pollution control mechanisms, emission threshold controls, and post-combustion ash cleaning. Pollution control is carried out using two mechanisms, namely: (1) turning on the incinerator when fishing port activities are quiet, and (b) planting trees in the port area and coastal areas around the port. For emissions, it can be controlled by installing an emission detection device on the incinerator. This device provides information on emission conditions when the incinerator is operated, and its operation can be suspended if emissions exceed the threshold (Ji et al., 2022; Hendrawan, 2022). Ash cleaning can be done periodically, for example, every 5-7 days. Furthermore, the ash can be used to fertilising trees that function as air pollution controllers, and the rest can be shared with the community (as organic fertiliser). This is very good because the existence of the incinerator provides additional benefits to the community. According to Caramuta et al. (2021) and Firdaus et al. (2020), strategies that have a real impact on the community need to be prioritised, because apart from being highly acceptable, their implementation will definitely be more effective in fishing ports.

The strategy of recruiting skilled incinerator managers from the community (MANG) could be a back-up (priority II) and supporter of the CONT strategy. In its application, the strategy could be carried out after the environmental control system in incinerator operations had been adequately fulfilled. The control system was an important content in training incinerator managers recruited from the community. According to Ross et al. (2024) and Ewell et al. (2020), a combination of complementary strategies can increase the chances of success of the incinerator program as a solution for handling port waste. Meanwhile, the success of the program stages can increase the trust of fisheries stakeholders (McClanahan et al., 2024; Firdaus et al., 2020) and guarantee the long-term implementation of incinerators (Yang et al., 2019; Hendrawan, 2022). Table 4 presents several implications/benefits that could arise from the implementation of incinerators for the sustainability of fisheries activities at the Tanjung Luar FP.

Table 4. Implications of the implementation of incinerators on the sustainability of fisheries activities in the port

No	Fishery activities	Contribution of fisheries stakeholders to incinerators	Implications/benefits of implementing incinerators in fishing ports
1.	Fishing boat	Collection of fishing waste, prospective incinerator operators	Clean fish landing dock, faster fish unloading, more hygienic fish caught
2.	Fish marketing	Collection of solid waste at fish auction sites, prospective incinerator operators	Image of fish caught increases, fish auction is neater and more orderly, fish sells faster
3.	Port industry and fish processing	Collection of solid waste from port industry and fish processing, prospective incinerator operators	Complaints about industrial waste from ports and fish processing decrease, raw fish and processed products are of higher quality
4.	Sea supply kiosk	Collection of solid waste from supply preparation	Sea supply area is cleaner, visitor health is more assured
5.	Provision of fuel	Collection of solid waste from the port in the fuel station area	Fuel station area is cleaner, fire risk is reduced
6.	Provision of ice for fish	Collection of solid waste in the ice factory area	Ice factory area is cleaner, ice factory performance is improved, fish cold handling is more assured
7.	Food stalls	Collection of leftover food and vegetable waste	Food stalls are cleaner, visitor health is more assured
8.	Fishery services	Coordination of fish handling and fish transportation waste	Fishery services are better and demand is increasing, cleanliness of fish transportation facilities is more assured

If the fishing port successfully handles solid waste using an incinerator, it will encourage the development of fishing activities in the Tanjung Luar FP. Many fishing boats will land their catches at the port because the dock is clean and no longer disturbed by fishing waste (Table 4). Fish auction and marketing activities can run more orderly, and the solid waste produced can be sent to the incinerator at the end of each activity. The area around the sea supply kiosk is also cleaner because packaging waste is no longer piled up for days. This then invites many fish buyers, visitors, and the community to come to the fishing port. According to Mustaruddin et al. (2022b) and Wirajing and Nanfosso (2025), fish buyers and visitors pay close attention to the cleanliness and quality of fish in transactions, because fisheries activities at the

port are a food business. These fisheries transactions will affect other transactions, such as the provision of ice, food stalls, and fisheries services. Fisheries services, for example, there will be bank transfers and fish transportation services, if there is a fish purchase. This will continue, if there is comfort in activities at the fishing port, especially in solving the problem of solid waste that is widely complained about. This study has shown that incinerators have high suitability for handling this waste, and also presents a strategy for implementing it at fishing ports. Each fisheries stakeholder can contribute according to their role in supporting the implementation of the incinerator (Table 4). This finding can be applied to all fishing ports because they have the same waste typology, and also supports the ecofishing port program initiated by the Indonesian Government (Muninggar et al., 2020; Wahyuni et al., 2022).

4. CONCLUSION

The developing fishery activities in Tanjung Luar FP were fishing boat activities, fish marketing, port industry and fish processing, provision of supplies for going to sea, provision of fuel for going to sea, provision of ice for fish, food stalls, and other fisheries services. All these activities had the potential for solid waste. The solid waste from fishery activities is net scraps, fishing line pieces, used cardboard supplies, used plastic, fallen fish, pieces of fish, fish scales and guts, fish container waste, pieces of rope, wooden crate waste, used sacks, used jerry cans, pipe pieces, used hoses, used styrofoams, used spare parts, leaves, and food waste. The suitability of the incinerator for solid waste management at the port was relatively high, which was indicated by the fulfilment of good compliance criteria (3.20 on a scale of 1-4) and very good beyond compliance criteria (3.52 on a scale of 1-4). The development of an environmental control system in incinerator operations (CONT) was priority strategy I for the application of incinerators for solid waste management in fishing ports (IR=0.245, inconsistency 0.05). The supporting strategy was the recruitment of skilled incinerator managers from the community (MANG) (IR=0.232, inconsistency 0.05).

ACKNOWLEDGEMENTS

The author would like to thank the Directorate General of Higher Education, Research, and Technology of the Ministry of Education, Culture, Research and Technology of Indonesia for funding this research in accordance with the 2024 Research Program Implementation Contract Number: 027/E5/PG.02.00.PL/2024 dated June 11, 2024. The author would also like to thank IPB University, the Department of Marine Affairs and Fisheries of East Lombok Regency, and the Bangsal Fishermen Group of East Lombok Regency for their support in data collection.

AUTHORS CONTRIBUTION

Experimental Run and Data Collection, Mustaruddin, Iin Solihin, Gondo Puspito, and Fis Purwangka; **Methodology and Validation**, Mustaruddin, Iin Solihin, and Eko Sri Wiyono; **Writing-Original Draft Preparation**, Syifa Nurul Aini, Mustaruddin, and Gondo Puspito; **Formal Analysis, Data Curation, and Visualization**, Syifa Nurul Aini and Fis Purwangka; **Writing-Review and Editing**, Eko Sri Wiyono and Gondo Puspito; **Supervision**, Mustaruddin.

DECLARATION OF COMPETING INTEREST

The authors have no conflict of interest to declare.

REFERENCES

Azeez AS, Muraleedharan KR, Revichandran C, John S, Seena G, Ravikumar CN, et al. Modelling of sediment plume associated with the capital dredging for sustainable mangrove ecosystem in the Old Mangalore Port, Karnataka, India. Regional Studies in Marine Science 2022;56:Article No. 102693.

Caramuta C, Giacomini C, Longo G, Montrone T, Poloni C, Ricco L. Integration of BPMN modeling and multi-actor AHP-aided evaluation to improve port rail operations. Transportation Research Procedia 2021;52:139-46.

Cheng Y, Oleszek S, Shiota K, Oshita K, Takaoka M. Comparison of sewage sludge mono-incinerators: Mass balance and distribution of heavy metals in step grate and fluidized bed incinerators. Waste Management 2020;105:575-85.

Department of Environment and Sanitation (DES) of East Lombok Regency. Report on Environmental and Sanitation Management and Control. Selong, Indonesia: DES of East Lombok Regency; 2024. p. 58.

Department of Marine Affairs and Fisheries (DMAF) of East Lombok Regency. Marine Affairs and Fisheries Performance Report. Selong, Indonesia: DMAF of East Lombok Regency; 2024. p. 65.

Ewell C, Hocevar J, Mitchell E, Snowden S, Jacquet J. An evaluation of Regional Fisheries Management Organization at-sea compliance monitoring and observer programs. Marine Policy 2020;115:Article No. 103842.

Firdaus M, Shafitri N, Witomo CM. Fisheries empowerment in East Lombok Regency, West Nusa Tenggara Province. Marina Scientific Bulletin 2020;6(2):85-98 (in Indonesian)

Hendrawan A. The role of incinerators in preventing marine pollution in KM. Tanto Bersama. Jogja Maritime Scientific Magazine 2022;20(1):42-50 (in Indonesian).

Ji G, Chen Q, Ding Z, Gu J, Guo M, Shi L, et al. High mortality and high PCDD/Fs exposure among residents downwind of municipal solid waste incinerators: A case study in China. Environmental Pollution 2022;294(1):Article No. 118635.

Kamargo G, Simbolon D, Mustaruddin. Capture fisheries management strategy in the Lingga Regional Marine Conservation Area (LRMCA) in Lingga Regency. Albacore Journal 2018;2(3):333-42 (in Indonesian).

Liu S, Tian F, Pan YF, Xiang LH, Lin L, Hou R, et al. Contamination and ecological risks of steroid metabolites require more attention in the environment: Evidence from the fishing ports. Science of The Total Environment 2022;807(1):Article No. 150814.

McClanahan TR, Oddenyo RM, Kosgei JK. Challenges to managing fisheries with high inter-community variability on the Kenya-Tanzania border. Current Research in Environmental Sustainability 2024;7:Article No. 100244.

McClanahan TR, Azali MK, Kosgei JK. Fish catch responses to Covid-19 disease curfews dependent on compliance, fisheries management, and environmental contexts. Marine Policy 2022;144:Article No. 105239.

Ministry of Environment and Forestry (MEF) of Indonesia. Regulation of MEF for Company Performance Rating Assessment Program (Proper) in Environmental Management: Volume 1. Jakarta, Indonesia: MEF of Indonesia; 2021.

Muninggar R, Lubis E, Iskandar BH. Assessment of ecofishingport parameters at Jakarta Nizam Zachman Oceanic Fishingport. Journal of Fisheries and Marine Technology 2020;11(1):111-23 (in Indonesian).

Mustaruddin, Baskoro MS, Santoso D, Karnan. Attractor effectiveness and squid-enrichment strategies in Tanjung Luar, East Lombok Regency, West Nusa Tenggara. Albacore Journal 2022a;6(3):281-91 (in Indonesian).

Mustaruddin, Selomita E, Nugroho T, Kartini SS. Sanitation aspects on tuna landings on Bungus Fishing Port, West Sumatra. Indonesian Journal of Agricultural Sciences 2022b;27(4):536-43 (in Indonesian).

Mustaruddin, Nurani TW, Wisudo SH, Wiyono ES, Haluan J. Quantitative Approach to Developing Fisheries Industry Operations. Bandung, Indonesia: CV. Lubuk Agung; 2011.

Osmundsen L. Port reception facilities and a regional approach: A bridge for abating plastic pollution in the arctic? Marine Policy 2023;148:Article No. 105436.

Ozkaynak OH, Icemer GT. Based on stakeholder questionnaires of ship-derived waste, waste management re-planning in Ports and determining the need for inspection. Marine Policy 2024;159:Article No. 105912.

Rosalina D, Adi W, Martasari D. Analysis of sustainable catch and squid fishing season patterns in Sungailiat Nusantara Fishingport, Bangka. Maspari Journal 2011;2(1):26-38 (in Indonesian).

Ross J, Hammouche S, Chen Y, Rockall AG. Beyond regulatory compliance: Evaluating radiology artificial intelligence applications in deployment. Clinical Radiology 2024;79(5):338-45.

Saaty TL. Decision Making for Leaders. Jakarta, Indonesia: PT. Pustaka Binaman Pressindo; 1993. p. 270.

Shofa R, Hadi H. Study of environmental sanitation of fishermen's settlements in Tanjung Luar Village, Keruak District, East Lombok Regency. Journal of Geographical Science and Education Studies 2017;1(2):22-34.

Subhan M. Analysis of handling and strategy of fish waste management at Tanjung Luar Fish Auction Place, Keruak District, East Lombok Regency. Rinjani Scientific Journal 2018;6(1):79-83 (in Indonesian).

Thanassekos S, Scheld AM. Simulating the effects of environmental and market variability on fishing industry structure. Ecological Economics 2020;174:Article No. 106687.

Vaio AD, Varriale L, Trujillo L. Management control systems in port waste management: Evidence from Italy. Utilities Policy 2019;56:127-35.

Wahyudin I, Kamal MM, Fahrudin A, Boer M. Sustainability analysis of elasmobranch fisheries in Tanjung Luar, East Lombok Regency. Journal of Tropical Marine Science and Technology 2019;11(1):103-16 (in Indonesian).

Wahyuni DM, Mustaruddin, Muninggar R. Environmental management assessment of Kutaraja Oceanic Fishingport based on eco-fishingport parameters. Albacore Journal 2022;6(2):123-37 (in Indonesian).

Wirajing MAK, Nanfosso RT. Establishing a sustainable fishing industry: The role of environmental stringency, fishery training and education infrastructure in the Maritime Cameroon. Marine Policy 2025;178:Article No. 106730.

Yang L, Liu G, Zhu Q, Zheng M. Small-scale waste incinerators in rural China: Potential risks of dioxin and polychlorinated naphthalene emissions. Emerging Contaminants 2019;5:31-4.

Environment and Natural Resources Journal

Volume 23
Issue 5
2025

Groundwater Studies for Sustaining Peatlands against Fire Disasters and Supporting Water Resources

David Andrio[1,3*], Nur Islami[2], and Lita Darmayanti[1]

[1]*Environmental Engineering, Universitas Riau, Pekanbaru, Indonesia*
[2]*Physics Education, Universitas Riau, Pekanbaru, Indonesia*
[3]*Center for Technology and Energy Application, Universitas Riau, Pekanbaru, Indonesia*

ARTICLE INFO

Received: 2 Jan 2025
Received in revised: 15 May 2025
Accepted: 29 May 2025
Published online: 2 Jul 2025
DOI: 10.32526/ennrj/23/20250002

Keywords:
Peat fire/ Peatland/ Geoelectrical Resistivity

*** Corresponding author:**
E-mail:
davidandrio@lecturer.unri.ac.id

ABSTRACT

There are two main issues related to water resources in coastal areas covered by peat soil. The first problem is peat fires, which occur during the dry season and are difficult to extinguish because the characteristics of peat make it very flammable. The second problem is a lack of clean water resources for the needs of the surrounding community. This study investigates the feasibility of groundwater potential for prevention of peat fire tragedies, and groundwater resources for community use. This study employed an integrated approach that combined geoelectrical resistivity surveys with physical and chemical analyses of soil and groundwater to assess groundwater potential both as a water resource and as a preventive measure against peatland fires. The results of this study indicated that all groundwater samples were contaminated with seawater and exceeded the permissible limits set by the World Health Organization (WHO), making them unsuitable for human consumption. Except for the central and eastern parts of the study area, peat soil exhibited resistivity values ranging from 30 to 210 Ω·m, largely influenced by its fluid and clay content. Through interpretation of resistivity data, variations in sand and gravel content at different depths were identified. Shallow aquifers were present at a depth of 10 meters in the south and 12 meters in the north, and the peat soil had a thickness that varied up to 4 meters. Thus while the groundwater reserves in the study area are not fit for community use or consumption, they do appear sufficient to significantly reduce the risk of widespread peat fire disasters.

1. INTRODUCTION

Water is one of the most vital natural resources required by all living organisms and for maintaining environmental sustainability. Water quality in a region can be influenced by natural environmental factors as well as anthropogenic activities, including negligence, which may lead to in the contamination of water sources (Karunanidhi et al., 2021). Moreover, water plays a crucial role in maintaining the hydrological balance of peatlands, which is, which is essential for ensuring the long-term sustainability of peat ecosystems (Tanneberger et al., 2021). In peatland areas, shallow groundwater is often unsuitable for suitable for daily human use, as it is inevitably contaminated by the peat material itself (Dettmann et al., 2021; Szczepański et al., 2021). Near surface peat soil also dries out easily during the dry, making peatlands more prone to drought and increasingly susceptible to fire (Nelson et al., 2021; Taufik et al., 2022). Peat fires cause severe damage to both the ecosystems living in peat areas and the surrounding environment, especially through the production of hazardous smoke and haze.

Peatland fires can exhibit a wide temporal range and may smolder underground, persisting for extended periods. Extinguishing peat fires requires a very tiring effort, because most peatlands in remote areas and difficult to reach. Peat soil frequently experiences fire disasters during the dry season (Kurniawan et al., 2024; Rezanezhad et al., 2016). Typically, peat fires

Citation: Andrio D, Islami N, Darmayanti L. Groundwater studies for sustaining peatlands against fire disasters and supporting water resources. Environ. Nat. Resour. J. 2025;23(5):420-435. (https://doi.org/10.32526/ennrj/23/20250002)

are uncontrollable due to the large volume water needed to extinguish them. To effectively prevent sub-surface fires, it is essential to fully saturate the peat soil with water, beyond merely extinguishing surface flames. Research on peat soil has been documented in a number of studies. To preserve wet environment, Ghit et al. (2018) conducted research to the area of peat soil in Algeria. Crowson et al. (2019) mapped Sumatra Island's peat forests using satellite remote sensing fusion. In contrast, Chasmer et al. (2017) used Lidar data to measure the thickness of peat soil and the quantity lost due to peat fires. To preserve peat soil, Zak and McInnes (2022) carried out wetting of peatlands to maintain ecological conditions. The restoration of peatlands can help counteract detrimental impacts and deliver advantages for both local and global communities related to carbon, water, biodiversity, and human well-being (Farrell et al., 2024).

Silvestri et al. (2019) reported the application of geophysical techniques in the study of peat soil and how to compare aerial geophysics topographic method for determining the depth of peat soil measured from the surface. Several studies have reported their findings on the application of geophysical techniques to investigate groundwater characteristics, peat properties and potential, seawater intrusion in shallow aquifers, subsurface void, and even hydrothermal systems in hilly regions (Islami et al., 2025; Tajul Baharuddin et al., 2013; Islami, 2018; Islami et al., 2019). Taufik et al. (2022) developed the PFVI index for assessing fire risk in tropical peatlands, incorporating information on groundwater tables and groundwater retention. This PFVI index can be used as a peat fire risk management tool, and its application can minimize the risk of fire in tropical peatlands.

The amount of water needed for extinguishing fires in peatlands is significantly greater than in other forest fire cases. Utilizing local groundwater as a resource for firefighting could help address these major challenges more effectively. This study uses a combination of geoelectrical resistivity of soil and groundwater physical analysis to examine the potential of groundwater and peatland in the research area. Thus, it can be a foundation for the peat to protect it from fire hazards can cause disasters to the environment and also human life. The findings of this study should be useful in informing the local community and government about environmental factors that should be considered when allocating the peatland's water resources, and it also does not rule out the possibility of providing references for research in other parts of the world with the same case. With regard to the accessibility and utilization of water resources for the prompt containment of forest fires, particularly in the peatland region, this research is very significant for providing protection for peatlands from fires, it will contribute to climate resilience, sustainable peatland management and the long-term sustainability of the peat environment.

2. METHODOLOGY

2.1 The study area

The study was conducted in the eastern part of the central Sumatra Basin (Figure 1), Riau Province, Indonesia, which is the largest tertiary sedimentary basin in the country and a key source of hydrocarbons. In terms of its tectonic context, the region is classified as a back-arc basin, which primarily influences its geological characteristics. Peat soil is dominant on the surface, especially in the area near the coast (Zhao et al., 2022). Peat soil, wherever it is located, is very prone to burning during the dry season (Nelson et al., 2021). This situation is particularly alarming because nearly all of Indonesia's peatland areas have undergone changes in function for agricultural purposes (Juniyanti et al., 2021; Purwanto et al., 2020).

2.2 Methodology

In this study, an analysis of peat and soil characteristics, groundwater characteristics, and the relationship between electrical resistivity and the characteristics of the measured material was carried out.

2.2.1 Analysis of soil properties

Fourteen soil samples were gathered from various sites where the geoelectrical resistivity data survey was conducted. In order to improve our understanding of the properties of the soil in the study region, soil grain size was examined (Guo, 2009). To describe the original soil, a soil sample was taken at a depth of roughly 40-50 cm. A well was bored to obtain soil samples of subterranean soil at different depths in addition to the near-surface dirt. Sixteen soil samples of dirt were collected at certain depths. The dried soil was sieved and categorized based on the grain size classification system of Braja (2019) to obtain information on the soil's moisture content.

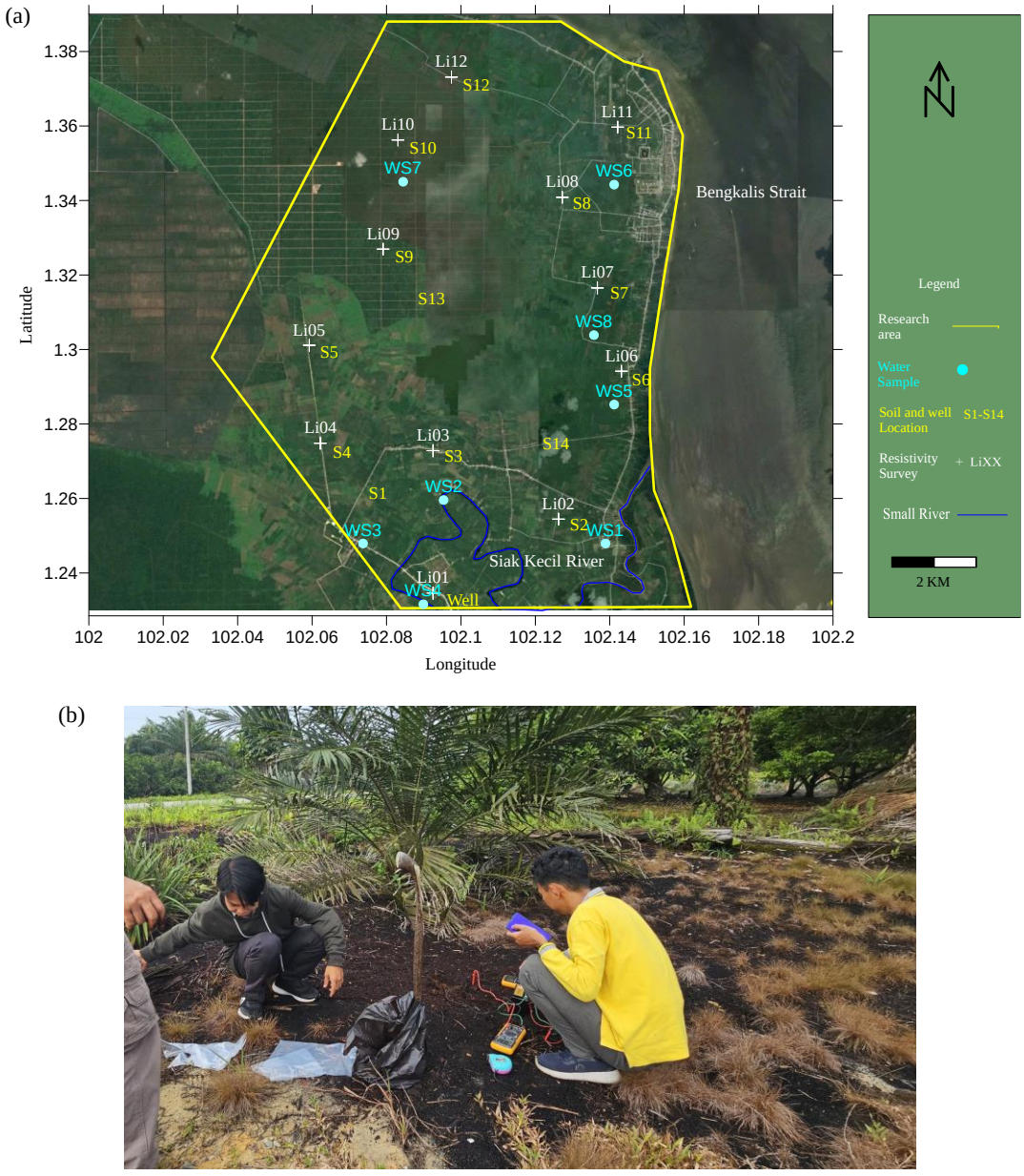

Figure 1. (a) Map of study area, (b) peatland condition in the study site

2.2.2 Measuring soil resistivity directly

At various locations near the resistivity survey, fifty direct readings of soil resistivity measurements were completed. To determine the genuine resistivity values of specific places of interest, direct measurements of soil resistivity were obtained for various soil environments and conditions, such as wet clay, dried clay, dry peat, and others. To find the genuine resistivity values, a Wenner setup with a narrow electrode spacing of 5 cm was employed. According to Telford et al. (1990), it is possible to determine the accurate resistivity value of the soil by measuring it with a reasonably small electrode directly, with the assumption that the soil is homogenous for small electrode spacing. At the measuring site, the type and color of the soil were noted and samples of the surface soil were collected to examine the grain size.

2.2.3 Chemical examination of groundwater

Six existing boreholes were used to gather groundwater samples, as shown in Figure 1. There were eight water samples taken. The paucity of existing wells in the research area made it challenging to gather groundwater samples at the same target zone depths. Based on information provided by the well owner, all of the current wells are deeper than 50 meters, with the exception of W5, a dig well, which is only about 5 meters deep. The wells' deepest point was where the well screen was positioned.

Regretfully, the well's owner could not recall the well's precise depth. Furthermore, because the wells were sealed with concrete, it was not possible to estimate the depth to the water's surface. The characteristics of the groundwater were investigated using a chemical examination of the water. Since the deeper aquifer is the primary supply of residential water, special attention has been paid to it. A peristaltic pump was used to gather groundwater samples. A number of in-situ characteristics were measured, including temperature, salinity, pH, total dissolved solids (TDS), water level, and well depth. Four hundred milliliters of water were sampled and stored in plastic bottles. Standard techniques were used to analyze each and every water sample (Clesceri et al., 1999). The water samples were transported to the Chemical Analysis Laboratory for less than 30 hours while being kept at a temperature of about 4°C in a thermos. There, they were analyzed for ion content using Ion Chromatography (IC) and Inductively Coupled Plasma (ICP), which is the latest method offering higher sensitivity, speed, and precision (Appelo and Postma, 2004).

2.2.4 Geoelectrical resistivity survey

Figure 1 shows all the locations where 1D geoelectrical resistivity surveys were conducted. At these sites, 12 traverse lines with lengths of between 200 and 260 meters were established using the Schlumberger configuration. This configuration was chosen due to its greater depth of investigation, less time and a high signal to noise ratio (Telford et al., 1990). A custom resistivity meter with a varied maximum output current and DC voltage was used. The amount of space in the field determined how long the survey would take. To improve the resolution of shallower layers, comparatively small 0.5 m increments in electrode spacing were employed for the first 10 measurements.

The apparent resistivity value was computed using the unprocessed field data, which included electric current, voltage, and electrode spacing. The actual subsurface resistivity value was then obtained by entering these data into the Res1D program for the inversion stage (Loke, 2001). The early model utilized in the data processing was the baseline for the initial data. The first set of data came from interpreting the trend line that the raw data's apparent resistivity had produced. Next, each geoelectrical layer's resistivity value and thickness were calculated using the Res1D software. In order to obtain the true resistivity value, both forward and inverse modeling techniques were used in the process. To compare with the measured value in forward modeling, the program computes the value of theoretical resistivity in the model created by repetitive inversion. The resistivity curve's layered-ground model, which represented the likelihood (expressed in terms of least squares) of corresponding to the field curves, was determined by inverse modeling. Finally, the data was mapped and contoured using Surfer 8.02 (Golden Software).

3. RESULTS AND DISCUSSION

3.1 Characteristics of the soil and a direct assessment of its resistivity

Table 1 shows the type of soil and resistivity measurement. The interpretation of subsurface resistivity was guided by these findings. The data given in Table 1 shows that the resistivity value of saturated peat soil will depend on the clay content in the peat pore. The magnitude of peat resistivity increases if the peat content increases. When peat is mixed with clay, the magnitude of resistivity will decrease as the clay content mixed with the peat increases. Peat without clay content shows a resistivity value of 195-210 Ω·m for wet conditions, and for relatively dry conditions it is 70-95 Ω·m. According to Basri et al. (2019), the pore fluid in the peat soil determines the peat resistance value especially in dry conditions. As the moisture content drops, the medium's ability to conduct current generally diminishes because of empty pores. For this reason, the resistivity value typically rises. Even though the medium in Table 1 was filled with water, the coarse sand was made of the electric current-resistant quartz crystal. This increased the medium's overall conductivity because the water in the pores served as a conductor to transfer electrical current.

3.2 Groundwater chemical analysis

The results of chemical analysis of groundwater samples from both the recently drilled well and the existing wells are presented in Table 2. The final rows of the table show the World Health Organization's (WHO, 2008) maximum concentration that suitable for human consumption. With the exception of WS5 and WS8 (5.68 and 5.91, respectively), the majority of water samples have pH values between 6 and 8 (not safe for human consumption). All groundwater samples have K, Ca, Mg, and Na cation levels that are within the permissible range for ingestion by humans. Furthermore, the SO_4^{-2} anion content was

comparatively low (<400 mg/L), making it safe for ingestion by humans. With the exception of WS3 and WS7, the Fe anion's content is unfit for human consumption which is more than 0.3 mg/L. The elevated seawater concentration but decreased pH content in the groundwater samples from these two wells is most likely the cause of the lower content of Fe. The organic content of the water is what causes the fluctuation in pH (Hounslow, 1995). Table 2 shows differences in the cation content, particularly in Fe, which are higher than the typical threshold for human intake that is safe.

Table 1. Actual resistivity readings of the drilled well's surface soil and soil sample

No	Type of soil	Soil sources	Number of samples	Colour	Resistivity range (Ω·m)	
					Wet condition (Moisture content >25%)	Dry condition (Moisture content<10%)
1	Peat (100%)	Near surface	5	Dark grey	70.33-95.6	195.2-210.6
2	Peat (50%-75%)	Near surface	5	Dark grey	40.3-55.6	78.6-98.3
3	Peat (25%-50%)	Near surface	4	Dark grey	31.4-36.2	80.7-89.1
4	Clay	New well	4	Dark grey	16.5-23.4	61.7-73.4
5	Clay	New well	4	Relatively white	55.3-67.4	241.2-269.3
6	Medium to fine Sand	New well	4	Relatively white, (fully saturated)	46.5-68.2	-
7	Coarse sand	New well	4	Relatively white, (fully saturated)	51.2-84.5	-

Table 2. Chemical content of the groundwater sample

Well name	pH	Salinity (0/00)	TDS (mg/L)	Cl (mg/L)	SO_4 (mg/L)	K (mg/L)	Ca (mg/L)	Mg (mg/L)	Na (mg/L)	Fe (mg/L)
WS1	7.12	0.73	2,270.7	834.75	291	1.93	42.6	35.69	55.86	0.23
WS2	7.36	1.13	3,060.2	1,189.25	273.4	2.33	72.3	48.19	67.36	0.34
WS3	7.18	0.54	2,100.8	634.85	292	1.72	32.8	35.67	55.84	0.16
WS4	6.87	0.82	2,050.2	517.5	382.4	1.88	38.1	27.57	39.13	3.16
WS5	5.68	0	163.4	63.3	124.8	1.24	14.4	3.23	22.18	2.73
WS6	6.92	0.22	1,092.3	276.5	368.6	1.53	44.7	21.43	10.25	5.83
WS7	6.97	0.31	1,130.6	411.3	317.4	1.68	36.5	17.52	37.12	2.22
WS8	5.91	0.21	1,102.4	306.6	378.6	1.72	47.8	19.44	17.24	6.82
WHO	6-8			250	400			150	200	0.3

The anion concentration of the water sample reveals that all of the water samples have comparatively greater chloride ion values than the 250 mg/L (human consumption limit) except WS5. The well WS5 location is relatively far from the coast and is the cause of the low concentration of chloride ion. A map showing TDS and chloride is shown in Figure 2. Circles indicate groundwater chloride concentrations, which are comparatively low in the southern portion of the research region. In the northern portion of the research region, they are, nevertheless, comparatively high. The north of the research region has higher chloride concentrations, which are related to its closeness to the coastline. In water samples that are quite close to the coastline, other researchers have also discovered relatively high concentrations of chloride (Telahigue et al., 2018; Ayed et al., 2018). For TDS, the same pattern was noted. All of the water in the aquifer, though, is thought to be a combination of freshly arrived non-brackish water and seawater that was previously trapped there.

In Figure 2, the chloride ions are plotted against other ions for all the water samples from the research area. Based on the plotted graph in Figure 2, it can be concluded that the groundwater comes from the same saltwater source. Chemical reactions like ion exchange activities or mixing can alter the chemical makeup of fresh groundwater. In reality, the data match those shown in Table 2. As seen in Figure 3, most ions generally exhibit a strong association with the chloride ions. In the deeper aquifer, K, Mg, and Na ions have a strong association with chloride, with the exception of Ca ions. This suggests that the source of these ions is the same saline water (Kim et al., 2003).

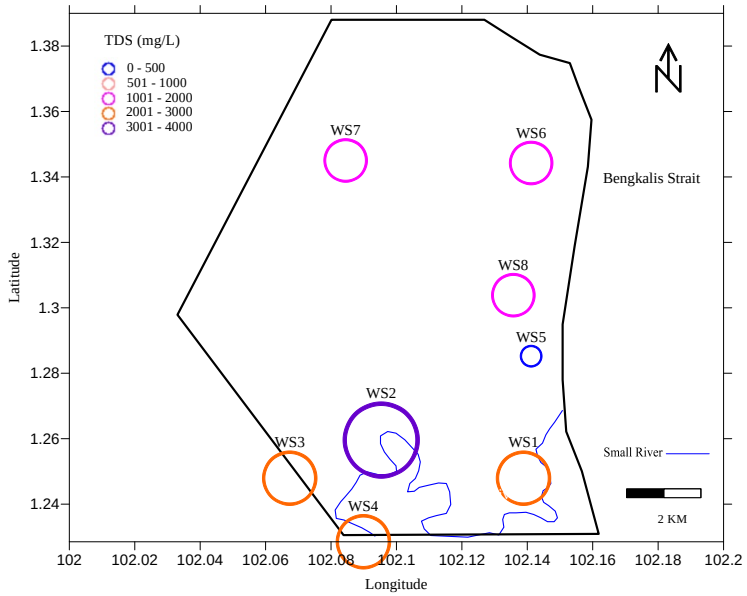

Figure 2. TDS distribution in the research area

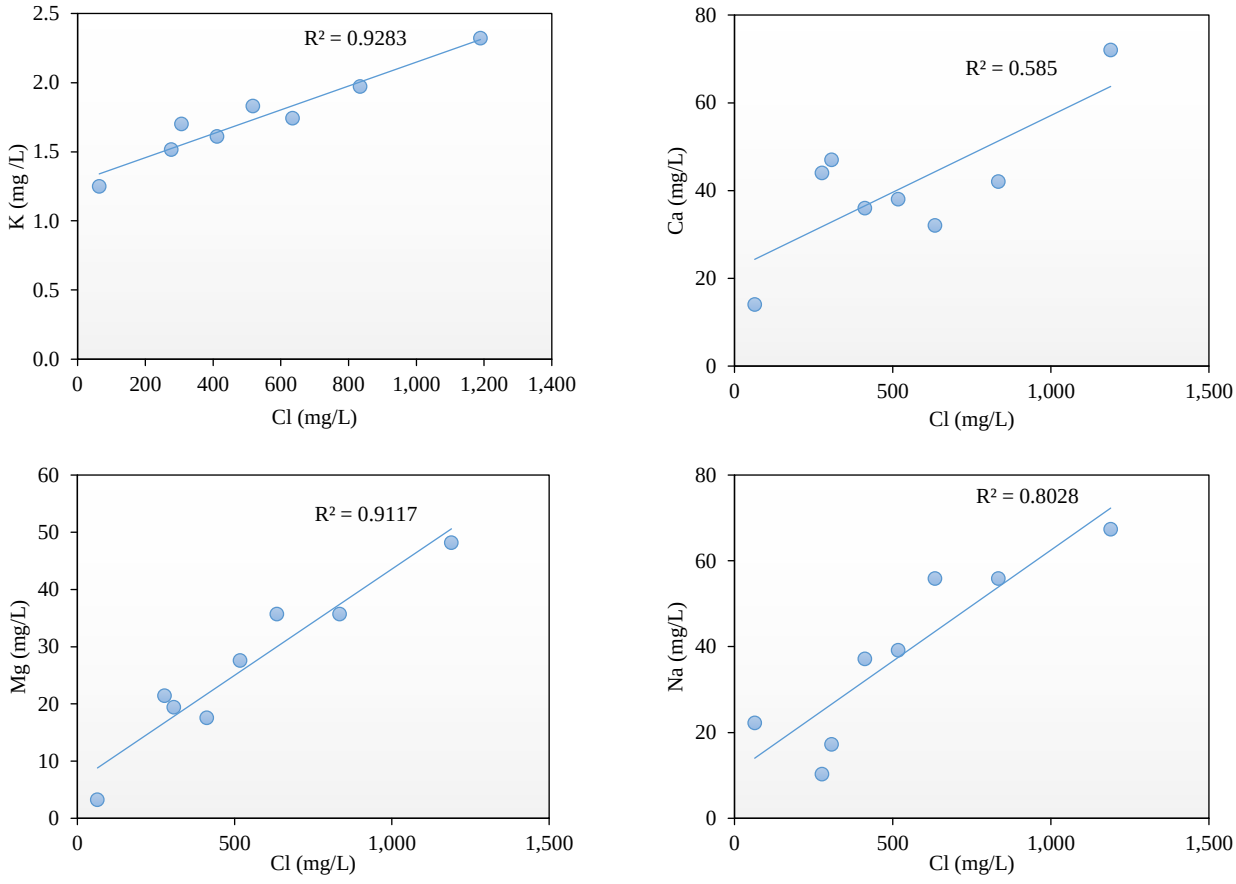

Figure 3. Scatter plot of Cl versus other anion content

3.3 Data from well-drilled

In order to acquire geological information for the purpose of calibrating and interpreting the resistivity data, a fresh well was dug approximately in the middle of the research region. Soil samples were collected during the drilling of the well. In order to get geological data for this study region, several researchers also took soil samples while digging (Zhuo et al., 2017; Li et al., 2019). The soil analysis findings are plotted against depth in Figure 4. There is clay soil, which is light grey, down to around two meters. A notable change in clay color to grey occurs

from 2 to 12 meters. Deeper than 12 to 19 meters is where fine sand can be found. During the site survey, the first aquifer was discovered in this depth range. At 52 meters below the surface, a second aquifer with fine-grained sand was discovered. The well's maximum depth was 70 meters, and coarse sand is found between 58 and 70 meters (Figure 4).

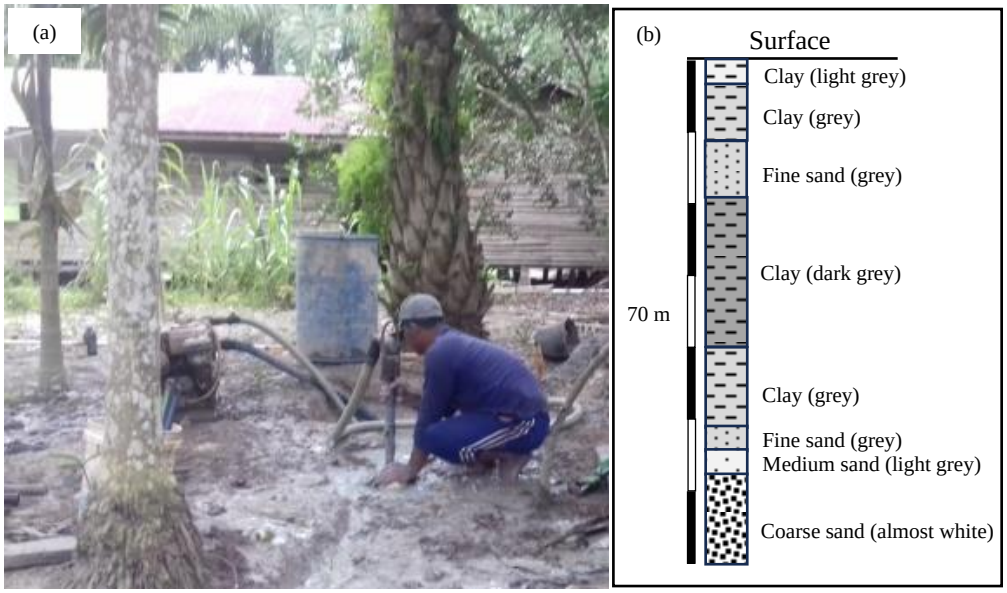

Figure 4. Well drilling photograph (a) and Lithology log (b)

3.4 Interpretation of resistivity below the surface

All the resistivity data were processed using Res1DInv to estimate the depth of each layer and true resistivity value of each layer. The inversion process was carried out using resistivity raw data collected from the field. The subsurface's geoelectrical resistivity for each site is interpreted in Figure 5. The result of the inversion shows the resistivity model that is represented by the block form in the picture, the computed apparent resistivity is displayed using a curve line and then the observed apparent resistivity data are shown by using the plus (+) sign.

Direct soil resistivity measurement in Table 1 for certain soil conditions was utilized as a guide during the interpretation process to interpret the subsurface resistivity (Figure 5). The direct resistivity measurement of the soil is also supported by well log data that was obtained from the drilled well (Figure 4). The different types of curves for the span from the top surface to the second aquifer were recognized in Figure 5. Res1D was used to process the geoelectrical resistivity curves with an RMS error of less than 5% for all line surveys. Similar types of resistivity undulation are seen in these twelve resistivity curves model. With the exception of the LS6 and LS7 lines, which have resistivities of about 150 Ω·m. In the near surface layer, resistivity data ranges from 30 to 50 Ω·m which shows layers of peat mixed with clay that are indicated by near-surface resistivity range from 30 to 50 Ω·m. A resistivity of about 150 Ω·m. indicates that there is rather dry clay present. Direct field observations made near each survey site substantiate this. The geoelectrical resistivity curve's form provides an indicator of lithology interchange, as seen in the following pattern. The rock formation and lithology in the study area are indicated by five distinct types of geoelectrical resistivity curves. This conclusion is based on the characteristic of block and guided by the lithology data. They are peat soil followed by clay, then layered by the first aquifer, and clay layer between the first and second aquifers, and the second aquifer. Nevertheless, the eastern and middle regions of the research area did not contain peat soil. This is the opposite of what was found in the resistivity study of LS6 and LS7, where the top surface had a resistivity value of roughly 150 Ω·m. The lithology information gleaned from the drilling procedure also lends credence to this hypothesis (Figure 4).

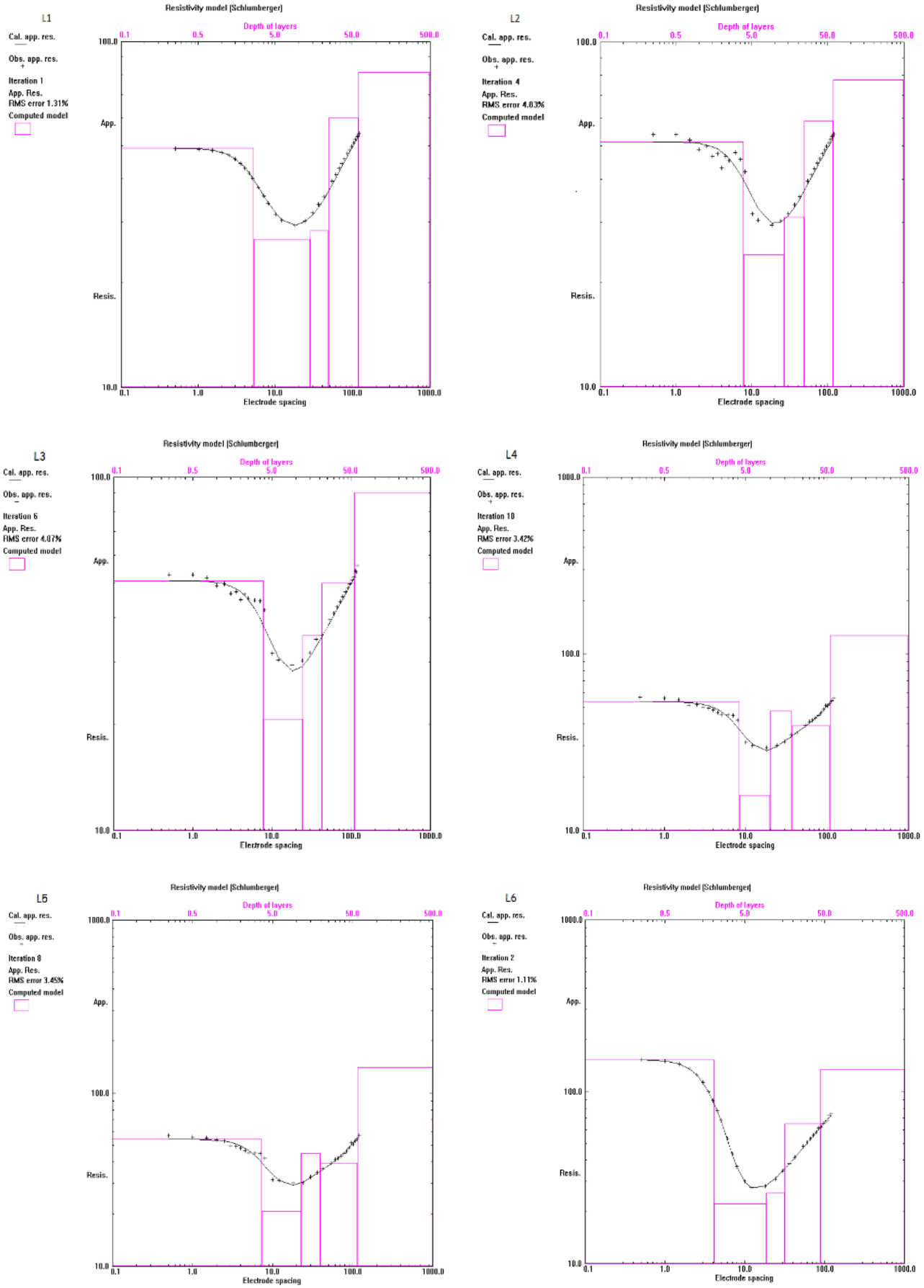

Figure 5. The resistivity plotted against depth

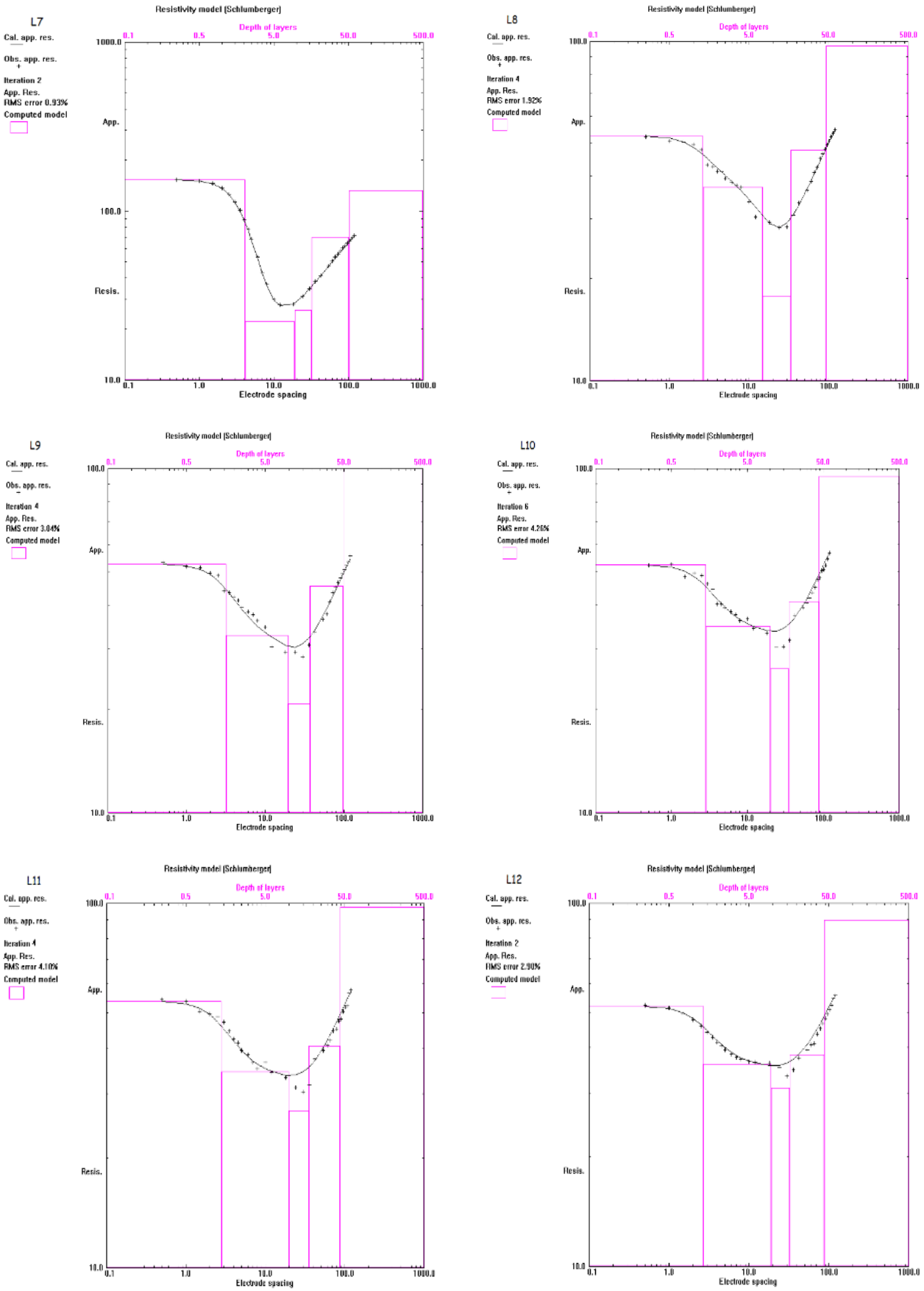

Figure 5. The resistivity plotted against depth (cont.)

In the southern portion of the research area (LS9, LS10, LS11, LS12, LS13, and LS14), the value of the resistivity data was found to be around 50 Ω·m from the surface down to a depth of 1.5 m based on the interpretation of the resistivity data in Figure 5. This resistivity value is consistent with the peat soil, which was determined by direct resistivity testing and ranged from 47 to 54 Ω·m (Table 1). In the northern portion (LS1, LS3, and LS4), the peat soil resistivity values range from 48 to 53 Ω·m, indicating a relatively thick peat layer averaging 2.60 m. As seen in the LS7 and eastern portions as well (LS5 and LS6), no peat soil was discovered in the middle of the research area. The resistivity value in these locations is 150 Ω·m, or dried clay soil, close to the surface. The following layer has a resistivity of 22 to 35 Ω·m, which is indicative of saturated clay soil. Because the north portion of this stratum was closer to the beach, there was a comparatively greater resistivity difference between it and the south. Out of all the layers, the third layer has the lowest resistance (25-38 Ω·m). This suggests that the layer on top of it is an aquifer that is full of brackish water. This aquifer gets deeper as it moves northward. This aquifer gets deeper as it moves northward. Nonetheless, this aquifer's resistivity rises toward the south, suggesting that the groundwater's brackishness gradually diminishes as one moves landward. Beneath the first aquifer lies a clay layer with resistivity between 50 and 59 Ω·m. The resistivity values of the deepest layer, which matches to the second aquifer, range from 80 to 120 Ω·m. In the deeper depth, the second aquifer is located at a depth of roughly 60 meters in the north and 40 meters in the south. The fresh aquifer has comparatively less chlorides and sulphates in the groundwater in the southern portion, and these kinds progressively rise in the direction of the north, according to the relatively large resistivity difference in the second aquifer.

The resistivity distribution in the subsurface is displayed in Figure 6. The resistivity readings were utilized to contour it laterally using a kriging method. The kriging spreading was based on a variogram modelled with a lag distance of 0.056 (unit is in degree) for individually depth below the surface (0 m). The resistivity distribution at the surface is comparatively higher (>120 Ω·m) in the middle and eastern regions of the research area. Peat soil was represented by the dark grey zone. The resistivity value is typically about 25 Ω·m at depths of 10 and 20 m, indicating the presence of a brackish water zone in the first aquifer. The clay zone was grey at 30, 40, and 50 meters below the surface. The second aquifer, which is light blue in hue, is the last stratum.

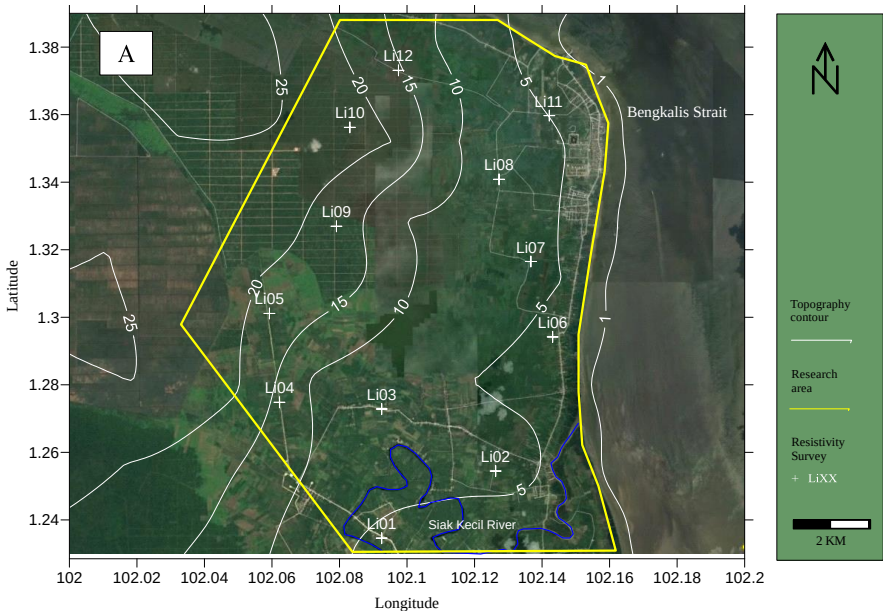

Figure 6. Topography map (a) and distribution of resistivity value at the surface to -60 m depth (b-h)

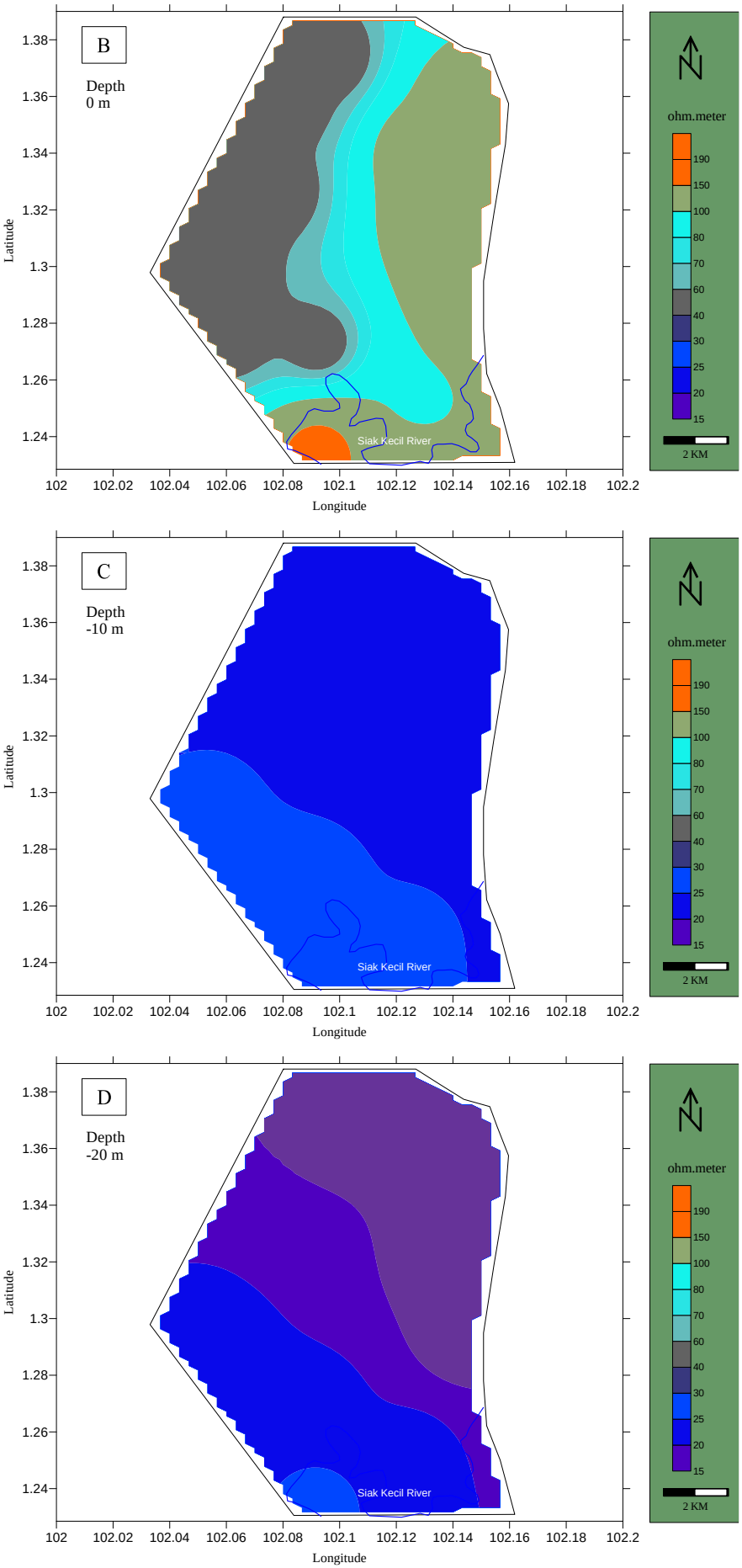

Figure 6. Topography map (a) and distribution of resistivity value at the surface to -60 m depth (b-h) (cont.)

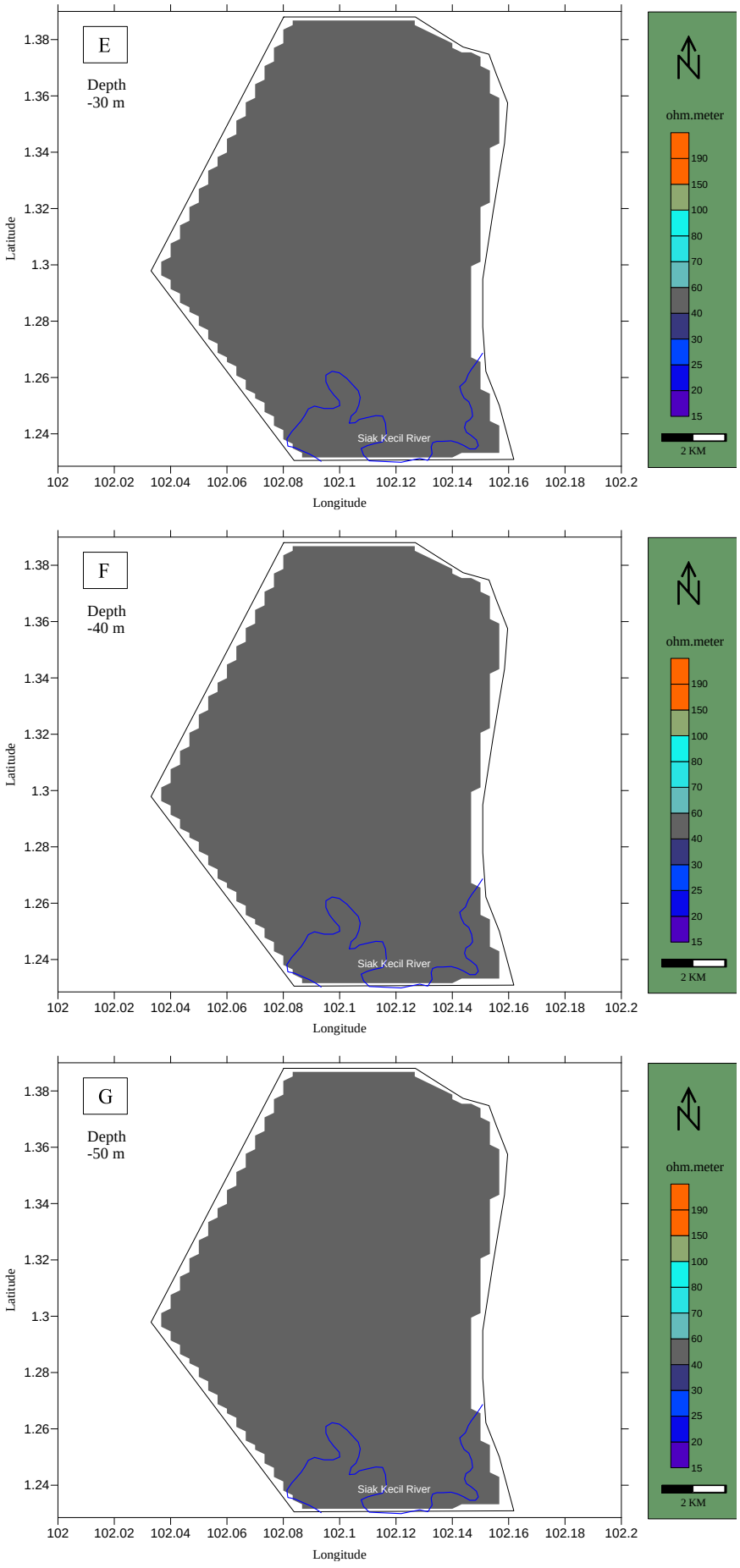

Figure 6. Topography map (a) and distribution of resistivity value at the surface to -60 m depth (b-h) (cont.)

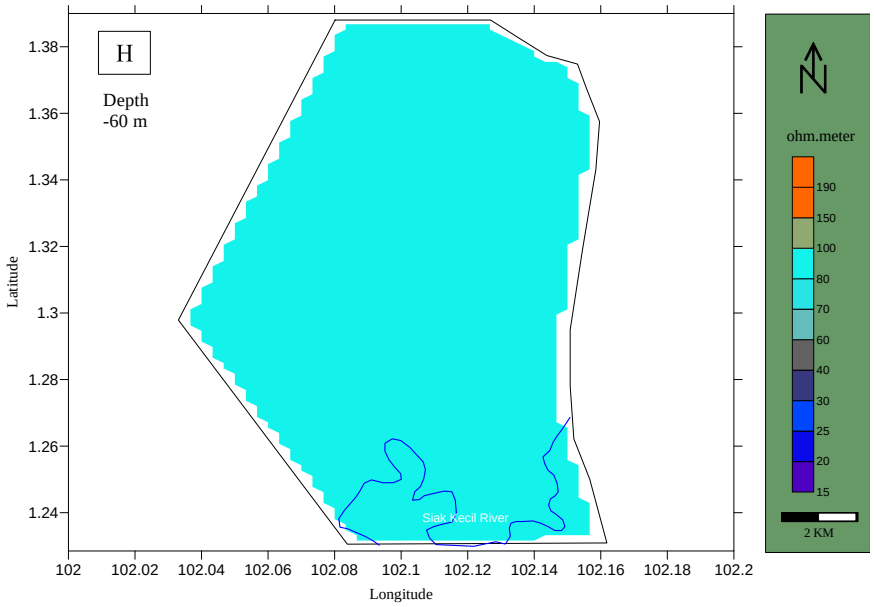

Figure 6. Topography map (a) and distribution of resistivity value at the surface to -60 m depth (b-h) (cont.)

3.5 Anticipation for prevent Peat fire disaster

Based on the resistivity data interpretation, the thickness of peat soil was estimated for all the research area. These data's trends show that resistivity changes dramatically at a depth of roughly two meters. This suggests that the soil had changed from being peat to becoming clay. In contrast, the southern region of the research area experiences no such change. This suggests that in the southern part of the research area, the peat soil is not found in the near surface (0-3 m deep). The reason these zones don't have peat soil is because the Siak River overflowed and inundated their surface, leaving clay as the predominant material covering these places.

The total bounded study area is 1.88×10^8 m^2 which is used in the estimation peat and aquifer volume. The peat's thickness ranges from 0 m in the southern area but is found to be about 4 m thick in the northern area, with an average thickness of roughly 2 m. The depth of peatland is according to the geoelectrical resistivity interpretation for the entire region. Figure 7 displays the soil thickness that is only 4 m thick in the north portion. Other studies indicate that peat thickness varies from 1 meter to tens of meters, depending on the depositional environment during peat formation (Crezee et al., 2022; Islami and Irianti, 2021; Anda et al., 2021; Islami et al., 2023). Finally, the total volume of the peat soil within the study area is about 3.72×10^8 m^3. This volume prognosis is based on the boundary of the countering and the depth in each location. Peat porosity in this region is about 41% (Sutejoa et al., 2016), and then the peat,s total pore volume can reach about 1.54×10^8 m^3.

In order to do early anticipation of the peat fire disaster, the need of water is important to investigate. The thickness of the first aquifer as determined by interpreting the resistivity data depicted in Figure 8 is roughly 8 m thick in the south region. The aquifer is thicker just about 12.8 m thick in the north region. Because thickness is not recorded uniformly, the increase in thickness from the south to the middle area is less than the increase in thickness from the middle to the northern area; therefore, the first aquifer's thickness does not increase gradually to the north. Since the first aquifer has an average thickness of 10.2 meters, the approximate total volume of water resources in the pores with average porosity of 30% in the shallow aquifer is predicted to be as much as 5.75×10^8 m^3.

The overall amount of water in the reservoir of the shallow aquifer is expected to be greater than what would be required to plug all of the peat soil pores, which helps to prevent peat fire disasters. Because the peat soil has significantly high of porosity and permeability (Sutejoa et al., 2016), water can naturally seep to the bottom part of the material of the pores in the peat. To put it another way, all of the water in the first aquifer can be used to predict the amount of water needed to avoid a peat fire. This eliminates the need for helicopters to carry water to other sites, which has historically been the method used when peat fires occur.

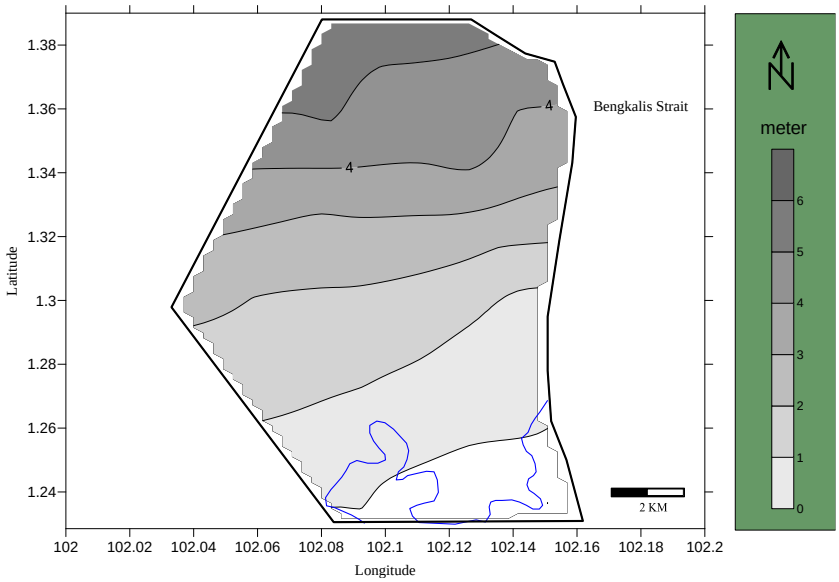

Figure 7. Thickness of peat soil obtained from the resistivity interpretation

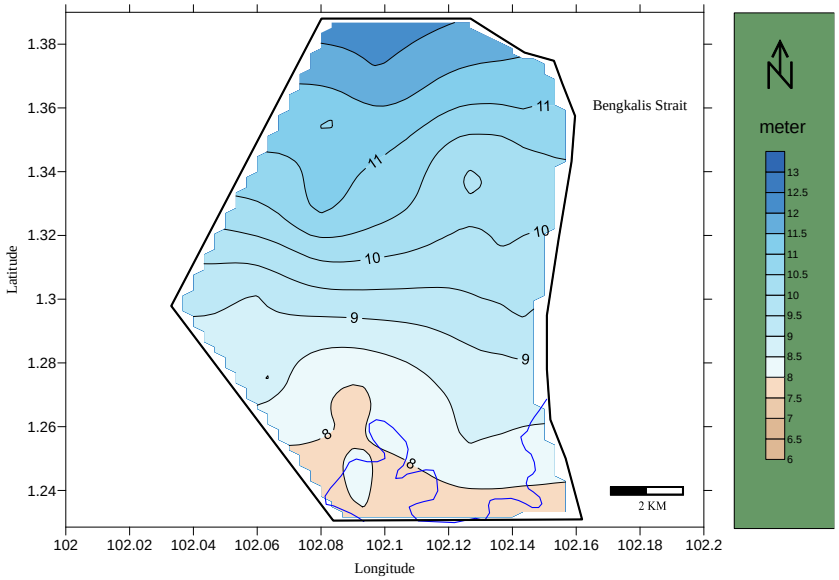

Figure 8. Thickness of the first aquifer

Finally, according to a volume analysis of both peat soil and groundwater, the water resources from the first aquifer are quite feasible to supply water in this area to put out flames of the peat in the dry season. But if peat fires occurred in this area or perhaps in other locations of peatlands, the issue that can come up is that it is quite challenging to get the fire site in order to drill wells during a fire. Therefore, in the event of a drought, it would be wise to locate wells with automated pumps in case of peat fires. This would reduce the likelihood of a peat fire happening. In addition, the automated pumps would keep the peat's moisture content constant. Ultimately, it will maintain the peat wetland area's ecosystem's viability.

3.6 Future discussion

This study shows a snapshot of groundwater chemistry and resistivity but does not consider how seasonal variability may impact groundwater availability or quality for fire prevention. Future research should focus on how changes between the dry and wet seasons can affect important factors such as groundwater levels, salinity concentrations, and peat moisture dynamics in coastal areas. Multi-seasonal studies using long-term field monitoring approaches, hydrological modeling, and satellite imagery would be very useful in understanding the complex interactions between seasonal rainfall, seawater intrusion, and groundwater balance. Particular attention should be

paid to the impacts of prolonged dry seasons or extreme wet seasons on peat drying, increased oxidation, subsidence, and changes in groundwater and surface water quality. The study conducted by Ahmad shows the importance of maintaining the condition of peatlands from fires. They did this engaging with the community about how important it is to maintain the condition of peatlands.

4. CONCLUSION

The findings of this study suggest that the peat soil and aquifer conditions in the study area can be effectively investigated using the geoelectrical resistivity method. Direct surface resistivity measurement is a highly helpful tool for resistivity data interpretation and calibration. The north of the research area has rather brackish groundwater, as evidenced by the comparatively high chloride concentration of the water samples. According to the resistivity data interpretation, the study region is made up of coarse sand, clay, and peat soil. Based on the distribution of resistivity values, it was possible to detect and map the depths of the two aquifers and the peat. The research area's middle and eastern regions have no peat soil, and the thickness of the soil varies. The entire volume of water in the shallow aquifer appears to be more than sufficient to prevent a peat fire calamity in the future, even as the aquifer's depth grows toward the north.

REFERENCES

Anda M, Ritung S, Suryani E, Hikmat M, Yatno E, Mulyani A, et al. Revisiting tropical peatlands in Indonesia: Semi-detailed mapping, extent and depth distribution assessment. Geoderma 2021;402:Article No. 115235.

Appelo CA, Postma D. Geochemistry, Groundwater and Pollution. London: CRC press; 2004.

Ayed B, Jmal I, Sahal S, Bouri S. The seawater intrusion assessment in coastal aquifers using GALDIT method and groundwater quality index: The Djeffara of Medenine coastal aquifer (Southeastern Tunisia). Arabian Journal of Geosciences 2018;11(20):Article No. 609.

Basri K, Wahab N, Talib MK, Zainorabidin A. Sub-surface profiling using electrical resistivity tomography (ERT) with complement from peat sampler. Civil Engineering and Architecture 2019;7(6A):7-18.

Braja MD. Advanced Soil Mechanics. 4th ed. London: CRC Press; 2019.

Chasmer LE, Hopkinson CD, Petrone RM, Sitar M. Using multitemporal and multispectral airborne lidar to assess depth of peat loss and correspondence with a new active normalized burn ratio for wildfires. Geophysical Research Letters 2017;44(23):11,851-9.

Clesceri LS, Greenberg AE, Eaton AD. Standard Methods for the Examination of Water and Wastewater. Washington DC: APHA; 1999.

Crezee B, Dargie GC, Ewango CE, Mitchard ET, Emba BO, Kanyama TJ, et al. Mapping peat thickness and carbon stocks of the central Congo Basin using field data. Nature Geoscience 2022;15(8):639-44.

Crowson M, Warren-Thomas E, Hill JK, Hariyadi B, Agus F, Saad A, et al. A comparison of satellite remote sensing data fusion methods to map peat swamp forest loss in Sumatra, Indonesia. Remote Sensing in Ecology and Conservation 2019;5(3):247-58.

Dettmann U, Kraft NN, Rech R, Heidkamp A, Tiemeyer B. Analysis of peat soil organic carbon, total nitrogen, soil water content and basal respiration: Is there a 'best' drying temperature? Geoderma 2021;403:Article No. 115231.

Farrell CA, Connolly J, Morley TR. Charting a course for peatland restoration in Ireland: A case study to support restoration frameworks in other regions. Restoration Ecology 2024;32(7):e14216.

Ghit K, Muller S, Bélair GD, Belouahem Abed D, Daoud-Bouattour A, Benslama M. Palaeoecological significance and conservation of peat-forming wetlands of Algeria. Revue d'Écologie (La Terre et La Vie) 2018;73(4):414-30.

Guo M. Soil sampling and methods of analysis. Journal of Environmental Quality 2009;38(1):Article No. 375.

Hounslow A. Water Quality Data: Analysis and Interpretation. Boca Raton: CRC Press; 2018.

Islami N, Irianti M, Fakhruddin F, Zulirfan Z. A preliminary study of geothermal resources in the Rokan Hulu Regency, Riau, Indonesia. Journal of Physics: Conference Series 2019;1185(1):Article No. 012003.

Islami N, Irianti M, Yusoff I. An effective method for quantitative interpretation of seawater intrusion in shallow aquifers from electrical resistivity data. Current Applied Science and Technology 2025;25(1):1-14.

Islami N, Irianti M. A quantitative interpretation of salt water mixture in the shallow aquifer through the geoelectrical resistivity data. Journal of Physics: Conference Series 2023;2582(1):Article No. 012001.

Islami N, Irianti M. Resistivity characteristics of soil saturated with variation of salt water-fresh water mixture. Journal of Physics: Conference Series 2021;2049(1):Article No. 012029.

Islami N. Groundwater exploration in the bedrock area using geoelectrical resistivity survey. IOP Conference Series: Earth and Environmental Science 2018;186(3):Article No. 012016.

Juniyanti L, Purnomo H, Kartodihardjo H, Prasetyo LB. Understanding the driving forces and actors of land change due to forestry and agricultural practices in sumatra and kalimantan: A systematic review. Land 2021;10(5):Article No. 463.

Karunanidhi D, Aravinthasamy P, Deepali M, Subramani T, Shankar K. Groundwater pollution and human health risks in an industrialized region of southern India: Impacts of the COVID-19 lockdown and the monsoon seasonal cycles. Archives of Environmental Contamination and Toxicology 2021;80(1):259-76.

Kim Y, Lee KS, Koh DC, Lee DH, Lee SG, Park WB, et al. Hydrogeochemical and isotopic evidence of groundwater salinization in a coastal aquifer: A case study in Jeju volcanic island, Korea. Journal of Hydrology 2003;270(3-4):282-94.

Kurniawan A, Graham LB, Applegate G, Arifanti VB, Akbar A, Hadi EE, et al. Impacts of rainfall on peat fire during the dry season and wet dry season on degraded tropical peatland in South Sumatra, Indonesia. IOP Conference Series: Earth and Environmental Science 2024;1315(1):Article No. 012060.

Li S, Huang Z, Zhao K, Xu H, Fang Q. Comparative analysis of pit deformation characteristics in typical region soft soil deposits of China. Arabian Journal of Geosciences 2019;12:1-11.

Loke MH. Tutorial: 2-D and 3-D Electrical Imaging Surveys [internet]. 2001 [cited 2024 March 10]. Available from: http://www.geoelectrical.com.

Nelson K, Thompson D, Hopkinson C, Petrone R, Chasmer L. Peatland-fire interactions: A review of wildland fire feedbacks and interactions in Canadian boreal peatlands. Science of the Total Environment 2021;769:Article No. 145212.

Purwanto E, Santoso H, Jelsma I, Widayati A, Nugroho HY, van Noordwijk M. Agroforestry as policy option for forest-zone oil palm production in Indonesia. Land 2020;9(12):Article No. 531.

Rezanezhad F, Price JS, Quinton WL, Lennartz B, Milojevic T, Van Cappellen P. Structure of peat soils and implications for water storage, flow and solute transport: A review update for geochemists. Chemical Geology 2016;429:75-84.

Silvestri S, Knight R, Viezzoli A, Richardson CJ, Anshari GZ, Dewar N, et al. Quantification of peat thickness and stored carbon at the landscape scale in tropical peatlands: A comparison of airborne geophysics and an empirical topographic method. Journal of Geophysical Research: Earth Surface 2019;124(12):3107-23.

Sutejoa Y, Dewi R, Hastuti Y, Rustam RK. Engineering properties of peat in Ogan ilir regency. Jurnal Teknologi (Sciences & Engineering) 2016;78(7-3):61-9.

Szczepański M, Szajdak LW, Meysner T. Impact of shelterbelt and peatland barriers on agricultural landscape groundwater: Carbon and nitrogen compounds removal efficiency. Agronomy 2021;11(10):Article No. 1972.

Tajul Baharuddin MF, Taib S, Hashim R, Abidin MH, Rahman NI. Assessment of seawater intrusion to the agricultural sustainability at the coastal area of Carey Island, Selangor, Malaysia. Arabian Journal of Geosciences 2013;6(1):3909-28.

Tanneberger F, Appulo L, Ewert S, Lakner S, Ó Brolcháin N, Peters J, et al. The power of nature-based solutions: How peatlands can help us to achieve key EU sustainability objectives. Advanced Sustainable Systems 2021;5(1):Article No. 2000146.

Taufik M, Widyastuti MT, Sulaiman A, Murdiyarso D, Santikayasa IP, Minasny B. An improved drought-fire assessment for managing fire risks in tropical peatlands. Agricultural and Forest Meteorology 2022;312:Article No. 108738.

Telahigue F, Agoubi B, Souid F, Kharroubi A. Assessment of seawater intrusion in an arid coastal aquifer, south-eastern Tunisia, using multivariate statistical analysis and chloride mass balance. Physics and Chemistry of the Earth, Parts A/B/C 2018;106:37-46.

Telford WM, Geldart LP, Sheriff RE. Applied Geophysics. Cambridge University Press; 1990.

World Health Organisation (WHO). WHO Guidelines for Drinking-Water Quality. 3rd ed. Geneva: WHO; 2008.

Zak D, McInnes RJ. A call for refining the peatland restoration strategy in Europe. Journal of Applied Ecology 2022;59(11):2698-704.

Zhao J, Lee JS, Elmore AJ, Fatimah YA, Numata I, Zhang X, et al. Spatial patterns and drivers of smallholder oil palm expansion within peat swamp forests of Riau, Indonesia. Environmental Research Letters 2022;17(4):Article No. 044015.

Zhuo L, Han D, Dai Q. Exploration of empirical relationship between surface soil temperature and surface soil moisture over two catchments of contrasting climates and land covers. Arabian Journal of Geosciences 2017;10:1-11.

Environment and Natural Resources Journal

Volume 23
Issue 5
2025

Comparative Study of the Removal Efficiency of *Chrysopogon zizanioides* (L.) and *Zea mays* (L.) of Copper (Cu) and Lead (Pb): Harnessing Phytoremediation Potential for Soil Recovery in a Former Dumpsite of El Salvador City, Misamis Oriental Philippines

Lynnel Boter-Uayan[1,2*] and Gina C. Lacang[1]

[1]*Department of Environmental Science and Technology, College of Science and Mathematics, University of Science and Technology of Southern Philippines, Cagayan de Oro City, Philippines*
[2]*Department of Education - El Salvador City Division, Himaya National High School, Himaya, Misamis Oriental Northern Mindanao, Philippines*

ARTICLE INFO

Received: 26 Feb 2025
Received in revised: 12 Jun 2025
Accepted: 16 Jun 2025
Published online: 14 Jul 2025
DOI: 10.32526/ennrj/23/20250050

Keywords:
Heavy metals/ Phytoremediation/ Translocation/ Bioaccumulation/ Efficiency removal/ Dumpsite

*** Corresponding author:**
E-mail: boterlynnel@gmail.com

ABSTRACT

Inorganic pollutants, like heavy metals found in soil with high levels of concentration, post a serious threat to the environment. However, heavy metals such as Cu and Pb produced by waste treated with a phytoremediation technique project a positive input. An experimental-descriptive analysis was used to quantify the phytoremediation potential of vetiver grass (*Chrysopogon zizanioides* L.) and maize (*Zea mays* L.) in accumulating Cu and Pb in a former El Salvador City dumpsite, located in Misamis Oriental Philippines. The study found that the initial amounts of Cu and Pb (1,368 and 38.1 mg/kg) decreased significantly to (850 and 20.5 mg/kg) respectively. The results also showed vetiver grass exhibited concentrations of lead (of 15.12±1.20 µg/g) and copper (506.36±8.44 µg/g) in its roots. In comparison, maize concentrations were found to be: lead (10.22±5.92 µg/g) and copper (486.85±3.12 µg/g) respectively. The Translocation Factor (TF) of vetiver grass had a 0.40 value, while maize showed 0.16 and 0.17 values (for Cu and Pb). The Bioaccumulation Factor (BAF) of vetiver grass was 47.55, and for maize 32.14. The results rendered significant over the three-month study period at a 0.95 confidence level. This study concludes that vetiver grass generally accumulates higher concentrations of both lead and copper in roots and shoots compared to maize, with roots consistently showing higher metal accumulation than shoots. For future research, these results provide a foundational scientific framework for soil evaluation of dumpsite areas, and give further support to policy implementations.

HIGHLIGHTS

The study utilized phytoremediation technique with applied complete randomized block design of pot experiment using vetiver grass and maize on the contaminated soil. High concentration of heavy metals accumulated on plant system in three months was also investigated.

1. INTRODUCTION

Environmental pollution in air, water and soil as a result of human activities marked a tremendous threat to the current era (Chirilă Băbău et al., 2024). Waste materials that brought adverse effect to the environment, has been carelessly managed causing serious environmental dilemma. These unproperly manage wastes contribute high content of organic pollutants and heavy metals on soil (Khalid et al., 2017). Soil pollutants is one of the foremost environmental issues worldwide (Abriha-Molnár et al., 2023). This issue projects a serious threat for this leads to the altered physical, chemical and biological environmental composition.

In the Philippines, R.A. 9003, also known as the Ecological Solid Waste Management Act of 2000, have been put in place to address the underlying issues. The goal is to manage solid waste efficiently

Citation: Boter-Uayan L, Lacang GC. Comparative study of the removal efficiency of *Chrysopogon zizanioides* (L.) and *Zea mays* (L.) of copper (Cu) and lead (Pb): Harnessing phytoremediation potential for soil recovery in a former dumpsite of El Salvador City, Misamis Oriental Philippines. Environ. Nat. Resour. J. 2025;23(5):436-447. (https://doi.org/10.32526/ennrj/23/20250050)

by reducing waste volume and promoting eco-friendly disposal methods. However, the Act's provisions on waste dumping have led to the accumulation of heavy metals, which has negatively impacted soil quality. This may lead to the increase of toxicity level in the soil ecosystem exceeding beyond the threshold limit if not properly monitored (Obasi et al., 2021). To address this environmental problem, strategies like phytoremediation have been introduced to mitigate the high concentrations of heavy metals in the soil resulting from increased waste dumping activities.

El Salvador City with its growing population, has opened its landfill on 2000 and started its operation on the year 2001. The area is specifically situated in the upland location of barangay Himaya. The area can hold wide range of wastes, that as it started its operation, it can accommodate approximately 108,000 kilos of waste per month. Wastes generated are combination of wastes coming from establishments, infrastructures, industries and household wastes. Through the years the landfill becomes an open-dumpsite due to the uncontrolled bulk of mixed-waste being dumped in the area. Such dumped wastes can have significant heavy metal contamination to soil (Bisht et al., 2024).

Heavy metals in contaminated soil which cannot be degraded are toxic elements that naturally occur in the environment and have an atomic density greater than 4×106 mg/kg. Such metals influence plant growth and development through biological and non-biological means. Exceeding the threshold limit beyond (20-100 mg/kg) Cu and (30-50 mg/kg) Pb may post an ecological and nutritional toxicity disrupting balance in soil ecosystem (Obasi et al., 2021). Increased level of heavy metals results to oxidative stress in plants leading to production of free radicals and reactive oxygen species, resulting in cellular damage, reduced growth, and lower biomass production (Goyal and Kahlon, 2022). These metal concentration that exceeds the WHO organization standards for plants and soil caused serious harm to the environment (Chibuike and Obiora, 2014). Hence, phytoremediation is vital.

Phytoremediation is a remediation technique that utilizes plants to absorb, sequester, and detoxify a range of pollutants from soil, water, and air (Zhang et al., 2020; Tiwari et al., 2019). It is environment friendly, cost effective and sustainable approach since it utilize plants to remove metals and organic contaminants in the soil. Common plant species that is being used for phytoremediation is the vetiver grass *Chyrsopogon zizanioides* (L.), a hyper accumulator plant belonging to the Poaceae family (Suelee et al., 2017). Maize *Zea Mays* (L.) belonging to the Poaceae family which is also globally known to being one of the most important cereal crops worldwide also renowned for its ability to tolerate heavy metals and grow rapidly with high biomass yield (Atta et al., 2023). Both plant species are tolerant to heavy metals specifically copper (Cu) and Lead (Pb), and is use as an alternative method to eliminate the presence of heavy metals on soil. Both plants are native species found in south and South-East Asia (Phusantisampan et al., 2016; Oshunsanya et al., 2023).

Numerous plant species that naturally inhabit contaminated areas have been investigated for their potential ability in phytoremediation. This includes dumpsites, landfills, mining, and quarrying sites. Certain plants are capable of thriving and surviving in metal-rich soils and are categorized as metal-tolerant species or bioindicators (Borymski et al., 2018). Such plants can effectively phytoremediate soil through exclusion from the plasma membrane, immobilization, ligand sequestration and chelation (Zhang et al., 2023).

In this light, the researcher utilized plant species, specifically vetiver grass and maize to determine the translocation and bioaccumulation factor of identified heavy metals to mitigate soil pollutants and improve soil quality. The utilized growth of plant species was observed in the study area.

2. METHODOLOGY

2.1 The study site

The study was conducted in Himaya El Salvador City, Misamis Oriental, Philippines. Situated approximately 8.5247, 124.5183, in the island of Mindanao. It geographically lies between the coordinates of 8º 28" to 8º 33" North Latitude and between 124º 27" to 124º 34" East Longitude. It is bordered by the Municipality of Alubijid to the west, Opol to the east and Manticao and Naawan to the south. On the north, lies Macajalar Bay of the Bohol Sea. The site presented in Figure 1 has an approximate elevation of 136.9 meters or 449.1 feet above mean sea level. The general land uses of the of the City's total land area of 14,265 hectares comprising of forestland with 8,271.20 hectares having the highest percent (57.98) stipulated in the existing general land use map. The area falls under climatic type III, which is relatively dry seasons from November to April and wet during the rest of the year with no pronounced maximum rain period. November to April is the relatively dry months, while May to October is often the period of heavy rainfall.

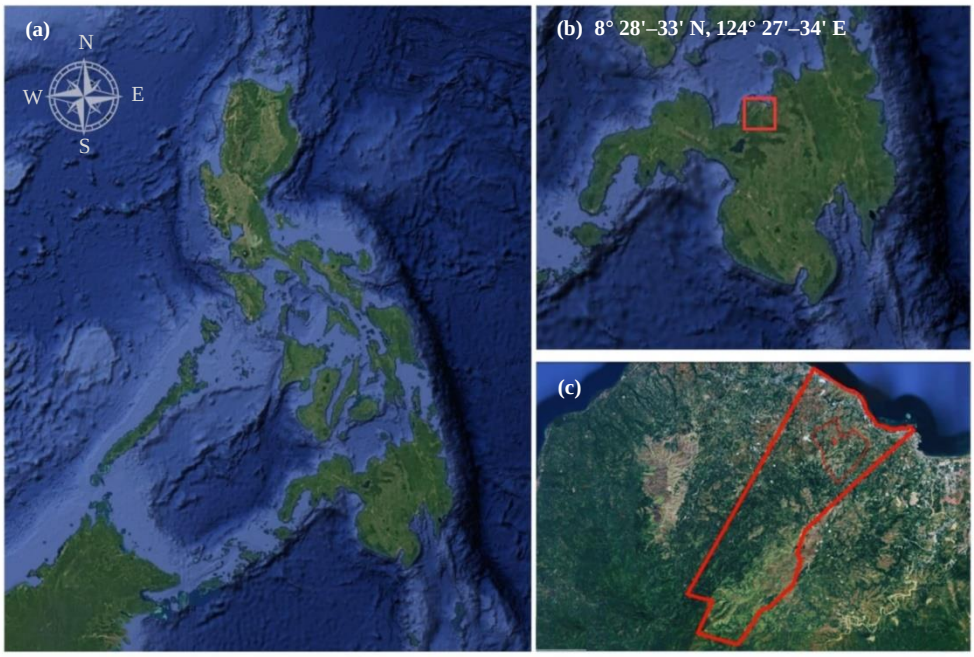

Figure 1. Location Map of the Philippines, Mindanao and Himaya El Salvador City, Misamis Oriental

2.2 Soil physicochemical analysis

2.2.1 Soil texture

To measure the relative proportion of sand, silt, and clay particles in a soil sample the research utilized the hydrometer or sedimentation method based on Stokes' Law to measure the settling rates of soil particles (University of Illinois, 2023).

In determining the soil texture, the amount of sand, silt and clay was determined using the hydrometer method or sedimentation test. One half (0.5) cup of soil sample was placed in 100ml graduated cylinder and added 3.5 cups of water. Using digital pH meter, the pH of soil water was set to ≤4.0 by adding hydrochloric acid (HCl), the graduated cylinder was covered, wobbled for five minutes, and allow to settle for 24 hours, the total depth including the depth of each layer of the soil was separated, measured and recorded. The soil separated (particle) was at the bottom, followed by the silt in the middle and the clay at the top.

The total depth, and the depth of the three separates, was calculated using the percentage of each soil separates using the formula below.

$$\% \text{ Sand} = \frac{\text{sand depth}}{\text{total depth}} \times 100 \quad (1)$$

$$\% \text{ Silt} = \frac{\text{silt depth}}{\text{total depth}} \times 100 \quad (2)$$

$$\% \text{ Clay} = \frac{\text{clay depth}}{\text{total depth}} \times 100 \quad (3)$$

After determining the proportion of the soil separates, the texture was determined using the soil triangle method to classify soil types based on relative proportions (Groenendyk et al., 2015).

2.2.2 Soil pH

To measure the hydrogen ion concentration in the soil solution, the research determines the soil pH a critical factor influencing nutrient availability, microbial activity, and overall soil quality (Jean-Philippe et al., 2012).

The pH meter probe was dipped into a solution- a mixture of soil and deionized water in a 1:1 ratio volume by weight. The solution was prepared by placing twenty (20 g) soil and deionized water in a 50 mL beaker. The samples were brought to a final volume of 40 mL and was shaken for one minute and allowed to settle for one (1) hour before pH was determined.

2.2.3 Soil organic matter

To be able to determine the key indicator of soil fertility, structure, and biological activity and traced the amount of decomposed plant and animal residues, cells and tissues of soil organisms, and substances, loss on ignition (LOI) method was utilized in the research. A technique used to estimate the amount of soil organic matter (Miller et al., 2013).

In soil organic matter analysis, samples that was collected dried overnight on the drying oven and set to

150°C, this process in to remove the undesirable water content in the soil. After drying, the soil was placed in a huge ceramic mortar and crushed thoroughly using mortar and pestle. The crushed soil was filtered in a 5mm soil sieved to ensure that only fine-earth fraction of the soil was analyzed. A 10 mL crucible was placed in electronic scale into zero (0) with the crucible on top. Using a soil scoop, exactly 5 grams of sieved soil was placed on the crucible and the weight was recorded. Same procedure was applied for the remaining soil samples. The samples were weighed again and the weight of the organic matter combusted was calculated.

The percent of organic matter was calculated using the formula below:

$$\% \text{ OM} = \frac{\text{weight of soil before combustion} - \text{weight of soil after combustion}}{\text{weight of soil before combustion}} \times 100 \quad (4)$$

2.3 Sampling procedure

Random Composite sampling was employed in the collection of soil samples within the dumpsite area. Multiple subsamples points were randomly identified across the area and mix into one composite sample. Pre-soil analysis was conducted. Subsurface soil samples were collected in the site using a shovel. Soil samples in triplicates was taken at a depth of 30-35 cm. Seven hundred fifty grams (750 g) of soil sample was subjected to lead (Pb) and copper (Cu) analysis. Two hundred fifty grams (250 g) of same soil sample was subjected to physicochemical analysis (Chafik et al., 2025). Unwanted debris like leaves, rocks, roots and alike was removed, and each soil sample was placed separately in a secured zip locked polyethylene bags and labelled using a waterproof marking pen. The soil samples were oven dried at 35°C to remove moisture prior to pot experiments. Background physiochemical properties of the tested soil before contamination was measured.

2.4 Plant preparation

Disease free, healthy vetiver and maize plants was grown on dumpsite soil in earthen pots (size-diameter 20 cm; height 17 cm) for a period of three months January to March 2024. Plants roots and shoots was pre-analyzed. Plastic vessels were placed below the earthen pots to collect the water that seeped out from the pots. Pot experiment of the plants was employed in the plant nursery area at home. Plants grown on the garden soil served as a control set. Two plants were planted per pot and three sets was prepared for each treatment. Plants was allowed to grow under normal environmental conditions.

2.5 Pot experiment

Pot experiments was employed for assessing the application of plants on contaminated soils. Eighteen (18) polyethylene pots were used in the conduct of the study, nine (9) experimental pots and (9) controlled pots. The pots were placed onto 240 mm plastic plant saucers. Pots were rinsed with 10% alcohol solution to sterilize the surface and eliminate microbial contaminants such as bacteria, fungi, or spores that may interfere with experimental results (Chauhan et al., 2020). In the plant nursery garden, polyethylene pots with identified plant samples were laid out completely in randomize block design with replicates. Enough space between the pots were ensured to keep plants from shading each other. Plants were planted in each pot with the same depth and amount of exposure to sunlight.

2.6 Soil preparation

Soil samples were collected from the designated subsurface sampling sites at a depth of 30-35 cm, air-dried at room temperature, and sieved through a 2 mm mesh to remove debris and coarse particles. Approximately 1.0 gram of each prepared soil sample was subjected to acid digestion to extract heavy metals. Digestion process followed adding 10 mL of concentrated nitric acid (HNO_3) to the soil sample in a digestion flask, followed by gentle heating until the reaction subsided. Subsequently, 5 mL of concentrated hydrochloric acid (HCl) was added, and the mixture was heated further until a clear solution was obtained. Standard solutions of the target Cu and Pb heavy metals were prepared to calibrate the Atomic Absorption Spectrophotometer. Flame Atomic Absorption Spectrophotometry (FAAS) was employed to determine the concentration of specific metal present. Calibration was performed using standard solutions of known concentrations, and the instrument was set to the appropriate wavelengths for Cu (324.8 nm) and Pb (283.3 nm). The method detection limits for copper and lead in soil were approximately 0.5 to 2 mg/kg and 1 to 2 mg/kg,

respectively, based on standard EPA and NIST analytical procedures.

In three-month experimental period, plant roots and shoots were systematically monitored at monthly intervals. At the end of each month, representative samples were harvested from both garden and dumpsite soil treatments. Plant tissue samples were collected for heavy metal analysis to determine the concentrations of Cu and Pb accumulated over time. Plant root and shoot samples were thoroughly washed with deionized water to remove soil particles, oven-dried at 70°C until constant weight, and ground to a fine powder using a stainless-steel mill. Approximately 0.5 grams of each powdered sample was digested using a mixture of concentrated nitric acid (HNO_3) and perchloric acid ($HClO_4$) in a digestion block under controlled heating until a clear solution was obtained. The digested samples were filtered and diluted to a known volume with deionized water. The concentrations of Cu and Pb were determined using Direct Air-Acetylene Flame Atomic Absorption Spectrophotometry (FAAS). The instrument was calibrated using standard solutions of Cu and Pb, and measurements were taken at wavelengths of 324.8 nm for Cu and 283.3 nm for Pb. The method detection limits for Cu and Pb in plant tissues using this technique were approximately 0.5 to 2 mg/kg and 1 to 2 mg/kg, respectively, based on standard EPA and NIST analytical protocols.

2.7 Statistical analysis

Gathered data were subjected to statistical analysis to ensure the reliability and significance of the results. To assess differences between dumpsite and garden soil plants samples, one-way analysis of variance (ANOVA) was performed. The level of significance was established at 0.95 confidence level.

3. RESULTS AND DISCUSSION

3.1 Soil physicochemical properties

Soil physical and chemical analysis results showed that the subsurface soil in the former dumpsite area has a clay texture with high water-holding capacity. It is slightly alkaline and is more likely to be suitable for most crops (Table 1).

Table 1. Pre-analysis of physicochemical and heavy metals analysis of the experimental subsurface soil

Soil characteristics	Value/Characterization	WHO/DUTCH Standards (mg/kg)	Method
Soil texture (%)			ASTM D 422-63 (2007) E2
Sand	44.60	40-50	
Silt	7.24	30-40	
Clay	48.16	20-30	
OM (%)	7.48		Walkley-Black (Colorimetric)
pH	7.8		
Pb (mg/kg)	38.1	85/55	Direct Air-Acetylene
Cu (mg/kg)	1,368	36/3.5	Flame AAS

Standard Method of Analysis for Soil, Plant, Tissue, water and fertilizer 1980

Table 1 shows the result obtained for the concentration of physicochemical and heavy metals on subsurface in the former dumpsite area. Soil texture identified as clay with the greatest value of 48.16 on its composition, indicating high water-holding capacity but poor drainage ability (Bradley et al., 2025). The level of pH with the value 7.8 indicates the subsurface soil to be slightly alkaline and is more likely to be suitable for most crops (Tian et al., 2024). Numerical value of the data gathered is being compared to the World Health Organization (WHO) and Dutch Standards for soil.

The lead (Pb) level of 38.1 mg/kg is below both WHO (85 mg/kg) and Dutch (55 mg/kg) standards, indicating that the lead concentration is within safe limits for soil health and plant growth. Content concentration on the subsurface soil did not exceed on the set standards. However, for copper (Cu) content level of 1,368 mg/kg is significantly higher than both WHO (36 mg/kg) and Dutch (3.5 mg/kg) standards. The high concentration of copper reveals alarming toxicity to plants and soil microorganisms, potentially leading to reduced plant growth and soil health concentration, numerical value exceeded far more beyond the tolerable amount on soil (Poggere et al., 2023).

The ratios of sand (44.60), silt (7.24), and clay (48.16) are indicated by the texture, with factors that

have impacts on nutrient availability and water retention (Wei et al., 2023). Lead and copper concentrations identified in the soil samples reveals possible contamination, while the pH level shows slightly alkaline composition.

3.2 Estimated concentration of heavy metals of plant roots and shoots

The data provided in Table 3 highlights the estimated concentrations of heavy metals, specifically lead (Pb) and copper (Cu), in the roots and shoots of vetiver grass (*Chrysopogon zizanoides* L.) and maize (*Zea mays* L.). The samples were taken from two different soil types: former dumpsite soil and garden soil (Table 2).

The concentration of lead in the roots of vetiver is significantly higher (15.12±1.20 µg/g) compared to maize (10.22±5.92 µg/g). This indicates that vetiver has a higher capacity to accumulate lead in its roots from contaminated soil (Gravand et al., 2021). Similarly, the lead concentration in the shoots of vetiver (6.21±2.23 µg/g) is higher than in maize (4.10±4.11 µg/g) with 0.95 level of significance. This suggests that vetiver is more efficient in translocating lead from roots to shoots, and a heavy metal tolerant species. This result is consistent to claims that vetiver not only accumulates lead effectively in its roots but also translocate a significant portion to its shoots (Singh et al., 2024).

Table 2. Estimated concentration (µg/g) of heavy metal concentration of plant roots and shoots

	Lead (Pb)		Copper (Cu)	
	Chrysopogon zizanoides (L.)	*Zea mays* (L.)	*Chrysopogon zizanoides* (L.)	*Zea mays* (L.)
Former dumpsite soil				
Roots	15.12±1.20	10.22±5.92	506.36±8.44	486.85±3.12
Shoots	6.21±2.23	4.10±4.11	90.28±12.60	80.24±5.11
Garden soil				
Roots	<0.01	<0.01	<0.01	<0.01
Shoots	<0.01	<0.01	<0.01	<0.01

Values are mean of 3 samples±SD

The copper concentration in the roots of vetiver (506.36±8.44 µg/g) is slightly higher than in maize (486.85±3.12 µg/g). Both plants show a high capacity for copper accumulation in their roots, but vetiver is marginally more effective. The copper concentration in the shoots of vetiver (90.28±12.60 µg/g) is also higher than in maize (80.24±5.11 µg/g). This indicates that vetiver is more efficient in translocating copper from roots to shoots (Kumar et al., 2018).

For both plant samples, the concentrations of lead and copper in roots and shoots are below detectable levels (<0.01 µg/g) in garden soil. This suggests that the garden soil is not contaminated with these heavy metals, and both plants do not accumulate significant amounts of lead or copper in garden soil sample.

3.3 Translocation and bioaccumulation of heavy metals in plant roots and shoots

The data gathered provides insights into the relative translocation and bioaccumulation of heavy metals in the roots and shoots of vetiver and maize. Translocation factor (TF) of plant utilized in the research study was used to measure the plant's ability to transfer heavy metals from its roots to its shoots (Table 3).

Data gathered revealed that. vetiver, for both lead (Pb) and copper (Cu) has a TF of 0.40 value. This indicates that 40% of the heavy metals absorbed by the roots are translocated to the shoots. This relatively high TF suggests that vetiver is efficient in moving heavy metals from roots to shoots. Maize has a TF value for lead 0.17, and copper 0.16 value. The lower values indicate that maize is less efficient in translocating heavy metals from roots to shoots compared to vetiver (Dorafshan et al., 2023).

The bioaccumulation factor (BAF) was used in the research study to measure the ability of a plant to accumulate heavy metals from the soil into plant tissues (Sabir et al., 2022). For the BAF value in shoots, values indicate that vetiver has a higher capacity to accumulate lead and copper in its shoots compared to maize (Dorafshan et al., 2023).

Table 3. Relative translocation and bioaccumulation of heavy metals in plant roots and shoots

	Lead		Copper	
	Chrysopogon zizanoides (L.)	*Zea mays* (L.)	*Chrysopogon zizanoides* (L.)	*Zea mays* (L.)
Translocation factor	0.40	0.40	0.17	0.16
Bioaccumulation factor shoot	19.53	12.89	6.60	5. 87
Bioaccumulation factor root	47.55	32.14	37. 01	35.59

The BAF values in roots show that both plants have a high capacity to accumulate heavy metals in their roots. However, vetiver has a slightly higher BAF for lead with the value of 47.55, indicating it is more efficient in accumulating lead in its roots compared to maize with of 32.14 value. For copper, the BAF values are relatively similar, suggesting both plants are effective in accumulating copper in their roots (Darajeh et al., 2019; Parihar et al., 2021).

The data suggests that vetiver has a higher capacity for both bioaccumulation shoots and roots of lead 19.53 and 47.55, copper 6.60 and 37.01 and translocation lead 0.40 and copper 0.17 value of heavy metals compared to maize. This makes vetiver a more suitable candidate for phytoremediation strategies aimed at both phytoextraction and phytostabilization (Singh et al., 2024).

3.4 Plant lead (Pb) and copper (Cu) concentration analysis

3.4.1 Bioaccumulation factor analysis (BFA)

Biological accumulation factor is the ability of plants to accumulate metals into their tissues. It was calculated as ratio of heavy metal in shoots to that in the soil (Balabanova et al., 2016). In order to determine the bioaccumulation of lead and copper on plant tissues, the ratio of the contaminant in plant and the concentration in the environment at a steady state was calculated using the formula:

$$\text{Bioaccumulation Factor} = \frac{\text{metal concentration in shoots}}{\text{metal concentration in soil}}$$

3.4.2 Translocation factor analysis (TFA)

After the determination of bioaccumulation factor of pant species, translocation factor was calculated to determine the ability of the plant to accumulate metals from the roots to the aerial parts of the plants. The translocation factor is defined as the ratio of metal concentration in the shoots to the roots (Yoon et al., 2006). Translocation may also move the absorb substances throughout the plant parts. To obtain the translocation factor of lead and copper in plants the formula was used:

$$\text{Translocation Factor} = \frac{\text{metal concentration in shoots}}{\text{metal concentration in roots}}$$

Translocation factor with value greater than 1 mg/kg, indicates that the plant translocates metals effectively from root to the shoot (Bu-Olayan and Thomas, 2014).

Phytoremediation performance was evaluated using the removal efficiency factor. The equation below was applied:

$$\text{Removal Efficiency (\%)} = \frac{C_0 - C}{C_0} \times 100$$

Where; C_o the primary metal concentration in the soil and C referred to the final concentration. The higher the amount of removal efficiency factor means the phytoremediation process was more effective.

3.5 Heavy metal concentration of plants in three months span

The table provides insights into the concentration of heavy metals, specifically lead and copper in the roots and shoots of vetiver and maize grown in soil from a former dumpsite over a three-month period (Table 4-5).

Data gathered showed that the concentration of lead in both shoots and roots revealed a decreasing trend over the three-month period. This suggests that vetiver is capable of initially accumulating lead from the soil, but the rate of accumulation decreases over time. The concentration of lead is consistently higher in the roots compared to the shoots. This indicates that vetiver tends to sequester lead in its root system, which is beneficial for phytostabilization as it prevents the translocation of lead to the above-ground parts of the plant.

The concentration of copper in the shoots decreases significantly over the three-month period. This suggests that the initial uptake of copper is high, but the plant's ability to translocate copper to the shoots diminishes over time. The concentration of copper in the roots shows a slight decrease from first to second month but then increases slightly in third month. This fluctuation could be due to various factors

such as changes in soil chemistry, root growth dynamics, or microbial activity in the rhizosphere.

Similar to lead, the concentration of copper is significantly higher in the roots compared to the shoots. This indicates that vetiver is effective in accumulating copper in its root system, making it suitable for phytostabilization.

Table 4. Heavy metal concentration (µg/g) of roots and shoots of vetiver grown using former dumpsite soil in three months span

Months	Lead		Copper	
	Shoot	Root	Shoot	Root
1	3.02	7.89	40.45	187.03
2	1.76	4.07	30.65	156.14
3	1.43	3.16	19.18	163.19

Vetiver accumulates higher concentrations of copper compared to lead in both roots and shoots. Plant possesses a dense and deep fibrous root system significantly increasing the root-soil interface, enhancing its ability to absorb soluble metal ions such as copper. This suggests that the plant has a higher affinity for copper uptake from the soil. The higher accumulation of copper in the roots indicates that grass utilized in the research study can be particularly effective in stabilizing copper-contaminated soils.

The data in Table 5 provides insights into the concentration of heavy metals, specifically lead and copper in the roots and shoots of maize grown in soil from a former dumpsite over a three-month period.

Table 5. Heavy metal concentration (µg/g) of roots and shoots of maize grown using former dumpsite soil in three months span

Months	Lead		Copper	
	Shoot	Root	Shoot	Root
1	2.87	4.03	30.46	168.28
2	1.03	3.46	26.74	161.55
3	0.2	2.73	23.04	157.02

The concentration of lead in both shoots and roots decreases over the three-month period from 2.87 to 0.2 value in shoots and 4.03 to 2.73 value in roots. This suggests that maize initially accumulates lead from the soil, but the rate of accumulation decreases over time from 30.46 to 23.04 value in shoots and 168.28 to 157.02 value in roots. The concentration of lead is consistently higher in the roots compared to the shoots. This indicates that maize tends to sequester lead in its root system, which is beneficial for phytostabilization as it prevents the translocation of lead to the above-ground parts of the plant.

The concentration of copper in the shoots decreases over the three-month period. This suggests that the initial uptake of copper is high, but the plant's ability to translocate copper to the shoots diminishes over time. The concentration of copper in the roots shows a slight decrease over the three months. This indicates that while maize continues to accumulate copper in its roots, the rate of accumulation slows down over time. Similar to lead, the concentration of copper is significantly higher in the roots compared to the shoots. This indicates that maize is effective in accumulating copper in its root system, making it suitable for phytostabilization.

Maize has a well-developed fibrous root system with large surface area that enhances plant ability to absorb nutrients and trace elements from the soil. Plant root epidermis and cortex are structured to facilitate the movement of water and solutes, including copper ions, into the vascular system. Results showed that it accumulates higher concentrations of copper compared to lead in both roots and shoots. This suggests that the plant has a higher affinity for copper uptake from the soil. The higher accumulation of copper in the roots indicates that maize can be particularly effective in stabilizing copper-contaminated soils.

The observed trend in Figure 2(a-b), where lead concentration in vetiver shoots decreases from 3.02 µg/g in the first month to 1.43 µg/g in the third month, and in roots from 7.89 µg/g to 3.16 µg/g, suggests a declining uptake and translocation of lead over time. Pattern may be attributed to several physiological and environmental factors, including the plant's saturation threshold for lead, changes in bioavailability of lead in the soil, or the plant's adaptive detoxification mechanisms that limit further uptake to avoid toxicity.

Maintained higher value concentrations of lead in roots compared to shoots indicate that plant primarily functions as a phytostabilizer, sequestering lead in the root zone and minimizing movement to aerial parts. Result is consistent with findings that vetiver grass accumulated 107-911 mg/kg of lead in roots and only 8.3-180 mg/kg in shoots, even under high soil lead concentrations (Rotkittikhun et al., 2006).

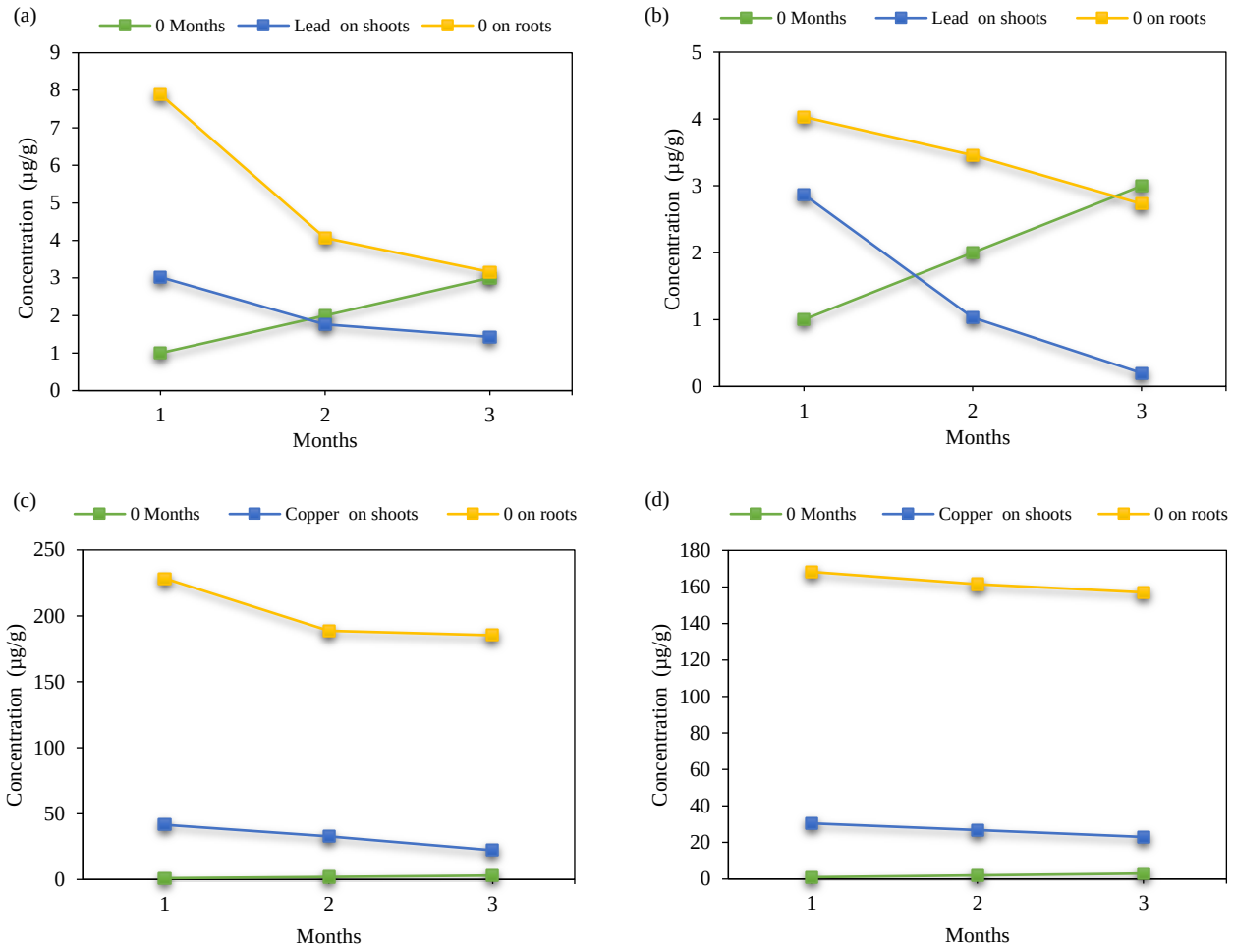

Figure 2. Heavy metal concentration in three months of vetiver and maize

Figure 2(c-d) presents Pb accumulation in maize over a three-month period. The concentration of lead in the shoots decreased markedly from 2.87 µg/g in the first month to 0.20 µg/g by the third month. Similar but less pronounced decline was observed in the roots, Pb levels dropped from 4.03 µg/g to 2.73 µg/g. Findings suggest that maize initially absorbs and translocate Pb efficiently, but its capacity to do so reduced over time, potentially it may due to physiological regulation or a reduction in the bioavailable fraction of Pb in the soil.

The consistently higher concentrations of lead in the roots compared to the shoots indicate that maize, like other cereal crops, tends to retain heavy metals in the root zone. Similar patterns have been reported that maize roots accumulated significantly more lead than shoots, with translocation factors typically below one (Sharma and Dubey, 2005).

3.6 Post analysis of the experimental soil

Soil post analysis was employed to assess how soil quality and contamination levels change over time, specifically in response to the utilization of hyperaccumulator species like maize and vetiver grass.

In the gathered data on post-analysis of the experimental soil, result revealed significant changes in heavy metal concentrations, particularly for Cu and Pb with the three-month phytoremediation period using maize and vetiver grass. The initial concentrations of Cu and Pb were 1,368 mg/kg and 38.1 mg/kg, respectively. After the experimental period, values decreased to 850 mg/kg for Cu and 20.5 mg/kg for Pb (Table 6). Reduction suggests effective uptake and accumulation of heavy metals by the experimental plants, supporting potential use in phytoremediation strategies.

Observable decrease in heavy metal concentrations was significant when compared to international safety thresholds. According to the World Health Organization (WHO), the acceptable limits for Cu and Pb in soil are 36 mg/kg and 85 mg/kg, respectively, for Dutch standards 3.5 mg/kg for Cu and 55 mg/kg for Pb. Although the post-analysis

values remain above thresholds, the downward trend indicates progress toward safer soil conditions and highlights the potential of continued phytoremediation for long-term remediation (Du et al., 2022).

Table 6. Post Analysis of Physicochemical and Heavy metals Analysis of the Experimental Soil

Soil Characteristics	Value/Characterization	WHO/DUTCH Standards (mg/kg)	Method
Soil texture (%)			ASTM D 422-63 (2007) E2
Sand	44.60	40-50	
Silt	7.24	30-40	
Clay	48.16	20-30	
OM (%)	7.48		Walkley-Black (Colorimetric)
pH	7.8		
Pb (mg/kg)	20.5	85/55	Direct Air-Acetylene
Cu (mg/kg)	850	36/3.5	Flame AAS

Physicochemical properties namely soil texture and pH remained stable throughout the experiment, with a consistent pH of 7.48 and a soil texture dominated by clay (48.16%), followed by sand (44.6%) and silt (7.24%). Characteristics were favorable for heavy metal retention and plant growth, as clay-rich soils with neutral pH tend to immobilize metals and reduce their leaching potential. The stability of these parameters suggests that the remediation process did not adversely affect the soil's structural integrity or fertility.

3.7 Comparative removal efficiency of plants

Removal efficiency of plant species was determined to assess plants' ability to extract, accumulate, and reduce heavy metal concentrations on soil (Table 7).

Over a three-month phytoremediation period, a comparative analysis of vetiver and maize grown in dumpsite soil revealed notable differences in heavy metal removal efficiencies, particularly for Pb and Cu. Vetiver demonstrated a higher initial uptake of both metals, especially in root tissues. In the first month, vetiver roots accumulated 7.89 mg/kg of Pb and 187.03 mg/kg of Cu, while maize roots absorbed only 4.03 mg/kg of Pb and 168.28 mg/kg of Cu (Table 8).

However, maize exhibited a more pronounced reduction in metal concentrations over time, particularly for Pb. By the third month, Pb levels in maize shoots dropped from 2.87 mg/kg to just 0.2 mg/kg, indicating a removal efficiency of approximately 93%. In contrast, vetiver shoots showed a reduction from 3.02 mg/kg to 1.43 mg/kg, reflecting a lower efficiency of about 53%. For copper, vetiver still maintained higher uptake levels, but maize showed a steadier decline, suggesting a more consistent removal pattern.

Table 7. Removal efficiency of plants

Plant species	Shoots (mg/kg)				Roots (mg/kg)			
	Lead		Copper		Lead		Copper	
	Initial	Final	Initial	Final	Initial	Final	Initial	Final
Vetiver	3.02	1.43	40.45	19.18	7.89	3.16	187.03	163.19
Maize	2.87	0.2	30.46	23.04	4.03	2.73	168.28	157.02

Table 8. Lead and copper removal efficiency

Plant species	Pb removal efficiency (%)	Cu removal efficiency (%)	Remarks
Vetiver			
Shoots	52.65	52.28	Highly efficient
Roots	52.58	52.58	Highly efficient
Maize			
Shoots	93.03	24.36	Highly efficient for Pb; less efficient for Cu
Roots	24.36	24.36	Highly efficient for Pb; less efficient for Cu

Philippine National Standard (PNS/BAFS 40:2014)

The findings were consistent with the work of (Otunola et al., 2023), emphasizing vetiver's strong phytoremediation potential due to its high biomass and tolerance to heavy metal stress. More so, maize was also recognized for its gradual and sustained metal uptake, making it suitable for long-term remediation strategies (Ali et al., 2013; Otunola et al., 2023). The complementary use of both species could enhance the overall efficiency of phytoremediation efforts in contaminated sites.

4. CONCLUSION

Vetiver grass was effective in absorbing and storing heavy metals from the soil with the roots acting as the primary site of accumulation. The initial concentration of Pb in the soil was 38.1 mg/kg, which decreased to 20.5 mg/kg by the end of the study, corresponding to a 46.19% reduction. Similarly, Cu levels declined from 1,368 mg/kg to 850 mg/kg, indicating a 37.87% reduction. These results highlight vetiver's strong phytoremediation potential, attributed to its extensive root system, high biomass production, and tolerance to heavy metal stress. The substantial accumulation of Pb and Cu in vetiver roots, particularly during the initial month, further supports its capacity for stabilizing and extracting contaminants from polluted soils. Pb and Cu concentrations in plant shoots and roots generally decrease over the three-month period of the study. Plant roots consistently show higher concentrations of lead and copper compared to plant shoots, indicating that the roots were more effective in absorbing and storing heavy metals. Vetiver grass in research study shows strong potential for phytoremediation, particularly for soils contaminated with Pb and Cu. Plant ability to accumulate higher concentrations of heavy metals makes the plant suitable candidate for soil remediation like areas of El Salvador City dumpsite area.

ACKNOWLEDGEMENTS

The authors would like to extend its deep gratitude to the faculty of the Department of Environmental Science and Technology, College of Science and Mathematics, University of Science and Technology, Southern Philippines, Cagayan de Oro City, Philippines for offering laboratory assistance on the conduct of the experimental work.

AUTHOR CONTRIBUTIONS

Boter-Uayan, L.B.U.: Supervision, Conceptualization, Investigation, Methodology, Experiment, Validation, Formal Analysis, Visualization, Writing-Original and Revised Editing. Lacang, G.L.: Supervision, Visualization.

DECLARATION OF COMPETING INTEREST

The authors declare that they have no known competing financial interests or personal relationships that could have appeared to influence the work reported in this paper.

REFERENCES

Abriha-Molnár VÉ, Szabó S, Magura T, Tóthmérész B, Abriha D, Sipos B, et al. Assessment of environmental impacts based on particulate matter, and chlorophyll content of urban trees. Scientific Reports 2024;14:Article No. 19911.

Ali H, Khan E, Sajad MA. Phytoremediation of heavy metals: Concepts and applications. Chemosphere 2013;91(7):869-81.

Atta MI, Zehra SS, Ali H, Ali B, Abbas SN, Aimen S, et al. Assessing the effect of heavy metals on maize (*Zea mays* L.) growth and soil characteristics: Plants-implications for phytoremediation. PeerJ 2023;11:e16067.

Balabanova B, Stafilov T, Baceva K. Bioaccumulation of heavy metals in *Salix alba* and *Acer negundo* from polluted soils in the vicinity of a lead and zinc smelter. Environmental Science and Pollution Research 2016;23(6):5479-88.

Bisht A, Kamboj V, Kamboj N, Bharti M, Bahukahndi KD, Saini H. Impact of solid waste dumping on soil quality and its potential risk on human health and environment. Environmental Monitoring and Assessment 2024;196:Article No. 763.

Borymski S, Cycoń M, Beckmann M, Mur LAJ, Piotrowska-Seget Z. Plant species and heavy metals affect biodiversity of microbial communities associated with metal-tolerant plants in metalliferous soils. Frontiers in Microbiology 2018;9:Article No. 1425.

Bradley O, Keßler D, Gadermaier J, Mayer M, Leitgeb E. Soil: The foundation for ecological connectivity of forest ecosystems. In: Kraus D, editor. Ecological Connectivity of Forest Ecosystems. Cham: Springer; 2025.

Bu-Olayan AH, Thomas BV. Assessment of the ultra-trace mercury levels in selected desert plants. International Journal of Environmental Science and Technology 2014;11:1413-20.

Chafik Y, Sena-Velez M, Henaut H, Missbah El Idrissi M, Carpin S, Bourgerie S, et al. Synergistic effects of compost and biochar on soil health and heavy metal stabilization in contaminated mine soils. Agronomy 2025;15(6):Article No. 1295.

Chauhan A, Jindal T. Methods of sterilization and disinfection. In: Chauhan A, Jindal T, editors. Microbiological Methods for Environment, Food and Pharmaceutical Analysis. Cham: Springer; 2020. p. 67-72.

Chibuike GU, Obiora SC. Heavy metal polluted soils: Effect on plants and bioremediation methods. Applied and Environmental Soil Science 2014;2014(1):Article No. 752708.

Chirilă Băbău AM, Micle V, Damian GE, Sur IM. Lead and copper removal from sterile dumps by phytoremediation with *Robinia pseudoacacia*. Scientific Reports 2024;14(1):Article No. 9842.

Darajeh N, Truong P, Rezania S, Alizadeh H, Leung DW. Effectiveness of vetiver grass versus other plants for

phytoremediation of contaminated water. Environmental Science and Pollution Research 2019;26(25):25736-52.

Dorafshan MM, Abedi-Koupai J, Eslamian S, Amiri MJ. Vetiver grass (*Chrysopogon zizanoides* L.): A hyper-accumulator crop for bioremediation of unconventional water. Sustainability 2023;15(4):Article No. 3529.

Du Z, Lin D, Li H, Li Y, Chen H, Dou W, et al. Bibliometric analysis of the influencing factors, derivation, and application of heavy metal thresholds in soil. International Journal of Environmental Research and Public Health 2022;19(11):Article No. 6561.

Goyal R, Kahlon MS. Soil physico-chemical properties and water productivity of maize as affected by biochar application under different irrigation regimes in northwest India. Communications in Soil Science and Plant Analysis 2022;53(9):1068-84.

Gravand F, Rahnavard A, Pour GM. Investigation of vetiver grass capability in phytoremediation of contaminated soils with heavy metals (Pb, Cd, Mn, and Ni). Soil and Sediment Contamination: An International Journal 2021:30(2):163-86

Groenendyk DG, Ferré TPA, Thorp KR, Rice AK. Hydrologic-process-based soil texture classifications for improved visualization of landscape function. PLoS One 2015;10(6):e0131299.

Jean-Philippe D, Deguine JP, Goebel FR, Lamichhane JR. Soil and plant health in relation to dynamic sustainment of Eh and pH homeostasis: A review. Agronomy for Sustainable Development 2012;32(2):401-9.

Khalid S, Shahid M, Niazi NK, Murtaza B, Bibi I, Dumat C. A comparison of technologies for remediation of heavy metal contaminated soils. Journal of Geochemical Exploration 2017;182:247-68.

Kumar D, Bharti SK, Anand S, Kumar N. Bioaccumulation and biochemical responses of *Vetiveria zizanioides* grown under cadmium and copper stresses. Environmental Sustainability 2018;1:133-9.

Miller RO, Gavlak R, Horneck D. Soil, Plant and Water Reference Methods for the Western Region. 4th ed. WREP 125. Western Coordinating Committee on Nutrient Management (WERA-103); 2013. p. 77-8.

Obasi SE, Obasi NA, Nwankwo EO, Enemchukwu BN, Igbolekwu RI, Nkama JO. Effects of organic manures bioremediation on growth performance of maize (*Zea mays* L.) in crude oil polluted soil. International Journal of Recycling of Organic Waste in Agriculture 2021;10(4):415-26.

Oshunsanya SO, Yu H, Opara CC, Odebode AM, Oluwatuyi TS, Babalola O. Integration effect of vetiver grass strips with maize population density on soil erosion under two contrasting slopes of rainforest agroecology. Catena 2023;221:Article No. 106768.

Otunola BO, Aghoghovwia MP, Thwala M, Gómez-Arias A, Jordaan R, Hernandez JC, et al. Improving capacity for phytoremediation of Vetiver grass and Indian mustard in heavy metal (Al and Mn) contaminated water through the application of clay minerals. Environmental Science and Pollution Research 2023;30:53577-88.

Parihar JK, Parihar PK, Pakade YB, Katnoria JK. Bioaccumulation potential of indigenous plants for heavy metal phytoremediation in rural areas of Shaheed Bhagat Singh Nagar, Punjab (India). Environmental Science and Pollution Research 2021;28:2426-42.

Phusantisampan T, Meeinkuirt W, Saengwilai P, Pichtel J, Chaiyarat R. Phytostabilization potential of two ecotypes of Vetiveria zizanioides in cadmium-contaminated soils: Greenhouse and field experiments. Environmental Science and Pollution Research 2016;23:20027-38.

Poggere G, Gasparin A, Barbosa JZ, Melo GW, Corrêa RS, Motta ACV. Soil contamination by copper: Sources, ecological risks, and mitigation strategies in Brazil. Journal of Trace Elements and Minerals 2023;4:Article No. 100059.

Rotkittikhun P, Chaiyarat R, Kruatrachue M, Pokethitiyook P, Baker AJM. Effects of soil amendment on growth and lead accumulation in *Vetiveria zizanioides* and *Thysanolaena maxima* grown in lead-contaminated soil. Chemosphere 2006;65(1):42-9.

Sabir M, Baltrėnaitė-Gedienė E, Ditta A, Ullah H, Kanwal A, Ullah S, et al. Bioaccumulation of heavy metals in a soil–plant system from an open dumpsite and the associated health risks through multiple routes. Sustainability 2022;14(20):Article No. 13223.

Sharma P, Dubey RS. Lead toxicity in plants. Brazilian Journal of Plant Physiology 2005;17(1):35-52.

Singh L, Malik M, Babu R. Phytoremediation of heavy metals by vetiver grass near riverbeds. In: Madhav S, Gupta GP, Yadav RK, Mishra R, van Hullebusch E, editors. Phytoremediation: Biological Treatment of Environmental Pollution. Cham: Springer Nature Switzerland; 2024.

Suelee AL, Hasan SNMS, Kusin FM, Yusuff FM, Ibrahim ZZ. Phytoremediation potential of vetiver grass (*Vetiveria zizanioides*) for treatment of metal-contaminated water. Water, Air, and Soil Pollution 2017;228:Article No. 158.

Tian Y, Jiang W, Chen G, Wang X, Li T. Gypsum and organic materials improved soil quality and crop production in saline-alkali on the loess plateau of China. Frontiers in Environmental Science 2024;12:Article No. 1434147.

Tiwari J, Kumar S, Korstad J, Bauddh K. Ecorestoration of polluted aquatic ecosystems through rhizofiltration. In: Pandey VC, Bauddh K, editors. Phytomanagement of Polluted Sites. Amsterdam: Elsevier; 2019.

University of Illinois. Standard operating procedure: Particle size analysis for soil texture (hydrometer method). Urbana-Champaign (IL): Department of Crop Sciences, University of Illinois at Urbana-Champaign; 2023 [cited 2025 May 30]. Available from: https://margenot.cropsciences.illinois.edu/wp-content/uploads/2023/06/Particle-size-analysis-for-soil-texture-determination-hydrometer-method-UIUC-Soils-Lab.pdf

Wei B, Peng Y, Lin L, Zhang D, Ma L, Jiang L, et al. Drivers of biochar-mediated improvement of soil water retention capacity based on soil texture: A meta-analysis. Geoderma 2023;437:Article No. 116591.

Yoon J, Cao X, Zhou Q, Ma LQ. Accumulation of Pb, Cu, and Zn in native plants growing on a contaminated Florida site. Science of the Total Environment 2006;368(2-3):456-64.

Zhang F, Sun S, Rong Y, Mao L, Yang S, Qian L, et al. Enhanced phytoremediation of atrazine-contaminated soil by vetiver (*Chrysopogon zizanioides* L.) and associated bacteria. Environmental Science and Pollution Research 2023;30(15):44415-29.

Zhang L, Zhang P, Yoza B, Liu W, Liang H. Phytoremediation of metal-contaminated rare-earth mining sites using Paspalum conjugatum. Chemosphere 2020;259:Article No. 127280.

Environment and Natural Resources Journal

Volume 23
Issue 5
2025

Optimization of Breadfruit (*Artocarpus altilis*) via Succinylation Reaction on the Effect of Time Duration and Temperature

Cut Fatimah Zuhra*, Andriayani, and Venny Angelina Siregar

Department of Chemistry, Faculty of Mathematics and Natural Sciences, Universitas Sumatera Utara, Medan, North Sumatra 20155, Indonesia

ARTICLE INFO

Received: 15 Feb 2025
Received in revised: 17 Jun 2025
Accepted: 20 Jun 2025
Published online: 17 Jul 2025
DOI: 10.32526/ennrj/23/20250041

Keywords:
Breadfruit starch/ Catalyst/ Pyridine/ Succinic acid/ Succinylation reaction

*** Corresponding author:**
E-mail: cutfatimah@usu.ac.id

ABSTRACT

Native breadfruit starch exhibits limitations such as poor water solubility, low thermal stability, and restricted functional properties, which hinder its direct application in industrial fields. In this study, modified starch was synthesized using a succinylation reaction between breadfruit (*Artocarpus altilis*) starch and succinic acid on a pyridine catalyst with time variations of 3, 3.5, and 4 h, and temperature variations of 95°C, 105°C, and 115°C. From the isolation of breadfruit starch, a yield of 7.5% was obtained. The modified succinic starch was analyzed for functional groups using an FT-IR spectrophotometer, SEM, and TGA, and the degrees of substitution, solubility, and swelling power were then determined. The formation of succinylated starch was confirmed by FT-IR spectra, which exhibited a characteristic C=O ester vibrational band at 1,692 cm^{-1} and a supporting peak at 1,200 cm^{-1} corresponding to the C-O-C ester functional group. The DS values were measured across all variations of time and temperature, with the highest DS value of 0.5293 observed at 3.5 h and 105°C. Both swelling power and solubility increased with longer reaction times and higher temperatures. Thermal analysis indicated that the starch samples experienced significant degradation at 400.6°C, with a mass loss of 82.9%. SEM images revealed that the succinylation reaction caused fragmentation of starch granules, indicating a structural modification of the starch. Overall, the transformation of native breadfruit starch into succinylated starch enhanced its functional properties, demonstrating its potential as an environmentally friendly material for bioplastic applications. Further investigations are recommended to assess the mechanical performance and biodegradation behavior of the resulting bioplastics in order to comprehensively evaluate their potential for commercial application.

HIGHLIGHTS

- Modification of breadfruit starch by succinylation method with pyridine catalyst
- The modified succinic starch was analyzed for functional groups using FT-IR spectrophotometer, SEM, TGA, followed by determination of degree of substitution, solubility, and swelling power.
- Greater water absorption causes swelling power to increase

1. INTRODUCTION

Starch, a semi-crystalline biopolymer, is a highly versatile raw material with a wide range of applications, including as a staple food in human diets, food additives, biodegradable packaging materials, and more. For starch applications, the structure (semi-crystalline lamellae, crystalline structure, and molecular structure) and properties (swelling index, thermal properties, adhesive properties, and digestibility) of various starches have been extensively studied (Huang et al., 2016; Tan et al., 2015; Wongsagonsup et al., 2008). Specifically, corn starch, rice starch (Deng et al., 2014), cassava starch (Mei et al., 2015), and potato starch have been well-researched. However, the increasing demand for starch from modern industries has generated intense interest in new and underutilized polysaccharide sources, opening opportunities for other plants, given

Citation: Zuhra CF, Andriayani, Siregar VA. Optimization of breadfruit (*Artocarpus altilis*) via succinylation reaction on the effect of time duration and temperature. Environ. Nat. Resour. J. 2025;23(5):448-458. (https://doi.org/10.32526/ennrj/23/20250041)

the high starch demand. There are also less common starches, such as breadfruit starch, that are worth investigating for the development of new starch-based products with enhanced properties (Tan et al., 2017).

Breadfruit (*Artocarpus altilis*) is a tropical fruit native to Indonesia, the South Pacific, and the Caribbean, and belongs to the Moraceae family (Wang et al., 2011). Breadfruit is a popular starch-producing fruit widely developed in Indonesia. Its high carbohydrate content makes it a valuable source for starch production. Starch extracted from breadfruit yields 18.5 g/100 g with a purity of 98.86% and consists of 27.68% amylose and 72.32% amylopectin (Fatimah Zuhra et al., 2022). Due to the fruit's poor fresh storage quality, converting it into flour and starch offers a more stable form and enhances its versatility. Since ancient times, native breadfruit starch has been used as a raw material for preparing various products (Alam et al., 2024). To expand its applications, several physical and chemical modifications of breadfruit starch, such as acetylation, oxidation, HMT (heat moisture treatment), and fermentation, have been studied recently (Adebowale et al., 2005). However, the digestibility of breadfruit starch is rarely reported. Haydersah et al. (2012) studied the digestibility of breadfruit starch and found that fermentation can increase its resistant starch content.

Native starch is not soluble in water and contains granules whose size, composition, physicochemical, and functional properties depend on plant characteristics and environmental conditions. Native starch from various plant sources generally has properties that limit its use in different food products. Improvements in the physical and chemical properties of native starch can be made, among other ways, through starch modification (Volkert et al., 2010). Modified starch is starch whose hydroxyl groups have been altered through a reaction or by changing its original structure. Starch is treated with specific processes to produce better properties, improving its previous characteristics to meet industrial needs. Modified starch has properties that native starch does not, these include higher brightness (whiter starch), lower retrogradation, lower viscosity, more apparent gel formation, softer gel texture, lower tensile strength, starch granules that break more easily, higher gelatinization time and temperature, and lower time and temperature for starch granules to break.

Starch modification can be carried out chemically through cross-linking, oxidation, etherification, esterification, or substitution, as well as through a combination of these methods (dual and more modification). Modification via esterification is one of the best starch modifications used. Modification through esterification can slow the rate of starch retrogradation, which is caused by the inhibition of hydrogen bond formation between amylose and amylopectin molecules by the ester groups formed. The advantages of starch modified through esterification include reduced gelatinization temperature, increased viscosity, higher water-binding capacity, and a clearer paste. Compared to cross-linked starch, esterified starch still experiences a decrease in viscosity during the heating process (unstable under heating) and is less resistant to acidic conditions (Zhang et al., 2009; Hamid et al., 2024d). The esterification method using Succinic Acid catalyst has been widely discussed to become succinylated starch. The modification of starch through succinylation has become a significant area of research over the past decade. Succinylated starch is widely recognized as an essential stabilizer due to its surface-active properties. This type of starch displays distinctive features, as its hydrophilic regions acquire hydrophobic traits by introducing octenyl groups, giving the molecule amphiphilic properties. The stabilization mechanism of succinylated starch leverages both the hydrophobic interactions and steric hindrance provided by the succinyl group. Succinylated starch can be further utilized in frozen canned food products and flavor encapsulation materials (Błaszczak et al., 2007; Hamid et al., 2024c).

Then the research conducted by Sri Haryani Anwar is the synthesis of breadfruit pat with succinic acid getting FTIR results that, the peak at 1,720 cm^{-1} is the C=O stretch vibration of the ester carbonyl group, while the peak at 1,560 cm^{-1} is related to the $RCOO^-$ carboxylate stretch vibration (Anwar et al., 2020a). These results indicate that the hydroxyl group in starch is substituted with the carbonyl and carboxyl ester groups of succinic acid. Fourier transform infrared spectroscopy (FTIR) showed that the starch modification was successful (Degree of Substitution, 0.0241) (van der Burgt et al., 2000). The novelty of this research lies in optimizing the preparation of breadfruit (*Artocarpus altilis*) based materials through succinylation chemical reaction utilizing succinic acid as a catalyst, which has not been widely explored in the context of natural biomaterial modification (Rumahorbo et al., 2023). This study specifically highlights the effect of reaction time and temperature on the efficiency of the succinylation process, which

aims to improve the physicochemical and functional properties of breadfruit starch. With this approach, it is expected to obtain breadfruit starch derivative products that have better thermal stability, increased solubility, and wider applicative potential in the fields of pharmaceuticals, food, and bioplastics. This innovation provides a new contribution to the development of local biomaterials that are environmentally friendly and have high added value through controlled chemical modification techniques (Chabib et al., 2025; Fatimah Zuhra and Ginting, 2013).

Based on the background described above, the researcher was interested in modifying starch through a succinylation reaction between breadfruit starch (*Artocarpus altilis*) and succinic acid using pyridine as a catalyst, with variations in time and temperature. The succinylated starch was tested by analyzing functional group changes using FT-IR spectroscopy, morphological analysis using SEM, temperature change analysis using TGA, and determining the Degree of Substitution, swelling power, and solubility. This modification aims to produce starch that meets industrial needs.

2. METHODOLOGY

2.1 Materials

Breadfruit was taken from Sumatera Utara Province, Indonesia, and serves as a doping source for starch (Hamid et al., 2024b). Succinic Acid, Pyridine, Ethanol, Hydrochloric Acid, Sodium Hydroxide, and distilled water were bought from Merck in Germany.

2.2 Methods

2.2.1 Isolation of breadfruit starch

First, the breadfruit starch is peeled and the fruit stalk is removed in isolating breadfruit starch is to peel and remove the fruit stalk, then wash it until it is free of dirt and sap. The breadfruit was cut into pieces, pureed using a blender, and squeezed through a gauze filter to get the starch. This was left for 24 h until the starch settled, and then the liquid was washed several times with water until it was clear. The starch obtained was dried in an oven at 45°C for 24 h. The sample was then mashed, sieved, and weighed. Subsequently, it was analyzed using Fourier Transform Infrared (FT-IR) spectroscopy and Scanning Electron Microscopy (SEM) (Hamid et al., 2024a).

2.2.2 Modification of breadfruit starch with succinic acid

The following steps were used in the preparation of breadfruit starch modification using succinylation reaction. First, 10 g of breadfruit starch was suspended in 50 mL of pyridine and put into a 250 mL threeneck flask. Then, it was stirred at 85°C for two h, and 4 g of succinic acid was added and refluxed while stirring for 3.5 h at 105°C. Then, it is cooled at room temperature, washed with distilled water three or more times until a normal pH (7) is obtained, and washed with 70% alcohol twice to ensure that impurities were removed. Then, the starch was dried at 40°C for 24 h and filtered with a 100 mesh sieve. The same procedure was carried out for 3 h and 4 h time variations. Then, it was analyzed by FT-IR spectroscopy, and the degree of substitution was calculated. Then, the highest value of the degree of substitution is carried out the same procedure with temperature variations of 95°C, 105°C, and 115°C. Furthermore, it was characterized by FT-IR spectroscopy, SEM, solubility, and swelling power.

2.2.3 Degree of substitution (DS)

The degree of substitution was determined from the modified breadfruit starch samples using the modified titration method. First, 0.5 g of starch succinate was weighed and placed into an Erlenmeyer flask. Then, 30 mL of distilled water and 15 mL of 0.5 M NaOH were added. The mixture was heated at 30°C until fully dissolved. After that, two drops of phenolphthalein (PP) indicator were added, and the solution was titrated with 0.1 M HCl until it turned colorless (Zuhra et al., 2025). The degree of substitution was then calculated using Equation (1).

$$\text{Degree of substitution (DS)} = \frac{162A}{4300-42A} \quad (1)$$

Where; A=starch content (%).

2.2.4 Fourier transform infrared (FTIR) spectrophotometer

Fourier-transform infrared spectroscopy (FTIR) analysis was performed using a Shimadzu spectrometer. Spectral visualization and processing were carried out using Spectragryph software for optical spectroscopy, version 1.2.13, developed by Dr. Friedrich Menges (Copyright 2019-2020). All spectra

were recorded in the range of 4,000-400 cm^{-1}, with an average of 32 scans and a resolution of 8 cm^{-1} (Nasr et al., 2020).

2.2.5 Scanning electron microscopy (SEM)

The surface morphologies of the native and modified starch granules were examined using a scanning electron microscope (SEM) model Phenom Pro Desktop SEM and JEOL JSM-IT200. All samples were carefully mounted on aluminum stubs using double-sided conductive carbon tape and coated with a thin layer of gold to enhance electrical conductivity. The observations were conducted under a high-vacuum mode at an accelerating voltage of 25 kV. Morphological features of the starch granules were captured at a magnification of 5.000 times to allow for detailed visualization of surface texture, granule integrity, and any structural alterations resulting from the modification process (Humaidi et al., 2024).

2.2.6 Thermogravimetric analysis (TGA)

Starch sample thermal decomposition was determined using a Pyris-1 DSC apparatus (PerkinElmer DSC 4000, Shelton, USA). Samples were heated between 30 and 650°C at 10°C/min in an inert atmosphere of nitrogen flowing at 20 mL/min (Oderinde et al., 2020).

2.2.7 Determination of swelling power and solubility

Swelling power and solubility of succinate starch can be used in the method used to cut (Zuhra et al., 2020). Starch is suspended with distilled water (1%, w/v) in a test tube of known weight. Then, it was heated in a water bath at a temperature of 95°C for 30 min and then cooled to room temperature (±27°C). The starch suspension was centrifuged at 5.000 rpm for 15 min to separate the residue and supernatant. The supernatant (10 mL) is dried to constant weight at a temperature of 110°C. The residue from obtained from drying the supernatant shows the amount of starch dissolved in water (%). The residue and water retained after centrifugation ware then weighed. The swelling ability of starch (based on dry weight) was determined as follows is Equations (2) and (3):

$$\text{Swelling of starch} = \frac{\text{Weight of paste}}{\text{Weight of dry sample}} \quad (2)$$

$$\text{Solubility} = \frac{W2 - W1}{\text{Weight of starch}} \times 100\% \quad (3)$$

Where; W_1=mass of dry test tube + dry starch; W_2=mass of dry test tube + wet starch.

3. RESULTS AND DISCUSSION

3.1 Mechanism

Succinic starch was obtained from the succinylation reaction between breadfruit starch and succinic acid. Succinylation of breadfruit starch was carried out in stages. While at the stage of dissolving breadfruit starch with pyridine. This stage aims to smooth the starch granules so that they can react with succinic acid. Pyridine also serves as a catalyst that can activate the hydroxyl group. After reaching a temperature of 85ºC, succinic acid is added, forming a yellowish gel-shaped starch succinate mixture. The reaction pathway for the succinylation of breadfruit starch with succinic acid is depicted in Figure 1.

The result of the succinylation reaction will product the main product, starch succinate. The gel-shaped succinic starch mixture was then added with 70% alcohol and distilled water and dried in an oven. The resulting succinic starch has physical properties of yellowish color, is lump-shaped, and is more hydrophilic than natural starch. In the reaction mechanism of starch succinate formation, secondary C atoms are substituted by succinic acid because secondary OH groups, especially C-2 OH groups, are more reactive than primary OH groups. The reactivity of OH group C-2 is 60-65%, and OH group C-6 is 15-20% (Burgt et al., 2000).

3.2 Degree of substitution analysis

In this study, the DS results obtained at various times include a 3 h period with a value of 0.5159, then a 3.5 h period with a value of 0.5293, and finally, a 4 h period with a value of 0.4949. Based on the volume of HCl used in the titration, it can be seen that the value of the degree of substitution increases in the 3-h and 3.5-h time variations, namely from 0.5159 to 0.5293, but there is a decrease in the 4-h time variation with a value of 0.4949. Increase in heating time increased he solubility and the DS value of the starch. The decrease in DS value in the 4 h time variation was due to the hydrolysis reaction that decreased the reaction efficiency (Bhosale and Singhal, 2006). In the succinylation process of breadfruit starch, it is known that the highest reaction efficiency is obtained with a reaction time of 3.5 h.

In the temperature variation study, the degree of substitution (DS) obtained at 95°C was 0.4606,

increased to 0.5293 at 105°C, and slightly decreased to 0.5201 at 115°C. As shown in Figure 2, the volume of HCl used during titration indicates a trend consistent with the DS values: the DS increased with temperature from 95°C to 105°C, but a slight decline was observed at 115°C. The initial increase in DS with rising temperature is attributed to the enhancement in reaction kinetics; higher temperatures increase molecular motion and collision frequency, thereby accelerating the succinylation reaction (Chi et al., 2008). However, at excessively high temperatures, such as 115°C, partial degradation or structural disruption of the starch granules may occur, which can negatively affect the efficiency of the substitution reaction. Based on these findings, the optimal succinylation condition was achieved at 105°C, where the highest DS and reaction efficiency were observed. When combined with the optimal reaction time of 3.5 h, this temperature condition yielded the most effective modification of breadfruit starch. High temperatures cause starch to undergo gelatinization, leading to the formation of aggregates that hinder the succinylation reaction and reduce its effectiveness (Dewi et al., 2022).

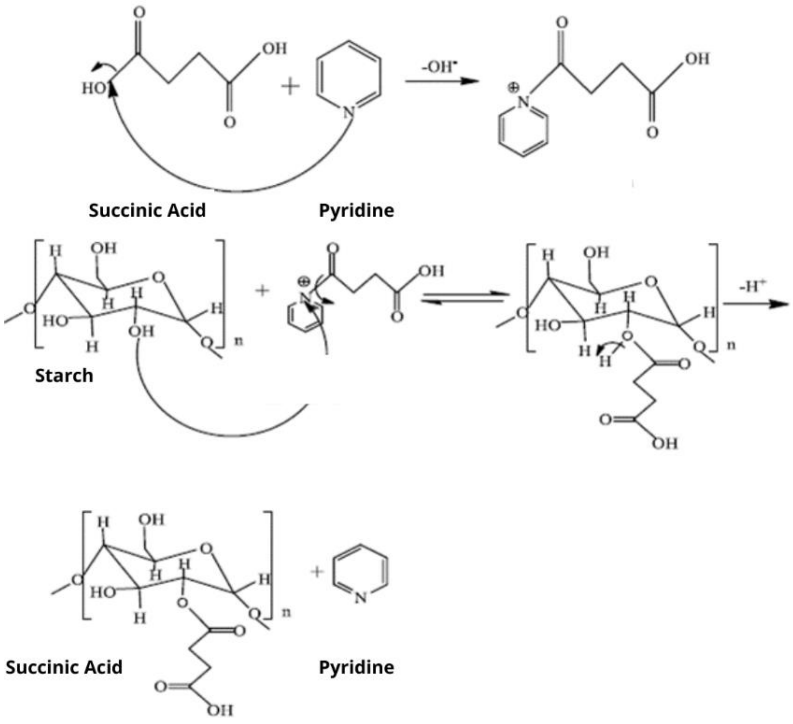

Figure 1. Reaction mechanism for the formation of modified starch

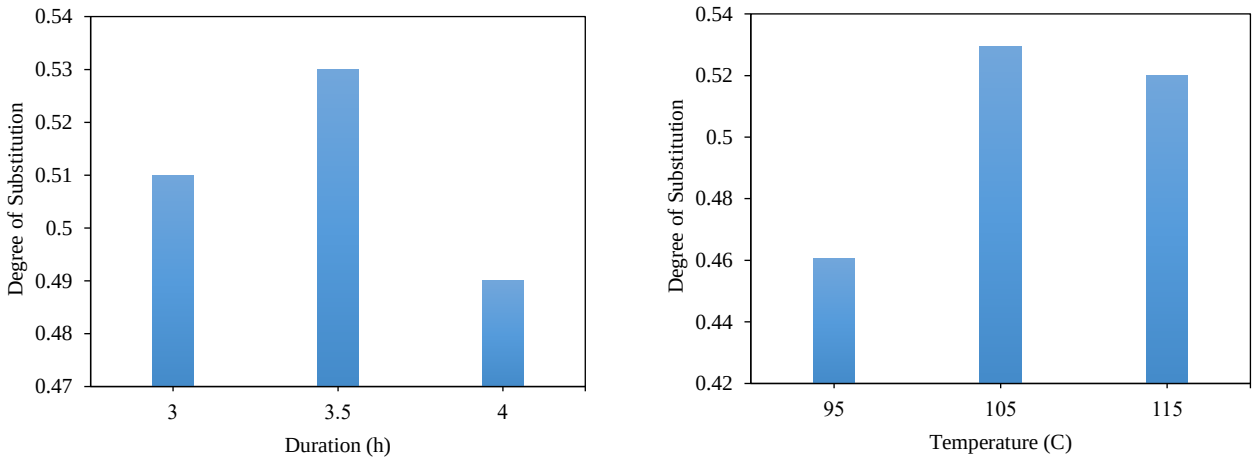

Figure 2. Degree of substitution value of modified breadfruit starch in different durations and the temperature of the reaction.

3.3 FTIR Analysis

FT-IR spectrophotometer test on breadfruit starch can be seen in Figure 3, which shows a spectrum with a peak vibration in the 3,265 cm^{-1} wave number region, indicating the -OH group. At wave number 2,922 cm^{-1}, the absorption shows the C-H alkane (-CH_3) stretching vibration. The absorption at wave number 1,640 cm^{-1} comes from rocking vibrations of -OH bound to water molecules contained in starch through hydrogen bonds the absorption band in the 1,334-1,500 cm^{-1} range shows bending vibrations on C-H. According to Chen et al. (2019), the area between 1,340 cm^{-1} to 1,500 cm^{-1} is the absorption area of rocking vibrations of C-H. The absorption band at wave number 1,148 cm^{-1} shows C-O stretching vibrations. Wave number 1,148 cm^{-1} shows the absorption of C-O stretching vibrations bound to the secondary alcohol hydroxyl group.

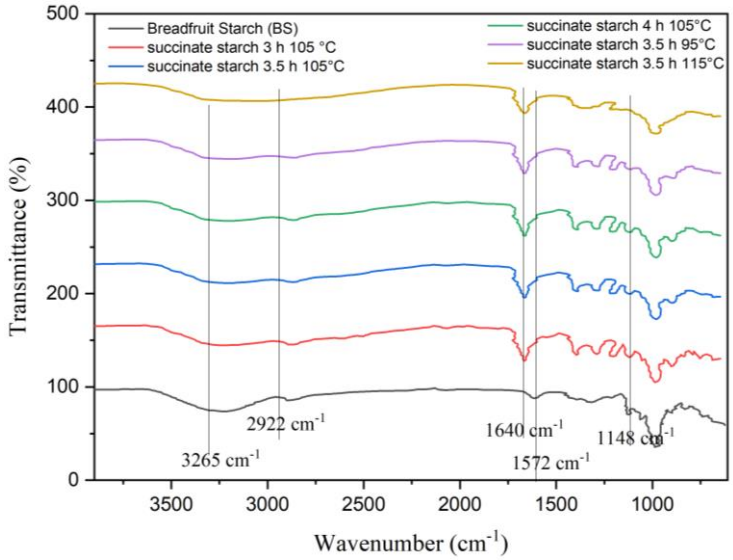

Figure 3. FT-IR spectra of isolated breadfruit starch (a), succinate starch 3 h 105°C (b), succinate starch 3.5 h 105°C (c), succinate starch 4 h 105°C (d), succinate starch 95°C 3.5 h (e), succinate starch 115°C 3.5 h (f).

The comparison of spectra between breadfruit starch (Figure 3) with succinic starch with time variation (Figure 3) showed a change in wave absorption bands, namely in the FT-IR spectrum of succinic starch with time variation showing the C=O ester group at 3 h wave number 1,692.2 cm^{-1} with low intensity, 3.5 h wave number 1,692.2 cm^{-1} with high intensity, 4 h wave number 1,692.2 cm^{-1} with low intensity. The comparison of the spectrum between breadfruit starch and succinic starch with temperature variation, shows a change in the absorption band, namely in the FT-IR spectrum of succinic starch with temperature variation showing the C=O ester group at 95°C wave number 1,692.2 cm^{-1} with medium intensity, at 105°C wave number 1,692.2 cm^{-1} with high intensity, at 115°C wave number 1,692.2 cm^{-1} with medium intensity. The band occurring at 1,572 cm^{-1} corresponds to the asymmetric stretching of the carboxylate RCOO group vibrations that are characteristic of esterified starch. In addition, the intensity of the absorption peaks around 1,692 cm^{-1} and 1,572 cm^{-1} increases as the degree of substitution increases, indicating that more OS groups are inserted into the starch (Hao et al., 2019). The higher intensity of the FT-IR spectrum indicates the increasing effectiveness of succinylation and the higher degree of substitution. In this study, the degree of substitution increased and decreased according to the intensity of the FT-IR spectrum.

3.4 Swelling power and solubility analysis

This study examined the swelling power and solubility of breadfruit starch and succinylated starch, as shown in Table 1. At the treatment condition of 3.5 h at 115°C, the starch sample exhibited a swelling power of 9.34% and a solubility of 57.32%. The increase in starch solubility is attributed to the higher heating of the starch suspension, which leads to the depolymerization of starch molecules, particularly amylose (Ojogbo et al., 2020). Depolymerized amylose consists of shorter and more linear chains that are more readily soluble in water. As a linear polymer, amylose naturally tends to dissolve in water, and this tendency increases when the molecular structure is

simplified due to thermal degradation. Therefore, the higher the heating temperature, the greater the extent of amylose breakdown, resulting in increased solubility of the starch. On the other hand, the increase in swelling power is related to a lower amylose content or a higher proportion of amylopectin in the starch. Amylopectin is predominantly located in the amorphous regions of starch granules. These amorphous regions are less dense and more porous, allowing water to penetrate more easily and causing the granules to swell. Thus, higher heating temperatures enhance the swelling power of starch by facilitating water absorption through the amorphous regions rich in amylopectin (Chen et al., 2020).

Table 1. Results of swelling power and solubility determination

Sample	Swelling power (%)	Solubility (%)	Sample	Swelling power (%)	Solubility (%)
Breadfruit starch	8.7646	29.80	-	-	-
3 h 105°C	8.8730	42.08	3.5 h 95°C	8.8372	30.88
3.5 h 105°C	9.0952	49.02	3.5 h 105°C	9.0952	49.02
4 h 105°C	10.5817	59.02	3.5 h 115°C	9.3449	57.32

Then, both swelling power and solubility of starch are strongly influenced by the molecular structure of starch, particularly the interactions between amylose and amylopectin, as well as the structural changes induced by thermal treatment. Succinylation modification alters these intermolecular hydrogen bonds by introducing bulky succinyl groups, which disrupt the native compact structure of starch. As a result, the molecular arrangement becomes more open and hydrophilic, thereby enhancing the starch's ability to absorb water and dissolve more easily. This structural disruption contributes significantly to the observed increases in both swelling power and solubility. The amorphous part is the part that absorbs water more efficiently. The more amylopectin in starch, the wider the amorphous area will be, so water absorption will be more excellent. It is known that swelling power in starch is influenced by water absorption. The greater the water absorption, the increased swelling power (Amari et al., 2021).

3.5 SEM analysis

SEM analysis was conducted to determine the modified starch compounds' morphology. In this study, SEM tests were carried out for breadfruit starch and succinate starch, which had the highest DS value, namely succinate starch with a time variation of 3.5 h at 105°C. Succinate reactions can change the structure of starch granules. This can be seen in succinic starch with a broken granule structure because breadfruit starch reacts with succinic acid compared to natural breadfruit starch granules. The granule shape of breadfruit starch and succinic starch is different at 5.000 times magnification, where the breadfruit starch granules are more rounded, while the succinic starch granules are more broken. This shows that adding succinic acid affects the shape of the starch granules (Luo et al., 2024). The morphology of breadfruit starch is shown in Figure 4(a), and the morphology of succinic starch is shown in Figure 4(b).

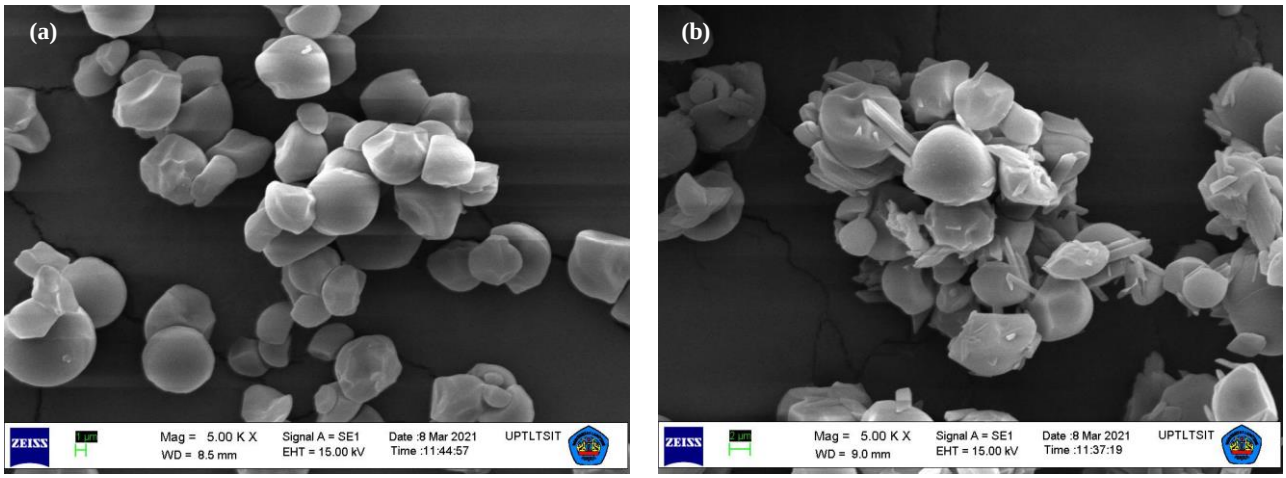

Figure 4. Morphology of breadfruit starch (a), starch succinate with time variation of 3.5 h at 105°C (b).

3.6 TGA analysis

Thermal properties describe the changes that occur during the heating of a starch until gelatinization occurs. These thermal properties can be analyzed using Thermogravimetric Analysis (TGA). The TGA pattern is presented in the form of the onset temperature (T0), peak temperature (Tp), and end temperature (Te). It also shows the changes in mass weight of the starch molecules that decrease as heat energy is applied. Based on Figure 5 for sample 0.5 h at 105°C, starch succinate has an onset temperature of 30°C, a peak temperature of 400°C, and an end temperature of 700°C. The decrease in temperature explains that starch succinate decomposes in three steps. At 150°C, the starch undergoes 10% decomposition, then decomposes at 400°C, resulting in a significant mass reduction of 82.9%, and finally loses mass at 650°C (94.7%). This aligns with the findings of Rudnik et al. (2005), which stated that starch decomposition begins at 150°C under both atmospheric and inert conditions. This indicates that the initiation of starch decomposition is non-oxidative. In addition to glass transition (TG) data, the DSC analysis includes a Differential Thermal Analysis (DTA) graph in Figure 5. DTA measures exothermic or endothermic changes with increasing temperature. The DTA curve shows an exothermic event, where a sharp peak appears at 420°C, corresponding to the complete breakdown of starch succinate (Wang et al., 2024).

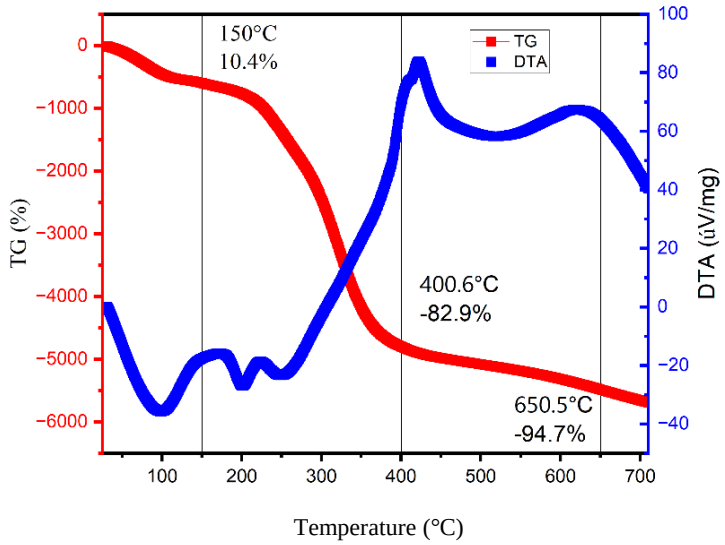

Figure 5. TGA graph

The data in the Table 2 shows the relationship among starch type, processing time, temperature, and degree of substitution (DS) in previous studies. Breadfruit starch processed for 2 h at 40°C had a DS value of 0.0241. Meanwhile, tannia (*Xanthosoma sagittifolium*) starch processed for 2 h at a higher temperature of 150°C had a greater degree of substitution (DS) of 0.0414. Cassava starch and Ginkgo starch, processed at a lower temperature (35°C) for 3 and 8 h respectively, showed smaller DS values of 0.008 and 0.006. Interestingly, Breadfruit starch in the designed study showed the highest DS value of 0.5293, which was much greater than the other samples. This indicates that the optimal combination of time and temperature can significantly increase the starch substitution rate. Based on the comparison of the degree of substitution (DS) value, the results are not worse than the previous research and are highly recommended for use in the industry (Altuna et al., 2018).

Table 2. Research results from previous studies

Sample	Time (h)	Temperature (°C)	Degree of substitution	Reference
Breadfruit starch	2	40	0.0241	Anwar et al. (2020b)
Tannia (*Xanthosoma sagittifolium*) starch	2	150	0.0414	Rosida et al. (2020)
Cassava starch	3	35	0.008	Zhang et al. (2017)
Ginkgo starch	8	35	0.006	Zheng et al. (2017)
Corn starch	3	40	0.086	Xie et al. (2024)
Potato starch	3	35	0.21	Chen et al. (2024)
Breadfruit Starch	3.5	105	0.5293	This study

4. CONCLUSION

This study successfully synthesized succinylated breadfruit starch through a succinylation reaction between native breadfruit starch and succinic acid using pyridine as a catalyst. The optimal reaction condition was achieved at 3.5 h and 105°C, yielding a degree of substitution (DS) value of 0.5293. The resulting modified starch appeared as a fine, homogeneous powder with a uniform texture. Fourier-transform infrared (FT-IR) spectroscopy confirmed the successful modification by detecting the characteristic ester carbonyl (C=O) absorption band at 1,692 cm^{-1}, indicating the formation of succinate ester groups. The succinylated starch synthesized under varying reaction times (3, 3.5, and 4 h) and temperatures (95, 105, and 115°C) exhibited increased swelling power and solubility compared to native starch. This enhancement is attributed to the molecular changes induced by the succinylation reaction and thermal treatment. Specifically, higher temperatures facilitate the depolymerization of amylose into shorter chains that are more soluble, while the increased proportion of amylopectin in the amorphous regions promotes greater water absorption and granule swelling. Thermogravimetric analysis (TGA) revealed that the starch underwent gelatinization in three distinct stages, with the most significant mass loss occurring at 400.6°C, corresponding to an 82.9% reduction in mass. Scanning Electron Microscopy (SEM) further demonstrated that succinylation altered the granule morphology; the starch granules became fragmented and exhibited surface disruption compared to the smooth, rounded granules of native breadfruit starch. These structural changes are consistent with the observed increases in swelling power and solubility, which were more pronounced with longer reaction times and higher temperatures. Overall, the results indicate that the succinylation reaction under optimized conditions effectively modifies the duration and temperature properties of breadfruit starch, enhancing its potential applicability in various industrial and food-related applications.

ACKNOWLEDGEMENTS

The authors would like to thank the Universitas Sumatera Utara for the TALENTA Universitas Sumatera Utara with contract number 399/ UN5.2.3.1/PPM/SPP-TALENTAUSU/2021.

AUTHORS CONTRIBUTION

Experimental run and Data Collection, Cut Fatimah Zuhra; Methodology, Validation, Supervision and Writing Original Draft Preparation, Andriayani.; Formal Analysis; Data Curation, Visualization, Writing - Review and Editing, Venny Angelina Siregar.

DECLARATION OF COMPETING INTEREST

The authors have no conflict of interest to declare.

REFERENCES

Adebowale KO, Olu-Owolabi BI, Olawumi EK, Lawal OS. Functional properties of native, physically and chemically modified breadfruit (*Artocarpus artilis*) starch. Industrial Crops and Products 2005;21:343-51.

Alam M, Pant K, Brar DS, Dar BN, Nanda V. Exploring the versatility of diverse hydrocolloids to transform techno-functional, rheological, and nutritional attributes of food fillings. Food Hydrocolloids 2024;146:Article No. 109275.

Altuna L, Herrera ML, Foresti ML. Synthesis and characterization of octenyl succinic anhydride modified starches for food applications. A review of recent literature. Food Hydrocolloids 2018;80:97-110.

Amari A, Elboughdiri N, Ghernaout D, Lajimi RH, Alshahrani AM, Tahoon MA, et al. Multifunctional crosslinked chitosan/ nitrogen-doped graphene quantum dot for wastewater treatment. Ain Shams Engineering Journal 2021;12(4):4007-14.

Anwar SH, Hasni D, Rohaya S, Antasari M, Winarti C. The role of breadfruit OSA starch and surfactant in stabilizing high-oil-load emulsions using high-pressure homogenization and low-frequency ultrasonication. Heliyon 2020a;6(7):e04341.

Anwar SH, Hasni D, Rohaya S, Antasari M, Winarti C. The role of breadfruit OSA starch and surfactant in stabilizing high-oil-load emulsions using high-pressure homogenization and low-frequency ultrasonication. Heliyon 2020b;6(7):e04341.

Bhosale R, Singhal R. Process optimization for the synthesis of octenyl succinyl derivative of waxy corn and amaranth starches. Carbohydrate Polymers 2006;66(4):521-7.

Błaszczak W, Fornal J, Kiseleva VI, Yuryev VP, Sergeev AI, Sadowska J. Effect of high pressure on thermal, structural and osmotic properties of waxy maize and Hylon VII starch blends. Carbohydrate Polymers 2007;68(3):387-96.

van der Burgt YEM, Bergsma J, Bleeker IP, Mijland PJHC, van der Kerk-van Hoof A, Kamerling JP, et al. Distribution of methyl substituents in amylose and amylopectin from methylated potato starches. Carbohydrate Research 2000; 325(3):183-91.

Chabib L, Nursal, Miskam M, Mohd Kaus NH, Shafie MH, Hamid M, et al. Optimization of g-C3N4 nanoparticles on structural, morphological, and optical properties as organic pollutants adsorbent in glycerin. Case Studies in Chemical and Environmental Engineering 2025;11:Article No. 101057.

Chen R, Ma Y, Chen Z, Wang Z, Chen J, Wang Y, et al. Fabrication and characterization of dual-functional porous starch with both emulsification and antioxidant properties. International Journal of Biological Macromolecules 2024;264(2):Article No. 130570.

Chen Y, Dai G, Gao Q. Preparation and properties of granular cold-water-soluble porous starch. International Journal of Biological Macromolecules 2020;144:656-62.

Chen Y, Hao Y, Ting K, Li Q, Gao Q. Preparation and emulsification properties of dialdehyde starch nanoparticles. Food Chemistry 2019;286:467-74.

Chi H, Xu K, Wu X, Chen Q, Xue D, Song C, et al. Effect of acetylation on the properties of corn starch. Food Chemistry 2008;106(3):923-8.

Deng Y, Jin Y, Luo Y, Zhong Y, Yue J, Song X, et al. Impact of continuous or cycle high hydrostatic pressure on the ultrastructure and digestibility of rice starch granules. Journal of Cereal Science 2014;60:302-10.

Dewi AMP, Santoso U, Pranoto Y, Marseno DW. Dual modification of sago starch via heat moisture treatment and octenyl succinylation to improve starch hydrophobicity. Polymers (Basel) 2022;14:Article No. 1086.

Fatimah Zuhra C, Ginting M, Masyita A, Fithri Az-zahra W. Carboxymethyl starch synthesis from breadfruit starch (*Artocarpus Communis*) through esterification reaction with monochloro acetate. Proceedings of the 1st International MIPAnet Conference on Science and Mathematics IMC-SciMath; Medan, Indonesia; 2022. p. 143-8.

Fatimah Zuhra C, Ginting M. Effect of essential oil of attarasa leaves (*Litsea Cubeba* Lour. Pers) on physico-mechanical and microstructural properties of breadfruit starch-alginate edible film. Malaysian Journal of Analytical Sciences 2013; 17(3):370-5.

Hamid M, Dayana I, Satria H, Siregar MF, Rianna M, Wijoyo H. Chitosan/CNDs coated Cu electrode surface has an electrical potential for electrical energy application. South Africa Journal Chemistry Enginering 2024a;50:445-50.

Hamid M, Humaidi S, Wijoyo H, Isnaeni I, Saragi IR, Simanjuntak C, et al. Solvothermal synthesized N-S doped carbon dots derived from cavendish banana peel (*Musa paradisiaca*) for detection of Fe(III) and Pb(II). Case Studies in Chemical and Environmental Engineering 2024b;10:Article No. 100832.

Hamid M, Kaus NHM, Humaidi S, Isnaeni I, Daulay A, Saragi IR. Activated carbon from biomass waste candlenut shells (*Aleurites moluccana*) doped ZIF-67/Fe_3O_4 as advanced materials for supercapacitor. Material Science Energy Technologies 2024c;7:381-90.

Hamid M, Humaidi S, Saragi IR, Simanjuntak C, Isnaeni I, Azizah, et al. The effectiveness of activated carbon from nutmeg shell in reducing ammonia (NH_3) levels in fish pond water. Carbon Trends 2024d;14:Article No. 100324.

Hao Y, Chen Y, Li Q, Gao Q. Synthesis, characterization and hydrophobicity of esterified waxy potato starch nanocrystals. Industrial Crops and Products 2019;130:111-7.

Haydersah J, Chevallier I, Rochette I, Mouquet-Rivier C, Picq C, Marianne-Pépin T, et al. Fermentation by amylolytic lactic acid bacteria and consequences for starch digestibility of plantain, breadfruit, and sweet potato flours. Journal Food Science 2012;77(8):466-72.

Huang TT, Zhou DN, Jin ZY, Xu XM, Chen HQ. Effect of repeated heat-moisture treatments on digestibility, physicochemical and structural propertiokres of sweet potato starch. Food Hydrocolloid 2016;54:202-10.

Humaidi S, Hamid M, Wijoyo H. Study and characterization of BaFe12O19/PVDF composites as electrode materials for supercapacitors. Biosensor Bioelectronic X 2024;19:Article No. 100507.

Luo H, Liu Q, Sun Z, Liang D, Zheng Y, Zhao L, et al. Removal of the out-shell for lotus root starch improved the effect of heat-moisture modification on multi-structure, physicochemical and digestibility properties. Food Hydrocolloid 2024;151:Article No. 109865.

Mei JQ, Zhou DN, Jin ZY, Xu XM, Chen HQ. Effects of citric acid esterification on digestibility, structural and physicochemical properties of cassava starch. Food Chemistry 2015;187:378-84.

Nasr JJM, Al-Shaalan NH, Shalan SM. Sustainable environment-friendly quantitative determination of three anti-hyperlipidemic statin drugs and ezetimibe in binary mixtures by first derivative Fourier transform infrared (FTIR) spectroscopy. Spectrochimica Acta Part A: Molecular and Biomolecular Spectroscopy 2020;237:Article No. 118332.

Oderinde AA, Ibikunle AA, Bakre LG, Babarinde NAA. Modification of African breadfruit (*Treculia africana*, Decne) kernel starch: Physicochemical, morphological, pasting, and thermal properties. International Journal Biology Macromolecular 2020;153:79-87.

Ojogbo E, Ogunsona EO, Mekonnen TH. Chemical and physical modifications of starch for renewable polymeric materials. Materials Today Sustainability 2020;7-8:Article No. 100028.

Rosida, Finatsiyatull D, Nusandari R. Modification of native and hydrolyzed tannia (*Xanthosoma sagittifolium*) starch by succinic acid (succinylation). EurAsian Journal of BioSciences 2020:14(2):1-2

Rudnik E, Matuschek G, Milanov N, Kettrup A. Thermal properties of starch succinates. Thermochimica Acta 2005; 427(1-2):163-6.

Rumahorbo CGP, Ilyas S, Hutahaean S, Zuhra CF, Situmorang PC. The improvement of the physiological effects of Nanoherbal Sikkam leaves (*Bischofia javanica*). Rasayan Journal of Chemistry 2023;16:766-72.

Tan X, Li X, Chen L, Xie F, Li L, Huang J. Effect of heat-moisture treatment on multi-scale structures and physicochemical properties of breadfruit starch. Carbohydrat Polymer 2017;161:286-94.

Tan X, Zhang B, Chen L, Li X, Li L, Xie F. Effect of planetary ball-milling on multi-scale structures and pasting properties of waxy and high-amylose cornstarches. Innovative Food Science and Emerging Technologies 2015;30:198-207.

Volkert B, Lehmann A, Greco T, Nejad MH. A comparison of different synthesis routes for starch acetates and the resulting mechanical properties. Carbohydrat Polymer 2010;79(3):571-7.

Wang X, Chen L, Li X, Xie F, Liu H, Yu L. Thermal and rheological properties of breadfruit starch. Journal Food Science 2011;76(1):55-61.

Wang Yitong, Teng H, Bai S, Li C, Wang Ye, Ma L, et al. Pickering emulsion of camellia oil stabilized by Octenyl succinic acid starch: Interaction, lipid oxidation and digestibility. International Journal Biology Macromolecular 2024;279:Article No. 135108.

Wongsagonsup R, Varavinit S, BeMiller JN. Increasing slowly digestible starch content of normal and waxy maize starches and properties of starch products. Cereal Chemistry 2008;85(6):738-45.

Xie F, Liu X, Liu N, Feng X, He Z, Din Z ud, et al. Effect of degree of substitution of octenyl succinate on starch micelles for synthesis and stability of selenium nanoparticles: Towards selenium supplements. International Journal Biology Macromolecular 2024;280:Article No. 135586.

Zhang B, Mei JQ, Chen B, Chen HQ. Digestibility, physicochemical and structural properties of octenyl succinic anhydride-modified cassava starches with different degree of substitution. Food Chemistry 2017;229:136-41.

Zhang L, Xie W, Zhao X, Liu Y, Gao W. Study on the morphology, crystalline structure and thermal properties of yellow ginger starch acetates with different degrees of substitution. Thermochima Acta 2009;495(1-2):57-62.

Zheng Y, Hu L, Ding N, Liu P, Yao C, Zhang H. Physicochemical and structural characteristics of the octenyl succinic ester of ginkgo starch. International Journal Biology Macromoleculerl 2017;94:566-70.

Zuhra CF, Ginting M, Azzahra WF, Hardiyanti R. Synthesis of bread fruit (*Artocarpus communis*)-based hydroxypropyl starch through etherification using propylene oxide. Rasayan Journal of Chemistry 2020;13:2445-54.

Zuhra CF, Sinaga MZE, Suharman, Situmorang PJ. Preparation of starch from breadfruit (*Artocarpus altilis*) with dual modification through oxidation and cross-linking methods. Applied Food Research 2025;5(1):Article No. 100787.

Environment and Natural Resources Journal

Volume 23
Issue 5
2025

Effect of Climate Variability on Chili Pepper (*Capsicum frutescens* L.) Cultivation in Indonesia

Bayu Dwi Apri Nugroho[1*], Aristya Ardhitama[1,2], Junun Sartohadi[3], Muamar Qadafi[4], Bowo Dwi Siswoko[5], and Afifatul Husna Al Adilah[6]

[1]*Department of Agricultural and Biosystems Engineering, Faculty of Agricultural Technology, Universitas Gadjah Mada Yogyakarta, Indonesia*
[2]*BMKG - Climatology Station of Yogyakarta, Sleman, Yogyakarta, Indonesia*
[3]*Department of Soil Science, Faculty of Agriculture, Universitas Gadjah Mada, Yogyakarta, Indonesia*
[4]*Research Center for Environmental and Clean Technology, National Research and Innovation Agency (BRIN), Indonesia*
[5]*Department of Forest Management, Faculty of Forestry, Universitas Gadjah Mada, Yogyakarta, Indonesia*
[6]*Center of Land Resources Management, Universitas Gadjah Mada, Sleman, Yogyakarta, Indonesia*

ARTICLE INFO

Received: 17 Apr 2025
Received in revised: 20 Jun 2025
Accepted: 24 Jun 2025
Published online: 22 Jul 2025
DOI: 10.32526/ennrj/23/20250097

Keywords:
ENSO/ Chili productivity/ Climate factors/ Rainfall variability/ Seasonal variability/ Statistical analysis

*** Corresponding author:**
E-mail: bayu.tep@ugm.ac.id

ABSTRACT

Significant shifts in climate patterns, particularly in rainfall and frequency of rainy days, are factors contributing to high variability in cultivation of agricultural products such as chili peppers. Therefore, this study investigated the impact of seasonal climate variability on chili pepper (*Capsicum frutescens* L.) production in Sleman Regency, of Central Java, Indonesia. Statistical methods including analysis of variance (ANOVA), principal component analysis (PCA), and Pearson correlation were used to examine the influence of various climate and seasonal factors such as rainfall, air temperature, humidity, rainy days, dry season onset, and duration on chili productivity. The results showed that total rainfall and frequency of rainy days significantly affected chili productivity, with correlation coefficients of +0.579 and +0.492 ($p<0.05$), and ANOVA confirming a strong relationship ($F=260.75$, $p<0.001$). This showed that rainfall distribution and frequency were critical factors influencing yield variability. Statistical analyses correlated with climate variability index calculations further confirmed significant climate changes in the region. Based on the results, both total rainfall and seasonal distribution were critical factors influencing chili pod productivity, emphasizing the importance of agricultural planning and adaptation strategies under changing climate conditions. The novelty of this study was in local-scale seasonal analysis, which used a climate variability index to detect extreme variability. When combined with multivariate statistical triangulation (correlation, PCA, and ANOVA), it offered robust evidence for region-specific adaptation strategies for chili farmers. The results showed the importance of including climate indicators in agricultural policy planning. Moreover, further studies were recommended to explore spatial climate trends across broader regions.

HIGHLIGHTS

- Climate data from 2010-2023 is analyzed for chili productivity trends.
- Rainfall and rainy days show a strong correlation with productivity.
- PCA identifies rainfall as the dominant factor influencing chili yield.
- ANOVA confirms rainfall's significant effect on yield variability.
- Study offers local adaptation insights for climate-sensitive crops.

1. INTRODUCTION

Indonesia is recognized as one of the world's most agriculture-dominated nations, where the sector serves as a cornerstone of the national economy (Hajad et al., 2023). The abundant natural resources, tropical climate, year-round sunshine, sufficient water availability, and fertile soils provide highly favorable conditions for agricultural development (Malihah,

Citation: Nugroho BDA, Ardhitama A, Sartohadi J, Qadafi M, Siswoko BD, Adilah AHA. Effect of climate variability on chili pepper (*Capsicum frutescens* L.) Cultivation in Indonesia. Environ. Nat. Resour. J. 2025;23(5):459-468. (https://doi.org/10.32526/ennrj/23/20250097)

2022). A significant portion of the population depends on this sector, where the majority is engaged in farming activities, making farmers significant contributors to national food production and rural livelihoods (Arvianti et al., 2019; Khotimah and Purnomo, 2018). Fertile soils are among key assets in Indonesia, advancing the agricultural sector (Pewista and Harini, 2013; Rondhi et al., 2018).

The availability of natural resources offers substantial opportunities for cultivating various food and horticultural crops (Setiyanto and Pasaribu, 2021). Among these crops, chili pepper (*Capsicum frutescens* L.) is a high-value commodity (Pertami et al., 2022). In addition to the economic importance, chili plays an essential role in Indonesian cuisine by contributing the distinctive spiciness and nutritional value (Siebert et al., 2022; Aprilia et al., 2023). However, the volatility of chili prices and supply often triggers public as well as governmental concerns, directly influencing national inflation and food security (Zelviyani, 2022).

The rising demand for chili production has driven both land expansion and production intensification, including through large-scale agricultural initiatives such as "food estates." National development strategies for chili focus on four objectives, namely ensuring year-round availability, stabilizing market prices, reducing imports, and boosting exports (Swastika et al., 2017). Despite these efforts, chili pepper is highly sensitive to environmental and climate factors, particularly temperature, humidity, and precipitation. Moreover, optimal growth occurs at temperatures between 24-28°C and humidity levels of 78-88%, with a weekly water requirement of approximately 2.5 to 3.5 cm (Yahwe and Isnawaty, 2016).

The sensitivity to environmental factors makes chili pepper vulnerable to climate variability and extreme weather events, leading to flower drop, crop failure, as well as high pest and disease outbreaks (Ayu et al., 2021). Climate change disrupts traditional agricultural practices by altering planting schedules, sowing periods, and overall yield as well as quality (Hidayati and Suryanto, 2015). For chili and other vegetable crops, intense rainfall causes direct damage, fostering fungal and bacterial diseases such as anthracnose, potentially reducing yields by approximately 50% (Emilia, 2020; Ardhitama et al., 2025).

Although previous studies have identified key climate factors influencing agricultural productivity, the specific seasonal impacts on chili yield remain underexplored (Herlina and Prasetyorini, 2020). Due to the varying climate changes, generalizations regarding temperature and humidity effects are insufficient without localized analysis. Therefore, this study aimed to investigate the impact of seasonal climate variability on chili pepper (*Capsicum frutescens* L.) production in Sleman Regency, Central Java, Indonesia. The experiment was conducted in Sleman Regency, Central Java, designated as a national chili production center under Decree No. 472/Kpts/RC.040/6/2018.

Despite the strategic role, there is limited understanding of how seasonal climate variability affects chili productivity in this region. Although several studies have explored the effect of rainfall on crop productivity, there is still limited quantitative analysis of seasonal climate variability using statistical indices and combined statistical validation at the local level in high-value horticultural crops like chili. Few studies have also focused on strategic agricultural regions like Sleman Regency, where climate risks are compounded by orographic and monsoonal influences.

The novelty of this study is in the focus on seasonal shifts, the application of climate variability indices, and the use of multivariate statistical analysis (PCA, ANOVA, and Pearson correlation) to validate the influence of several factors on productivity. The results are expected to offer practical adaptation strategies for local farmers. Additionally, this study explores the influence of seasonal rainfall and frequency of rainy days on chili production, providing locally relevant adaptation recommendations to enhance agricultural resilience under climate change.

2. METHODOLOGY

This study was conducted in Sleman Regency, Yogyakarta, located at coordinates 110°18'47" to 110°29'50" E and 7°34'13" to 7°49'57" S from August to December 2023, using secondary data collected between 2010-2023. Climate data (rainfall, rainy days, and temperature) were obtained from the BMKG Climatology Station, while chili productivity data were from the Sleman Agriculture Department. A statistical method was applied to analyze the influence of weather and climate variability on chili productivity.

Sleman Regency is located on the southern slope of Mount Merapi in the Yogyakarta Special Region, Java Island. This region is characterized by undulating to mountainous terrain, which contributes

to the unique rainfall pattern through orographic influences. Figure 1 shows the administrative boundaries and key topographic features relevant to the spatial variability of climate.

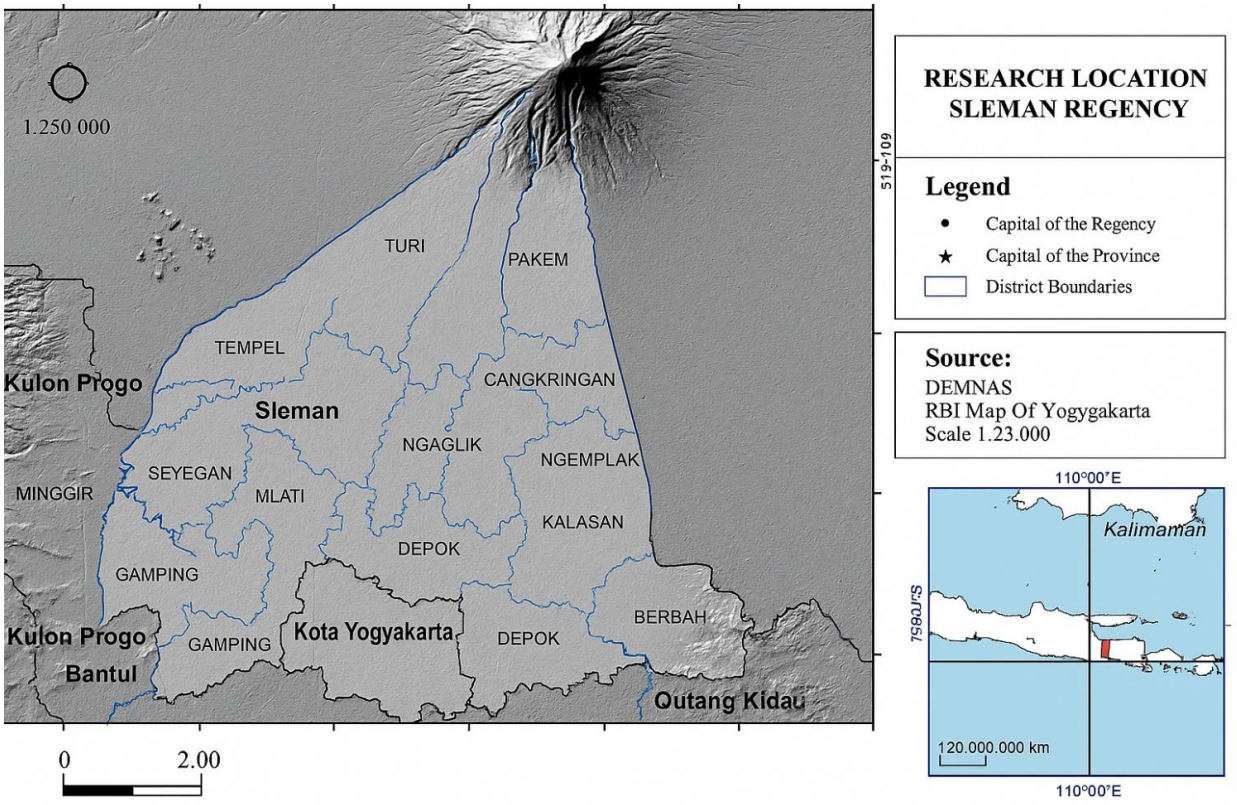

Figure 1. Map of study location

Secondary data were collected from the Sleman Geophysics Station under the BMKG Climatology Station of the Special Region of Yogyakarta. The data obtained covered rainfall, rainy days, humidity, temperature, onset and shift of dry season, dry season rainfall characteristics, and dry season duration for the 2010-2023 period. Data on chili pepper productivity and harvested region for the same period were obtained from the Sleman Department of Agriculture, Food, and Fisheries. The analysis focused on evaluating the influence of climate factors on chili productivity in Sleman Regency from 2010 to 2023. The onset and retreat of the wet and dry seasons were determined using BMKG's rainfall-based thresholds, where the start of the rainy season was defined by a sequence of five consecutive days with rainfall ≥50 mm. Seasonal duration was calculated based on monthly rainfall distribution. These definitions were consistently applied to ensure objectivity and transparency in seasonal classification across years. The stages of data processing in this study comprised, analysis of climate change variability, which included calculating climate data as follows:

$$\text{Variability} = (90p - 10p) / 50p \quad (1)$$

Climate change variability is found by taking away the rainfall amount at the 90th percentile from the 10th percentile value, and then this number is divided by the value obtained at 50th percentile. (Eldridge and Beecham, 2017). The values of climate factors in region are essential indicators of variability coefficient, as shown in Table 1.

Table 1. Climate variability coefficient

Variability coefficient	Category
0-0.50	Low
0.50-0.75	Low to moderate
0.75-1.00	Moderate
1.00-1.25	Moderate to high
1.25-1.50	High
1.50-2.00	Very high
>2.00	Extreme

Source: Eldridge and Beecham (2017)

Conducting chili productivity analysis from 2010 to 2023 in Sleman Regency using the following calculations:

Productivity = (Production (Kw))/(Harvested area) (2)

In order to see how climate affects chili productivity, this study checked the connection between rainfall, temperature, rainy days, when the dry season starts and ends, and some farming activities like harvested area. The objective was to find out how much these weather parts matter for chili production.

Before performing the actual analysis, the data from 2010 to 2023 was looked at to ensure availability and followed a normal pattern. If any data was missing, methods like filling in gaps with straight lines or using average values from seasons were used to fix it for everything to be consistent over the 14 years. The ways to study the data were picked based on usual practices in climate and farming practices. Pearson correlation was used to tell whether there was a strong or weak connection between each climate factor and how much chili was produced. To check more things at the same time and facilitate easy understanding, PCA was used to point out the most important factors. ANOVA helped to check if differences in rainfall or rainy days really made a difference in how much chili was grown.

All the analysis was done in RStudio using known packages like stats, car, FactoMineR, and factoextra. PCA was useful in picking out which weather things had the most effect on changes in productivity. This methodological framework reflects current advances in data-driven climate-agriculture studies, offering valuable insights by integrating multiple statistical methods for robust interpretation. The results have the potential to contribute novel understanding to the field, particularly in the context of climate variability impacts on horticultural production in tropical regions.

Climate data on rainfall, temperature, and rainy days were obtained from the Gamping Climatology Station, which served as the primary reference for Sleman Regency. However, this study used meteorological data from a single climatological station, which might not fully capture the microclimatic heterogeneity across this region. The limitation could affect the generalizability of the results and was acknowledged in the interpretation of the results.

This study applies a triangulated statistical method combining correlation, PCA, and ANOVA, each serving complementary purposes. Pearson correlation identifies the strength and direction of bivariate relationships between individual climate factors and productivity. PCA is used to reduce dimensionality and detect the most influential factors among multiple correlated indicators. ANOVA is applied to test whether differences in productivity across climate categories (high vs. low rainfall years) are statistically significant. These tools enable a comprehensive and layered interpretation of how seasonal climate variability affects chili productivity at local level.

3. RESULTS AND DISCUSSION

3.1 Analysis of chili productivity in Sleman Regency

The productivity of chili pepper in Sleman Regency from 2010 to November 2023, measured in quintals per hectare (q/ha), shows considerable fluctuation, as presented in Figure 2. The time-series analysis shows an unstable trend, with productivity ranging between 22 and 37 q/ha over the 14-year period. Based on the results, the highest yield was recorded in 2010, while the lowest occurred in 2022 and 2023, showing the influence of environmental and climate factors.

The fluctuation in chili production in Sleman Regency seem to be much because of changes in climate. One big reason for this is how the El Niño-Southern Oscillation (ENSO) affects the rain. During years with El Niño, like 2015, 2019, and 2023, it rained significantly less, and chili yields also dropped. On the other hand, in La Niña years such as 2011, 2020, and 2022, there was more rain, which had mixed results, sometimes helping and affecting crops. This shows that large climate system like ENSO affects local rain patterns and can really change how much chili is grown in the region.

Recent studies indicate that Sleman Regency has been increasingly affected by climate disturbances associated with El Niño and La Niña events (Siswanto et al., 2022). During El Niño years 2015, 2019, and 2023 chili productivity declined markedly, reaching 25 q/ha in 2015, decreasing further to 22 q/ha in both 2019 and 2023. The drop in chili production matches with dry conditions and hotter weather that usually come with El Niño, which makes water harder to get and slows down photosynthesis, limiting much yield (Aditya et al., 2021). But in La Niña years like 2011, 2020, and 2022, productivity was also affected, rising substantially in 2020. Even though La Niña represents more rain and cooler air that can help plants grow better at first, too much rain is not good for productivity. It can flood the soil and bring more root problems, which makes the crops less healthy. A good example is the Triple Dip La

Niña from 2020 to 2022, which showed how longer periods of this kind of weather can be risky (Anggraini et al., 2022). This shows that climate factors do not always work the same way and can have complicated effects on farming.

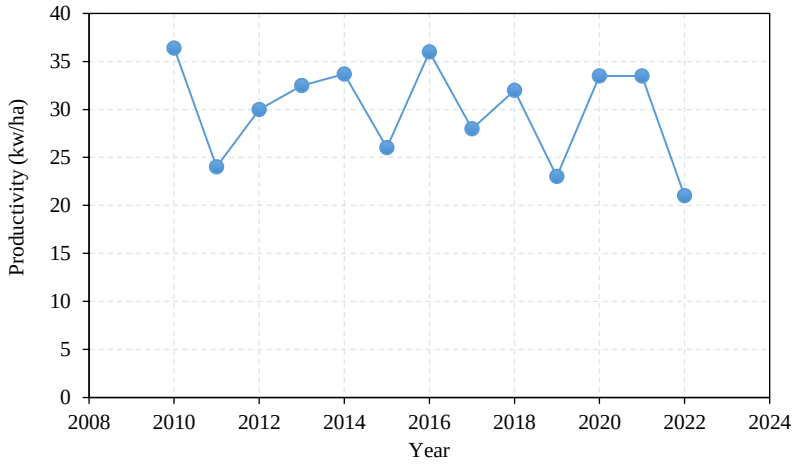

Figure 2. Calculation of chili pod productivity in Sleman Regency 2010-2023

3.2 Climate variability analysis

At the Gamping Geophysical Station, calculations were conducted for each climate factor, namely rainfall, air temperature, air humidity, and rainy days. The analysis was conducted to examine the response to climate factors that occurred between 2010 and 2023. From the calculation results in Table 2, climate variability values indicate that factors experiencing changes over the 14-year period are rainfall as well as the frequency of rainy days. Rainfall and rainy days have average variability values of 1.84 and 1.18, respectively. Based on the Climate Variability Index (CVI), rainfall showed very high variability, while frequency of rainy days had medium to high variability. In comparison, air temperature and relative humidity showed low inter-annual changes, with CVI values below 0.05, indicating minimal fluctuations during this study.

Table 2. Calculated value of climate variability

Year	Rainfall	Temperature	Relative humidity	Number of rainfall days
2010	1.30	0.03	0.05	0.45
2011	1.63	0.10	0.25	1.15
2012	1.29	0.05	0.54	1.14
2013	2.32	0.06	0.09	1.10
2014	2.37	0.07	0.12	1.28
2015	1.68	0.08	0.13	1.04
2016	0.92	0.04	0.04	0.51
2017	2.71	0.05	0.07	1.28
2018	2.46	0.10	0.06	1.39
2019	2.66	0.11	0.12	1.39
2020	1.86	0.04	0.10	1.24
2021	1.44	0.03	0.07	1.64
2022	1.15	0.04	0,07	0.97
2023	2.03	0.06	0.09	1.92
rata-rata	1.84	0.06	0.13	1.18

Source: Data Processed 2023

Rainfall intensity, distribution, and frequency of rainy days in Sleman Regency have been increasingly influenced by climate change, showing high variability compared to other equatorial regions such as West Kalimantan (Firdauzi and Suarma, 2023). Compared to Sleman, which is in the southern

monsoonal zone of Java with strong orographic effects, West Kalimantan is situated near the equator with flatter terrain and more uniform rainfall patterns. Although rainfall in equatorial climate tends to be more evenly distributed throughout the year, making seasonal shifts less pronounced, Sleman shows greater fluctuation in rainfall distribution. This is due to the geographical position and topographic complexity, which amplify the sensitivity of rainfall to seasonal and climate changes. In equatorial zones, like West Kalimantan, rainfall variability is generally classified as medium, with stations showing minor fluctuations in specific months (Aditya et al., 2021). These regions typically experience two rainy seasons and a brief dry season, driven by the sun's apparent biannual passage across the equator, causing relatively small temperature and seasonal amplitude (Liebmann et al., 2014). In Sleman Regency, the changes between the wet and dry times are becoming more bigger, showing that the normal equator rain system is not happening like before (Azizah and Zaki, 2025; Sundararaj et al., 2024).

Table 3 is showing the information on the monthly data like rain, air temperature, humidity, number of rainy days, when the dry season starts, and how long the dry season. The data are obtained from 2010 until 2023. The rainfall is changing significantly, from very small (18.2 mm) to very high (567.3 mm), which is representing big variations every season and year. Rainy days are also very different, with numbers between 3 and 27 days in a month. Meanwhile, temperature and humidity are not changing much, with standard numbers being just 1.1°C and 4.3%. The dry season mostly starts at the end of May and can last from 2 months to 6 months. This kind of data numbers is used for helping to look at how much the climate is changing and the effect on farming and crop growing.

Table 3. Summary statistics of climate and seasonal factors in Sleman Regency (2010-2023)

Factors	Mean	Min	Max	Standard deviation	Unit	Notes
Rainfall (monthly total)	215.8	18.2	567.8	110.4	mm/month	Higher values in Nov-Mar (wet season)
Rainy days (monthly count)	14.1	3	27	5.6	days/month	Strong El Niño years had lowest values
Temperature (monthly mean)	27.4	24.3	30.9	1.1	°C	Relatively stable throughout the year
Relative Humidity	83.5	70	94	4.3	%	Higher during La Niña periods
Dry season Onset (average)	3rd week of May	April	June	-	-	Defined per BMKG onset criteria (5 consecutive dry days)
Dry season duration	4.2	2	6	1.2	months	Shorter in La Niña, longer in El Niño years

When comparing, Sleman Regency is considered to be tropical monsoon and also has orographic rain, which is the reason why the rainfall is more changing. The wet season has not many rainy days but many dry ones, which shows the rain is not spread properly. This is similar to what was found by Eldridge and Beecham (2017), who stated that places with mountains and high lands usually get more changing rain than regions near the sea. Since Sleman is on the side of Mount Merapi, the rain is affected by the mountain, where going up in height makes more rain problems happen.

Rainfall changes are very much affected by year-to-year climate factors like El Niño and La Niña, the Indian Ocean Dipole (IOD), and temperature in the sea near south Java (Izumo et al., 2020; Jun-Ichi et al., 2012; Pothapakula et al., 2020). These reasons make rain patterns more complicated, showing that the region is more prone to bad climate and needs special plans to help farming be better prepared.

3.3 Analysis of correlation coefficient values for climate and seasonal factors

The results of the correlation coefficient calculations relating productivity with climate and seasonal factors were computed individually. Table 4 shows the calculation results, indicating that the influential factors were rainy days and rainfall, with correlation coefficient values of +0.579 and +0.492, respectively. Among the 8 climate factors, only 2 showed Pearson correlation coefficients that were significant, with values exceeding 0.5. This showed a fairly strong relationship between chili productivity as well as climate and seasonal factors.

Table 4. Pearson correlation between climate and seasonal factors on chili productivity

	Rainfall	Temperature	RH	Number rainfall days	Start season	Shift	Season characteristics	Duration
Productivity	**0.579***	-0.049	0,045	**0.492****	0.083	0.083	0.218	-0.326

Note: *,** = p value<0.05 was taken to be significant. Source: Data Processed, 2023

Pearson correlation coefficient was calculated at a significance level of 0.05 to analyze the relationship between climate variability and chili productivity. Table 4 shows that the most influential factors were rainy days and rainfall, with correlation coefficients of +0.579 and +0.492, respectively. This showed a positive and fairly strong linear relationship between these climate factors and chili productivity. Generally, rainfall plays a key role in providing the necessary water for chili plant growth, which significantly impacts productivity, particularly in regions like Sleman Regency. Seasonal variability, particularly in rainfall intensity and temporal distribution, also affects chili productivity (Firdauzi and Suarma, 2023).

Excessive rainfall can negatively impact chili, due to high sensitivity to waterlogging. Chili requires specific water conditions to thrive, and prolonged rainfall can disrupt this balance, affecting plant growth. Therefore, chili growers often plant at seasonal transitions to avoid waterlogged conditions capable of hindering root respiration and overall plant health (Jinagool and Arom, 2023). In addition to rainfall, the onset and duration of dry season also influence productivity. This study found a weak correlation (0.218) between the dry season's characteristics and productivity. There was also a slightly stronger inverse correlation (0.326) between the length of the dry season and productivity. However, the onset and advance of the dry season did not significantly impact chili productivity.

A study in Malang Regency showed a different pattern, where the relationship between productivity as well as rainfall and temperature was weaker, with air humidity being the most influential factor on chili productivity (Ridho and Suminarti, 2020). In contrast to Malang Regency, with lower annual rainfall variation due to coastal proximity and differing agroclimatic zoning, Sleman Regency shows more pronounced dry season extremes. This suggests that temperature and humidity consistently affect different regions. For instance, excessive humidity from heavy rainfall can delay pollination, thereby promoting fungal growth, pests, and diseases, which negatively impact chili productivity (Ferdiyanto and Sujono, 2018). In one study about corn growing in Malang Regency, the air temperature was found to be the biggest thing that affected productivity. Rainfall did not have much effect because the amount of rain every month was already enough for the corn to get water (Herlina and Prasetyorini, 2020). This is showing that different crops need climate factors, because of variations across regions.

Table 5 summarizes the key statistical results showing that rainfall and rainy days consistently become the dominant factors influencing chili productivity in Sleman Regency. The correlation coefficients ($r=0.579$ and 0.492, respectively; $p<0.05$) indicate a moderate to strong positive relationship. These results are further supported by PCA analysis, where both factors contribute significantly to the variance in productivity. Additionally, ANOVA confirmed significant differences in productivity across different levels of these factors ($F=260.75$, $p<0.001$).

The results from three methods, correlation, PCA, and ANOVA, all showed that rainfall and rainy days are very important for chili productivity. Using these methods helped make the understanding more sure and matched with other studies in tropical places where rainfall was mostly the main factor stopping crops from growing well (Guido et al., 2020; Eldridge and Beecham, 2017). Although the correlation coefficients fall within a moderate range ($r=0.579$ and 0.492), their statistical significance ($p<0.05$) and consistent confirmation across multivariate analyses support their validity. More importantly, these results emphasize that, among various fluctuating factors, rainfall both in total volume and temporal distribution remains the most actionable and policy-relevant parameter for climate-sensitive crops such as chili.

There is a need to contextualize these findings in light of spatial variations reported in the literature. Some studies, particularly those conducted in more hydrologically stable or lowland regions, have found that rainfall does not significantly influence productivity. These differences show variations in agroecological regions, farming systems, and rainfall sufficiency thresholds. In comparison, Sleman

Regency experiences high seasonal rainfall variability due to orographic and monsoonal dynamics, making rainfall a far more critical determinant of crop outcomes. Therefore, this study shows the importance of conducting localized climate-productivity assessments focusing on regional conditions.

Table 5. Summary of statistical results on climate factors influencing chili productivity in Sleman Regency (2010-2023)

Method	Factors	Key result	Significance
Pearson correlation	Rainfall, Rainy Days	R=0.579, 0.492	p<0.05
PCA	Rainfall, Rainy Days	Dominant components	Cumulative variance < 80%
ANOVA	Rainfall, Rainy Days	F=260.75	p<0.001

In line with this study, rainfall and rainy days are dominant predictors, although other agronomic factors such as fertilizer application, pest outbreaks, irrigation management, seed variety, and market access also contribute significantly to productivity. These non-climate factors are not included due to data availability constraints, and their exclusion limits the comprehensiveness of the analysis. Therefore, future studies should consider integrating both climate and non-climate factors in a multivariate framework to develop a more holistic understanding of the determinants of chili productivity.

3.4 PCA analyses between climate variability and productivity

The PCA results for rainfall and rainy days in Figure 3 show that the total variance value is under 80%, which means it is important. By using PCA on the data about chili productivity and climate, the main part of the analysis was found to affect chili farming the most. These results provided more details about how much each climate and season factor added to the changes in chili productivity. Rainfall and rainy days were the biggest components that had the most effect on the change in chili pod productivity values.

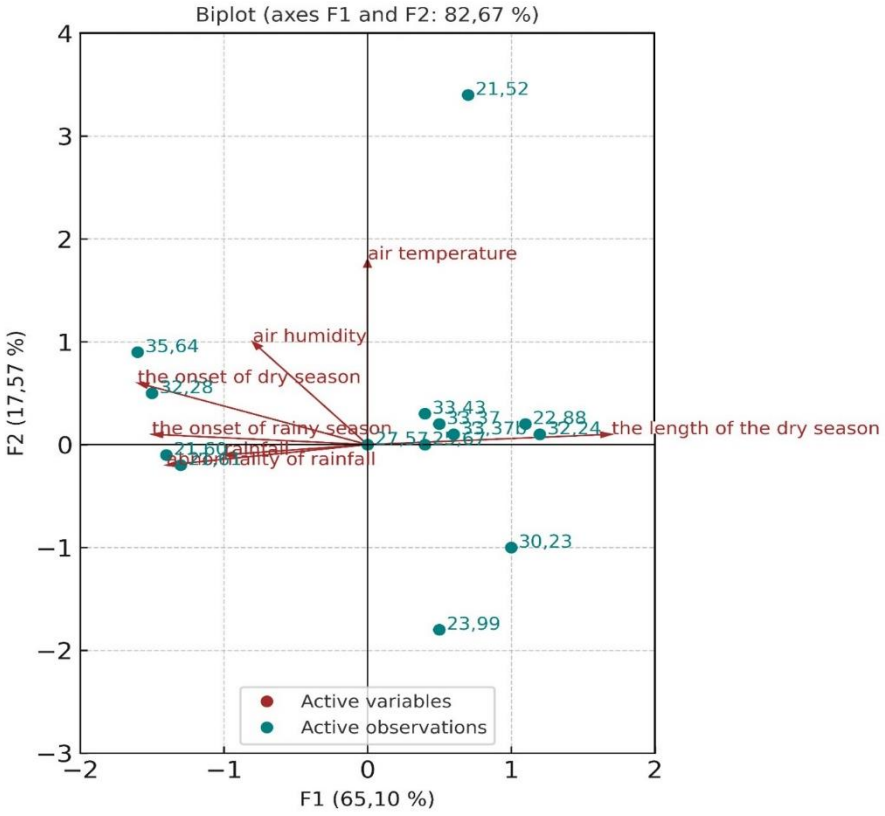

Figure 3. Principal component analysis results

The PCA results in Figure 3 showed that rainfall and rainy days were the main factors causing changes in productivity, with the total variance being less than 80%. To find which factors were most important, the analysis looked at three things, namely scree plot line, how much was explained in total, and eigenvalue. Because rainfall data is very important for how crops grow, knowing how rain occurs in each area is needed to help with making choices in farming (Guido et al., 2020). In some places, rain may not have a big effect on farming productivity (Aditya et al., 2021).

3.5 ANOVA analysis

ANOVA analysis of climate and seasonal factors as the main components influencing chili commodity (Table 4). After PCA results identified rainfall and rainy days as influential, ANOVA analysis was performed to observe the relationship between rainfall, rainy days, and chili productivity. The results showed that factors related to rainy days and rainfall significantly affected chili productivity. With a p-value<0.05, production was significantly impacted by the significant differences between the two factors, as shown in Table 6.

Table 6. Results of ANOVA analysis of the relationship between climate factors and productivity

Source of variation	SS	df	MS	F	p-value	F crit
Between groups	42228656	2	21114328	260.7484	2.6828E-23	3.238096
Within groups	3158059	39	80975.86			
Total	45386715	41				

Note: p-value<0.05 was taken to be significant. Source: Data Processed, 2023

4. CONCLUSION

In conclusion, this study showed that chili productivity in Sleman Regency was significantly influenced by climate factors, particularly rainfall and rainy days. The correlation analysis showed a positive relationship between these factors and chili productivity, with coefficients of +0.579 for rainy days and +0.492 for rainfall, indicating a moderately strong association. PCA further confirmed that rainfall and rainy days were the most influential factors contributing to productivity variability, accounting for a substantial proportion of the overall variance. Furthermore, ANOVA analysis supported these results, showing the significant role of seasonal and climate factors in determining chili productivity. This study also showed that changes in climate variability, particularly in rainfall patterns, had become more pronounced in recent years, further emphasizing the impact of climate change on agricultural productivity. Moreover, future studies should focus on integrating non-climate variability such as agronomic practices and socio-economic factors to build a more comprehensive resilience model. The investigations should be carried out by exploring spatial climate patterns and incorporating additional factors to provide a more comprehensive understanding of the factors affecting crop productivity in Sleman Regency.

ACKNOWLEDGEMENTS

This study is supported by the Research Center for Land Resources Management, Universitas Gadjah Mada.

AUTHOR CONTRIBUTIONS

Conceptualization, B.D.A.N and A.H.A.A.; Methodology, B.D.A.N.; Software, B.D.A.N.; Validation, B.D.A.N and J.S.; Formal Analysis, B.D.A.N and A.H.A.A.; Investigation, B.D.A.N.; Resources, M.Q.; Data Curation, B.D.A.N.; Writing-Original Draft Preparation, B.D.A.N.; Writing-Review and Editing, A.H.A.A and J.S.; Visualization, B.D.A.N.; Supervision, J.S and B.D.S.; Project Administration, B.D.A.N.; Funding Acquisition, A.H.

DECLARATION OF CONFLICT OF INTEREST

The authors declare that there are no conflicts of interest.

REFERENCES

Aditya F, Gusmayanti E, Sudrajat J. The Impact of Rainfall Changes on Paddy Field Productivity in West Kalimantan. Jurnal Ilmu Lingkungan 2021;19(2):237-46 (in Indonesian).

Anggraini SD, Pane R, Haya SF. Food price highlights during the pandemic and the 2022 La Niña threat in Indonesia. Jurnal Ilmu Komputer Ekonomi dan Manajemen 2022;2(1):205-15 (in Indonesian).

Aprilia SE, Susilawati S, Hermawan A. Effectiveness pruning and planting media on the morphology and results of floating red chilies. Biovalentia: Biological Research Journal 2023; 9(2):97-102.

Ardhitama A, Nugroho BDA, Sartohadi J, Supari S, Qadafi M, Wulan IR. Mitigating methane emissions in chili farming with sustainable agricultural practices. Ecological Engineering and Environmental Technology 2025;26(3):220-32.

Arvianti EY, Masyhuri M, Waluyati LR, Darwanto DH. The crisis facing young Indonesian farmers. Agriekonomika 2019; 8(2):168-80 (in Indonesian).

Ayu IW, Suhada I, Kusumawardani W, Oklima AM, Novantara Y, Soemarno S. Assistance for healthy cultivation of chili plants on sub-optimal land in facing the impact of climate change in Sumbawa Regency. Mattawang: Jurnal Pengabdian Masyarakat 2021;2(1):1-7 (in Indonesian).

Azizah YN, Zaki MK. Characterization of the spatial and temporal distribution of precipitation and hydrometeorological disasters in Sleman, Yogyakarta. IOP Conference Series: Earth and Environmental Science 2025;1477(1):Article No. 012048.

Emilia V. The impact of climate change on the agricultural sector [Internet]. 2020 [cited 2025 Jun 6]. Available from: https://www.kompasiana.com/viee/5fdf699d8ede4827577b90e5/pengaruh-perubahan-iklim-terhadap-sektor-pertanian (in Indonesian).

Eldridge DJ, Beecham G. Climate Variability Impacts on Land Use and Livelihoods in Drylands. Cham, Switzerland: Springer; 2017.

Ferdiyanto A, Sujono S. Fuzzy logic-based soil moisture control for Chili plants. Maestro 2018;1(1):86-91 (in Indonesian).

Firdauzi L, Suarma U. Analysis of rainfall variability and shifts in season in relation to the rice cultivation period in Sleman Regency. IOP Conference Series: Earth and Environmental Science 2023;1233:Article No. 012052.

Guido Z, Zimmer A, Lopus S, Hannah C, Gower D, Waldman K, et al. Farmer forecasts: Impacts of seasonal rainfall expectations on agricultural decision-making in Sub-Saharan Africa. Climate Risk Management 2020;30:Article No. 100247.

Hajad V, Ikhsan I, Herizal H, Latif IR, Marefanda N. Poverty and the curse of natural resources in Indonesia. Journal of Contemporary Governance and Public Policy 2023;4(1):41-58.

Herlina N, Prasetyorini A. Effect of climate change on planting season and productivity of maize (*Zea mays* L.) in Malang Regency. Jurnal Ilmu Pertanian Indonesia 2020;25(1):118-28 (in Indonesian).

Hidayati IN, Suryanto S. The influence of climate change on agricultural production and adaptation strategies on drought-prone land. Jurnal Ekonomi and Studi Pembangunan 2015;16(1):42-52 (in Indonesian).

Izumo T, Vialard J, Lengaigne M, Suresh I. Relevance of relative sea surface temperature for tropical rainfall interannual variability. Geophysical Research Letters 2020;47(3): e2019GL086182.

Jinagool W, Arom P. Influence of watering regimes on physiological traits, growth, yield, and capsaicin content of chilies. ASEAN Journal of Science and Technology Reports 2023;26(1):20-31.

Jun-Ichi H, Mori S, Kubota H, Yamanaka MD, Haryoko U, Lestari S, et al. Interannual rainfall variability over northwestern Jawa and its relation to the Indian Ocean Dipole and El Niño-Southern Oscillation events. Scientific Online Letters on the Atmosphere 2012;8(1):69-72.

Khotimah KA, Purnomo D. Analysis of Factors Affecting Rice Imports in Indonesia from 1980 to 2016 [dissertation]. Surakarta: Universitas Muhammadiyah Surakarta; 2018 (in Indonesian).

Liebmann B, Hoerling M, Funk C, Bladé I, Dole R, Allured D, et al. Understanding recent Eastern Horn of Africa rainfall variability and change. Journal of Climate 2014;27(22):8630-45.

Malihah L. Challenges in addressing the impacts of climate change and supporting sustainable economic development: A review. Jurnal Kebijakan Pembangunan 2022;17(2):219-32 (in Indonesian).

Pertami RRD, Eliyatiningsih E, Salim A, Basuki B. Optimization of land use based on land suitability class for the development of red chillies in Jember Regency. Jurnal Tanah Sumberdaya Lahan 2022;9(1):163-70 (in Indonesian).

Pewista I, Harini R. Factors and impacts of agricultural land-use conversion on the socio-economic conditions of residents in Bantul Regency: A case study of urban, peri-urban, and rural areas from 2001 to 2010. Jurnal Bumi Indonesia 2013;2(2):96-103 (in Indonesian).

Pothapakula PK, Primo C, Sørland S, Ahrens B. The synergistic impact of ENSO and IOD on Indian summer monsoon rainfall in observations and climate simulations: An information theory perspective. Earth System Dynamics 2020;11(4):903-23.

Ridho MN, Suminarti NE. The effect of climate change on cayenne pepper (*Capsicum frutescens* L.) productivities in Malang Regency. Jurnal Produksi Tanaman 2020;8(3):304-14 (in Indonesian).

Rondhi M, Pratiwi PA, Handini VT, Sunartomo AF, Budiman SA. Agricultural land conversion, land economic value, and sustainable agriculture: A case study in East Java, Indonesia. Land 2018;7(4):Article No. 148.

Sundararaj SI, Chandramathy I, Jeykumar RKC, Chandramohan K. Urbanizational impact on climatic variables and geographical analysis of physical land use land cover variation of a city using remote sensing. Global Nest Journal 2024;26(5):1-15.

Setiyanto A, Pasaribu S. Predicting the impacts of climate change on Indonesia's five main horticulture commodities. IOP Conference Series: Earth and Environmental Science 2021;653:Article No. 012009.

Siebert E, Lee S, Prescott M. Chili pepper preference development and its impact on dietary intake: A narrative review. Frontiers in Nutrition 2022;9:Article No. 1039207.

Siswanto S, Wardani KK, Purbantoro B, Rustanto A, Zulkarnain F, Anggraheni E. Satellite-based meteorological drought indicator to support food security in Java Island. PLoS One 2022;17(6):e0260982.

Swastika S, Pratama D, Hidayat T, Andri KB. Technical manual on chili cultivation technology Indonesia: Universitas Riau [Internet]. 2017 [cited 2025 Jun 6]. Available from: https://www.academia.edu/40395361/BUKU_PETUNJUK_TEKNIS_TEKNOLOGI_BUDIDAYA_CABAI_MERAH_Editor_Rustam_Oni_Ekalinda_Lay_Out_Andi.html (in Indonesian).

Yahwe CP, Isnawaty LFAR. Design and development of a prototype soil moisture monitoring system via SMS based on irrigation events: a case study on chili and tomato plants. SemanTIK 2016;2(1):97-110 (in Indonesian).

Zelviyani. Supply and demand analysis of large red chili commodities: A case study at Karisa Market, Binamu District, Jeneponto Regency. Journal Agritech Science 2022;6(2):64-75 (in Indonesian).

Environment and Natural Resources Journal

Volume 23
Issue 5
2025

Predicting Habitat Suitability for the Endangered Green Peafowl (*Pavo muticus* L., 1766) in Thailand's Western Stronghold under Future Climate Scenarios

Kornkanok Prommakul[1], Jedsada Noowong[1], Khwanrutai Charaspet[2], Bunyatiporn Kaewdee[1], Kittiwara Siripattaranukul[1], Prateep Duengkae[1], Saksit Simchareon[1], and Ronglarp Sukmasuang[1*]

[1]Department of Forest Biology, Faculty of Forestry, Kasetsart University, Thailand
[2]Wildlife Research Division, Wildlife Conservation Office, Department of National Parks, Wildlife and Plant Conservation, Thailand

ARTICLE INFO

Received: 4 Apr 2025
Received in revised: 1 Jul 2025
Accepted: 7 Jul 2025
Published online: 31 Jul 2025
DOI: 10.32526/ennrj/23/20250081

Keywords:
Green peafowl/ Habitat suitability/ Species distribution modeling/ Conservation planning/ Huai Kha Khaeng Wildlife Sanctuary

*** Corresponding author:**
E-mail: ronglarp.s@ku.th

ABSTRACT

The green peafowl (*Pavo muticus* L., 1766) is endangered globally. This study evaluates environmental factors shaping its habitat in key Thai strongholds to identify current habitat suitability and predict future changes under climate scenarios. Current and projected climate data from 2020 to 2100 were analyzed under four scenarios of 20 years each: at present, in the near future, mid future and far future, using species distribution modelling with MaxEnt and SSP2-4.5 to assess potential impacts. The results show that the key green peafowl habitat factors included elevation, slope, streams, isothermality and annual precipitation. Mixed deciduous forests were the most critical forest types for the species. Moderately and highly suitable habitats for the green peafowl covered approximately 5% of the sanctuary. However, well suitable habitat is projected to decrease markedly, representing a 21.25% decline. Strict management of these crucial areas is essential. Moreover, expanding protected areas, networks, and conservation strategies are vital for addressing challenges arising from rapid global environmental change.

HIGHLIGHTS

Camera traps captured twenty-nine ground bird species in Huai Kha Khaeng Wildlife Sanctuary. The green peafowl was the most abundant species. Topography and climate factors strongly influenced green peafowl habitat suitability. The suitable habitat is projected to decrease markedly representing a 21.25% decline. Conservation efforts must focus on the key habitats and climate impacts to conserve the species and their stronghold habitat.

1. INTRODUCTION

The green peafowl, *Pavo muticus* L., 1766, is native to the tropical and subtropical forests of Southern and Southeast Asia, including Northeast India, southern China, Myanmar, Laos, Cambodia, Thailand, Vietnam and Java (IUCN, 2025). The species is classified into three subspecies: the Burmese green peafowl (*P. muticus spicifer*), the Indochinese green peafowl (*P. muticus imperator*), and the Javan green peafowl (*P. muticus muticus*) (Patil and Vijay, 2024). Two subspecies occur in Thailand: the Javan green peafowl (also known as the Southern green peafowl), and the Indochinese green peafowl (or Northern green peafowl). Overall, the green peafowl is extinct across several countries while surviving in fragmented, small populations in others (Saridnirun et al., 2023). Major threats include habitat loss (Kong et al., 2018) as well as environmental changes (Weiskopf et al., 2020; Shwe et al., 2021). Thus, environmental studies are an urgent priority for conservation.

Citation: Prommakul K, Noowong J, Charaspet K, Kaewdee B, Siripattaranukul K, Duengkae P, Simchareon S, Sukmasuang R. Predicting habitat suitability for the endangered green peafowl (*Pavo muticus* L., 1766) in Thailand's Western Stronghold under future climate scenarios. Environ. Nat. Resour. J. 2025;23(5):469-482. (https://doi.org/10.32526/ennrj/23/20250081)

Sukumal et al. (2022) identified six green peafowl strongholds in Southeast Asia: eastern Cambodia, south-central Vietnam, northeastern Cambodia, western Thailand, northern Thailand, and Myanmar's Bago Yoma range. In Thailand, scattered populations have been reported in several National Parks and Wildlife Sanctuaries (Sukumal et al., 2020; Nasoongnern et al., 2024). The most critical habitat of green peafowl in Thailand is Huai Kha Khaeng Wildlife Sanctuary (HKKWS) because there is a large population of green peafowl living naturally without overlapping with agricultural areas. (Sukumal et al., 2017).

In the case of climate factors, climate markedly influences species' habitats and distribution patterns (Odeny et al., 2019). Rising temperatures have raised concerns about declining bird populations (Bhagarathi et al., 2024). In recent years, studies have shown that >20% of bird species face extinction due to climate change (Pacifici et al., 2017; Yu et al., 2022; Halupka et al., 2023; Lawer, 2024; Mota et al., 2024; Weinhäupl and Devenish-Nelson, 2024). Climate also determines the availability of suitable habitat, making it the most critical factor in predicting future distribution (Singh et al., 2021). Understanding and forecasting range shifts and habitat changes due to climate are essential for effective conservation management (Holbrook et al., 2017; Bhasin et al., 2024). Protected areas remain central to conservation strategies for long-term biodiversity preservation (Vimal et al., 2021; Williams et al., 2022). Species distribution models play a key role in conservation by bridging research and policymaking (Coreau et al., 2018), offering hope for sustaining bird populations despite climate challenges (Bernath-Plaisted et al., 2024).

However, studies predicting habitat ranges at varying conservation hotspot levels are lacking in Thailand. Understanding and identifying suitable habitats are critical for long-term conservation. This study aims to examine the relationship between the occurrence of green peafowl and key environmental factors, including climate, topography, and vegetation cover, and to assess the suitability of habitat under these conditions.

This study aimed to investigate the environmental factors that affected the occurrence of peafowl in an area that had never been studied before, despite its significance as a conservation area. MaxEnt and the SSP2-4.5 scenario were used to predict changes in peafowl distribution every 20 years from 2020 to 2100 at four intervals. The results of the study provided insights into how peafowl habitats have changed due to climate change. These findings contributed to a better understanding that could be applied to develop management guidelines for the conservation of green peafowls and other ground-dwelling wildlife in the area, enhancing ecosystem integrity and future conservation benefits.

2. METHODOLOGY

2.1 Study area

The study was conducted in HKKWS (Figure 1). The area is primarily covered by mixed deciduous (MDF) and dry evergreen forests (DEF), with patches of dry deciduous forest (DDF). Elevation in HKKWS ranges from 200 to 1,600 m, characterized by low-slope alluvial valleys along major rivers and rugged hills. The dominant vegetation includes MDF (48.3%), DEF (24.7%), hill evergreen forest (13.4%), and DDF (6.9%) (Saisamorn et al., 2024). The sanctuary is home to threatened species (Charaspet et al., 2021). Annual temperatures fall within the 8-38°C range, with mean annual rainfall of 1,375 mm (Simcharoen et al., 2014).

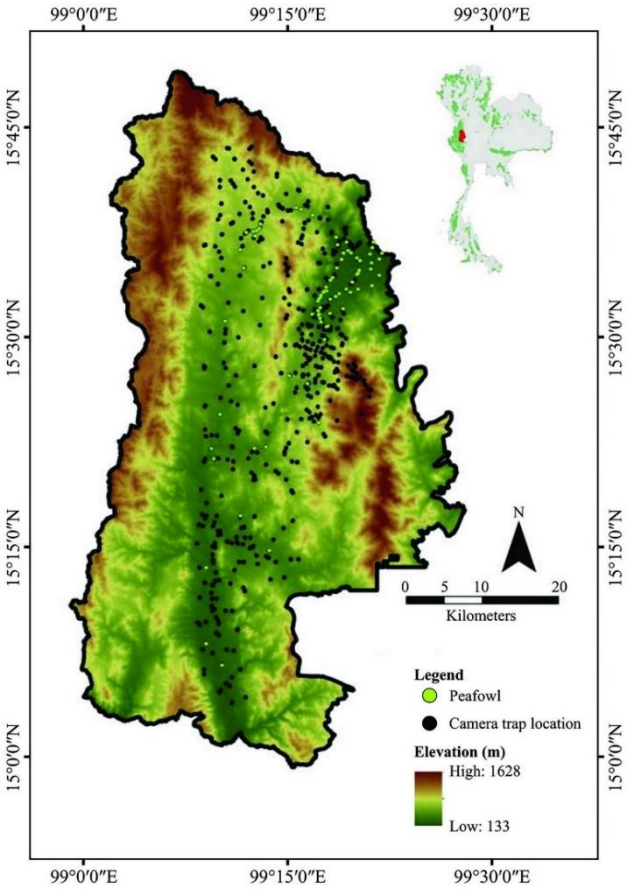

Figure 1. Study area and occurrence locations of green peafowl in HKKWS (646 locations)

2.2 Data collection

Camera traps were deployed in HKKWS from November 2017 to March 2019 across 646 locations, totaling 9,640 trap nights, with green peafowl photographed at 106 locations. In total, 40 Bushnell Trophy Cam HD Essential E2 12MP Trail Cameras were used. The study divided a 1:50,000 geographic map into 1-km^2 grid cells, 646 grid cells totally, placing a camera in each grid, with 15-20 grids surveyed per field trip. Cameras were spaced at least 500-m apart to ensure independent detections and reduce the probability of photographing the same animal with multiple cameras (Charaspet et al., 2019a; Charaspet et al., 2019b; Charaspet et al., 2020). Deployment locations were selected based on habitat suitability and the likelihood of green peafowl presence, especially along the main streams (Sukumal et al., 2017; Penjor et al., 2021).

Cameras were secured with metal casings and python locks, mounted on trees at 40-50 cm above ground level to capture terrestrial bird species, and positioned 3-4 m from target points or according to site suitability (Fontúrbel et al., 2020). They were set to hybrid mode (photo and video) with 24-h activation, three-photo capture per trigger, 10-s video length, and 10-s intervals, operating continuously (Leo et al., 2024). After each 30-day period, cameras were relocated.

All photographs were imported into a computer and organized using Camera Trap Manager (Zaragozí et al., 2015). Data was transferred to Microsoft Excel for analysis. Terrestrial bird species in photographs were identified by common name, scientific name, and family following IUCN (2025). Only clear photographs with date and time stamps were used. The recorded photographs were selected using independent event criteria according to Choo et al. (2020) for further abundance calculations. The relative abundance index was calculated as the number of independent event detections per one hundred camera-days or camera-nights (Zhao et al., 2020).

2.3 Species distribution model

Variable selection enhances model accuracy by reducing multicollinearity and minimizing the number of required predictors (Yi et al., 2016). The variance inflation factors (VIFs) of 22 environmental variables were tested using the "usdm" package in R studio (Naimi et al., 2014; R Core Team, 2018). VIFs, based on correlation coefficients (Shrestha, 2022), were used to eliminate variables with VIFs >5 (Akinwande et al., 2015), except for elevation, which is a key predictor of green peafowl habitat suitability (Chatterjee and Hadi, 2006). Ultimately, 12 variables were selected: percent tree cover, forest type, elevation, slope, distance to a stream, distance to a ranger station, mean diurnal range, isothermality, annual precipitation, precipitation of driest month, and precipitation of coldest quarter. These variables were used to model both present and future habitat scenarios (Abdelaal et al., 2019). The present model used bioclimatic data from 1970 to 2020, whereas future models incorporated projections from the IPSLCM6A-LR model, one of the best-performing models for HKKWS (Kamworapan et al., 2021), developed by the Institut Pierre Simon Laplace, France (Boucher et al., 2020). Future scenarios were based on Shared Socioeconomic Pathways (SSP2-4.5), which assume medium greenhouse gas emission stabilization (Lovino et al., 2021). All environmental variables were resampled using the bilinear resampling technique (Ren et al., 2016), clipped to a 30-arcsecond (~1 km) resolution in ASCII format, and processed using R studio. The environmental variables used in the analysis are listed in Appendix Table 1.

To further minimize multicollinearity among continuous environmental variables (topographic variables, land cover variables, anthropogenic variables and bioclimatic variables) and mitigate potential model uncertainty or overfitting, a threshold correlation value of 0.7 was applied (Dormann et al., 2013). Highly correlated variables were identified and removed using the "vifcor" function in the "sdm" package in R (Naimi and Araújo, 2016). The final variable sets minimized redundancy in modeling green peafowl habitat suitability (Table 1).

Species distribution modeling was performed using MaxEnt version 3.4.4 (Phillips et al., 2017). The model was run with default settings unless otherwise specified. Specifically, we used the default feature classes (linear, quadratic, product, and hinge) and the regularization multiplier was set to the default value of 1.0. These settings help control model complexity and reduce the risk of overfitting. These choices align with standard practices commonly adopted in species distribution modeling literature (e.g., Phillips et al., 2006; Elith et al., 2011). By using these default configurations, we ensured that the model was comparable with a wide range of previous studies and maintained a balance between model performance and interpretability.

Table 1. Predictor bioclimatic variables used after removing highly correlated variables to minimize multicollinearity in species distribution models.

Label	Variable	Scaling factor	Unit	Note
BIO2	Mean diurnal range	10	°C	Two effects are at play: one influencing BIO2 and one influenced by BIO2. Diurnal range impacts frost occurrence, whereas maritimity affects BIO2, i.e., proximity to the ocean increases temperature range.
BIO3	Isothermality	100	%	Isothermality is strongly affected by distance from the equator. In the tropics, temperatures are relatively stable year-round, whereas at the poles, winters and summers are distinctly different.
BIO12	Annual precipitation	1	mm	This variable reflects a region's aridity and wetness but represents total annual water availability. If precipitation varies markedly throughout the year, this may not be the most suitable variable.
BIO14	Precipitation of driest month	1	mm	
BIO19	Precipitation of coldest quarter	1	mm	

Models were trained and tested with 10 simulations and a maximum of 500 iterations, using an initial background dataset of 10,000 units. A sub-sample approach allocated 75% of the data for training and 25% for testing. Model results were expressed in log-log (clog-log) format (Trisurat et al., 2014; Bai et al., 2018; Mcgarvey et al., 2021; Khan et al., 2022). The AUC (area under the receiver operating characteristic curve) values vary from 0 to 1; values <0.5 indicate that the model performance is worse than random, 0.5 indicates performance that is not better than random, 0.5-0.7 indicates poor performance, 0.7-0.9 indicates reasonable or moderate performance, and >0.9 indicates high performance (Jiang et al., 2018). The future habitat suitability model incorporated projected changes in bioclimatic variables to assess green peafowl habitat suitability may shift under different climate conditions (Table 1). The model was used to identify suitable habitat areas in HKKWS while accounting for potential environmental changes.

The models were calibrated to produce suitability scores on a scale from 0 to 1, where 0 indicates the least suitable and 1 the most suitable. These scores were categorized into four suitability classes: unsuitable (0.00-0.25), poorly suited (0.25-0.50), moderately suited (0.50-0.75), and well suited (0.75-1.00) (Ab Lah et al., 2021; Luo et al., 2025).

3. RESULTS AND DISCUSSION

3.1 Green peafowl abundance

In total, 29 bird species from 18 families were photographed using camera traps. The most frequently captured species was the green peafowl, with 506 images recorded across 9,690 trap nights, representing 5.22% of all recorded terrestrial bird detections. These images were obtained from 95 of 646 camera locations. Focusing on species from the pheasant family (Phasianidae), six species were identified: green peafowl, red junglefowl, kalij pheasant (*Lophura leucomelanos*), grey peacock-pheasant (*Polyplectron bicalcaratum*), Siamese fireback (*Lophura diardi*), and silver pheasant (*Lophura nycthemera*). Collectively, these species accounted for 8.68% RAI of all recorded terrestrial bird detections, comprising most of the 10.16% RAI of total wildlife captured (Table 2).

Table 3 summarizes the environmental factors influencing the habitat suitability of green peafowl in HKKWS under present (2020) and near-future (2021-2040), medium-future (2041-2060), and far future (2081-2100) scenarios. The assessment considered topographic, bioclimatic, and anthropogenic variables. On average, topography was the most influential factor, accounting for 67.50% of green peafowl habitat suitability based on % relative contribution (%RC), with elevation (54.52%) being the dominant variable, followed by slope (12.45%). Bioclimatic variables also played a role (29.07%), particularly isothermality (21.55%), annual precipitation (4.82%) and mean diurnal range (2.35%), while land cover variables (1.87%), tree cover (0.01%), forest type (1.86%) and anthropogenic variables (1.65%) were of little influence on green peafowl.

Table 2. Ground-dwelling bird species photographed in HKKWS (November 2017-March 2019) using camera traps at 646 locations (9,690 trap nights), comparing Phasianidae and non-Phasianidae species.

Family/Common name	Scientific name	NIP	RAI	LOF	Naïve occupancy	IUCN 2025
Phasianidae						
Green peafowl	*Pavo muticus*	506	5.22	95	14.71	EN
Red junglefowl	*Gallus gallus*	327	3.37	123	19.04	LC
Kalij pheasant	*Lophura leucomelanos*	6	0.06	6	0.93	LC
Grey peacock-pheasant	*Polyplectron bicalcaratum*	1	0.01	1	0.15	LC
Siamese fireback	*Lophura diardi*	1	0.01	1	0.15	LC
Silver pheasant	*Lophura nycthemera*	1	0.01	1	0.15	LC
		842	8.68	227	35.13	
Charadriidae						
Red-wattled lapwing	*Vanellus indicus*	73	0.75	7	1.08	LC
Ardeidae						
Chinese pond heron	*Ardeola bacchus*	7	0.07	7	1.08	LC
Columbidae						
Grey-capped emerald dove	*Chalcophaps indica*	7	0.07	5	0.77	LC
Eastern spotted dove	*Spilopelia chinensis*	7	0.07	6	0.93	LC
Zebra dove	*Geopelia striata*	1	0.01	1	0.15	LC
Strigidae						
Brown fish-owl	*Ketupa zeylonensis*	7	0.07	2	0.31	LC
Bucerotidae						
Oriental pied hornbill	*Anthracoceros albirostris*	6	0.06	3	0.46	LC
Pittidae						
Blue-winged pitta	*Pitta moluccensis*	5	0.05	5	0.77	LC
Blue pitta	*Hydrornis cyaneus*	3	0.03	1	0.15	LC
Corvidae						
Red-billed blue magpie	*Urocissa erythroryncha*	5	0.05	5	0.77	LC
Caprimulgidae						
Large-tailed nightjar	*Caprimulgus macrurus*	4	0.04	4	0.61	LC
Accipitridae						
Crested serpent-eagle	*Spilornis cheela*	3	0.03	3	0.46	LC
Unidentified eagle species	-	6	0.06	6	0.93	-
Muscicapidae						
White-rumped shama	*Copsychus malabaricus*	2	0.02	2	0.31	LC
Oriental magpie-robin	*Copsychus saularis*	1	0.01	1	0.15	LC
Picidae						
Black-headed woodpecker	*Picus erythropygius*	2	0.02	2	0.31	LC
Grey-faced woodpecker	*Picus canus*	1	0.01	1	0.15	LC
Turdidae						
Blue rock-thrush	*Monticola solitarius*	1	0.01	1	0.15	LC
Coraciidae						
Indian roller	*Coracias benghalensis*	1	0.01	1	0.15	LC
Caprimulgidae						
Large-tailed nightjar	*Caprimulgus macrurus*	1	0.01	1	0.15	LC
Alcedinidae						
White-throated kingfisher	*Halcyon smyrnensis*	1	0.01	1	0.15	LC
Pycnonotidae						
White-throated bulbul	*Alophoixus flaveolus*	1	0.01	1	0.15	LC
Turnicidae						
Yellow-legged buttonquail	*Turnix tanki*	1	0.01	1	0.15	LC
	Total	988	10.16	294	45.42	

Note: NIP: number of independent photographs; RAI: relative abundance index; LOF: location found; IUCN (2025): The International Union for Conservation of Nature.

3.2 Factors affecting green peafowl occurrence

All habitat suitability models demonstrated robust predictive performance, with high mean area under the curve (AUC) values for present model=0.92; near-future model=0.91; mid-future=0.91; far-future=0.91. The overall mean AUC value across all scenarios was 0.920±0.001, indicating strong model accuracy. Analysis results showed that environmental factors influencing green peafowl occurrence were primarily related to topography, with an average relative contribution (RC) of 67.50±2.05%. Altitude above sea level was the primary factor (average RC=54.52±2.06%), with the average altitude of green peafowl occurrence being 307.40 m above sea level. Slope was the second most important topographic factor (average RC=12.45±0.13%) (Table 4). Climate was the second most influential factor after topography, contributing an average RC of 29.07±2.12% to habitat suitability. Five key bioclimatic variables were identified: mean diurnal range, isothermality, annual precipitation, precipitation of the driest month, and precipitation of the coldest quarter. Temperature consistency demonstrated the most significant effect (RC=21.55±2.47%), with a mean temperature consistency value of 56.00±0.12% across all scenarios, because the appearance of green peafowl was a response to temperature levels. Vegetation-related variables, including percentage tree cover and forest type (MD), contributed 1.87% to the total RC that played a minor role in green peafowl occurrence (Table 3). From examining trends from the present to 2100, the relative influence of environmental factors on green peafowl occurrence remained largely stable, except for annual precipitation, which showed a consistent increase in importance (Figure 2). Precipitation enhances environmental productivity and habitat complexity, which directly supports the ecological requirements of the green peafowl, thereby increasing their likelihood of presence in such areas. The changes in the mean values of key environmental variables across different time periods for green peafowl habitat are presented in Figure 3. Figure 4 displays the Jackknife test results, which assess the relative importance of individual environmental variables in determining green peafowl habitat suitability, which confirmed climatic and topographic conditions as the most informative variable.

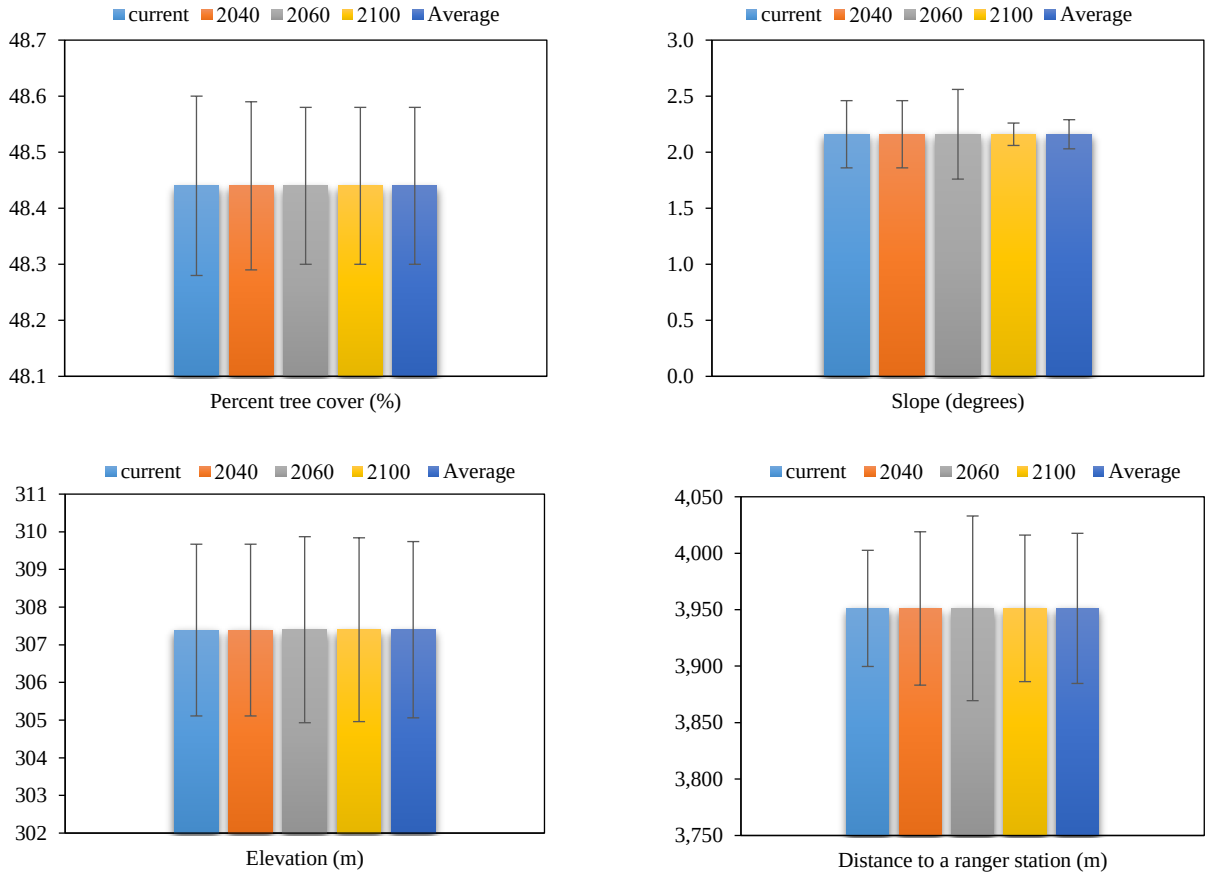

Figure 2. Change in the mean values of some key environmental variables across different time periods (2020-2100) for green peafowl habitat in HKKWS. Error bars indicate standard deviations.

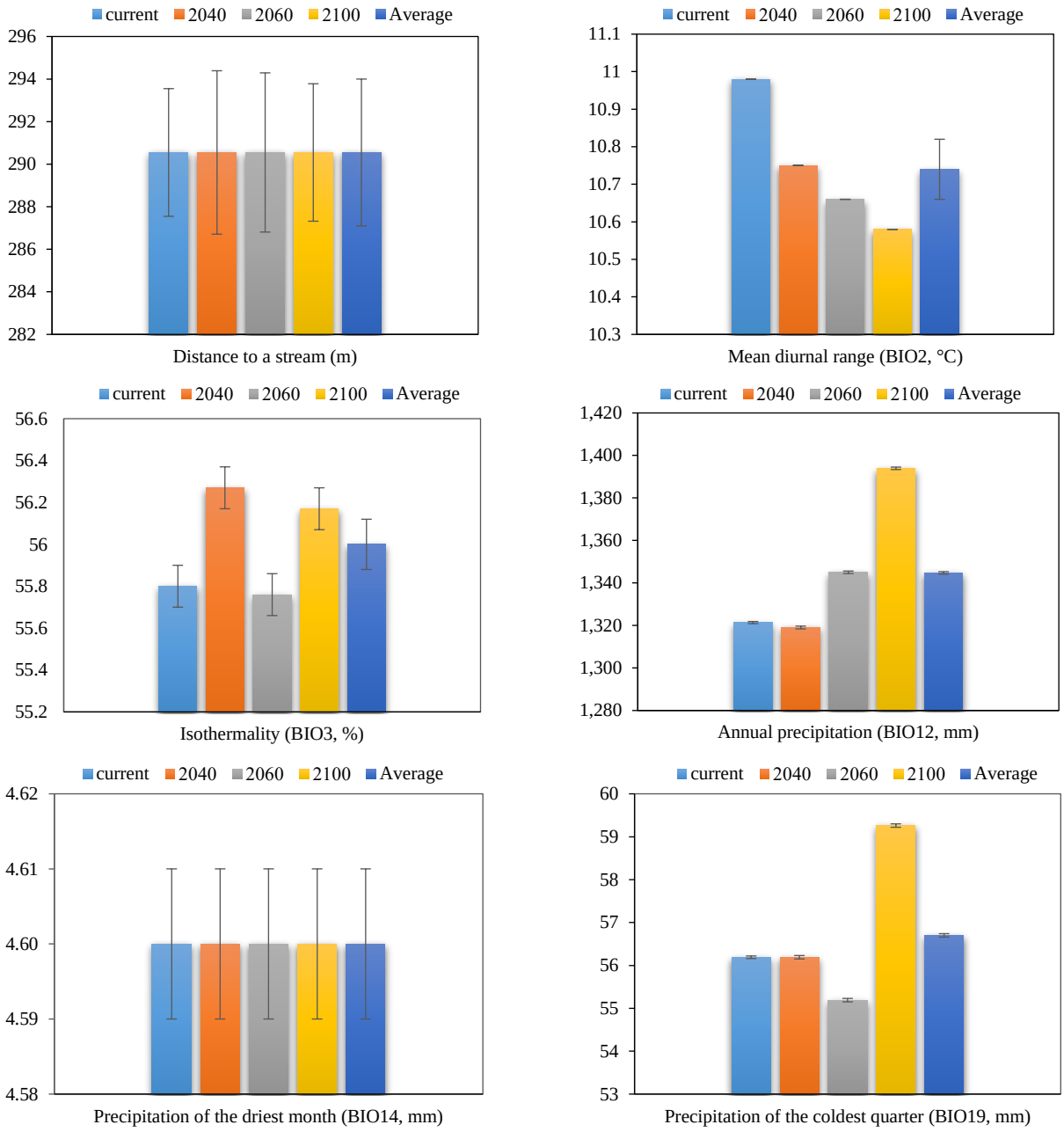

Figure 2. Change in the mean values of some key environmental variables across different time periods (2020-2100) for green peafowl habitat in HKKWS. Error bars indicate standard deviations (cont.).

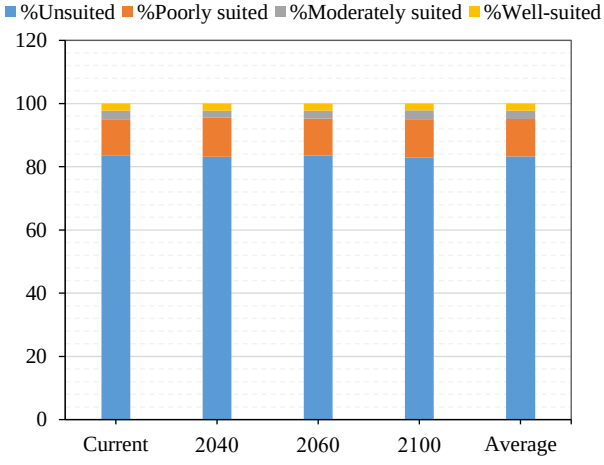

Figure 3. Predicted percentage changes in potential habitat suitability for green peafowl based on current and future environmental conditions.

Table 3. Percentage relative contributions (RCs) and mean values of key environmental variables used in habitat suitability models for green peafowl in HKKWS.

Environmental variables	Present (2020) AUC=0.922		Near-future (2021-2040) AUC=0.915		Mid-future (2041-2060) AUC=0.916		Far-future (2081-2100) AUC=0.916		Average Present-2100 AUC=0.92 ± 0.001	
	RC (%)	Sample average (±SD)	RC (%)	Sample average (±SD)	RC (%)	Sample average (±SD)	RC (%)	Sample average (±SD)	RC (%)	Sample average (±SD)
Land cover variables	1.7		1.9		1.7		2.2		1.87±0.11	
Percent tree cover (%)	0	48.44±0.16	0.1	48.44±0.15	0.1	48.44±0.14	0.1	48.44±0.14	0.01±0.00	48.44±0.14
Forest type	1.7	MDF	1.8	MDF	1.6	MDF	2.1	MDF	1.86±0.10	MDF
Topographic variables	62.7		71.5		65.5		70.3		67.50±2.05	
Elevation (m)	50	307.39±2.28	58.5	307.39±2.45	52.1	307.4±2.47	57.5	307.4±2.44	54.52±2.06	307.40±2.34
Slope (degrees)	12.2	2.16±0.03	12.5	2.16±0.03	12.8	2.16±0.04	12.3	2.16±0.04	12.45±0.13	2.16±0.00
Distance to a stream (m)	0.5	290.55±3.00	0.5	290.55±3.84	0.6	290.55±3.74	0.5	290.55±3.23	0.52±0.02	290.55±3.45
Anthropogenic variables	1.8		1.5		1.7		1.6		1.65±0.06	
Distance to a ranger station (m)	1.8	3,951.15±51.43	1.5	3,951.08±67.92	1.7	3,951.21±81.79	1.6	3,951.19±64.89	1.65±0.06	3,951.15±66.50
Bioclimatic variables	34		25.1		31.2		26		29.07±2.12	
Mean diurnal range (BIO2,°C)	2.6	10.98±0.00	1.9	10.75±0.00	2.5	10.66±0.00	2.4	10.58±0.00	2.35±0.15	10.74±0.08
Isothermality (BIO3, %)	27.4	55.8±0.01	17.6	56.27±0.01	23.9	55.76±0.01	17.3	56.17±0.01	21.55±2.47	56.00±0.12
Annual precipitation (BIO12, mm)	3.8	1,321.37±0.5	5.4	1,319.05±0.66	4.6	1,345.02±0.59	5.5	1,393.95±0.58	4.82±0.39	1,344.74±0.58
Precipitation of the driest month (BIO14, mm)	0.1	4.6±0.01	0.1	4.6±0.01	0.1	4.6±0.01	0.2	4.6±0.01	0.12±0.02	4.60±0.01
Precipitation of the coldest quarter (BIO19, mm)	0.1	56.19±0.03	0.1	56.19±0.04	0.1	55.19±0.04	0.6	59.26±0.04	0.22±0.12	56.70±0.0.04

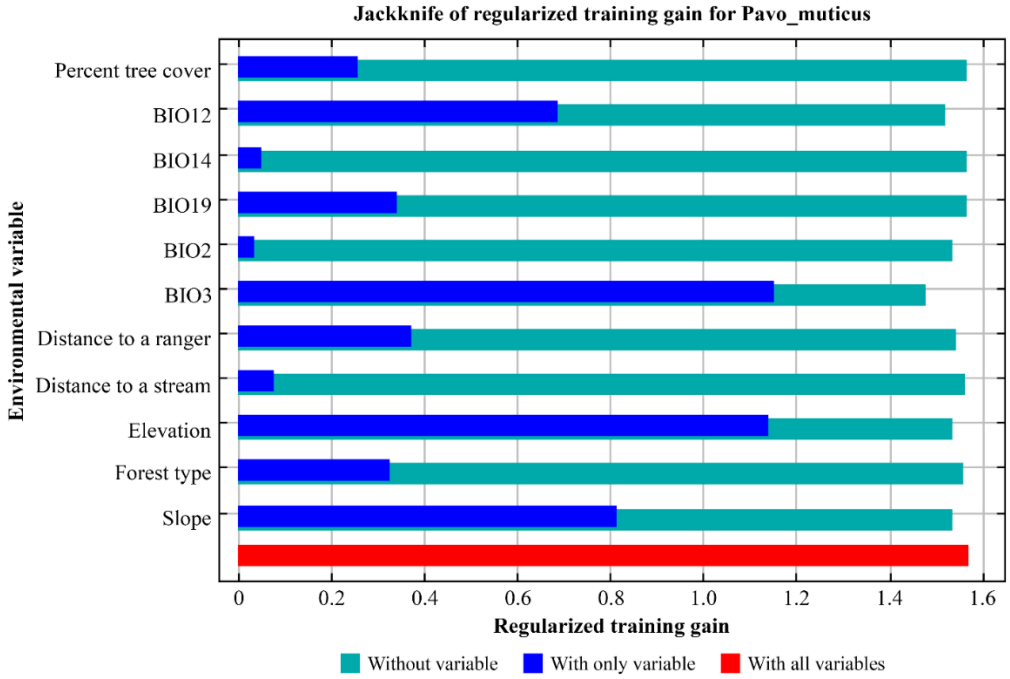

Figure 4. Jackknife test results assessing the relative importance of individual environmental variables in determining green peafowl habitat suitability under current conditions which confirmed Isothermality (BIO3, %) as the most informative variable

3.3 Habitat suitability

Results revealed that a highly suitable habitat is limited to 80 km^2, accounting for only 2.22% of the total area (Table 4 and Figure 5). Future projections suggest a slight decrease in unsuitable areas, with low- and medium-suitability areas showing minor increases. However, the extent of highly suitable habitat is predicted to remain relatively lower, ranging from 63 to 80 km^2.

Table 4. Present and future habitat suitability for green peafowl in HKKWS.

Habitat suitability		Current (2020)	Near-future (2021-2040)	Mid-future (2041-2060)	Far-future (2081-2100)	Average
Unsuited	Area (km^2)	2,442	2,435	2,446	2,428	2,437.75
	% (of HKK)	83.46	83.22	83.60	82.98	83.32
Poorly suited	Area (km^2)	339	361	341	346	346.75
	% (of HKK)	11.59	12.34	11.65	11.83	11.85
Moderately suited	Area (km^2)	80	65	74	89	77.00
	% (of HKK)	2.73	2.22	2.53	3.04	2.63
Well-suited	Area (km^2)	80	65	65	63	68.25
	% (of HKK)	2.22	2.22	2.22	2.15	2.20
Total area of HKK (km^2)		2,926	2,926	2,926	2,926	

This study recorded 29 species of ground-dwelling birds from 18 families using camera traps in HKKWS, making it the second most diverse site after Khao Yai National Park, where Kanka et al. (2023) identified 36 species from 21 families. The pheasant family was prominent in HKKWS, with six species recorded. Notably, the occurrence of green peafowl has increased in the eastern part of HKKWS, particularly along Huai Thap Salao Stream, a trend consistent with the findings of Suwanrat et al. (2015), who observed higher green peafowl numbers in forest-edge habitats near human settlements.

In addition to biological factors, especially food, water, roosting, shelter and nesting site that is essential to the species (Hernowo, 2017), this study showed that the key factors affecting green peafowl presence were topographic variables, followed in order of influence by climatic, anthropogenic and tree

cover factors. This contrasts with the findings of Sukmasuang et al. (2023) who demonstrated that the distribution of Siamese fireback and red junglefowl in lowland regions was largely influenced by climatic factors, with biophysical and topographic factors playing secondary roles.

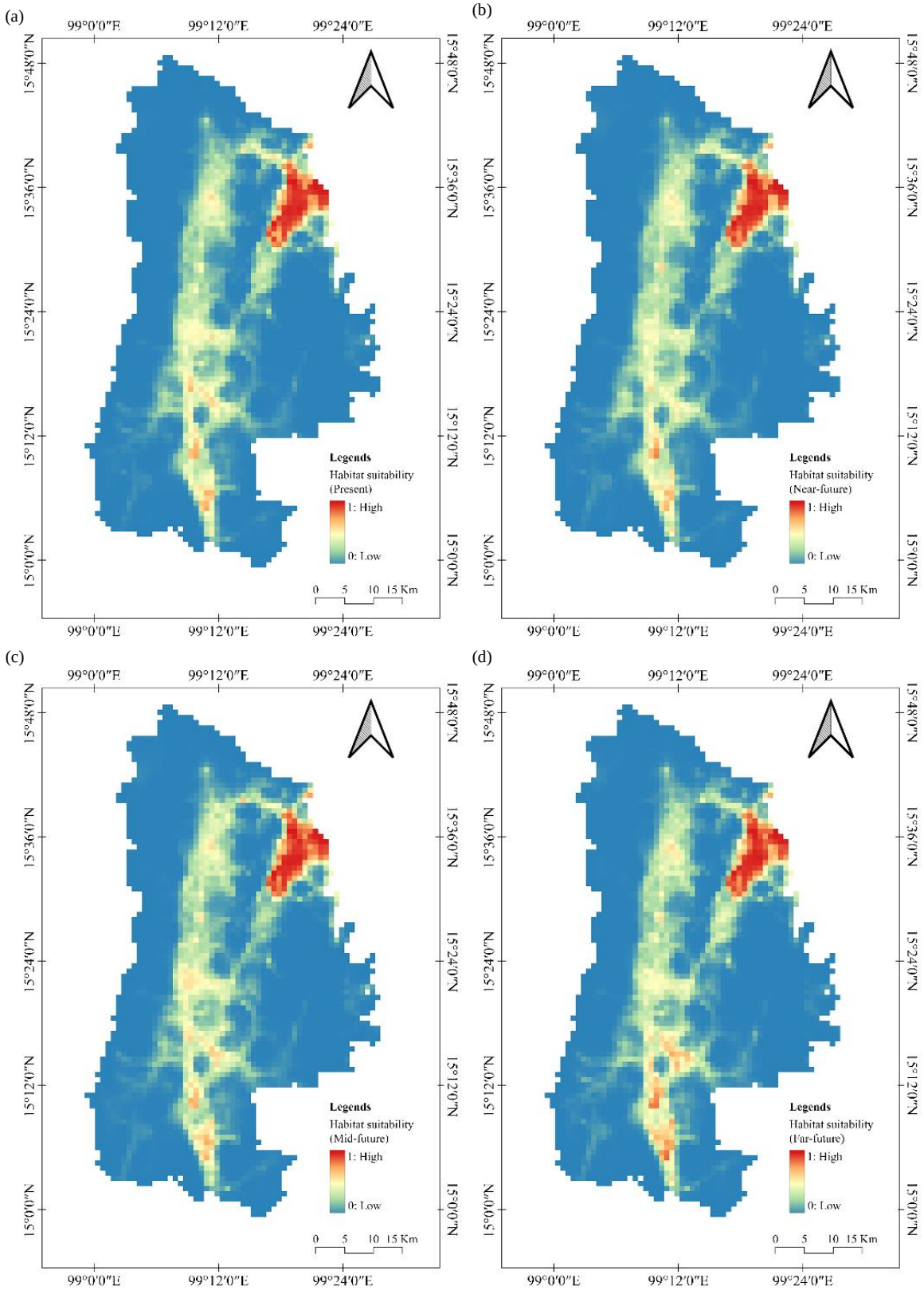

Figure 5. (a) Present, (b) near-future, (c) mid-future, and (d) far-future for green peafowl habitat suitability in HKKWS.

Topographic features, like slopes and terrain, influence where green peafowl can live and move around. They use these features to find food, shelter and avoid predators (Saridnirun et al., 2023). Different slopes and terrains affect their ability to forage, roost and care for their young. In essence, green peafowls adapt their behavior and movement patterns to the specific topographic conditions of their habitat, making use of the landscape to meet their daily needs, indicating that green peafowl prefer habitats with specific slope characteristics, because they offer a balance of safety, visibility, food availability, roosting and nesting sites (Hernowo, 2017). In the case of anthropogenic variables, there is no evidence of community habitation in this area, there is only a forest protection unit, so it has very little influence on the appearance of the green peafowl (Yan et al., 2021).

Additionally, percent tree cover, annual precipitation and elevation were key factors contributing to higher AUC values. Among climatic factors, isothermality had the strongest influence on green peafowl occurrence, followed by annual precipitation, mean diurnal range, precipitation of the driest month and precipitation of the coldest quarter, Isothermality represents the ratio of diurnal to annual temperature variations (O'Donnell and Ignizio, 2012), with values close to 100 indicating similar day-to-night and seasonal temperature fluctuations (Lu et al., 2022). Isothermality has previously been identified as a major determinant of species distribution (Xie et al., 2023). Additionally, the mean temperature of the wettest quarter has been shown to positively influence green peafowl habitat suitability, whereas the mean temperature of the driest quarter has a negative impact (Lawer, 2024). These findings align with those of Phipps et al. (2017) and Rehman et al. (2024) who reported isothermality being a key factor influencing habitat suitability. Given the projected long-term significance of isothermality (Xie et al., 2023), it remains a critical variable for future green peafowl conservation. Similarly, Nameer (2020) noted that temperature and precipitation seasonality during the driest quarter play a major role in determining the distribution of Indian peafowl (*Pavo cristatus*). The present findings underscore the need for green peafowl conservation strategies that prioritize habitats at specific elevations with stable climatic conditions.

Although highly suitable habitat will continue to decline, it comprises a small proportion of the total area, underscoring the challenges in green peafowl conservation. These constraints may stem from climate change which is difficult to control directly. These findings suggest that habitat conservation and management efforts should prioritize landscape characteristics to ensure the long-term survival of green peafowl in the HKKWS, in addition to linking with large-scale forest conservation to counter climate change as essential for the long-term survival of this endangered species.

4. CONCLUSION

This study identified the green peafowl as the most recorded ground bird in the sanctuary, with its presence strongly influenced by topographic and bioclimatic factors such as elevation and isothermality. MDF was identified as the most critical factor for green peafowl survival. Currently, only 5% of HKKWS (143.25 km²) is classified as moderately to highly suitable habitat for green peafowl. Future projections indicate a decline in highly suitable habitat, from 80 km^2 at present to 63 km^2, representing a 21.25% decrease. This highlights the need for proactive conservation measures to ensure the long-term survival of green peafowl in HKKWS; conservation efforts should focus on protecting key habitats. Managing and expanding protected areas strategically are key for conserving green peafowl in the long term and addressing environmental issues like biodiversity loss, climate change, and habitat degradation through large-scale conservation landscapes.

ACKNOWLEDGEMENTS

We would like to express our sincere gratitude to the Director of the Department of National Parks, Wildlife, and Plant Conservation for granting permission for this research, Mr. Somphot Duangchantrasiri, head of Khao Nang Rum Wildlife Research Station and his staff for their kindly help.

AUTHOR CONTRIBUTIONS

Conceptualization, Ronglarp Sukmasuang; Methodology, Ronglarp Sukmasuang and Saksit Simchareon; Software, Jedsada Noowong; Validation, Ronglarp Sukmasuang and Jedsada Noowong; Formal Analysis, Kornkanok Prommakul and Jedsada Noowong; Investigation, Kittiwara Siripattaranukul; Resources, Prateep Duengkae; Data Curation, Bunyatiporn Kaewdee; Writing-Original Draft Preparation, Ronglarp Sukmasuang; Writing-Review and Editing, Khwanrutai Charaspet and Kornkanok Prommakul; Visualization, Kornkanok Prommakul; Supervision, Saksit Simchareon and Prateep Duengkae; Project Administration, Ronglarp Sukmasuang; Funding Acquisition, Ronglarp Sukmasuang.

DECLARATION OF CONFLICT OF INTEREST

The authors declare no conflict of interest.

REFERENCES

Abdelaal M, Fois M, Fenu G, Bacchetta G. Using MaxEnt modeling to predict the potential distribution of the endemic plant *Rosa arabica* Crép. in Egypt. Ecological Informatics 2019;50:68-75.

Ab Lah NZ, Yusop Z, Hashim M, Mohd Salim J, Numata S. Predicting the habitat suitability of *Melaleuca cajuputi* based on the MaxEnt species distribution model. Forests 2021;12(11):Article No. 1449.

Akinwande MO, Dikko HG, Samson A. Variance inflation factor: As a condition for the inclusion of suppressor variable(s) in regression analysis. Open Journal of Statistics 2015;5(7): 754-67.

Bai DF, Chen PJ, Atzeni L, Cering L, Li Q, Shi K. Assessment of habitat suitability of the snow leopard (*Panthera uncia*) in Qomolangma National Nature Reserve based on MaxEnt modeling. Zoological Research 2018;39(6):373-86.

Bernath-Plaisted JS, Correll MD, Somershoe SG, Dwyer AM, Bankert A, Beh A, et al. Review of conservation challenges and possible solutions for grassland birds of the North American Great Plains. Rangeland Ecology and Management 2023;90:165-85.

Bhagarathi LK, Da Silva PNB, Maharaj G, Pestano F, Cossiah C, Kalika-Singh S, et al. Comprehensive review on the impact of climate change on the ecology, breeding seasonality, abundance and distribution of birds and possible approaches to address and conserve bird populations. International Journal of Science and Technology Research Archive 2024;6(2):21-44.

Bhasin A, Ghosal S, Raina P, Hore U. Climate change impacts on high altitude wildlife distribution: Predicting range shifts for four ungulates in Changthang, Eastern Ladakh. Ecological Frontiers 2024;44(2):365-80.

Boucher O, Servonnat J, Albright AL, Aumont O, Balkanski Y, Bastrikov V, et al. Presentation and evaluation of the IPSL-CM6 A-LR climate model. Journal of Advances in Modeling Earth Systems 2020;12(7):e2019MS002010.

Charaspet K, Sukmasuang R, Khoewsree N, Pla-Ard M, Paansri P, Keawdee B, et al. Spatial and temporal overlaps of top predators: Dhole, tiger and leopard, and their potential prey in Huai Kha Khaeng Wildlife Sanctuary, Thailand. Biodiversitas 2021;22(2):580-92.

Charaspet K, Duengkae P, Khiowsree N, Simchareon S, Sukmasuang R, Songsasen N. Some ecological aspects of dhole (*Cuon alpinus*) in the Huai Kha Khaeng Wildlife Sanctuary, Uthai Thani Province, Thailand. Folia Oecologica 2019a;46(2):91-100.

Charaspet K, Sukmasuang R, Khoewsree N, Pla-ard M, Songsaen N, Simchareon S. Movement, home range size and activity pattern of the golden jackal (*Canis aureus*, Linneaus, 1758) in Huai Kha Khaeng Wildlife Sanctuary, Thailand. Biodiversitas 2019b;20(11):3430-8.

Charaspet K, Sukmasuang R, Khoewsree N, Pla-ard M, Chanachai Y. Prey species and prey selection of dholes at three different sites in Thailand. Biodiversitas 2020;21(11):5248-62.

Chatterjee S, Hadi AS. Regression Analysis by Example. Hoboken, New Jersey: Jonh Wiley and Sons; 2006.

Choo YR, Kudavidanage EP, Amarasinghe TR, Nimalrathna T, Chua MAH, Webb EL. Best practices for reporting individual identification using camera trap photographs. Global Ecology and Conservation 2020;24:e01294.

Coreau A, Guillet F, Rabaud S. The influence of ecological knowledge on biodiversity conservation policies: A strategic challenge for knowledge producers. Journal for Nature Conservation 2018;46:97-105.

Dormann CF, Elith J, Bacher S, Buchmann C, Carl G, Carré G, et al. Collinearity: A review of methods to deal with it and a simulation study evaluating their performance. Ecography 2013;36(1):27-46.

Elith J, Phillips SJ, Hastie T, Dudík M, Chee YE, Yates CJ. A statistical explanation of MaxEnt for ecologists. Diversity and Distributions 2011;17(1):43-57.

Halupka L, Debora Arlt, Tolvanen J, Millon A, Bize P, Adamík P, et al. The effect of climate change on avian offspring production: A global meta-analysis. Proceedings of the National Academy of Sciences 2023;120(19):e2208389120.

Hernowo JB. Determinant factors of the Javan green peafowl (*Pavo muticus muticus* Linnaeus 1758) habitat in Baluran and Alas Purwo National Parks, East Java, Indonesia. Tropical Drylands 2017;1(1):50-6.

Holbrook JD, Squires JR, Olson LE, DeCesare NJ, Lawrence RL. Understanding and predicting habitat for wildlife conservation: The case of Canada lynx at the range periphery. Ecosphere 2017;8(9):e01939.

Fontúrbel FE, Rodríguez-Gómez GB, Fernández N, García B, Orellana JI, Castaño-Villa GJ. Sampling understory birds in different habitat types using point counts and camera traps. Ecological Indicators 2020;119:Article No. 106863.

International Union for Conservation of Nature (IUCN). The IUCN Red List of Threatened Species. Version 2024-2 [Internet]. 2025 [cited 2025 Jan 9]. Available from: http://iucnredlist.org.

Jiang D, Chen S, Hao M, Fu J, Ding F. Mapping the potential global codling moth (*Cydia pomonella* L.) distribution based on a machine learning method. Scientific Reports 2018; 8(1):Article No. 13093.

Kamworapan S, Thao PTB, Gheewala SH, Pimonsree S, Prueksakorn K. Evaluation of CMIP6 GCMs for simulations of temperature over Thailand and nearby areas in the early 21st century. Heliyon 2021;27:7(11):e08263.

Kanka P, Sukmasuang R, Duengkae P, Siripattaranugul K. Abundance and physical factors affecting the appearance of selected terrestrial birds in Khao Yai National Park using camera trapping. Biodiversitas 2023;24(1):222-32.

Khan AM, Li Q, Saqib Z, Khan N, Habib T, Khalid N, et al. MaxEnt modelling and impact of climate change on habitat suitability variations of economically important chilgoza pine (*Pinus gerardiana* Wall.) in South Asia. Forests 2022; 13(5):Article No. 715.

Kong D, Wu F, Shan P, Gao J, Yan D, Luo W, et al. Status and distribution changes of the endangered Green Peafowl (*Pavo muticus*) in China over the past three decades (1990s-2017). Avian Research 2018;9:Article No. 18.

Lawer EA. Predicting the impact of climate change on the potential distribution of a critically endangered avian scavenger, Hooded Vulture *Necrosyrtes monachus*, in Ghana. Global Ecology and Conservation 2024;49:e02804.

Leo S, Izz Q, Finley NL, Sumardi I, Andiani J. Wildlife species recorded by camera traps in reforested lowland rainforest and peat swamp forest of Gunung Palung National Park, Indonesia. Tropical Natural History 2024;24(1):8-19.

Lovino MA, Pierrestegui MJ, Müller OV, Berbery EH, Müller GV, Pasten M. Evaluation of historical CMIP6 model simulations and future projections of temperature and precipitation in Paraguay. Climatic Change 2021;164:Article No. 46.

Luo Y, Yang J, Liu L, Zhang K. MaxEnt modeling and effects of climate change on shifts in habitat suitability for *Sorbus alnifolia* in China. Plants 2025;14(5):Article No. 677.

Lu Q, Rao J, Shi C, Guo D, Fu G, Wang J, et al. Possible influence of sudden stratospheric warmings on the atmospheric environment in the Beijing-Tianjin-Hebei Region. Atmospheric Chemistry and Physics; Katlenburg-Lindau 2022;22(19):13087-102.

McGarvey DJ, Brown AL, Chen EB, Viverette CB, Tuley PA, Latham OC, et al. Do fishes enjoy the view? A MaxEnt assessment of fish habitat suitability within scenic rivers. Biological Conservation 2021;263:Article No. 109357.

Mota FMM, Kittelberger KD, Florez-Pa´ı C, Sekercioglu CH. Climate-driven distributional shifts in Choco´ endemic birds of southwest Colombia. Frontiers in Conservation Science 2024;5:Article No. 1412440.

Naimi B, Hamm ASS, Groen TA, Skidmore AK, Toxopeus AG. Where is positional uncertainty a problem for species distribution modelling? Ecography 2014;37(2):191-203.

Naimi B, Araújo MB. sdm: A reproducible and extensible R platform for species distribution modelling. Ecography 2016;39(4):368-75.

Nameer PO. The expanding distribution of the Indian peafowl (*Pavo cristatus*) as an indicator of changing climate in Kerala, southern India: A modelling study using MaxEnt. Ecological Indicators 2020;110:Article No. 105930.

Nasoongnern J, Suksavate W, Noowong J, Kaewdee B, Pisarn N, Sukmasuang R. Abundance, activity pattern and habitat suitability of the selected wildlife species in Ob Khan National Park, Northern Thailand. Journal of Wildlife and Biodiversity 2024;8(2):81-102.

Odeny D, Karanja F, Mwachala G, Pellikka P, Marchant R. Impact of climate change on species distribution and carbon storage of agroforestry trees on isolated east African mountains. American Journal of Climate Change 2019;8(3):364-86.

O'Donnell MS, Ignizio DA. Bioclimatic Predictors for Supporting Ecological Applications in the Conterminous United States: U.S. Geological Survey Data Series 691 [Internet]. 2012 [cited 2024 Dec 2]. Available from: https://pubs.usgs.gov/publication/ds691.

Pacifici M, Visconti P, Butchart SHM, Watson JEM, Cassola FM, Rondinini C. Species' traits influenced their response to recent climate change. Nature Climate Change 2017;7:205-8.

Phillips SJ, Anderson RP, Dudík M, Schapire RE, Blair ME. Opening the black box: An open-source release of Maxent. Ecography 2017;40(7):887-93.

Phillips SJ, Anderson RP, Schapire RE. Maximum entropy modeling of species geographic distributions. Ecological Modelling 2006;190(3-4):231-59

Phipps WL, Diekmann M, MacTavish LM, Mendelsohn JM, Naidoo V, Wolter K, et al. Due South: A first assessment of the potential impacts of climate change on Cape vulture occurrence. Biological Conservation 2017;210:16-25.

Penjor U, Kaszta Z, Macdonald DW, Cushman SA. Prioritizing areas for conservation outside the existing protected area network in Bhutan: The use of multi-species, multi-scale habitat suitability models. Landscape Ecology 2021;36:1281-309.

Patil AB, Vijay N. Conservation implications of diverse demographic histories: The case study of green peafowl (*Pavo muticus* Linnaeus 1766). Conservation Genetics 2024;25:455-68.

R Core Team. R: A Language and Environment for Statistical Computing. Vienna, Austria: Foundation for Statistical Computing [Internet]. 2018 [cited 2024 Dec 2]. Available from: https://cran.r-project.org/doc/manuals/r-release/fullrefman.pdf .

Rehman S, Iqbal Z, Qureshi R, Khan AM, Qaseem MF, Siddiqui MH. Bioclimatic and remote sensing factors are better key indicators than local topography and soil: Vegetation composition variability in forests of Pakistan's Spin Ghar Mountain range. Ecological Indicators 2024;163:Article No. 112111.

Ren Z, Wang D, Ma A, Hwang J, Bennett A, Sturrock HJWB. Predicting malaria vector distribution under climate change scenarios in China: Challenges for malaria elimination. Scientific Reports 2016;6:Article No. 20604.

Saisamorn A, Duangchantrasiri S, Sornsa M, Suksavate W, Pattanavibool A, Duengkae P. Recovery of globally threatened ungulate species in Huai Kha Khaeng Wildlife Sanctuary, Thailand. Global Ecology and Conservation 2024;53:e03012.

Saridnirun G, Sukumal N, Grainger MJ, Savini T. Low-intensive agricultural landscapes could help to sustain Green Peafowl *Pavo muticus* inhabiting surrounding forest patches in Northern Thailand. Global Ecology and Conservation 2023;44:e02487.

Shrestha SL. Quantifying effects of meteorological parameters on air pollution in Kathmandu valley through regression models. Environmental Monitoring and Assessment 2022; 194(10):Article No. 684.

Shwe NM, Sukumal N, Oo KM, Dowell S, Browne S, Savini T. Importance of isolated forest fragments and low intensity agriculture for the long-term conservation of the green peafowl *Pavo muticus*. Oryx 2021;55(2):311-7.

Simcharoen A, Savini T, Gale GA, Simcharoen S, Duangchantrasiri S, Pakpien S, et al. Female tiger *Panthera tigris* home range size and prey abundance: Important metrics for management. Oryx 2014;48(3):370-7.

Singh C, Solomon D, Rao N. How does climate change adaptation policy in India consider gender? An analysis of 28 state action plans. Climate Policy 2021;21(7):958-75.

Sukumal N, Dowell SD, Savini T. Micro-habitat selection and population recovery of the Endangered Green Peafowl *Pavo muticus* in western Thailand: Implications for conservation guidance. Bird Conservation International 2017;27(3):414-30.

Sukumal N, Dowell SD, Savini T. Modelling occurrence probability of the endangered green peafowl *Pavo muticus* in mainland South-East Asia: Applications for landscape conservation and management. Oryx 2020;54(1):30-9.

Sukumal N, Thunhikorn S, Savini T. Assessing the status of the Green Peafowl's expected stronghold in dry forests along the Salawin River, North-West Thailand. Bird Conservation International 2022;33:e32.

Suwanrat S, Ngoprasert D, Sutherland C, Suwanwaree P, Savini T. Estimating density of secretive terrestrial birds (*Siamese fireback*) in pristine and degraded forest using camera traps and distance sampling. Global Ecology and Conservation 2015;3:596-606.

Sukmasuang R, Chaisomboon P, Paansri P, Trisurat Y, Kanka P, Khiowsree N, et al. A. Abundance and factors affecting the appearance of *Siamese fireback* and red junglefowl in the lowland forest of Thailand. Biodiversitas 2023;24(10): 5718-30.

Trisurat Y, Kanchanasaka B, Kreft H. Assessing potential effects of land use and climate change on mammal distributions in northern Thailand. Wildlife Research 2014;41(6):522-36.

Williams DR, Rondinini C, Tilman D. Global protected areas seem insufficient to safeguard half of the world's mammals from human-induced extinction. Proceedings of the National Academy of Sciences of the United States of America 2022;119(24):e2200118119.

Vimal R, Navarro LM, Jones Y, Wolf F, Moguédec GL, Réjou-Méchain M. The global distribution of protected areas management strategies and their complementarity for biodiversity conservation. Biological Conservation 2021;256:Article No. 109014.

Weinhäupl C, Devenish-Nelson ES. Potential impacts of climate change on terrestrial Aotearoa New Zealand's birds reveal high risk for endemic species. Biological Conservation 2024;296:Article No. 110668.

Weiskopf SR, Rubenstein MA, Crozier LG, Gaichas S, Griffis R, Halofsky JE, et al. Climate change effects on biodiversity, ecosystems, ecosystem services, and natural resource management in the United States. Science of the Total Environment 2020;733:Article No. 137782.

Xie C, Chen L, Li M, Jim CY, Liu D. BIOCLIM modeling for predicting suitable habitat for endangered tree *Tapiscia sinensis* (Tapisciaceae) in China. Forests 2023;14:Article No. 2275.

Yan M, Gu B, Zhang M, Wang W, Quan RC, Li J, et al. The Range Contraction and Future Conservation of Green Peafowl (*Pavo muticus*) in China. Sustainability 2021;13:Article No. 11723.

Yi YJ, Cheng X, Yang ZF, Zhang SH. Maxent modeling for predicting the potential distribution of endangered medicinal plant (*H. riparia* Lour) in Yunnan, China. Ecological Engineering 2016;92:260-9.

Yu Y, He G, Li DY, Zhao XM, Chang J, Liu XC, et al. Climate change challenge, extinction risk, and successful conservation experiences for a threatened primate species in China: Golden snub-nosed monkey (*Rhinopithecus roxellana*). Zoological Research 2022;43(6):940-4.

Zaragozí B, Belda A, Giménez P, Navarro JT, Bonet A. Advances in camera trap data management tools: Towards collaborative development and integration with GIS. Ecological Informatics 2015;30:6-11.

Zhao G, Yang H, Gong Y, Xie B, Ge J, Feng L. Spatio-temporal coexistence of sympatric mesocarnivores with a single apex carnivore in a fine-scale landscape. Global Ecology and Conservation 2020;21(3):e00897.

Environment and Natural Resources Journal

Volume 23
Issue 5
2025

Environmental Health Risk and Spatial Distribution of $PM_{2.5}$ in The Cement Industry

Anwar Daud[1], Agus Bintara Birawida[1*], and Muhammad Rachmat[2]

[1]Department of Environmental Health, Faculty of Public Health, Hasanuddin University, Indonesia
[2]Department of Health Promotion and Behavior Science, Faculty of Public Health, Hasanuddin University, Indonesia

ARTICLE INFO

Received: 4 Jul 2024
Received in revised: 24 Jun 2025
Accepted: 7 Jul 2025
Published online: 15 Aug 2025
DOI: 10.32526/ennrj/23/20240182

Keywords:
Spate/ $PM_{2.5}$/ Cement industry/ EHRA

*** Corresponding author:**
E-mail: agusbirawida@gmail.com

ABSTRACT

The proximity of cement factories to residential areas raises concerns about air pollution and health risks associated with particulate matter (PM) emissions, particularly $PM_{2.5}$. This study aims to assess environmental health risks and spatial $PM_{2.5}$ exposure around the cement industry in South Sulawesi, Indonesia. Methods involved descriptive quantitative techniques, with data collected from eight sampling locations using purposive sampling, encompassing 160 individuals. Data analysis included intake calculations and risk quotient assessments. Hazard identification, dose-response analysis, exposure evaluation, and risk characterization were conducted to assess the health risks of $PM_{2.5}$ exposure. Results indicate that $PM_{2.5}$ levels in areas near the cement plant often exceed acceptable safety limits, posing notable health risks, especially among sensitive populations such as children and the elderly. The spatial analysis identifies Taraweang and Mangilu Villages as moderately exposed, Mangilu village is 1.6 km away from the cement factory, while Taraweang village is 1.55 km away, underscoring the necessity for targeted mitigation strategies and policies to safeguard public health in similar industrial settings.

1. INTRODUCTION

Particulate Matter (PM) refers to airborne mixtures of fine solid particles and liquid droplets originating from both anthropogenic and natural processes. Prolonged and repeated exposure to PM is associated with numerous adverse health outcomes, notably affecting respiratory and cardiovascular functions. PM typically comprises chemical constituents such as sulfates, nitrates, ammonia, sodium chloride, black carbon, mineral particles, and water content (WHO, 2023). In the cement manufacturing sector, particulate emissions are considered a major environmental pollutant. These emissions, primarily in the form of dust, can be released during almost every operational phase, including raw material handling, processing, and the distribution of finished cement products (Fitriyanti and Fatimura, 2019).

$PM_{2.5}$ is particulate dust with an aerodynamic diameter of 2.5 μm originating from fuel combustion, vehicle smoke, forest fires, and industry, smaller than PM_{10} (≤10 μm). $PM_{2.5}$ can be inhaled through the nose or mouth, pass through the respiratory tract, and reach the lung alveolus because its small size allows it to escape the body's natural filtration. These pollutants are collected with 50% efficiency by PM sampling collection 2.5 (Liang et al., 2021). $PM_{2.5}$ forming composition consists of sulfates, nitrates, organic compounds, ammonium compounds, metals, acidic materials, and other contaminants, which are believed to harm health.

$PM_{2.5}$ refers to fine particulate matter with an aerodynamic diameter of 2.5 micrometers or less, which is primarily generated from sources such as combustion of fossil fuels, motor vehicle emissions, industrial activities, and biomass burning, and is significantly smaller in size compared to PM_{10}

Citation: Daud A, Birawida AB, Rachmat M. Environmental health risk and spatial distribution of $PM_{2.5}$ in the cement industry. Environ. Nat. Resour. J. 2025;23(5):483-493. (https://doi.org/10.32526/ennrj/23/20240182)

particles (≤10 μm). $PM_{2.5}$ can be inhaled through the nose or mouth, pass through the respiratory tract, and reach the lung alveolus because its small size allows it to escape the body's natural filtration.

The generation of $PM_{2.5}$ originates from multiple sources, such as the combustion of biomass and coal, emissions from motor vehicles and industrial processes, as well as the resuspension of particulate dust (Sun et al., 2023). Among the identified sources, the combustion of solid fuels contributes substantially to $PM_{2.5}$ emissions, primarily because of its inherently low thermal efficiency and the high emission rates of pollutants released during the process (Xu et al., 2019; Yun et al., 2020). In the cement industry, $PM_{2.5}$ is produced by processing raw materials, burning limestone into cement, packaging, and storage (Regia et al., 2021).

Rapidly growing industrial activities cause an increase in energy consumption, which can indirectly cause air pollution (Ouyang et al., 2022). The physicochemical characteristics of $PM_{2.5}$ exhibit considerable variability depending on the emission source. Combustion of solid fuels is known to generate $PM_{2.5}$ laden with high concentrations of organic compounds and trace heavy metals. These chemical constituents can potentiate the cytotoxic potential of $PM_{2.5}$ by inducing cellular dysfunction and enhancing oxidative stress upon inhalation and systemic absorption in the human body (Sun et al., 2023). Cytotoxicity is defined as the capacity of a substance, process, or agent to induce toxicity in cells, either by causing cell death or impairing cellular functions (Saroyo and Saputri, 2021). Figure 1 explains the flow or scheme of environmental impacts related to fly ash exposure to human health and ecosystems, with details of sources, exposures and impacts. Wind can transport particulate matter over long distances, leading to its deposition in soil and water bodies.

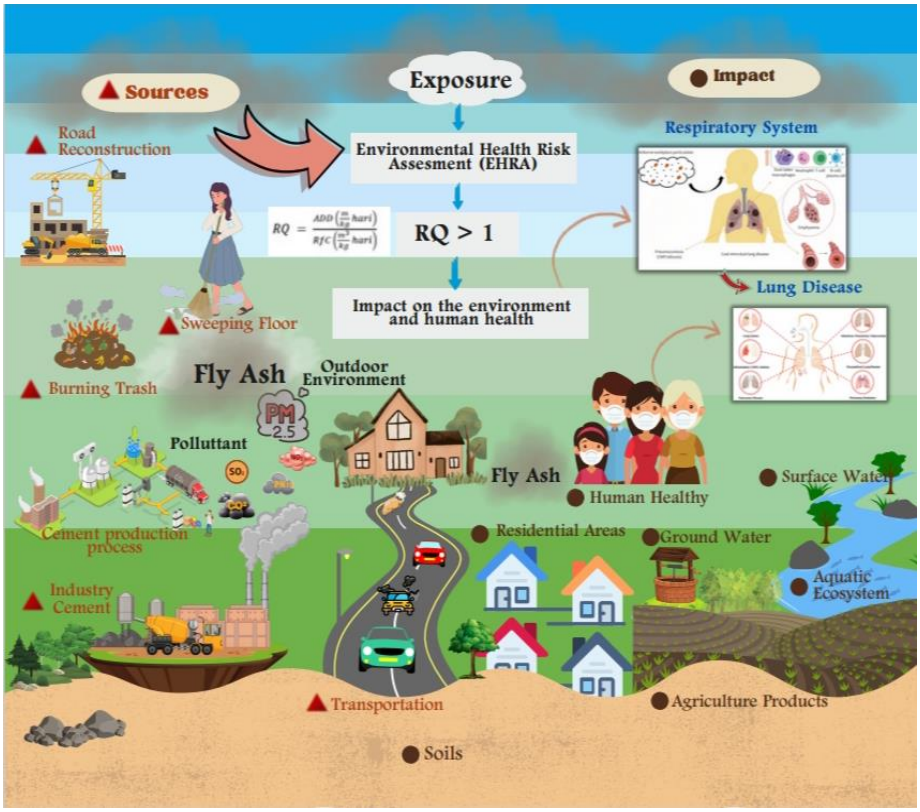

Figure 1. Exposure of $PM_{2.5}$ in the cement industry

Airborne particulate matter (PM) can undergo long-range atmospheric transport via wind and subsequently deposit on terrestrial or aquatic surfaces (United States Environmental Protection Agency, 2022). Air humidity also plays a crucial role in influencing PM behavior, with humid conditions accelerating the deposition of fine particles such as $PM_{2.5}$ (Duppa et al., 2020). Exposure to $PM_{2.5}$ poses substantial public health risks, as it has been epidemiologically associated with cardiovascular and respiratory disorders such as myocardial infarction, arrhythmias, asthma aggravation, reduced pulmonary

function, and elevated mortality among individuals with preexisting cardiopulmonary conditions (United States Environmental Protection Agency, 2022). Environmental impacts associated with PM include land degradation, water pollution, solid waste generation, and dust accumulation. In the cement industry, PM emissions are particularly influenced by the use of calcareous materials, primarily derived from natural limestone ($CaCO_3$). Calcium, which constitutes nearly 50% of CO_2 emissions during clinker production, is a key contributor to air pollution in this sector (Abubakar et al., 2022).

Global estimates indicate that $PM_{2.5}$ exposure contributes to approximately 5 million premature deaths annually, with an additional 0.5 million deaths linked specifically to $PM_{2.5}$ pollution exacerbated by climate change (Lin et al., 2018). According to the Global Burden of Disease (GBD) study, outdoor air pollution—primarily from $PM_{2.5}$ and ground-level ozone—was responsible for an estimated 4.5 million premature deaths in 2019 (Roser, 2021). The 2020 World Air Quality Report indicates that Indonesia recorded the highest average $PM_{2.5}$ concentration in Southeast Asia, reaching 40.8 µg/m³, ranking first among countries in the region (Dwi Safira et al., 2022).

Assessing the environmental health risks associated with $PM_{2.5}$ exposure is critical, particularly in communities residing near cement industry zones. Due to its ultrafine size, $PM_{2.5}$ is capable of penetrating deep into the respiratory tract, reaching the alveolar region, and potentially translocating into the bloodstream. Consequently, populations in these areas are at elevated risk for developing cardiopulmonary diseases linked to prolonged $PM_{2.5}$ exposure (Chanda et al., 2024; Wan Mahiyuddin et al., 2023). Research by Novirsa and Achmadi (2012) analyzed the risk of $PM_{2.5}$ in the PT Semen Padang area. Lifetime risk assessment results indicate that three zones—Ring 2 (500-1,000 m), Ring 4 (1,500-2,000 m), and Ring 5 (2,000-2,500 m)—exceed the acceptable Risk Quotient (RQ) threshold of 1, signifying potential health hazards. The RQ, defined as the ratio between estimated exposure and a reference concentration, serves as an index for evaluating the likelihood of adverse effects from chemical exposure. The analysis suggests that residential areas located beyond 2.5 km from the cement industry are considered the safest, with $PM_{2.5}$ concentrations not exceeding 0.028 mg/m³ (Novirsa and Achmadi, 2012).

Environmental health risk analysis (EHRA) is a process used to calculate or estimate risks to human health now or in the future (Fitra et al., 2022; Kasim et al., 2023). Analyzing environmental health risks for people living in cement industrial areas is essential to understanding the community's current and future environmental health risks. In addition, related parties (government) can create policies and risk mitigation efforts to reduce disease due to exposure to $PM_{2.5}$ and PM_{10}. Apart from carrying out risk analysis, it is also essential to determine the spatial pattern of people at risk of exposure to $PM_{2.5}$ and PM_{10} from the cement industrial area. GIS is a technology that can store, manipulate, analyze, and display natural conditions with the help of attribute and spatial data (Devi MLS, 2020).

PT Semen Tonasa, recognized as the largest cement manufacturer in Eastern Indonesia, operates on a 715-hectare site located in Biringere Village, Bungoro District, Pangkep Regency, approximately 68 kilometers from the city of Makassar. The facility comprises four production units, each equipped with key components such as limestone and clay crushers, raw mills, kilns, coal mills, silos, and packing systems. Utilizing a dry processing method, Units II and III have a combined annual production capacity of 590,000 tons, while Unit IV and Unit V produce 2,300,000 and 2,500,000 tons of cement per year, respectively.

$PM_{2.5}$ emissions in cement factory are generated through various stages of production, including raw material crushing, grinding, rotary kiln combustion, clinker cooling, and final grinding. These fine particles originate from material dust, fuel combustion, and the condensation of volatilized compounds. The level of $PM_{2.5}$ emissions is influenced by the efficiency of emission control systems such as bag filters and electrostatic precipitators (ESP). The proximity of the cement plant to residential zones increases the potential for ambient air pollution and associated health risks among the surrounding population due to industrial emissions. Exposure to $PM_{2.5}$ in industrial environments often becomes a primary concern in public health risk management.

The novelty of this study resides in the integration of environmental health risk assessment with geospatial analysis to characterize the spatial distribution patterns of $PM_{2.5}$ exposure in the vicinity of the PT Semen Tonasa industrial complex. The implication of this study underscores the importance of integrating spatial information in environmental health risk management to identify the most vulnerable zones to the negative impacts of $PM_{2.5}$ exposure. These findings provide a strong foundation

for developing more effective mitigation strategies and environmental protection policies in similar industrial areas.

2. METHODOLOGY

2.1 Study area

PT Semen Tonasa represents the largest cement production facility in Eastern Indonesia. Production Units II and III are situated in Mangilu Village, whereas Unit IV is located in Biring Ere Village, Bungoro District, Pangkep Regency, within the province of South Sulawesi. The activities of the cement factory include mining exploration activities, especially blasting and storing coal fuel, factory operations from Biring Ere to Biringkassi, and supporting raw materials. Figure 2 illustrates the sampling points of respondents and research locations within the PT Semen Tonasa industrial area.

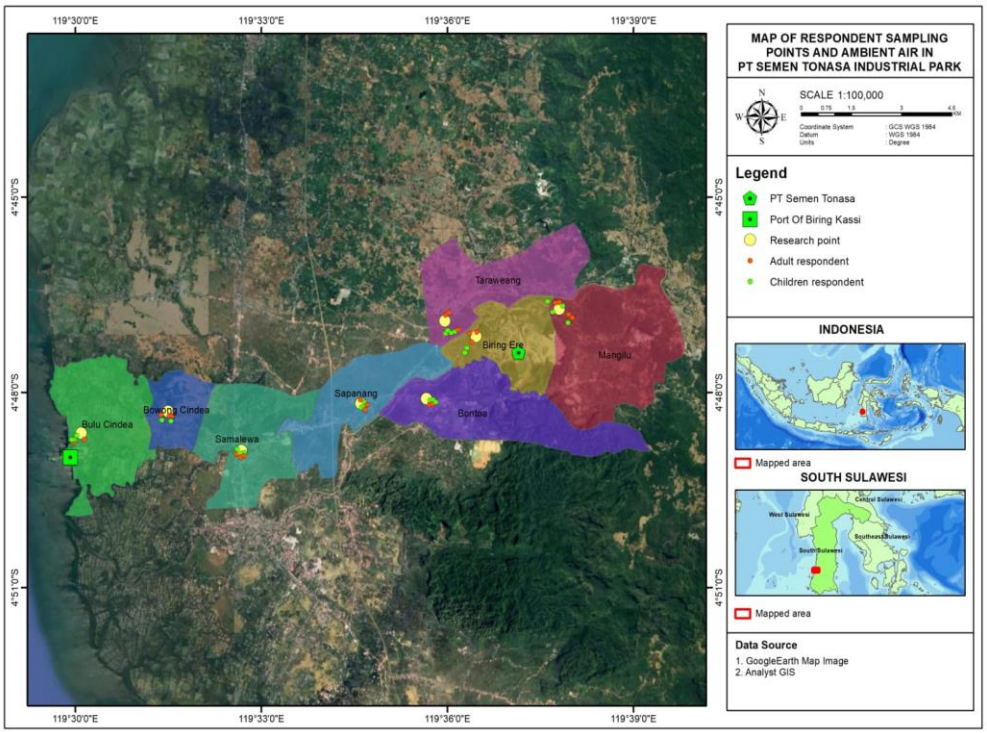

Figure 2. Sampling location

2.2 Sampling method

This study employs a descriptive quantitative approach, with observational findings analyzed using spatial mapping techniques to identify regions with varying levels of $PM_{2.5}$ exposure risk. The samples in this study are human samples and environmental samples used to analyze environmental health risks. The data used in the study all come from primary data. Sampling was conducted at eight sites surrounding the PT Semen Tonasa cement industrial area using a purposive sampling technique. A total of 160 human subjects, comprising both adults and children, were included alongside eight environmental sampling points focused on measuring ambient $PM_{2.5}$ concentrationsAmbient air samples were obtained from eight villages in the vicinity of the PT Semen Tonasa cement industrial complex, specifically Mangilu, Biring Ere, Sapanang, Samalewa, Bulu Cindea, Bowong Cindea, Bontoa, and Taraweang. One air quality sampling point was selected in each village to evaluate the ambient air quality in residential areas near PT Semen Tonasa.

2.3 Environmental health risk assessment

2.3.1 Hazard identification

Hazard identification aims to determine the concentration of specific hazardous agents that may pose health risks upon short- or long-term exposure (Fitra et al., 2022). The risk agents analyzed in this research are particulate matter ($PM_{2.5}$).

2.3.2 Dose-response analysis

The dose-response assessment was conducted using the Reference Concentration (RfC) for $PM_{2.5}$ established by the United States Environmental

Protection Agency (US-EPA), which is set at 0.0012 milligrams per kilogram per day (mg/kg/day).

2.3.3 Exposure analysis (exposure assessment)

Exposure analysis is intended to quantify the exposed population and determine the duration of exposure to the hazardous agent (Paustenbach et al., 2024). Exposure to airborne pollutants is quantified by estimating the intake dose absorbed into the human body (Regia et al., 2021). Exposure assessment is conducted by inputting anthropometric parameters and activity patterns into a standardized computational formula, typically processed using Microsoft Excel (Novirsa and Achmadi, 2012).

In this study, the environmental health risk assessment (EHRA) was carried out through the following sequential stages:

1) Hazard identification

This stage involves identifying the types of particulate matter generated from combustion processes during cement raw material processing that contribute to ambient air pollution.

2) Dose-response analysis

The dose-response analysis was conducted in accordance with the Reference Concentration (RfC) for $PM_{2.5}$ established by the U.S. Environmental Protection Agency (US-EPA), set at 0.0012 mg/kg/day.

3) Exposure analysis

$$ADD = \frac{C \times InhR \times ET \times EF \times ED}{BW \times AT}$$

Where; ADD=average daily dose (mg/kg/day); C=concentration of contaminant in air (mg/m^3); InhR=inhalation rate (m^3/hour); ET=exposure time (hour/day); EF=frequency of exposure (day/year); ED=duration (year); BW=body weight (kg); AT=averaging time (day).

4) Risk characterization

Non-carcinogenic risk characterization was performed by calculating the ratio of estimated intake to the reference dose or concentration of the hazardous agent. The resulting Risk Quotient (RQ) is used to assess the potential for adverse health effects based on established non-carcinogenic exposure guidelines.

$$RQ = \frac{ADD}{RfC}$$

Where; RQ=risk characterization; RfC= reference concentration.

5) Risk management

Upon completion of the environmental health risk assessment, if the Risk Quotient (RQ) is found to be ≥1, mitigation measures must be initiated. As part of the risk management process, appropriate strategies should be implemented, including the establishment of safe exposure thresholds.

The Environmental Health Risk Analysis by the US EPA estimates human health risks from ambient air pollution. The equation for the non-carcinogenic risk analysis of the inhalation route is shown in Figure 3:

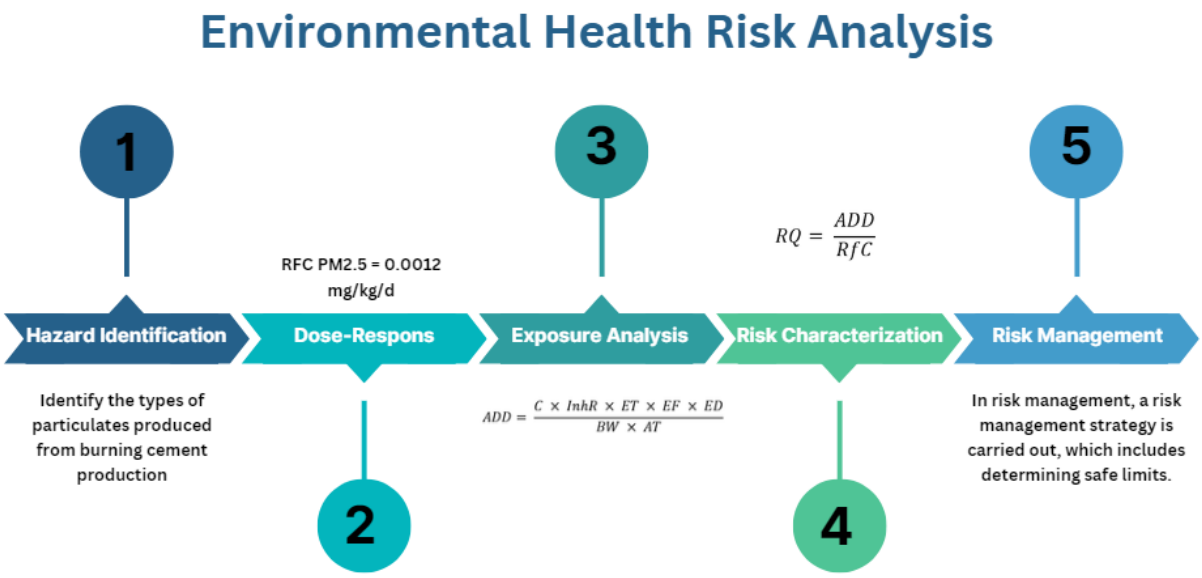

Figure 3. Environmental health risk analysis

3. RESULTS AND DISCUSSION

The environmental sample in this study consists of ambient air quality measurements of $PM_{2.5}$ collected by the researchers at eight locations, with one air quality monitoring point established in each village. Meteorological parameters—such as temperature, relative humidity, and wind speed—were sourced from the Meteorology, Climatology, and Geophysics Agency (BMKG) to ensure data reliability and consistency in representing standardized environmental conditions throughout the study.

Figure 4 The data illustrate ambient $PM_{2.5}$ concentrations along with temperature, humidity, and wind speed in the vicinity of PT Semen Tonasa, Pangkajene Islands Regency. The highest $PM_{2.5}$ level was recorded in Bontoa Village at 20.8 µg/m³, while the lowest was observed in Mangilu Village at 8.3 µg/m³. Two locations exceed the PM concentration quality standards$_{2.5}$ (15 µg/m^3), namely Bontoa Village as much as 20.8 µg/m^3 and Samalewa Village by 16.1 µg/m^3. The temperature at the eight research locations ranged from 32.3-36.5ºC, humidity from 42.9-64.8%, and wind speed from 1.1-2.3 (m/s). A high concentration of $PM_{2.5}$ is influenced by temperature, humidity and wind speed. The higher the temperature, the higher the PM concentration$_{2.5}$, while the higher the humidity, the lower the PM concentration$_{2.5}$. (Keyvani et al., 2020).

High $PM_{2.5}$ concentrations in Bontoa Village are due to the distance from the PT Semen Tonasa industry which is less than 1 km. People complained about scattered dust because of the mobilization of factory production in Biring Ere to Biringkassi. The elevated $PM_{2.5}$ concentration observed in Samalewa Subdistrict is attributed to heavy traffic conditions, particularly from frequent truck movement transporting cement, which contributes to the resuspension of dust particles into the ambient air.

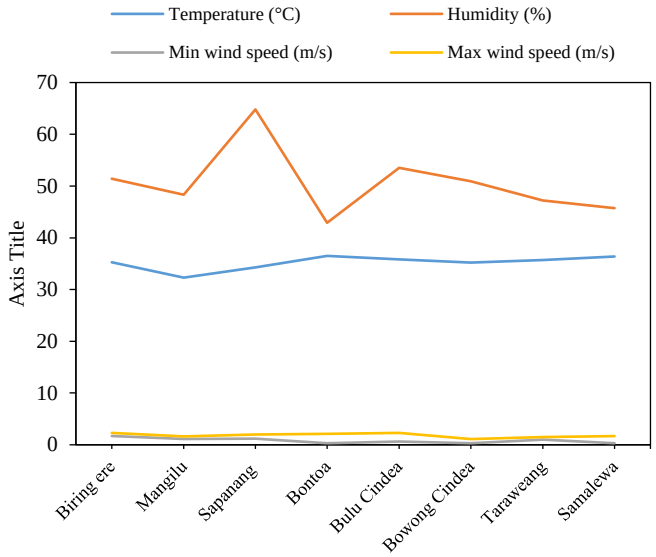

Figure 4. Ambient air quality parameters, $PM_{2.5}$ concentrations and meteorological data in Pangkajene Islands Regency, Indonesia

Meteorological variables such as wind direction, relative humidity, and temperature significantly influence ambient PM concentrations. Wind, in particular, plays a crucial role in the dispersion and transport of atmospheric pollutants. Measurement data indicate wind speeds ranging from 1.1 to 2.3 m/s. Prior research suggests that low wind velocities contribute to pollutant accumulation near emission sources, whereas higher wind speeds facilitate the dispersion of contaminants to more distant locations (Abbasi et al., 2019).

Figure 5 shows the wind direction for 6 months around the cement industry, where the dominant wind direction at the study site is towards the west and shows the frequency distribution of wind classes, where most are in the wind class 2.10-3.60 m/s. Wind serves as a primary driver in the atmospheric dispersion of pollutants, directing the movement of particulate matter along its flow. Wind velocity also determines the rate at which these pollutants are transported away from their emission sources (Istiqomah et al., 2023).

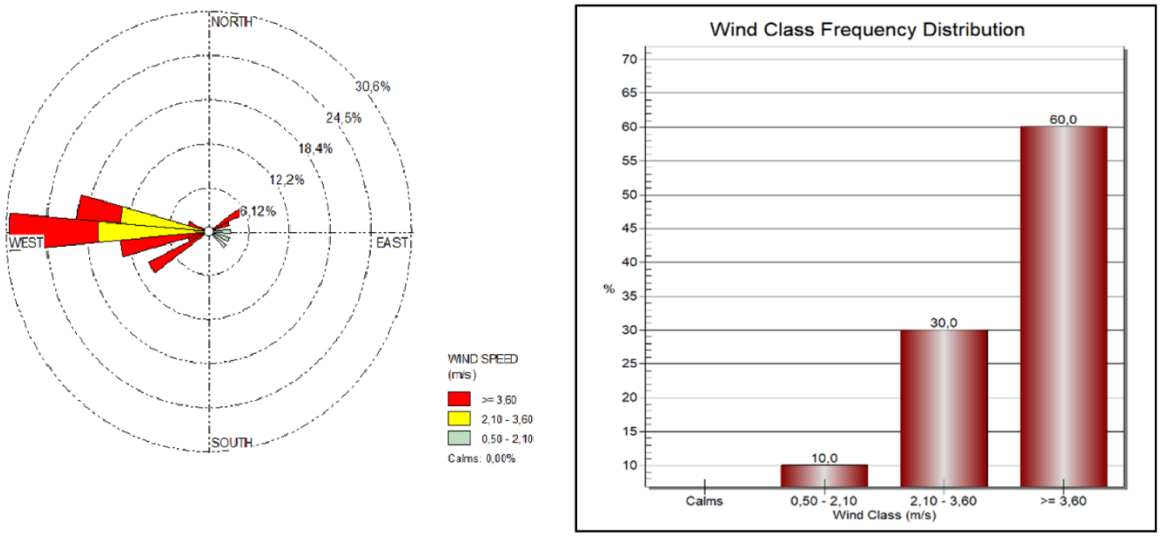

Figure 5. Wind rose and frequency distribution of wind classes

Table 1 shows the data indicate that respondents were aged between 6 and 45 years, with a mean age of 23 years. Body weight ranged from 11 to 92 kilograms, averaging 43 kg. The inhalation rate was recorded at 0.5 m³/hour for children and 0.83 m³/hour for adults. Annual exposure frequency varied from 317 to 365 days, with a mean of 358 days/year.

Intake values represent the level of exposure, and respondent characteristics are analyzed to identify the specific risk agents present in ambient air within Pangkajene Islands Regency. The real-time projected intake (Dt) values—minimum, maximum, and mean—are summarized in the following Table 2.

Based on Table 2. ADD intake value *real-time* non-carcinogenic $PM_{2.5}$ From 160 respondents, the result was showed that the mean real-time ADD for adults was 0.0047 mg/kg/day, exceeding that of children, which was 0.0016 mg/kg/day. For the lifetime exposure projection of non-carcinogenic $PM_{2.5}$ over a 5-30 year period, children's mean ADD ranged from 0.0009 to 4.6679 mg/kg/day, higher than adults whose values ranged from 0.0006 to 4.1989 mg/kg/day. Notably, the projected mean ADD in the 5th year remained below the Reference Concentration (RfC) for PM2.5 of 0.0012 mg/kg/day, indicating compliance with safety thresholds at that stage.

Table 1. Characteristics of respondents based on body weight and community activity patterns in Pangkep Regency 2023

Variabel	Min	Max	Mean	Total respondents
Age (years)	6	45	23	160
Body Weight (kg)	11	92	43	
Inhalation Rate (inhR) (m^3/jam) (USEPA, 2022)	0.5	0.83	0.665	
Exposure Frequency (EF) (hari/tahun)	317	365	358	

Table 2. Min, max and mean values of respondents' non-carcinogenic ADD for duration of PM exposure$_{2.5}$ around the PT industrial area. Tonasa Cement Pangkajene Islands District

Duration Time	ADD (mg/kg/day)							
	Min		Max		Mean		Is	
	Children	Mature	Children	Mature	Children	Mature	Children	Mature
Realtime	0.0005	0.0014	0.0043	0.0132	0.0016	0.0047	TMS	TMS
Lifetime								
5	0.0004	0.0002	0.0023	0.0015	0.0009	0.0006	MS	MS
10	0.0013	1.0150	9.8910	9.8520	2.7194	4.1989	TMS	TMS
15	1.0510	1.0380	7.0390	9.5360	2.7435	2.4284	TMS	TMS
20	1.4010	1.0640	9.3850	8.5020	3.6443	2.7060	TMS	TMS
25	1.0250	1.0620	9.6480	7.5670	4.2082	3.2630	TMS	TMS
30	1.1190	1.2750	9.9270	9.0810	4.6679	3.9157	TMS	TMS

3.1 Risk level characteristics

The Risk Quotient (RQ) serves as an indicator for assessing non-carcinogenic health risks. An RQ value exceeding 1 signifies the need for risk management interventions, whereas values below 1 indicate an acceptable risk level. Nonetheless, RQ values should consistently be maintained below the threshold of 1 to ensure continued protection of human health. The non-carcinogenic risk level is presented in Table 3 as follows.

Based on the results of Table 3 shows that the value of the real-time non-carcinogenic risk level or RQ $PM_{2.5}$ of 160 respondents (children and adults) is the average value for adult respondents 3.9845 higher than children, namely 1.4036, which means that the average community around the PT. Semen Tonasa industrial area is at risk of respiratory problems and decreased lung function in children's respondents because the RQ value >1. While the lifetime RQ projection for years 5-30 for children's respondents is 0.7631 to 4.5811 and adult respondents are 0.5342 to 3.2630. The projected mean RQ in the 5th year of the community living around the PT. Semen Tonasa industry is not at risk because the RQ value is <1, while the projected average RQ in the 10th-30th years increases, meaning that people are at risk of premature death, especially in people suffering from chronic heart or lung disease because the RQ value is >1.

Table 3. Min, max and average risk quotient (RQ) PM values$_{2.5}$ around the Industrial Area PT. Semen Tonasa Regency Pangkajene Islands

Duration time	RQ (mg/kg/day)							
	Min		Max		Average		Is	
	Children	Mature	Children	Mature	Children	Mature	Children	Mature
Realtime	0.4260	1.1330	3.6490	11.0000	1.4036	3.9845	Risk	Risk
Lifetime								
5	0.2600	0.1770	1.8600	1.2610	0.7631	0.5342	No risk	No risk
10	0.5840	0.3540	3.9100	2.5220	1.5268	1.0873	Risk	Risk
15	0.8760	0.5310	5.8660	3.7830	2.2904	1.6313	Risk	Risk
20	1.1680	0.7080	7.8210	5.0450	3.0540	2.1752	Risk	Risk
25	9.7770	0.8850	1.4600	6.3060	3.8177	2.7191	Risk	Risk
30	1.7520	1.0620	11.7300	7.5670	4.5811	3.2630	Risk	Risk

In developing countries, PM concentration$_{2.5}$ around cement factories is often above exposure limits, causing an increase in the number and severity of disease (Kholodov et al., 2020). In addition to air pollution, the cement industry contributes to various environmental and societal challenges, including land degradation, water pollution, and adverse health effects associated with particulate emissions (Rasmi and Türkay, 2023). Populations residing in proximity to cement manufacturing facilities are at risk of exposure to airborne pollutants emitted during production processes (Kholodov et al., 2020).

Health risks increase with the duration of exposure (Palacio et al., 2023). Elevated rates of illness among children residing near cement production facilities have been documented even in developed nations, despite ambient PM concentrations remaining within established regulatory limits (Kholodov et al., 2020). Individuals exposed to $PM_{2.5}$ face an elevated risk of developing pulmonary disorders and impaired cardiovascular function. Vulnerable populations, such as children and the elderly, are particularly susceptible to exacerbated respiratory symptoms, including airway irritation and dyspnea (He, 2021).

3.2 Risk management

In the context of Environmental Health Risk Analysis, risk management involves establishing protective exposure thresholds by regulating the duration, frequency, and timing of exposure to ensure population safety. The primary objective of risk management is to ensure that individuals or populations at risk of exposure to hazardous agents remain protected from associated health effects. This is achieved by adjusting relevant exposure parameters to maintain the Risk Quotient (RQ) below 1. The risk management thresholds for $PM_{2.5}$ are detailed in Table 4.

Risk reduction at the research location can be carried out by implementing scenario three, which shows that $PM_{2.5}$ exposure times are safe, around 5-7 hours daily obtained from the interview results. If respondents are exposed to more than the safe limit,

there will be a risk to their health. This scenario can apply to research sites; determining the exact timing of exposure can help identify the health risks associated with a particular exposure. Reducing exposure times is an essential preventive strategy in environmental health risk management. People can time their outdoor activities to avoid exposure to high levels of air pollution. Avoid outdoor activities when the cement factory operates, or the air conditions are particularly poor.

Table 4. $PM_{2.5}$ risk management

$PM_{2.5}$ risk management	Children	Mature
Scenario 1 EDaman (year)	7,2	9,4
Scenario 2 EFaman (days/year)	86,5	112
Scenario 3 ETaman (hours/days)	5,8	7,5

3.3 Spatial patterns

The following is the distribution of respondents' real-time RQ at each research location.

Figure 6 illustrates the risk of PM exposure$_{2.5}$ real-time projection of 5-30 years for respondents (children and adults) living around the PT Tonasa Cement industrial area. The study findings indicate that Samalewa, Sapanang, and Bontoa Villages fall within the moderate-risk category for $PM_{2.5}$ exposure, whereas Mangilu, Biring Ere, Taraweang, Bulu Cindea, and Bowong Cindea Villages are classified as low-risk areas.

This study shows that communities in Samalewa, Sapanang, and Bontoa villages are at moderate risk of environmental and health impacts due to proximity to the Semen Tonasa plant, including operational sites and raw material transportation routes. While the relationship between proximity to the plant and increased risk is clear, this study provides quantitative evidence by measuring $PM_{2.5}$ levels and documenting health complaints, such as coughing and shortness of breath in children based on interviews. In addition, the study also examined whether more remote villages were affected by cement-containing winds by analyzing $PM_{2.5}$ dispersion patterns and meteorological data, including wind direction and speed. The findings show that particulate matter can disperse beyond the immediate area of the plant under certain meteorological conditions, potentially impacting more remote areas, albeit to a lesser extent. These results emphasize the broader environmental and public health implications of plant operations, particularly regarding the dispersion of airborne particulates.

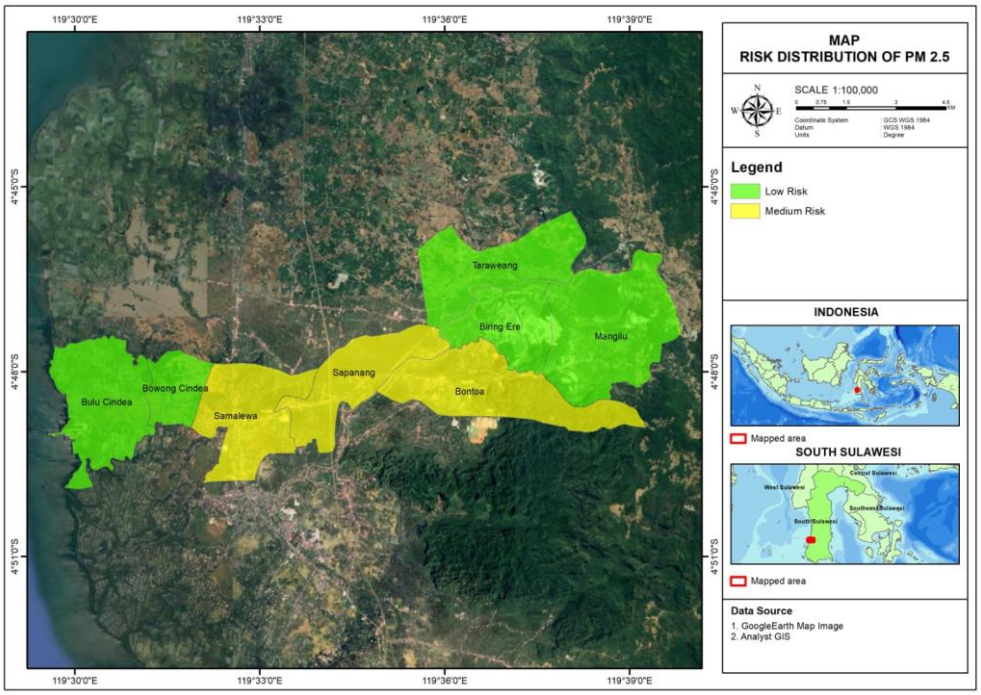

Figure 6. Distribution of PM real-time risk levels$_{2.5}$ respondent

The moderate risk classification for Taraweang and Mangilu Villages reflects the complex interplay of factors influencing $PM_{2.5}$ concentration, not just proximity to the cement factory. While the villages are near the factory, wind direction plays a significant role in dispersing or concentrating particulate matter, with specific patterns leading to localized accumulation of $PM_{2.5}$. Other contributing factors include emissions from blasting operations, transportation of raw materials, and dust released during material handling. Meteorological factors—such as wind velocity, temperature inversions, and relative humidity—significantly influence the dispersion dynamics of particulate matter, while local topographic features may contribute to the accumulation of pollutants in specific areas. This multifaceted assessment highlights that risk levels are shaped by a combination of environmental and operational influences, rather than proximity alone.

4. CONCLUSION

Ambient air monitoring around the PT Semen Tonasa industrial complex in Pangkajene Kepulauan Regency identified two locations—Bontoa Village and Samalewa Village—where $PM_{2.5}$ concentrations exceeded the permissible air quality standard of 15 µg/m³. The environmental health risk assessment indicates that residents living in proximity to the PT Semen Tonasa industrial area are exposed to $PM_{2.5}$ levels resulting in a Risk Quotient (RQ) greater than 1, which means that on average people are at risk of non-carcinogenic diseases. The spatial pattern shows that Samalewa, Sapanang, and Bontoa villages are at moderate risk of $PM_{2.5}$ exposure.

REFERENCES

Abbasi SA, Ponni G, Tauseef SM. Potential of joyweed Alternanthera sessilis for rapid treatment of domestic sewage in SHEFROL® bioreactor. International Journal of Phytoremediation 2019;21(2):160-9.

Abubakar IR, Maniruzzaman KM, Dano UL, AlShihri FS, AlShammari MS, Ahmed SMS, et al. Environmental sustainability impacts of solid waste management practices in the global South. International Journal of Environmental Research and Public Health 2022;19(19):Article No. 12717.

Chanda F, Lin Kai-Xuan, Chaurembo AI, Huang Jian-Yuan, Zhang Hui-Juan, Deng Wen-Hui, et al. $PM_{2.5}$-mediated cardiovascular disease in aging: Cardiometabolic risks, molecular mechanisms and potential interventions. Science of The Total Environment 2024;954:Article No. 176255.

Devi MLS WP. Distribution of Tsp (Total Suspended Particulate) dust to public health in Pt Semen Padang Industrial Area. Buana 2020;4(6):1245-61 (in Indonesian).

Duppa A, Daud A, Bahar B. Ambient air quality around Bosowa Cement Industry in Maros Regency. Journal of Maritime Public Health 2020;3(1):86-92 (in Indonesian).

Dwi Safira M, Syafiuddin A, Hakim A, Fasya Z, Setianto B, S1 PS, et al. Literature review: Air quality in industrial estates in various locations in Indonesia. Jurnal Public Health 2022;9(2):38-47 (in Indonesian).

Fitra M, Awaluddin S, Sejati, Elanda Fikri. Environmental Health Risk Analysis Revised Edition. Miladil Fitra; 2022 (in Indonesian).

Fitriyanti R, Fatimura M. Cleaner production applications in the cement industry. Jurnal Redoks 2019;3(1):10-5 (in Indonesian).

He B. A risk and decision analysis framework to evaluate future $PM_{2.5}$ risk: A case study in Los Angeles-Long Beach Metro Area. International Journal of Environmental Research and Public Health. 2021;18(9):Article No. 4905.

Istiqomah Q, Irsan R, Satria A. Analysis of distribution of NO_2 pollutants in PT. X Sanggau Regency, West Kalimantan. Journal of Civil Engineering 2023;23(3):359-62.

Kasim S, Daud A, Birawida AB, Mallongi A, Arundhana AI, Rasul A, et al. Analysis of environmental health risks from exposure to polyethylene terephthalate microplastics in refilled drinking. Global Journal of Environmental Science and Management 2023;9:301-18.

Keyvani S, Mohammadyan M, Chimehi E. Effect of the meteorological parameters on the indoor $PM_{2.5}$ and PM_{10} concentrations in a hospital. Scientific Research Publishing House 2020;2(4):1-7.

Kholodov A, Zakharenko A, Drozd V, Chernyshev V, Kirichenko K, Seryodkin I, et al. Identification of cement in atmospheric particulate matter using the hybrid method of laser diffraction analysis and Raman spectroscopy. Heliyon 2020;6(2):e03299.

Liang Y, Sengupta D, Campmier MJ, Lunderberg DM, Apte JS, Goldstein AH. Wildfire smoke impacts on indoor air quality assessed using crowdsourced data in California. Proceedings of the National Academy of Sciences 2021;118(36): e2106478118.

Lin C, Huang RJ, Ceburnis D, Buckley P, Preissler J, Wenger J, et al. Extreme air pollution from residential solid fuel burning. Nature Sustainability 2018;1(9):512-7.

Novirsa R, Achmadi UF. Risk analysis of exposure to $PM_{2.5}$ in daytime ambient air to people in the cement industry area. Public Health: National Public Health Journal 2012;7(4):Article No. 173 (in Indonesian).

World Health Organization (WHO). WHO Ambient Air Quality Database, 2022 Update: Status Report. World Health Organization; 2023.

Ouyang H, Tang X, Kumar R, Zhang R, Brasseur G, Churchill B, et al. Toward better and healthier air quality: Implementation of WHO 2021 global air quality guidelines in Asia. Bulletin of the American Meteorological Society 2022;103(7):1696-703.

Palacio LC, Durango-Giraldo G, Zapata-Hernandez C, Santa-González GA, Uribe D, Saiz J, et al. Characterization of airborne particulate matter and its toxic and proarrhythmic effects: A case study in Aburrá Valley, Colombia. Environmental Pollution 2023;336:Article No. 122475.

Paustenbach DJ, Madl AK, Massarsky A. Exposure assessment. Human and Ecological Risk Assessment: Theory and Practice 2024;1:157-261.

Rasmi SAB, Türkay M. Sustainability analysis of cement supply chains considering economic, environmental and social

effects. Cleaner Logistics and Supply Chain 2023;8:Article No. 100112.

Regia RA, Bachtiar VS, Solihin R. Analysis of health risks due to exposure to particulate Matter 2.5 ($PM_{2.5}$) in residential homes in housing X Cement Industrial Area. Journal of Environmental Science 2021;19(3):531-40 (in Indonesian).

Roser M. Data Review: How Many People Die from Air Pollution? Our World in Data; 2021.

Saroyo H, Saputri NFM. Cytotoxicity of mangrove leaves (rhizophora) ethanolic extract on cancer cells. Journal of Nutraceuticals and Herbal Medicine 2021;4(1):43-52.

Sun J, Yu J, Niu X, Zhang X, Zhou L, Liu X, et al. Solid fuel derived $PM_{2.5}$ induced oxidative stress and according cytotoxicity in A549 cells: The evidence and potential neutralization by green tea. Environment International 2023;171:Article No. 107674.

United States Environmental Protection Agency. Applying or Implementing Particulate Matter (PM) Standards. USEPA; 2022.

Wan Mahiyuddin WR, Ismail R, Mohammad Sham N, Ahmad NI, Nik Hassan NMN. Cardiovascular and respiratory health effects of fine particulate matters ($PM_{2.5}$): A review on time series studies. Atmosphere 2023;14(5):Article No. 856.

Xu H, Léon JF, Liousse C, Guinot B, Yoboué V, Akpo AB, et al. Personal exposure to $PM_{2.5}$ emitted from typical anthropogenic sources in southern West Africa: Chemical characteristics and associated health risks. Atmospheric Chemistry and Physics 2019;19(10):6637-57.

Yun X, Shen G, Shen H, Meng W, Chen Y, Xu H, et al. Residential solid fuel emissions contribute significantly to air pollution and associated health impacts in China. Science Advances 2020;6(44):eaba7621.

INSTRUCTION FOR AUTHORS

Publication and Peer-reviewing processes of Environment and Natural Resources Journal

Environment and Natural Resources Journal is a peer reviewed and open access journal that is published in six issues per year. Manuscripts should be submitted online at https://ph02.tci-thaijo.org/index.php/ennrj/about/submissions by registering and logging into this website. Submitted manuscripts should not have been published previously, nor be under consideration for publication elsewhere (except conference proceedings papers). A guide for authors and relevant information for the submission of manuscripts are provided in this section and also online at: https://ph02.tci-thaijo.org/index.php/ennrj/author. All manuscripts are refereed through a **single-blind peer-review** process.

Submitted manuscripts are reviewed by outside experts or editorial board members of **Environment and Natural Resources Journal**. This journal uses double-blind review, which means that both the reviewer and author identities are concealed from the reviewers, and vice versa, throughout the review process. Steps in the process are as follows:

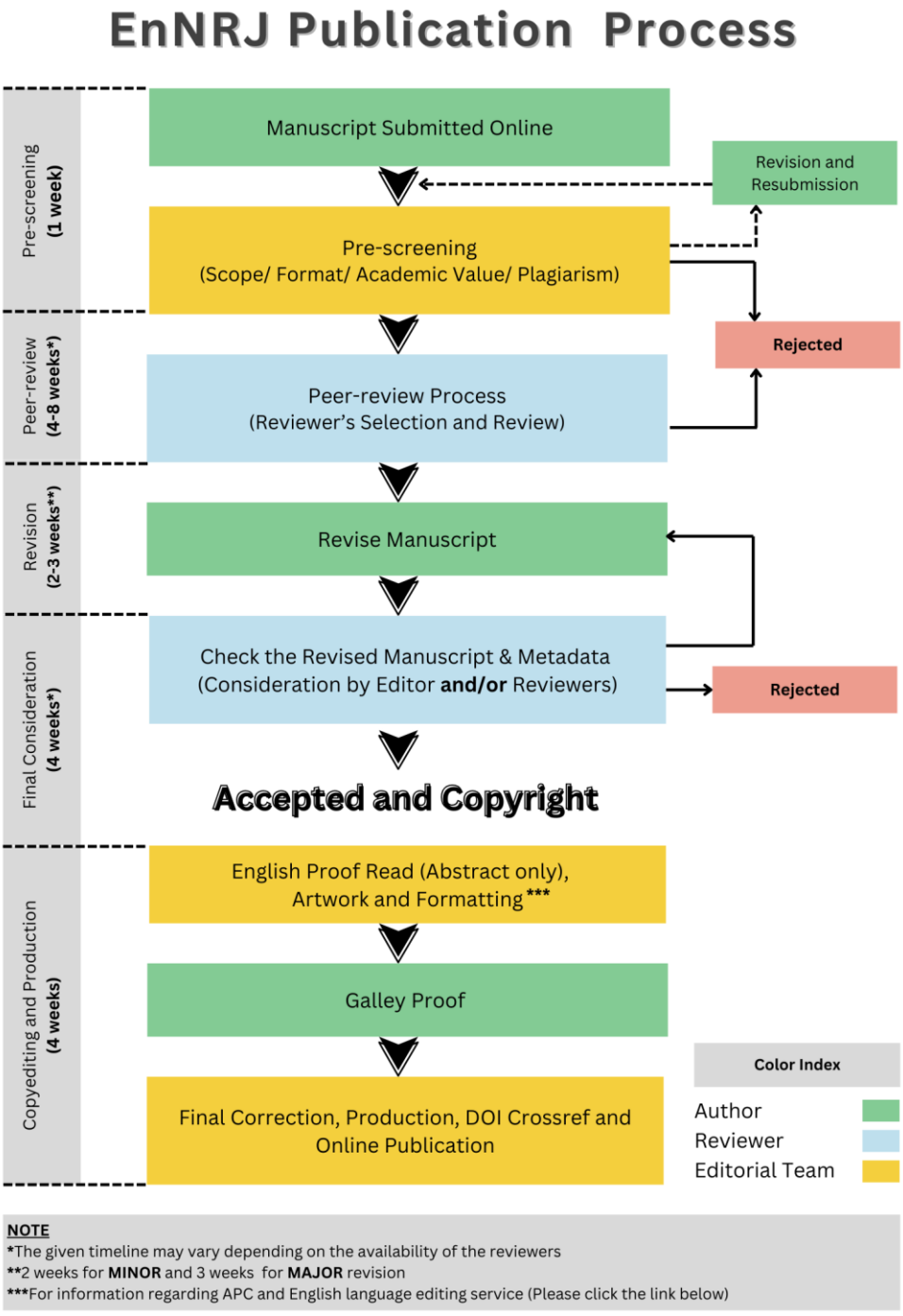

The Environment and Natural Resources Journal (EnNRJ) considers and accepts two types of articles for publication as follows:

- *Original Research Article*: This is the most common type of article. It showcases new, innovative or unique findings surrounding a focused research question. Manuscripts should not exceed 4,000 words (excluding references) - see more details in the Preparation of Manuscript section below.
- *Review Article (by invitation)*: This type of article focuses on the in-depth critical review of a special aspect of an environmental-related research question, issue, or topic. It provides a synthesis and critical evaluation of the state of the knowledge of the subject. Manuscripts should not exceed 6,000 words (excluding references).

Submission of Manuscript

The items that the author needs to upload for the submission are as follows:

Manuscript: The manuscript must be submitted as a Microsoft Word file (.doc or .docx). Refer to the **Preparation of Manuscript** section below for detailed formatting instructions.

Cover Letter: The letter should address the Editor and include the following: a statement declaring that the author's paper has not been previously published and is not currently under consideration by another journal.

- a brief description of the research the author reports in the paper, including why the findings are important and why the journal readers should be interested
- contact information of the author and any co-authors
- a confirmation that the author has no competing interests to disclose

Graphical Abstract (Optional): The author is encouraged to submit a graphical abstract with the manuscript. The graphical abstract depicts the research and findings with visuals. It attracts more potential readers as it lets them understand the overall picture of the article within a few glances. Note that the graphical abstract must be original and unpublished artwork. It should be a high-quality illustration or diagram in any of the following formats: TIFF, PDF, JPEG, or PNG. The minimum required size is 750 × 750 pixels (height × width). The size should be of high quality (600 dpi or larger) in order to reproduce well.

Reviewers Suggestion (mandatory): Please provide the names of three potential reviewers, with information about their affiliations as well as their email addresses. The recommended reviewers should not have any conflict of interest with the authors. Each reviewer must represent a different affiliation and not have the same nationality as the author. Please note that the editorial board retains the sole right to decide whether or not the recommended reviewers will be selected.

Declaration of Competing Interest: The author must include a declaration of competing interest form during submission. If there is no conflict of interest, please state, "The authors declare no conflict of interest." Otherwise, authors should declare all interests to avoid inappropriate influence or bias in their published work. Examples of potential conflicts of interest in research projects include but are not limited to financial interests (such as employment, consultancies, grants, and other funding) and non-financial interests (such as personal or professional relationships, affiliations, and personal beliefs).

CrediT (Contributor Roles Taxonomy) Author Statement or Author Contributions: For research articles with several authors, we require corresponding authors to provide co-author contributions to the manuscript using the relevant CRediT roles. CRediT is a taxonomy that shows the contributions of the author and co-author(s), reduces possible authorship disputes, and facilitates collaboration among research team members. The CRediT taxonomy includes 14 different roles describing each contributor's specific contribution to the scholarly output.

The roles are: Conceptualization; Data curation; Formal analysis; Funding acquisition; Investigation; Methodology; Project administration; Resources; Software; Supervision; Validation; Visualization; Roles/Writing – original draft; and Writing – review & editing.

Note that authors may have contributed through multiple roles, and those who contributed to the research work but do not qualify for authorship should be listed in the acknowledgments.

An example of a CRediT author statement is given below:
"Conceptualization, X.X. and Y.Y.; Methodology, X.X.; Software, X.X.; Validation, X.X., Y.Y. and Z.Z.; Formal Analysis, X.X.; Investigation, X.X.; Resources, X.X.; Data Curation, X.X.; Writing – Original Draft Preparation, X.X.; Writing – Review & Editing, X.X.; Visualization, X.X.; Supervision, X.X.; Project Administration, X.X.; Funding Acquisition, Y.Y."

Artwork for the Journal Cover: The author may provide and propose a piece of artwork (with a description) for the journal issue cover. This is an excellent opportunity for the author to promote their article, if accepted, on the cover of a published issue. Alternatively, the editorial team may invite the author to submit a piece of artwork for the cover after their manuscript has been accepted for publication. The final cover artwork selection will be made by the editorial team.

Final Author Checks: In addition to the basic requirements, the author should review this checklist before submitting their manuscript. Following it ensures the manuscript is complete and in accordance with all standards.

Preparation of Manuscript

Format and Style

The manuscript should be prepared strictly as per the guidelines given below. Any manuscript with an incorrect format will be returned, and the corresponding author may have to resubmit a new manuscript with the correct format.

Overall Format

The manuscript must be submitted as a Microsoft Word file (.doc or .docx). The formatting should be as follows:

- File format - .doc or .docx
- Page size - A4
- Page orientation - portrait (some landscape pages are accepted if necessary)
- Page margin - 2.54 cm (left and the right margin) and 1.9 cm (bottom and the top margin)
- Page number (bottom of the page)
- Line number
- Line spacing - 1.5
- Font - 12 point, Times New Roman (unless stated otherwise)

Unit - The use of abbreviation must follow the International System of Units (SI Unit) format.

- The unit separator is a virgule (/) and not a negative coefficient: 10 mg/L not 10 mgL^{-1}
- Liter always has a capital letter: mg/L

Equations

- Insert equations using the dedicated tool in Microsoft Word. Do not use pictures or text boxes.
- Equations that are referenced in the text should be identified by parenthetical numbers, such as (1), and should be referred to in the manuscript as “Equation 1”.

Inclusive Language: The language used in the manuscript acknowledges diversity, promotes equal opportunity, respects all people, and is sensitive to all aspects of differences. The manuscript content should not make assumptions about the beliefs or commitments of any individual. It should not imply superiority regarding age, race, ethnicity, culture, gender, sexual orientation, disability, or health conditions. Moreover, the manuscript must be free from bias, stereotypes, slang, and derogatory terms.

Reference Style: Vancouver style should be used for the reference list and in-text citations throughout the manuscript. Please follow the format of the sample references and citations, as shown in the Body Text Sections portion below.

Front Page

Title: The title of the manuscript should be concise and not longer than necessary. The title should be bold, 12-point size, and Times New Roman. The first letter of major words should be capitalized (as in standard title case).

Author(s) Name: The first and last names of all authors must be given, in bold, Times New Roman, and 12-point font.

Affiliation of All Author(s): Affiliation(s) must be in italics, Times New Roman, and 11-point font. Specify the Department/School/Faculty, University, City/Province/or State, and Country of each affiliation. Do not include positions or fellowships, or postal zip codes.
Each affiliation should be indicated with superscript Arabic numerals. The Arabic numeral(s) should appear immediately after the author’s name, and represent the respective affiliation(s).

Corresponding Author: One author should be responsible for correspondence, and their name must be identified in the author list using an asterisk (*).

- All correspondence with the journal, including article submission and status updates, must be handled by the corresponding author.

- The online submission and all associated processes should be operated by the corresponding author.

*Corresponding author: followed by the corresponding author's email address.

Example:

Papitchaya Chookaew[1], Apiradee Sukmilin[2], and Chalor Jarusutthirak[1*]
[1]Department of Environmental Technology and Management, Faculty of Environment, Kasetsart University, Bangkok, Thailand
[2]Environmental Science and Technology Program, Faculty of Science and Technology, Phranakhon Rajabhat University, Bangkok, Thailand
**Corresponding author: abcxx@xx.ac.th*

Abstract Page

Abstract: The abstract should include the significant findings paired with relevant data. A good abstract is presented in one paragraph and is limited to 250 words. Do not include a table, figure, or references.
Keywords - Up to six keywords are allowed, and they should adequately index the subject matter.

Highlights: Please include 3-5 concise sentences describing innovative methods and the findings of the study. Each sentence should contain at most 85 characters (not words).

Body Text Sections
The main body text of the manuscript normally includes the following sections: 1. Introduction 2. Methodology 3. Results and Discussion 4. Conclusions 5. Acknowledgments 6. Author Contributions 7. Declaration of Competing Interests 8. References

Introduction should include the aims of the study. It should be as concise as possible, with no subheadings. The significance of the problem and the essential background should also be given.

Methodology is sufficiently detailed so that the experiments can be reproduced. The techniques and methods adopted should be supported with standard references.
There should be no more than three levels of headings in the **Methodology and Results and Discussion** sections. Main headings are in bold letters, second-level headings are in bold and italic letters, and third-level headings are in normal letters.

Here is an example:

2. Methodology
2.1 Sub-heading
2.1.1 Sub-sub-heading

Results presents the key findings in figures and tables with descriptive explanations in the text.

Tables
- Tables - look best if all the cells are not bordered; place horizontal borders only under the legend, the column headings, and the bottom.

Figures
- Figures - should be submitted in color. The author must ensure that the figures are clear and understandable. Regardless of the application used to create them, when electronic artworks are finalized, please 'save as' or convert the images to TIFF or JPG and send them separately to EnNRJ. Images require a resolution of at least 600 dpi (dots per inch) for publication. The labels of the figures and tables must be Times New Roman, and their size should be adjusted to fit the figures without borderlines.
- Graph - The font style in all graphs must be Times New Roman, 9-10 size, and black color. Please avoid bold formatting, and set the border width of the graphs to 0.75 pt.

- Graph from MS Excel: Please attach an editable graph from MS Excel within your manuscript. Then please also submit the full MS Excel file used to prepare the graph as a separate document. This helps us customize our layout for aesthetic beauty.
- Graph from another program: Feel free to use whichever program best suits your needs. But as noted above, when your artwork is finalized, please convert the image to TIFF or JPG and send them separately Again, images should be at least 600 dpi. Do not directly cut and paste.

***All figures and tables should be embedded in the text, and also mentioned in the text.**

Discussion shows the interpretation of findings with supporting theory and comparisons to other studies. The Results and Discussion sections can be either separated, or combined. If combined, the section should be named Results and Discussion. **Conclusions** should include a summary of the key findings and take-home messages. This should not be too long, or repetitive but this section is absolutely necessary so that the argument of the manuscript is not uncertain or left unfinished.

Acknowledgments should include the names of those who contributed substantially to the work, but do not fulfill the requirements for authorship. It should also include any sponsor or funding agency that supported the work.

Author Contributions: For research articles with several authors, we require corresponding author contributions listed using the relevant CRediT roles. This should be done by the author responsible for correspondence.

Declaration of Competing Interest: The author must include a declaration of competing interest form during submission. If there is no conflict of interest, please state, "The authors declare no conflict of interest." Otherwise, authors should declare all interests to avoid inappropriate influence or bias in their published work.

References should be cited in the text by the surname of the author(s) and the year. This journal uses the author-date method of citation. The author's last name and date of publication are inserted in the text in the appropriate place. If there are more than two authors, “et al.” must be added after the first author’s name. Examples: (Frits, 1976; Pandey and Shukla, 2003; Kungsuwas et al., 1996). If the author’s name is part of the sentence, only the date is placed in parentheses: “Frits (1976) argued that . . .”

Please ensure that every reference cited in the text is also in the reference list (and vice versa).

In the list at the end of the manuscript, complete references must be arranged alphabetically by the surnames of the first author in each citation. Examples are given below.

Book

Tyree MT, Zimmermann MH. Xylem Structure and the Ascent of Sap. Heidelberg, Germany: Springer; 2002.

Chapter in a book

Kungsuwan A, Ittipong B, Chandrkrachang S. Preservative effect of chitosan on fish products. In: Steven WF, Rao MS, Chandrkachang S, editors. Chitin and Chitosan: Environmental and Friendly and Versatile Biomaterials. Bangkok: Asian Institute of Technology; 1996. p. 193-9.

Journal article

Muenmee S, Chiemchaisri W, Chiemchaisri C. Microbial consortium involving biological methane oxidation in relation to the biodegradation of waste plastics in a solid waste disposal open dump site. International Biodeterioration and Biodegradation 2015;102(3):172-81.

Journal article with Article Number

Sah D. Concentration, source apportionment and human health risk assessment of elements in $PM_{2.5}$ at Agra, India. Urban Climate 2023;49:Article No. 101477.

Non-English articles

Suebsuk P, Pongnumkul A, Leartsudkanung D, Sareewiwatthana P. Predicting factors of lung function among motorcycle taxi drivers in the Bangkok metropolitan area. Journal of Public Health 2014;44(1):79-92 (in Thai).

Article in press

Dhiman V, Kumar A. Biomass and carbon stock estimation through remote sensing and field methods of subtropical Himalayan Forest under threat due to developmental activities. Environment and Natural Resources Journal 2024. DOI: 10.32526/ennrj/22/20240018.

Published in conference proceedings

Wiwattanakantang P, To-im J. Tourist satisfaction on sustainable tourism development, Amphawa floating market Samut Songkhram, Thailand. Proceedings of the 1st Environment and Natural Resources International Conference; 2014 Nov 6-7; The Sukosol hotel, Bangkok: Thailand; 2014.

Ph.D./Master thesis

Shrestha MK. Relative Ungulate Abundance in a Fragmented Landscape: Implications for Tiger Conservation [dissertation]. Saint Paul, University of Minnesota; 2004.

Website

Orzel C. Wind and temperature: why doesn't windy equal hot? [Internet]. 2010 [cited 2016 Jun 20]. Available from: http://scienceblogs.com/principles/2010/08/17/wind-and-temperature-why-doesn/.

Report organization

Intergovernmental Panel on Climate Change (IPCC). IPCC Guidelines for National Greenhouse Gas Inventories: Volume 1-5. Hayama, Japan: Institute for Global Environmental Strategies; 2006.

Royal Gazette

Royal Gazette. Promotion of Marine and Coastal Resources Management Act 2059. Volume 132, Part 21, Dated 26 Mar B.E. 2558. Bangkok, Thailand: Office of the Council of State; 2015a. (in Thai).

Remark

** Please be note that manuscripts should usually contain at least 15 references and some of them must be up-to-date research articles.*

** Please strictly check all references cited in text, they should be added in the list of references. Our Journal does not publish papers with incomplete citations.*

Changes to Authorship

This policy of journal concerns the addition, removal, or rearrangement of author names in the authorship of accepted manuscripts:

Before the accepted manuscript

For all submissions, that request of authorship change during review process should be made to the form below and sent to the Editorial Office of EnNRJ. Approval of the change during revision is at the discretion of the Editor-in-Chief. The form that the corresponding author must fill out includes: (a) the reason for the change in author list and (b) written confirmation from all authors who have been added, removed, or reordered need to confirm that they agree to the change by signing the form. Requests form submitted must be consented by corresponding author only.

After the accepted manuscript

The journal does not accept the change request in all of the addition, removal, or rearrangement of author names in the authorship. Only in exceptional circumstances will the Editor consider the addition, deletion or rearrangement of authors after the manuscript has been accepted.

Copyright transfer

The copyright to the published article is transferred to Environment and Natural Resources Journal (EnNRJ) which is organized by Faculty of Environment and Resource Studies, Mahidol University. The accepted article cannot be published until the Journal Editorial Officer has received the appropriate signed copyright transfer.

Online First Articles

The article will be published online after receipt of the corrected proofs. This is the official first publication citable with the Digital Object Identifier (DOI). After release of the printed version, the paper can also be cited by issue and page numbers. DOI may be used to cite and link to electronic documents. The DOI consists of a unique alpha-numeric character string which is assigned to a document by the publisher upon the initial electronic publication. The assigned DOI never changes.

Environment and Natural Resources Journal (EnNRJ) is licensed under a Attribution-NonCommercial 4.0 International (CC BY-NC 4.0)

Mahidol University

Wisdom of the Land

Faculty of Environment and Resource Studies, Mahidol University, Thailand
999 Phutthamonthon Sai 4 Rd, Salaya, Phutthamonthon District, Nakhon Pathom 73170
E-mail: ennrjournal@gmail.com